EBERHARD KARLS
UNIVERSITÄT
TÜBINGEN

Applied numerical modeling of saturated / unsaturated flow and reactive contaminant transport - evaluation of site investigation strategies and assessment of environmental impact

Dissertation
zur Erlangung des Grades eines
Doktors der Naturwissenschaften
der Geowissenschaftlichen Fakultät
der Eberhard-Karls-Universität Tübingen

vorgelegt von

Christof Beyer
aus Braunschweig

2007

Applied numerical modeling of saturated / unsaturated flow and reactive contaminant transport - evaluation of site investigation strategies and assessment of environmental impact

Dissertation

zur Erlangung des Grades eines Doktors der Naturwissenschaften

der Geowissenschaftlichen Fakultät
der Eberhard-Karls-Universität Tübingen

vorgelegt von
Christof Beyer
aus Braunschweig

2007

Tag der mündlichen Prüfung: 23.02.2007

Dekan: Prof. Dr. Peter Grathwohl

1. Berichterstatter: Prof. Dr.-Ing. Olaf Kolditz

2. Berichterstatter: Priv. Doz. Dr. rer. nat. Sebastian Bauer

3. Berichterstatter: Prof. James F. Barker

Applied numerical modeling of saturated / unsaturated flow and reactive contaminant transport - evaluation of site investigation strategies and assessment of environmental impact

CHRISTOF BEYER

Abstract

In this thesis numerical models of variably saturated flow and reactive transport processes in porous media are employed as assessment tools in two different fields of application.

The first thematic complex studied is the computer based evaluation of investigation strategies for contaminated soils and aquifers. For this purpose the "Virtual Aquifer" (VA) concept is introduced and demonstrated by an assessment of the so called center line method for contaminant plume investigation. Errors and uncertainties in the estimation of contaminant degradation rates from center line data, which is often collected at field sites, are analysed. This is done by application at synthetic contaminated aquifers models, which are generated in the computer by numerical simulation of contaminant spreading. Monte Carlo simulations and sensitivity studies are performed to quantify the influences of sampling error magnitude, aquifer heterogeneity and model parameterisation on the estimated rate constants. In a second application example, the VA concept is used for the development and testing of a new approach for biodegradation parameter estimation. The performance of this method is studied in heterogeneous synthetic aquifers. Also, the propagation of errors and uncertainties from estimated rate parameters to a prognosis of the contaminant plume lengths is studied to obtain an indicator for the significance of the estimated degradation potential. The performance of the new parameter estimation method is assessed by comparison to frequently used approximations by first order kinetics.

The second thematic complex addressed in this thesis is the evaluation of environmental impact of contaminant emissions from road constructions by type scenario modelling. Two general concepts for modelling of flow and transport, i.e. the Eulerian and the Lagrangian points of view, are combined in this study to assess the extent of leaching from contaminated demolition waste within road structures to the groundwater surface. Transport simulations are performed for a number of typical subsoil units of Germany to analyse the sensitivity of contaminant transport behaviour on subsoil properties. The relevant contaminant transport and attenuation processes in road constructions and the different subsoils are identified. The study allows to draw important conclusions on how these mechanisms could be used or enhanced to reduce contaminant leaching to groundwater.

Angewandte numerische Modellierung der gesättigten / ungesättigten Strömung und des reaktiven Schadstofftransports- Evaluierung von Strategien der Standorterkundung und Umweltwirkungsprognose

CHRISTOF BEYER

Kurzfassung

Diese Arbeit stellt die Verwendung numerischer Modelle gesättigt / ungesättigter Strömungs- und reaktiver Stofftransportprozesse in porösen Medien als Bewertungsinstrument in zwei verschiedenen Anwendungsfeldern vor.

Der erste hier betrachtete Themenkomplex behandelt die computerbasierte Evaluierung von Erkundungsstrategien für kontaminierte Böden und Grundwasserleiter. Hierzu wird das Konzept der „Virtuellen Aquifere“ (VA) eingeführt und anhand einer Bewertung der sogenannten Center-Line Methodik zur Schadstofffahnenerkundung demonstriert. Die Center-Line Methode wird in der Praxis häufig zur Erhebung von Daten angewendet, auf deren Grundlage Schadstoff-Abbauratenkonstanten abgeschätzt werden können. Die Bewertung dieser Vorgehensweise wird durch eine Analyse der dabei auftretenden Fehler und Unsicherheiten vorgenommen, indem die Methode bei synthetischen kontaminierten Aquifermodellen angewendet wird, die am Computer durch numerische Simulation der Schadstoffausbreitung generierten wurden. Durch Monte-Carlo Simulationen und Sensitivitätsanalysen werden die Einflüsse von Messfehlern, Aquifer-Heterogenität und Modellparametrisierung quantifiziert. In einem zweiten Anwendungsbeispiel wird die VA-Methodik zur Ableitung und Prüfung eines neuen Ansatzes zur Schätzung von Parametern mikrobieller Abbaukinetiken angewendet. Die Eignung des Verfahrens wird in synthetischen heterogenen Aquiferen geprüft. Darüber hinaus wird die Fehler- und Unsicherheitspropagation von den geschätzten Abbauparametern zu mit diesen prognostizierte Schadstofffahnenlängen untersucht, um Indikatoren für die Aussagekraft der Parameter zu erhalten. Das Verfahren wird durch einen Vergleich mit häufig angewendeten Näherungen durch Kinetiken erster Ordnung bewertet.

Der zweite im Rahmen dieser Arbeit behandelte Themenkomplex ist die Bewertung der Umweltauswirkungen von Schadstoffausträgen aus Straßenbauten durch Typszenarien-modellierung. Hier werden zwei allgemeine Konzepte zur Modellierung von Strömung und Transport, der Eulerische und der Larangesche Ansatz, miteinander kombiniert. Das Ausmaß des Schadstoffeintrags aus belastetem im Straßenbau eingesetztem Recycling-Bauschutt ins Grundwasser wird durch Einsatz der mit einander gekoppelten numerischen Modelle GeoSys/Rockflow und SMART bewertet. Die Transport-simulationen werden für eine Reihe typischer Unterbodeneinheiten Deutschlands durchgeführt, um die Sensitivität des Schadstofftransportverhaltens auf die Unterbodeneigenschaften zu untersuchen. Die relevanten Schadstofftransport- und Attenuierungsprozesse im Straßenaufbau und den Unterböden werden identifiziert. Die Studie ermöglicht wichtige Schlüsse im Hinblick eine Nutzung und Förderung dieser Mechanismen zu einer weiteren Reduktion der Schadstoffeinträge ins Grundwasser.

Vorwort

Die zurückliegenden drei Jahre am ZAG in Tübingen waren für mich eine sehr spannende Zeit und nicht nur im Hinblick auf meine Promotion sehr lehrreich. Aus diesem Grund möchte ich hier die Gelegenheit nutzen, ein paar persönliche Worte zu verlieren und einigen Personen zu danken, ohne deren Beteiligung diese Arbeit so sicher nicht hätte entstehen können.

Die im Rahmen dieser Arbeit vorgestellten Ergebnisse wurden innerhalb der beiden Projekte "Virtueller Aquifer" (Förderkennzeichen 033 05 12/033 05 13) und "Übertragung der Ergebnisse des BMBF - Förderschwerpunktes „Sickerwasserprognose" auf repräsentative Fallbeispiele" (Förderkennzeichen 02WP0517) erarbeitet. Beide Projekte wurden durch das Bundesministerium für Bildung und Forschung (BMBF) finanziell gefördert, wofür diesem hiermit gedankt sei.

Besonders bedanken möchte ich mich bei den Betreuern dieser Arbeit. Herrn Prof. Dr.-Ing. Olaf Kolditz danke ich sehr für die Ermöglichung meiner Promotion, das in mich gesetztes Vertrauen und die stete Unterstützung. Seine immer optimistische Sicht der Dinge hat sich im Laufe der Zeit auch ein Wenig auf mich übertragen. Herr Dr. Sebastian Bauer ist mit Sicherheit die Person, die die Richtung meiner Arbeit am stärksten mitgeprägt hat. Sein aufrichtiges Interesse (auch abseits der fachlichen Dinge), viele ausführliche Diskussionen und immer konstruktive Kritik haben maßgeblich zu ihrem Gelingen beigetragen. Eine bessere Betreuung für seine Doktorarbeit kann man sich eigentlich kaum wünschen.

Herrn Prof. Dr. James F. Barker danke ich für die Erstellung des dritten Gutachtens dieser Arbeit.

Herzlich danken möchte ich Herrn Prof. Dr. Peter Grathwohl und Herrn Prof. Dr. Rudolf Liedl, die mir die Bearbeitung des Sickerwasserprognose-Projekts anvertrauten und mir so zu einem in jeder Hinsicht spannenden letzten Dreivierteljahr verhalfen.

Ein herzlicher Dank geht an meine Kollegen Dr. Cui Chen, Dipl.-Geol. Jan Gronewold, Dr. Wilfried Konrad, Dr. Thomas Kalbacher, Dr. Chan Hee Park, Dr. Wenqing Wang, Dr. Chris McDermott, Dr. Martin Beinhorn, Robert Walsh, M.Sc., Dr. Dirk Schäfer von der Uni Kiel, Dr. Hermann Rügner und Dr. Peter Dietrich vom UFZ in Leipzig, sowie an zahlreiche weitere Kollegen für angenehm reibungslose Zusammenarbeit, viele hilfreiche Diskussionen und gemeinsame Pausen vom Zahlen hin und her schubsen.

Mein größter Dank gilt meinen Eltern, da Ihr mir durch Eure Unterstützung diesen Weg erst ermöglicht habt, und Frauke für Deine große Geduld, Dein Verständnis, Deine Liebe und dafür, dass Du es trotz aller Umstände und Entfernungen gemeinsam mit mir bis hierhin geschafft hast.

Table of Contents

List of abbreviations and mathematical symbols

a	empirical sorption constant [-]
b	empirical sorption constant [-]
C	concentration [M L^{-3}]
C_0	equilibrium concentration [M L^{-3}]
C_l	liquid phase concentration [M L^{-3}]
C_s	solid phase concentration [M M^{-1}]
C_{org}	soil organic carbon content [%]
$C_w(\psi)$	water capacity function
D	tensor of hydrodynamic dispersion [L^2 T^{-1}]
D_a	aqueous molecular diffusion coefficient [L^2 T^{-1}]
D_{ae}	effective diffusion coefficient [L^2 T^{-1}]
D_{ap}	apparent diffusion coefficient [L^2 T^{-1}]
$\mathbf{D_e}$	tensor of effective hydrodynamic dispersion [L^2 T^{-1}]
$\mathbf{D_m}$	tensor of mechanical dispersion [L^2 T^{-1}]
DW	demolition waste
FE	finite element
FEM	finite element method
g	travel time probability density function
h	hydraulic head [L]
h'	erroneous head measurement [L]
I	identity tensor
I_C	inhibition concentration [M L^{-3}]
K	tensor of hydraulic conductivity [L T^{-1}]
k_{max}	maximum degradation rate [M L^{-3} T^{-1}]
l	pore connectivity parameter [-]
m	empirical Van Genuchten parameter [-]
M_C	half-saturation concentration [M L^{-3}]
MM	Michaelis-Menten
n	empirical Van Genuchten parameter [-]
OOP	object-oriented programming
PDE	partial differential equation
pdf	probability density function
Q	source or sink term [M L^{-3} T^{-1}]
r	radial distance [L]
REV	representative elementary volume
S	specific storativity [L^{-1}]
S_r	relative saturation [-]
t	time [T]
V	magnitude of velocity vector [L T^{-1}]
v_{max}	maximum growth rate [T^{-1}]
v	average linear velocity [L T^{-1}]
v	vector of average linear velocity [L T^{-1}]
VA	Virtual Aquifer
X	microbial population [M L^{-3}]
Y	yield coefficient [-]
z	elevation [L]
α	empirical Van Genuchten parameter [L^{-1}]
α_L	longitudinal dispersivity [L]
α_T	transverse dispersivity [L]
Γ	reaction function
γ	tortuosity related coefficient [-]
δ	random number
ε	intraparticle porosity [-]
$\Delta\varepsilon_h$	maximum measurement error [L]
η	empirical sorption constant [-]
η_e	effective porosity [-]
θ	volumetric water content [-]
θ_r	residual water content [-]
θ_s	saturated water content [-]
κ	empirical sorption constant [$M^{1-\eta}$ $L^{3\eta}$ M^{-1}]
λ	first order degradation rate constant [T^{-1}]
ξ	microbial decay term
ρ	density [M L^{-3}]
σ_Y^2	ln(K) variance
τ	travel time [T]
τ_f	tortuosity factor [-]
ψ	matric head [L]

Applied numerical modeling of saturated / unsaturated flow and reactive contaminant transport – evaluation of site investigation strategies and assessment of environmental impact

1. Introduction

In the field of subsurface hydrology, mathematical models are used to simulate fluid flow and solute transport by translating physical and biogeochemical processes into mathematical equations, which can be solved by either analytical or numerical methods. Understanding of individual processes in domains of simple geometry is already a challenging task for itself. In large scale applications, however, we are faced with heterogeneous environments and interactions of many different types of spatially and temporally variable processes, which leave the numerical treatment of such complex coupled problems often as the only way to reach meaningful conclusions (Zheng and Bennett, 1995). As a benefit of the rapid development of computational capabilities (e.g. high performance parallel computing, specialized software implementation methods, data pre- and post-processing tools, graphical display routines) the numerical simulation of complex coupled problems in subsurface hydrology is continuously advanced. In general, numerical models of flow and transport in geosystems are used as tools for

- qualitative and quantitative analysis of single or coupled processes
- identification of relevant parameters
- parameter estimation / inverse modeling
- sensitivity and uncertainty analysis
- prediction of system response to changes in initial or boundary conditions

These capabilities as well as the spectrum of application would not have been achieved without the ever growing demand for groundwater resources and the concern about its quality. Groundwater is one of the main drinking water supplies and increasingly used for agricultural field irrigation (Morris et al., 2003). At the same time pollution from industrial activities, waste disposal, agricultural use of fertilizers or pesticides and urban waste waters (Scheidleder et al., 1999) poses a serious threat to our groundwater resources.

In this thesis numerical modeling is used in three applications within the context of contaminant hydrology. The term applied numerical modeling here emphasizes the field scale application of computational methods to obtain solutions to systems of partial differential equations describing flow and reactive transport process interactions in porous media. Application 1 introduces the "Virtual Aquifer" (VA) concept, in which numerical modeling is used as a tool for the evaluation of investigation and remediation strategies for contaminated soils and aquifers. The concept is demonstrated by an assessment of the so called center line method for site investigation. In application 2 the VA concept is applied for the development and testing of a new approach for biodegradation parameter estimation. Both applications make use of the GeoSys / Rockflow code (Kolditz et al., 2006) for the numerical simulations. In application 3 the Eulerian and Lagrangian concepts for contaminant transport modeling are combined. GeoSys / Rockflow is coupled with the SMART model (Finkel et al., 1998) and used for type scenario modeling to assess the environmental impact of recycling materials in road constructions.

This synthesis is organized as follows: Chapter 2 presents the mathematical process models and numerical schemes used

for the application studies outlined. The chapter is based on fundamental publications in the field of computational hydrology. However, it is not intended to serve as a comprehensive review of processes and model concepts, as this would be beyond the scope of this synthesis. Chapter 3 and its subsections present the results and conclusions of the three application examples. Chapter 4 closes this synthesis with general conclusions and an outlook.

2. Mathematical models

The three-dimensional structure of natural porous media is manifested in its composition of three constituting phases, i.e. the solid (mineral or biophase), water and gaseous phases. At scales larger than the pore scale, a description of porous medium geometry becomes very complex and thus infeasible for modeling applications. To understand and formulate the dynamics of fluids in the subsurface the so called representative elementary volume (REV) concept is introduced (Bear, 1972): In the transition from the microscale to a larger macroscale material, parameters are averaged over a volume which is sufficiently large to describe the porous medium at that larger scale (see Fig. 1).

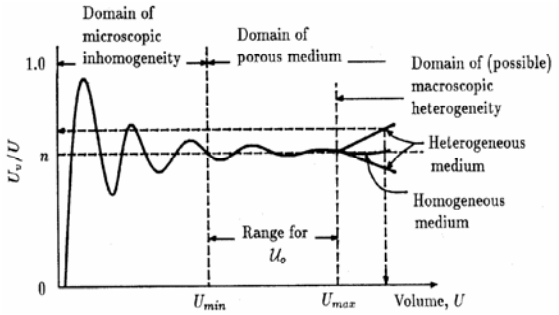

Fig. 1: Representative elementary volume concept (Bear and Bachmat, 1990).

This may also require a reformulation of the mathematical process descriptions. The derivation of representative or effective new material parameters and the corresponding governing equations is termed upscaling. Within the REV the detailed structure of the medium is lost and becomes a continuous field. Parameters like porosity, permeability or dispersivity are considered constant over the averaging volume. In the following sections material parameters and governing equations are based on this continuum approach.

2.1. Saturated / unsaturated flow

The dynamics of the water in fully saturated three dimensional porous media can be described by the combination of the mass balance for the water phase (eq. (1)) and Darcy's law (eq. (2)) as a constitutive equation (Bear, 1972)

$$S\frac{\partial h}{\partial t} = -\nabla \cdot \mathbf{q} + Q \qquad (1)$$

$$\mathbf{q} = -\mathbf{K}\nabla h \qquad (2)$$

where S [m^{-1}] is specific storativity, h [m] is the hydraulic head, given as the sum of elevation z [m] and the pressure head ψ [m], t [s] is time, $\mathbf{q}$ [$m\ s^{-1}$] is the Darcy flux vector, $\mathbf{K}$ [$m\ s^{-1}$] is the tensor of hydraulic conductivity and Q [s^{-1}] is a source or sink term. The governing equation for groundwater flow under transient conditions is thus given by (Bear, 1972)

$$S\frac{\partial h}{\partial t} = \nabla \cdot \left(\mathbf{K}\nabla h\right) + Q \qquad (3)$$

which at steady state converts to

$$\nabla \cdot \left(\mathbf{K}\nabla h\right) = -Q \qquad (4).$$

This model of steady state flow in saturated porous media is employed in applications 1 and 2 (sections 3.1, 3.2) of this synthesis. For unsaturated conditions, which are prevalent in application 3 (section 3.3), a more general form of eq. (2), the Buckingham-Darcy-law, can be used (Jury et al., 1991)

$$\mathbf{q} = -\mathbf{K}(\psi)\nabla h \qquad (5)$$

where $\mathbf{K}$ is a function of the pressure (or matric) head ψ, which itself depends on the volumetric water content θ [-] of the porous medium. As for saturated conditions, the

Buckingham-Darcy law is combined with mass balance principles to yield the governing equation of flow for unsaturated conditions, i.e. the Richards equation. This equation exists in three main forms with ψ, θ or both quantities as dependent variables (Jury et al., 1991). In GeoSys / Rockflow the ψ-based form (Freeze and Cherry, 1979) is implemented (Du et al., 2005)

$$C_w(\psi)\frac{\partial \psi}{\partial t} = \nabla \cdot \left(\mathbf{K}(\psi)\nabla \psi\right) + \frac{\partial K(\psi)}{\partial z} + Q \tag{6}$$

where $C_w(\psi)$ is the water capacity function defined by $d\theta / d\psi$ and with z positive in a downward direction. For the functional description of unsaturated hydraulic properties different mathematical formulations have been proposed in literature. A frequently used constitutive relation is the Van-Genuchten-Mualem model (Van Genuchten, 1980) which is based on the statistical pore space model of Mualem (1976) and is given by

$$K(S_r) = KS_r^l\left[1-\left(1-S_r^{-m}\right)^m\right]^2 \tag{7}$$

$$S_r = \frac{\theta-\theta_r}{\theta_s-\theta_r} = \frac{1}{\left[1+(\alpha\psi)^n\right]^m} \tag{8}$$

$$m = 1-1/n \tag{9}$$

where S_r [-] is defined as the relative saturation, l [-] is a pore connectivity parameter, θ, θ_r and θ_s are the actual, residual and saturated volumetric water contents, α [m^{-1}], n [-], and m [-] are empirical parameters. Other constitutive relationships comprise approaches such as the Brooks-Corey model (Brooks and Corey, 1966), the Haverkamp model (Haverkamp et al., 1977), potential functions as introduced by Huyakorn and Pinder (1983) or the multimodal model of Durner (1994). Recently, also free form parameterizations were suggested (Bitterlich et al., 2004). An overview on the prevalent approaches is given e.g. by Durner and Flühler (2005).

2.2. Transport processes

The most fundamental transport process of dissolved substances in saturated porous media is advection. Advection is passive with the flowing water. Purely advective transport of a solute plume is free of interference or mixing with the surrounding ambient water and is described with the advection equation (Zheng and Bennett, 1995)

$$\frac{\partial C}{\partial t} = -\mathbf{v}\nabla C + Q \tag{10}$$

where C [kg m^{-3}] is the concentration of a dissolved species, $\mathbf{v}$ [m s^{-1}] is the vector of average linear velocity which is given by division of $\mathbf{q}$ with the effective porosity η_e [-], and Q [kg m^{-3} s^{-1}] is a source or sink term for species C.

In natural aquifers or soils, purely advective transport is practically not established as dissolved molecules migrate from high to low concentration regions by Brownian motion. This concentration gradient driven mass transport is termed molecular diffusion and occurs even when the fluid itself is stagnant. For transient systems the diffusion process in water can be described using Fick's 2nd law, (Fetter, 1993)

$$\frac{\partial C}{\partial t} = -D_a\frac{\partial^2 C}{\partial x^2} \tag{11}$$

where D_a is the molecular diffusion coefficient in water [m^2 s^{-1}]. In porous media the diffusion process is hindered by the presence of the solid phase matrix and the tortous nature of the pores. Thus an effective diffusion coefficient D_{ae} is derived as (Grathwohl, 1998)

$$D_{ae} = D_a\frac{\eta_e\delta}{\tau_f} \tag{12}$$

where δ [-] is the constrictivity and τ_f [-] the tortuosity of the porous medium. Under unsaturated conditions D_{ae} can also be related to θ (e.g. Olsen and Kemper, 1968).

As water moves through a porous medium, single streamline velocities can be greater or less than v. This effect is due to different

path lengths of water molecules that bypass mineral grains of different size and shape, different pore diameters as well as inner pore friction which results in velocity contrasts along pore cross sections. The consequential divergence of transport velocities for dissolved solutes causes mixing with the ambient water along the flow path and thus results in solute spreading longitudinally and transversally to the main flow direction. This process is termed mechanical dispersion. For its mathematical description usually an analogy to the diffusion process is assumed. According to Bear (1972) the tensor of mechanical dispersion $\mathbf{D_m}$ is given by

$$\mathbf{D_m} = \alpha_T V \mathbf{I} + (\alpha_L - \alpha_T)\frac{\mathbf{vv}}{V} \quad (13)$$

where α_L and α_T [m] are longitudinal and transverse dispersivities, V is the magnitude of the velocity vector, $\mathbf{I}$ is the identity tensor and $\mathbf{vv}$ is the dyadic of the velocity vector. The tensor of hydrodynamic dispersion $\mathbf{D}$ [$m^2\ s^{-1}$] combines the dispersion and diffusion processes and is calculated by

$$\mathbf{D} = \mathbf{D_m} + D_{ae}\mathbf{I} \quad (14).$$

The mathematical formulation of advective-dispersive transport in fully saturated porous media assuming constant porosity is given by the sum of the advective and dispersive fluxes, i.e. the advection-dispersion-equation (Zheng and Bennett, 1995)

$$\frac{\partial C}{\partial t} = -\nabla \cdot (\mathbf{v}C) + \nabla \cdot (\mathbf{D}\nabla C) + Q \quad (15).$$

For unsaturated conditions the total solute flux in the water phase is described by

$$\frac{\partial \theta C}{\partial t} = -\nabla \cdot (\mathbf{q}\theta C) + \nabla \cdot (\theta \mathbf{D_e} \nabla C) + Q \quad (16)$$

where the effective hydrodynamic dispersion tensor $\mathbf{D_e}$ is used, as besides D_{ae} also α_L and α_T depend on θ (Bear, 1979).

2.3. Reactive processes

The source or sink terms Q in eq. (15) and (16) represent a large variety of processes other than advection or hydrodynamic dispersion, which may cause temporal changes in the solute concentration C. Hence, Q may represent transfer of species between solid, water, gaseous or biophase (e.g. volatilization, non aqueous phase liquid dissolution, sorption), or equilibrium and kinetic reactions of (geo-)chemical or biochemical nature. According to Rubin (1983) (Fig. 2) reactive processes can be classified by

- reaction velocity and reversibility (equilibrium or non-equilibrium; level A)
- involvement of only a single or several phases (homogeneous / heterogeneous; level B)
- reaction type: surface (e.g. sorption) or "classical" chemical reaction (level C)

For the sake of brevity, here only process concepts relevant for the model applications of chapter 3 are explained in more detail.

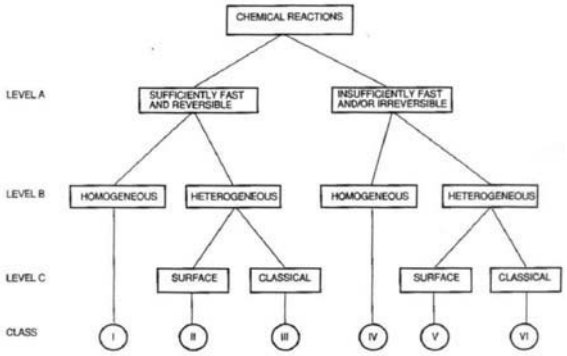

Fig. 2: Classification of reactions in porous media (Rubin, 1983).

Kinetic sorption

Transfer of dissolved species from the mobile phase to the solid matrix by physico-chemical processes is termed sorption. Sorbed species are immobilized and not transported with the water flux. Sorption is a reversible process, i.e. sorbed species can be remobilised by desorption. Temporary immobilisation by sorption results in lowered solute concentrations and retarded transport velocities. The manifold processes contributing to sorption phenomena include physical as well as chemical mechanisms (e.g. ion exchange and surface complexation through Coulomb or van der Waals forces, hydrogen-, hydrophobic- or

covalent bonding). To mathematically describe the sorption / desorption behaviour of a species so called sorption isotherms can be used, in which the sorbed amount of the species is a function of its dissolved concentration. A general nonlinear sorption model can be formulated as

$$C_s = \frac{\left(a\kappa C_l^{\eta}\right)}{\left(1 + abC_l^{\eta}\right)} \tag{17}$$

where C_s [kg kg^{-1}] is the sorbed solid phase and C_l [kg m^{-3}] the liquid phase concentration, κ, a, b and η are empirical constants. For $b = 0$, $a = 1$ [-] and $\eta = 1$ [-] eq. (17) is the linear Henry isotherm, in this case κ [m^3 kg^{-1}] is a simple equilibrium constant. For $\eta = 1$ and $b = 1$ eq. (17) is the Langmuir isotherm with κ [kg kg^{-1}] being the maximum amount of a species which can be sorbed to the solid phase and a [m^3 kg^{-1}] an adsorption constant. For $b = 0$, $a = 1$ [-] and $\eta \neq 1$ [-] (usually $\eta < 1$) the Freundlich isotherm is obtained, where κ [kg$^{1-\eta}$ m$^{3\eta}$ kg^{-1}] is the Freundlich coefficient and η [-] is the Freundlich exponent.

In general, sorption processes may be treated as equilibrium reactions because sorption is fast compared to transport. However, there are exceptions to this rule because for some solute species as well as soils or aquifers, equilibration is a slow process. Possible mechanisms include slow diffusion into intraparticle pores accompanied by equilibrium sorption to surfaces within the pores or slow diffusion in organic matter (Ball and Roberts, 1991; Grathwohl, 1998; Rügner et al., 1999). Hence, from a macroscopic point of view sorption equilibrium may not be reached within the available contact time between mobile and solid phases. Assuming spherical particles, intraparticle diffusion kinetics can be described by Fick´s 2nd law in radial coordinates (e.g. Grathwohl, 1998)

$$\frac{\partial C}{\partial t} = D_{ap}\left[\frac{\partial^2 C}{\partial r^2} + \frac{2}{r}\frac{\partial C}{\partial r}\right] \tag{18}$$

where r [m] is the radial distance from the particle center and D_{ap} [m^2 s^{-1}] is the apparent diffusion coefficient, which is calculated from D_a by

$$D_{ap} = \frac{D_a \varepsilon}{(\varepsilon + \kappa\rho)\,\tau_f} \tag{19}$$

where ε [-] is the intraparticle porosity, κ the linear equilibrium sorption coefficient and ρ [kg m^{-3}] the particle density. Other approaches to describe slow sorption / desorption kinetics comprise first- or second-order, two-stage models (e.g. Brusseau and Rao, 1989; Ma and Selim, 1994; Streck et al., 1995). A comparison of first-order and diffusion limited approaches was recently published by Altfelder and Streck (2006).

Kinetic degradation

Degradation, whether biotic or abiotic, is the only process that reduces the overall mass of contaminants in natural porous media without transfer to other phases. Biological degradation mechanisms are numerous, complex and by far not completely understood nor even identified. The vast amount of different types of microorganisms in the subsurface provides many metabolic pathways for contaminant degradation under aerobic and anaerobic conditions. Through successive oxidation or reduction reactions contaminants can be transformed to innocuous compounds like methane, chloride, water or carbon dioxide (Wiedemeier et al. 1999). However, intermediate products can even be of significantly higher toxicity and persistence than their parent compounds (e.g., dechlorination of dichloromethane to vinyl chloride; Wiedemeier et al. 1999).

Kinetic growth and decay of a microbial population X [kg m^{-3}] can be described by a generalized Monod-type equation as given e.g. in Schäfer et al. (1998)

$$\frac{\partial X}{\partial t} = v_{\max} X \prod_i \frac{C_i}{M_{C_i} + C_i} \times \prod_j \frac{I_{C_j}}{I_{C_j} + C_j} - \xi(X) \tag{20}$$

where v_{max} [s^{-1}] is a maximum growth rate, C_i [kg m^{-3}] is the concentration of the i^{th} substrate, M_{Ci} [kg m^{-3}] is the corresponding half velocity concentration [kg m^{-3}], C_j [kg m^{-3}] is the concentration of the j^{th} substance inhibiting microbial growth, I_{Cj} is the corresponding inhibition concentration [kg m^{-3}] and $\xi(X)$ is a microbial decay term, which is often modeled as being of first order. Consumption of substrates or production of k metabolites C_k [kg m^{-3}] is both coupled to microbial growth via (Schäfer et al., 1998)

$$\frac{\partial C_k}{\partial t} = \frac{-1}{Y_k}\left[\frac{\partial X}{\partial t}\right]_{growth} \tag{21}$$

where Y_k [-] is the yield coefficient for substrate or metabolite C_k, and $[\cdot]_{growth}$ refers to the growth term only in eq. (20). From the generalized Monod-type equation different more simple kinetic formulations can be derived. For a temporally constant microbial population, i.e. growth and decay terms are constant and of equal magnitude, no inhibition and dependence on only a single substrate, eq. (20) and (21) can be combined to yield the Michaelis-Menten (MM) kinetics model (Simkins and Alexander, 1984)

$$\frac{dC}{dt} = -k_{\max}\frac{C}{C + M_C} \tag{22}$$

where k_{max} is the maximum degradation rate [kg $m^{-3}s^{-1}$] and M_C is the MM half-saturation concentration [kg m^{-3}]. This approximation may be applicable e.g. when aquifer sediments have been exposed to contaminants for several years (Bekins et al., 1998) and is used in application 2 (section 3.2). Often, contaminant degradation is also described by simple first order kinetics, e.g. to simulate abiotic degradation reactions like hydrolysis and dehydrohalogenation of halogenated compounds (Wiedemeier et al., 1999). First order kinetics can be derived from eq. (22) for $C << M_C$

$$\frac{dC}{dt} = -\lambda C \tag{23}$$

where λ [s^{-1}] is the first order degradation rate constant, while for $C >> M_C$ eq. (22) approaches zero order kinetics. The first order model is used in application 1 and 3 (sections 3.1 and 3.3). Extensive reviews on kinetic models of biodegradation can be found e.g. in Baveye and Valocchi (1989), Rittmann and VanBriesen (1996) or Islam et al. (2001).

2.4. Numerics and software methods

Numerical solution of the governing equations

The governing equations for flow and reactive transport presented in sections 2.1 - 2.3 belong to the group of partial differential equations (PDE), containing derivatives of first order in time and of first as well as second order in space. The classification of PDE can be based on mathematical aspects (highest order derivatives in the dependent variables) or on a physical point of view (problem type of physical process) (Kolditz, 2002). Parabolic PDE are used for time-dependent problems with dissipation process, such as diffusion (eq. (11)) or transient groundwater flow (eq. (3)), which convert to elliptic PDE for steady state conditions (eq. (4)). A third class of PDE are hyperbolic equations like the linear advection equation (eq. (10)), which are used to describe time-dependent problems without dissipation process. The transport equations (15) and (16) are of mixed type with a parabolic dispersion-diffusion term and a hyperbolic advection term. Their behaviour for a particular problem depends on the relative magnitudes of these flux components. In general the transport equations are of parabolic character which changes to hyperbolic for large ratios of v/α_L as in this case the advective flux term is dominant (Kolditz, 2002).

In general, PDE describing physical problems are well-posed when appropriate initial and boundary conditions are specified for the domain where a solution is required. While analytical solutions can be

found for a number of problems with simple geometries and boundary conditions (e.g. Bear, 1979; Van Genuchten and Alves, 1982; Kinzelbach, 1983), for complex non-linear problems exact solutions may not exist and thus approximate numerical solutions must be obtained. Given the governing equations with appropriate initial and boundary conditions for a specified problem, the general strategy for a numerical solution is to first convert the PDE into a system of discrete algebraic equations and then to find the exact solution of the latter, which is the approximate solution of the PDE. An overview of approximation methods for the solution of PDE is given in Fig. 3.

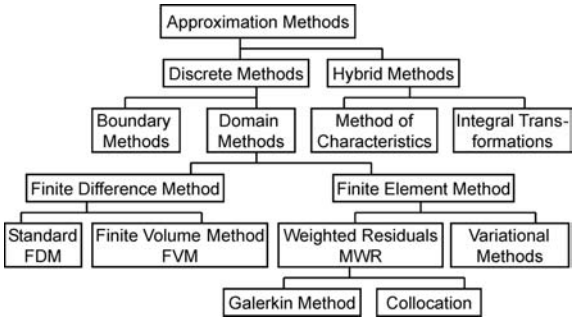

Fig. 3: Overview of approximation methods for PDE (Kolditz, 2002).

Among the many possible approaches for the numerical simulation of fluid dynamics and transport, finite difference, finite element and finite volume methods are the most frequently used. Their theory and implementation is content of numerous text books (e.g. Pinder and Gray, 1977; Baker, 1983; Zienkiewicz and Taylor, 1993; Helmig, 1997; Kolditz, 2002). Here, a short description of the finite element method (FEM) only is given, as it is the numerical scheme which is implemented in the GeoSys / Rockflow code (Kolditz et al., 2006) which is used in all applications presented in chapter 3.

The concept of the FEM is based on the spatial discretization ("meshing") of continuous structures into discrete substructures, i.e. the finite elements (FE). In comparison to finite differences, the big advantage of the FEM is its ability to also handle complex geometries by unstructured or arbitrarily shaped grids (Anderson and Woessner, 1992). The governing PDE are discretized by deriving integral formulations, e.g. by the method of weighted residuals. By introducing weighting functions the approximate solution is forced to satisfy the condition that the weighted average residual of the unknown true solution at the nodes over the computational domain is equal to zero. For any location within the domain the solution is obtained by linear combination of local interpolation functions and the solution at the nodes. With the standard Galerkin method (Huyakorn and Pinder, 1983) weighting and interpolation functions are selected identically. The FEM is globally mass conservative, locally, however, mass conservation problems may occur. Therefore mixed FEM approaches draw increasing attention (e.g. Starke, 2000; Knabner and Schneid, 2002; Korsawe et al., 2006).

The governing PDE of flow and reactive transport in porous media outlined in the previous sections are formulated from the point of view of an fixed observer with the fluid and solute moving on a fixed spatial grid. This approach is termed the Eulerian concept and is able to handle dispersion-dominated problems accurately and efficiently. For advection-dominated problems, however, the Eulerian concept is susceptible to numerical dispersion and artificial oscillations (Zheng and Bennett, 1995), For the price of increased computational effort this problem can be limited by sufficiently fine spatial and temporal discretization.

By contrast, the Lagrangian concept is well suited for advection-dominated problems, but problematic when advection and dispersion must be solved together (Thorenz, 2001). In the Lagrangian concept concentrations are not associated with fixed spatial points but rather with moving particles, that are transported with the prevailing flow velocity. The numerical model SMART (Finkel et al., 1998) is based on the Langrangian concept of Cvetkovic and Dagan (1996). In SMART the model

domain is discretized along advective flow paths of the Eulerian flow field by the travel time τ [s] of inert particles between an injection plane and a control plane, both oriented normal to the mean flow direction. Each particle trajectory is regarded as a separate one-dimensional stream tube of the flow field with an infinitesimal cross section. The probability density function (pdf) $g(\tau, x)$ of all particles travel times completely reflects all hydraulic heterogeneities of the model domain. Influences of reactions (e.g. biodegradation, intraparticle diffusion, sorption, etc.) are quantified by means of the reaction function $\Gamma(\tau, t)$, which is evaluated by the BESSY model (Jäger and Liedl, 2000) implemented in SMART. With given g and Γ the normalized breakthrough curve of a reactive solute at a control plane is calculated by (Finkel et al. 1998)

$$C(x,t) = \int_0^\infty g(\tau,x)\Gamma(\tau,t)d\tau \qquad (24).$$

To overcome the limitations of both the Eulerian and the Lagrangian concepts, mixed Eulerian-Lagrangian methods can be used, which take advantage of the particular appropriateness of both concepts for modeling advective and dispersive transport (e.g. Neumann, 1981; Thorenz, 2001; Park et al., 2006). In application 3 (section 3.3) a combination of the software codes GeoSys / Rockflow and SMART is used for a combined application of the Eulerian and the Lagrangian concepts. GeoSys / Rockflow is used to model the Eulerian flow field in a heterogeneous two dimensional domain and to derive the representative pdf $g(\tau, x)$. The SMART model then utilizes the pdf for the simulation of reactive transport in the model domain.

Object- and process-oriented methods

The GeoSys / Rockflow code, which is used for most of the numerical simulations described in chapter 3, is written in the C++ language and thus allows the implementation by object oriented programming (OOP) methods. The OOP concept is especially helpful for the development of complex software in programmer teams, as encapsulation and class-structures render the code more stable and errors are easier to detect. In GeoSys / Rockflow the OOP concept is met by so called process orientation (Kolditz and Bauer, 2004), which allows the coupling of two-phase flow, heat transport, mass transport, chemical reactions and deformation in an efficient way (Wang et al., 2006). The basic idea of process orientation is that between each physical process (e.g. single species transport) and its numerical approximation by an algebraic equation system (AES) exists a direct correspondence (Fig. 4). The AES originates from the temporal and spatial discretization of the PDE on the computational grid. For its solution the following steps are performed:

- AES assemblage and incorporation of initial conditions
- determination of element matrices
- incorporation of boundary conditions and source terms
- solving the AES by appropriate solvers

This procedure can be generalized for any physical process regardless of its specific type in an object oriented way by introducing the process object (Kolditz and Bauer, 2004) (Fig. 4).

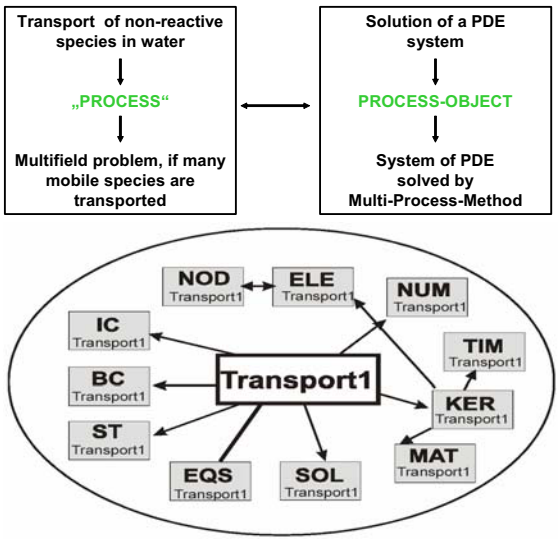

Fig. 4: Process analogy and process object, shown for an instance of a transport process (Kolditz and Bauer, 2004).

The process object has access to all required data structures and functions, and thus is self configuring, executing and destructing.

Contaminant transport problems usually involve a number of different processes as outlined in sections 2.1 – 2.3. The resulting multi-field problems can be approached by a multi-process algorithm, where one instance of the process object is created for each process considered. Solution of any number of flow or transport equations is fully automatic and encapsulated, guaranteeing high efficiency and flexibility.

In GeoSys / Rockflow saturated and unsaturated flow as well as conservative transport are solved using standard Galerkin FE. A non-iterative operator splitting technique for the coupling of conservative transport and (bio-)chemical reaction processes is used (Xie et al., 2006; Bauer et al., 2006b). First, the flow field is solved followed by conservative transport for all species. In the third step the calculation of kinetic biochemical reactions is performed. Finally chemical equilibrium reactions are calculated. This approach allows an easy handling of any number of species and reaction processes as well as employing optimised mathematical methods for the solution of the corresponding equation systems. The non-iterative approach, however, is limited to small time steps in order to avoid numerical instabilities. It is also known not to converge necessarily to the exact solution (Carrayrou et al., 2004). These limitations can be overcome using a computationally more demanding iterative operator splitting approach (e.g. Kinzelbach et al., 1991).

3. Modeling applications

In this chapter three application examples of numerical models for flow and reactive transport as established in chapter 2 are presented. Section 3.1 introduces the Virtual Aquifer (VA) concept, in which numerical modeling is used for the evaluation of investigation strategies for contaminated sites. In section 3.2 the VA concept is applied to derive and test a novel method for the estimation of biodegradation kinetic parameters from measured field data. Section 3.3 uses numerical modeling as a tool to predict the environmental impact of demolition waste used in road constructions

3.1. Evaluation of investigation strategies for contaminated aquifers using the Virtual Aquifer concept

Due to the limited accessibility of the subsurface, measurements of piezometric heads and pollutant concentrations at contaminated sites are sparse and may not be representative of the heterogeneous hydrogeologic conditions. Any site investigation is thus subject to uncertainty, reflecting the limited knowledge on aquifer properties and the extent of the contamination. Three main sources of uncertainty can be identified for site investigation, which are illustrated in Fig. 5. Conceptual model errors result from an incorrect identification of the governing processes at a site. Heterogeneity of the site causes an incomplete or wrong description of the relevant parameter distributions. For variables measured at observation wells like heads or concentrations measurement errors are inevitable. Due to this uncertainty, field investigation methods for plume screening and measuring of hydraulic conductivity or degradation rates can hardly be tested or verified in the field.

The VA approach is particularly aimed to overcome this problem. Its basic idea is the computer based evaluation of the performance and reliability of field investigation methods by application in heterogeneous synthetic (i.e. virtual) aquifers. In this it resembles the concept of “virtual realities” (Schäfer et al., 2002) which are used e.g. in car industry (“virtual crash test”), education (flight simulators) or medicine (interactive operation planning).

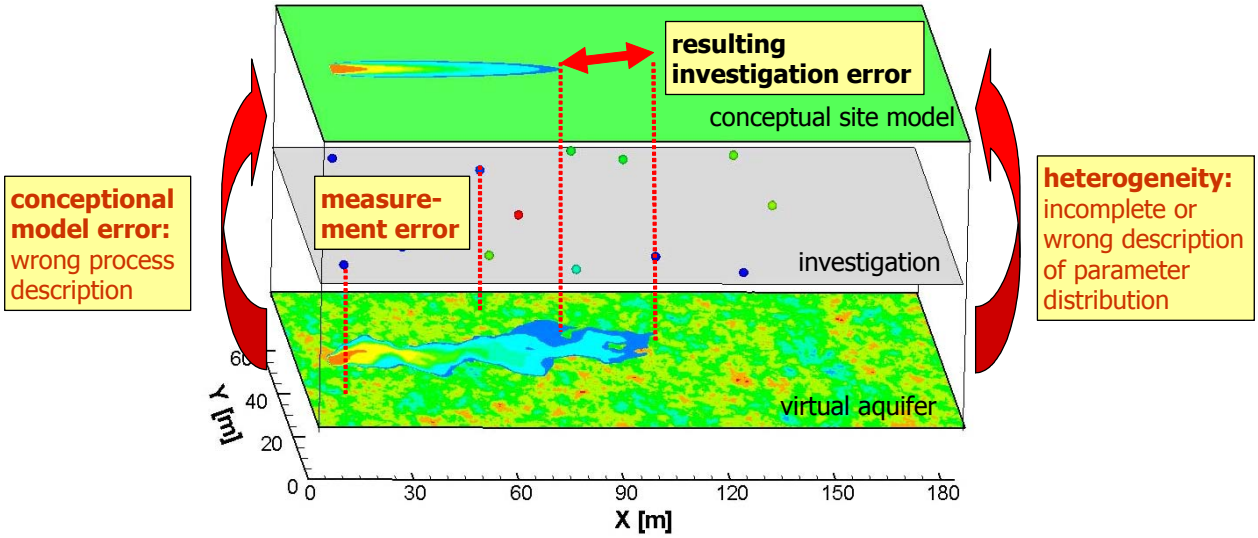

Fig. 5: Virtual aquifer concept and possible sources of investigation error.

An application of the VA concept requires the definition of a synthetic site model and its translation into a numerical model for the simulation of the identified relevant processes. Synthetic site models are generated based on statistical properties of natural aquifers. A defined contaminant source is then introduced and the evolution of aquifer contamination is simulated by numerical modeling, thus generating a realistic contaminant distribution in the synthetic aquifer. In comparison to the "real world", the unique advantage of the synthetic aquifer is that the spatial distribution of all physical and geochemical properties and parameters as well as contaminant concentrations are exactly known. Once the synthetic contaminated aquifer is generated, it can be studied by standard monitoring and investigation techniques, e.g. by emplacement of observation wells. Although the parameter distribution of the synthetic aquifer is known a priori, only the data "measured" at wells (i.e. hydraulic heads or concentrations) are used and interpreted. This is done because in a real site investigation also only a limited amount of measured data would be available. Finally, the results are compared to the "true" parameter distribution known from the synthetic aquifer, allowing an evaluation of the accuracy of the investigation method used. Using the VA concept, sources of uncertainty or error can be considered individually and the sensitivity of investigation results on these can be studied. Stochastic approaches like the Monte-Carlo method are applied to study the propagation of parameter variability and uncertainty into the investigation results. The VA has been first introduced by Schäfer et al. (2002) and was applied by Schäfer et al. (2004, 2006b), Bauer and Kolditz (2006), Bauer et al. (2005 [EP 1]; 2006a [EP 2], 2007 [EP 4]) and Beyer et al. (2006 [EP 3], 2007a [EP 5]). An overview of VA applications is given in Bauer et al. (2006b) and Schäfer et al. (2006a).

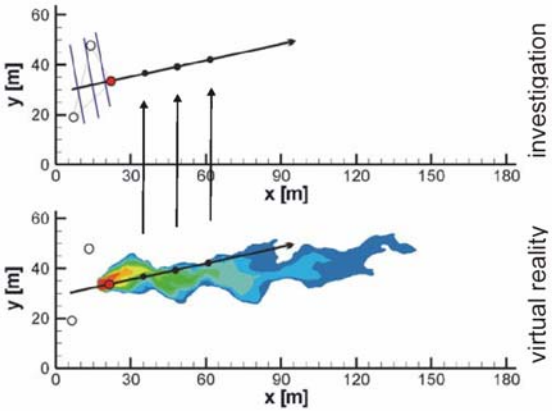

Fig. 6: Virtual investigation of a heterogeneous contaminant plume by the center line method (*Bauer et al., 2005 [EP 1]).*

The VA concept is used here to study errors and uncertainties in degradation rate constants estimated from data typically collected by site investigation with the so called

center line method (Fig. 6). This method is frequently used in field studies when natural attenuation is considered as a remediation alternative and is based on observation wells that are placed along the presumed center line of the contaminant plume.

Influence of measurement errors

The first aspect studied here is the influence of measurement errors in hydraulic heads on degradation rate constant estimates (Bauer et al., 2007 [EP 4]). The VA concept used in this study is based on a two dimensional conceptual model of the groundwater body using a homogeneous distribution of hydraulic conductivity K. The development of the contaminant plume originating from a rectangular source zone is simulated until steady state conditions are established. The numerical simulations are performed using the GeoSys / Rockflow code, which was introduced in the previous chapter. The contaminant is subject to a first order kinetics (eq. (23)) degradation reaction using a uniform degradation rate constant λ. Additionally, a conservative tracer is emitted from the source zone. The contaminant plume thus generated is then investigated by the center line method. From the hydraulic heads measured at three initial observation wells (one being located directly in the center of the source zone) first the direction of groundwater flow is estimated by construction of a hydrogeological triangle. Head measurements are obtained by reading the model output at the respective well locations and adding a random measurement error by

$$h' = h + \delta \Delta \varepsilon_h \tag{25}$$

where h' and h are the erroneous and exact (i.e. simulated) heads, respectively, δ is an evenly distributed random number from the interval [-1, 1] and $\Delta\varepsilon_h$ is the maximum measurement error. Along the estimated (and potentially erroneous) flow direction three new observation wells are installed, one at every 10 m. These wells were then used to measure local (erroneous) heads, contaminant concentrations and hydraulic conductivities along the presumed plume center line. From the hydraulic head difference, true porosity and well positions groundwater flow velocities are calculated. Together with the concentration data this allows the determination of λ using any of the analytical models presented in Tab. 1. As hydraulic conductivity K is distributed homogeneously and concentrations are assumed to be measured precisely, the only source of error here is the measured head.

Tab. 1: Analytical models for the estimation of the first order degradation rate constant λ.

method	formula	description	reference
1	$\lambda_1 = -\frac{v_a}{\Delta x}\ln\left(\frac{C(x)}{C_0}\right)$	analyt. solution of 1D advection equation with first order degradation	Newell et al. (2002)
2	$\lambda_2 = -\frac{v_a}{\Delta x}\ln\left(\frac{C(x)}{C_0}\frac{C_0^*}{C(x)^*}\right)$	same as method 1; concentrations normalized by conservative tracer	Wiedemeyer et al. (1996)
3	$\lambda_3 = \frac{v_a}{4\alpha_L}\left(\left(1-2\alpha_L\frac{\ln\left(C(x)/C_0\right)}{\Delta x}\right)^2 - 1\right)$	analyt. solution of 1D advection-dispersion equation with first order degradation	Buscheck and Alcantar (1995)
4	$\lambda_4 = \frac{v_a}{4\alpha_L}\left(\left(1-2\alpha_L\frac{\ln\left(C(x)/(C_0\beta)\right)}{\Delta x}\right)^2 - 1\right)$ with $\beta = erf\left(\frac{W_S}{4\sqrt{\alpha_T \Delta x}}\right)$	analyt. solution of 2D advection-dispersion equation with first order degradation and accounting for the source area width	Zhang and Heathcote (2003)

The conceptual model used is a rigorous simplification of the processes observed in natural aquifer systems, as K varies in space and contaminant degradation usually follows more complicated laws, depends on microorganism growth and may be limited or inhibited by other substances. The simplifications assumed here are however necessary to study the sole effects of measurement error on rate constant estimation under otherwise ideal conditions for the application of the center line method and the analytical models of Tab. 1.

In this synthesis only results for method 1 of Tab. 1 are presented. The degradation rate estimated from evaluation of measured heads and concentrations is divided by the true rate constant used in the numerical model yielding normalized overestimation factors. To assess the range of uncertainty resulting from the random measurement error a Monte Carlo analysis is conducted for five increasing values of $\Delta\varepsilon_h$, each with a sample size of 100. Fig. 7 presents the rate constants thus estimated versus $\Delta\varepsilon_h$. Without measurement error the correct rate constant is obtained. However, already for very small $\Delta\varepsilon_h < 1$ cm, a significant overestimation can be observed. This has two main reasons: Firstly, an erroneous head yields an incorrect transport velocity and thus results in rate constant overestimation for too high velocities and in underestimation for too low velocities. Secondly, erroneous heads result in an incorrect derivation of the flow direction using the hydrogeologic triangle. Thus the observation wells installed downgradient of the source may be placed off the true center line position (compare Fig. 6). Hence, concentrations measured in off center line wells are too low, indicating an overly high rate of degradation. Overestimation of the degradation rate increases with the maximum head error and reaches factors of more than 20 in the worst cases.

In Bauer et al. (2007 [EP 4]) also the influence of concentration measurement errors was studied. It was found that also this type of error results in overestimation of the rate constant on average. Erroneous heads, however, were found to have a larger impact on the rate constant estimates. For real field applications therefore much care has to be taken when measuring hydraulic heads for the derivation of the plume center line position.

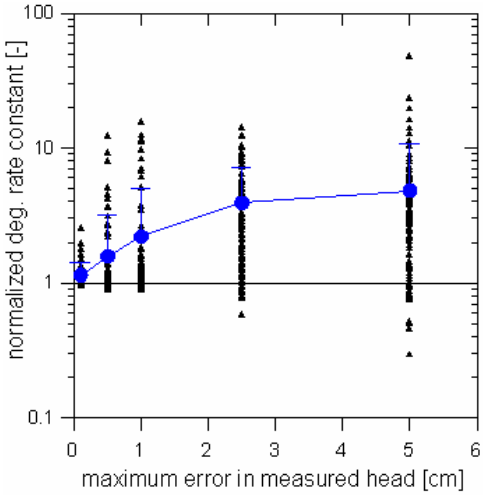

Fig. 7: Influence of head measurement error on rate constant estimates (Bauer et al., 2007 [EP 4]). The reference rate constant is indicated by the horizontal line, small symbols represent single estimates, big symbols are ensemble averages with standard deviation as error bars.

Influence of aquifer heterogeneity

The second aspect studied using the VA concept is the influence of spatially heterogeneous hydraulic conductivity distributions on the accuracy of rate constant estimation methods 1 – 4 of Tab. 1. For this end the conceptual model used so far is modified by assuming all head, concentration and K measurements to be free of measurement error and regarding K as a spatial random variable. This is done to study the sole influence of heterogeneous conductivity. Multiple realizations of heterogeneous K fields for four degrees of aquifer heterogeneity characterized by the ln-conductivity variance σ_Y^2 were generated, using a Monte Carlo approach to study the range of investigation result uncertainty. For each σ_Y^2 at least 100 different reali-

zations were generated. For all realizations the spreading of a conservative and a reactive contaminant plume subject to first order degradation was simulated. The resulting heterogeneous plumes were investigated as explained above. Fig. 8 presents normalized estimated rate constants for methods 1 – 4 (Tab. 1) versus σ_Y^2 (Bauer et al., 2005 [EP 1]). Clearly, most rate constants are larger than 1, i.e. the rate constant is generally overestimated. Single realizations show overestimation by several orders of magnitude. It is obvious that an increase in K heterogeneity causes higher overestimation. Also the spread of the 100 realizations and the resulting ensemble standard deviations increase significantly, causing higher uncertainty in the rate constant estimate. The main reasons for the observed overestimation are identified as deviation of observation wells from the true plume center line position, an incorrect approximation of the transport velocity and no or inadequate consideration of concentration reduction by longitudinal and transverse dispersion. Comparing the performance of methods 1 – 4 yields that method 2 is the most accurate and reliable among the four approaches. The superiority of method 2 follows from the correction of contaminant concentrations by normalization to the concentrations of a conservative tracer, which is spread from the same source. The tracer correction successfully accounts for the effects of dispersion and measuring off the center line. Method 3 explicitly accounts for longitudinal, method 4 for both, longitudinal and transverse dispersion. However, for each realization investigated, method 3 yields a higher rate constant estimate than methods 1 or 2. Longitudinal dispersion of a degrading contaminant results in a stronger spreading of the solute downstream and thus in higher concentrations along the center line of a steady state plume. To model an observed concentration reduction with a one-dimensional model like method 3 which accounts for α_L only

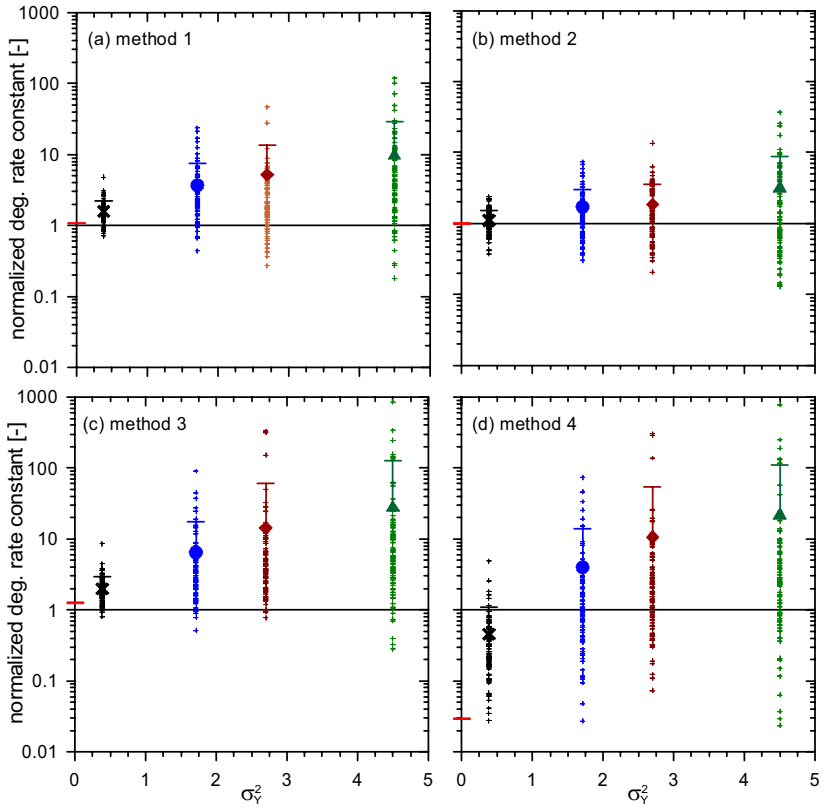

Fig. 8: Estimated degradation rate constants versus aquifer heterogeneity for methods 1 (a), 2 (b), 3 (c) and 4 (d) of Tab. 1 (Bauer et al., 2005 [EP 1]). Small symbols represent single realization results, large symbols ensemble averages of 100 realizations.

requires therefore a higher degradation rate constant. Method 4 yields significantly lower rate constant estimates than method 1, when aquifer heterogeneity is low, but almost the same results as method 3 for high heterogeneity. The rate constant underestimation for low heterogeneity is due to an "over correction" for transverse dispersion by the error function term β in the rate equation. Hence, both methods fail to yield closer rate constant estimates than the simpler approach of method 1, which completely neglects the dispersion process.

Influence of dispersivity parameterization

Since the results of methods 3 and 4 depend on longitudinal and transverse dispersivities, an adequate parameterization is crucial for their success. In this study, parameterization of α_L as well as α_T is based on the scale of the contamination problem, as common with many field applications. Clearly from the results in Fig. 8 derivation of α_L and α_T from the assumed length of the contaminant plume is not appropriate. As known from stochastic hydrogeology (e.g. Dagan, 1989) α_L as well as α_T strongly depend on travel time and distance as well as on the correlation structure of hydraulic conductivity and flow velocity. Therefore the influence of dispersivity parameterization on the performance of methods 3 and 4 was analyzed (Bauer et al., 2006a [EP 2]). From the often very limited amount of data on the degree of aquifer heterogeneity and the spatial correlation structure of hydraulic conductivity available for real field sites, the inference of dispersivities by methods of stochastic theory is rarely possible or at least afflicted by high uncertainty. Therefore a sensitivity analysis is performed to cover a wide range of values for α_L and α_T. Varying both parameters the heterogeneous plume realizations were re-evaluated using the different parameterizations of method 4. Fig. 9 shows results of method 4 in terms of ensemble medians of the 100 estimated rate constants for each of the four different degrees of heterogeneity and all combinations of α_L and α_T considered. As method 4 converges with method 3 for $\alpha_T = 0$, results for $\alpha_T = 0$ are also representative for method 3.

For all degrees of heterogeneity, decreasing median degradation rates are found with increasing α_T. For low and medium heterogeneity (Fig. 9 (a) and (b)) combinations of α_L and α_T can be found, which allow for an optimal estimation of the degradation rate constant, i.e. the results are of comparable accuracy as those of methods 1 or 2. For the highest degree of heterogeneity (Fig. 9 (d)), no such parameter combination is found within the range of dispersivities considered here. However, with an inadequate parameterization also for low heterogeneities severe over- as well as underestimation is possible. Moreover, with the exception of the low heterogeneity case, only unphysical combinations of low α_L and high α_T yield close estimates of the rate constant. These parameters do not represent actual dispersivities, but must be considered as mere lumped fitting parameters, as they are used to correct for off center line measurements and not the dispersion process only. As the magnitude of bias caused by off center line measurements is not known and the K correlation structure and degree of heterogeneity are usually not properly characterized at many field sites, choosing dispersivities for an application of method 4 would be highly uncertain and arbitrary.

From the results presented here, it can be concluded that for contaminated sites, where the assumption of first order degradation kinetics can be justified, method 2 should be preferably applied, if the degradation rate constant is to be derived with the center line approach. In situations, where a correction of concentrations by a conservative tracer is not possible, alternatively method 1 should be used, as its application implies the least amount of parameterization uncertainty.

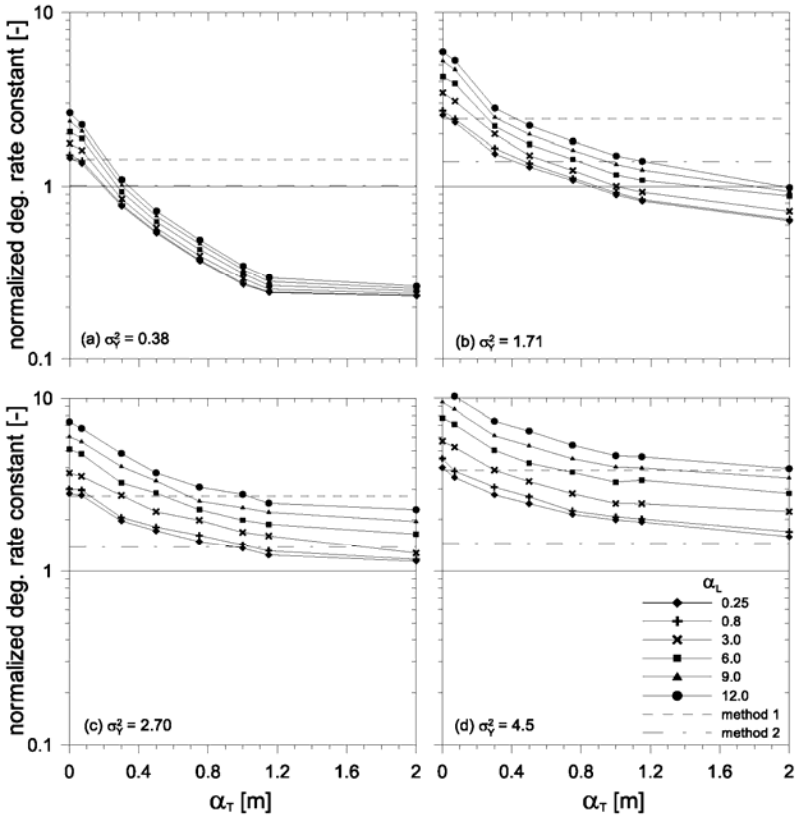

Fig. 9: Influence of dispersivity parameterization on estimated degradation rate constants for method 4 (and method 3 with $\alpha_T = 0$) of Tab. 1 and four degrees of aquifer heterogeneity σ_Y^2 (Bauer et al., 2006a [EP 2]). Symbols represent ensemble medians of 100 realizations.

Extensive monitoring networks

For the previous studies, linearly arranged center line observation wells have been used for the VA investigation (compare Fig. 6). Contaminant plumes in natural heterogeneous aquifers may however show a substantial amount of meandering (Wilson et al., 2004) resulting in non-linear center line orientations. As documented, an inappropriate assumption of a linear center line may result in misplacement of the observation wells and in significant overestimation, if degradation rate constants are to be derived. Moreover, only measurements in observation wells located on the plume axis are evaluated and additional information possibly at hand (i.e. well data downgradient from the source but not on the center line) is not explicitly accounted for in the rate estimation. Therefore the performance of methods 1, 3 and 4 of Tab. 1 was

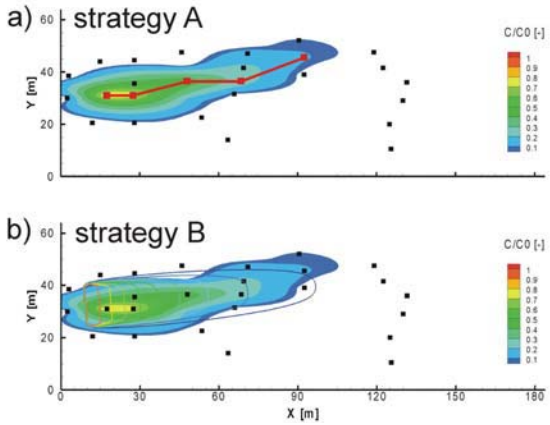

Fig. 10: Site investigation for degradation rate constant evaluation by (A) non-linearly positioned center line wells and (B) using all observation wells of the monitoring network (Beyer et al., 2007a [EP 5]). Small dark squares show observation well locations, larger squares show presumed center line well locations, contour lines are concentrations calculated analytically with the approach of Stenback et al. (2004).

studied for heterogeneous sites with extensive monitoring networks allowing the estimation of the degradation rate constant based on freely positioned observation wells from which a center line is constructed (strategy A, Fig. 10 (a)). Results are compared to a two-dimensional inverse modeling approach of Stenback et al. (2004), which accounts for information from all observation wells of a monitoring network (strategy B, Fig. 10 (b)). Both rate constant estimation strategies are applied to a set of synthetic contaminated sites with independently designed extensive monitoring networks (Beyer et al., 2007a [EP 5]).

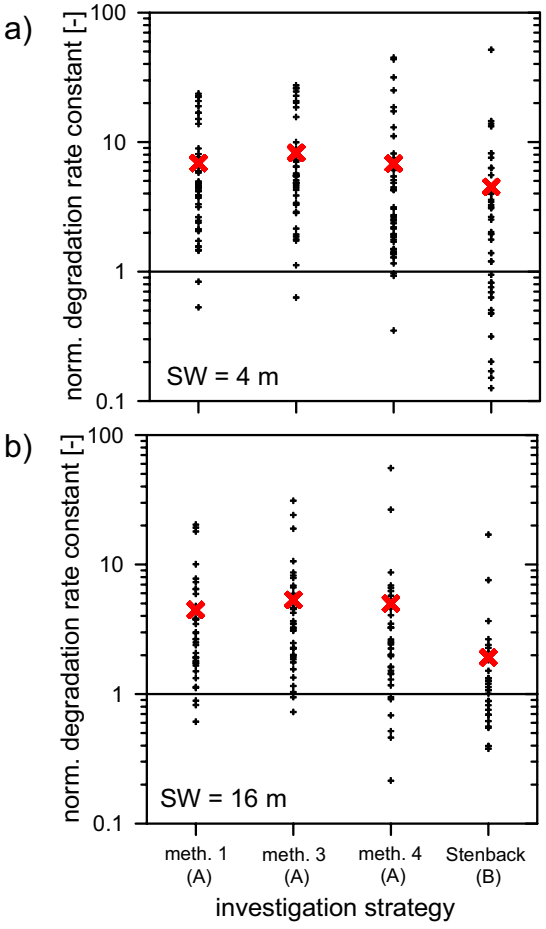

Fig. 11: Rate constant estimates obtained for investigation strategy A and methods 1, 3 and 4 as well as strategy (B) for a source width W_S of 4 (a) and 16 m (b) (Beyer et al., 2007a [EP 5]). Small symbols represent single realization results, large symbols ensemble averages.

Two different types of plumes are considered in this comparison: narrow contaminant plumes with a small source area width $W_S = 4$ m (Fig. 11 (a)) and wider plumes with $W_S = 16$ m (Fig. 11 (b)). For small source widths overestimation by strategy B is comparable to or at best slightly less than for approach A. For large source widths and wider plumes, however, strategy B yields closer estimates of the degradation rate constant than strategy A on average. The results of this study suggest that incorporation of off center line information for the estimation of the degradation rate constant can improve results of the plume investigation significantly.

3.2. Development and testing of a new approach to estimating biodegradation parameters from field data

In the previous section, the VA method was applied to evaluate the performance of different analytical models for the derivation of first order degradation rate constants from center line investigation data in heterogeneous aquifers. From the literature, however, it is well known that the use of first order kinetics may be problematic in some situations, as it is an inaccurate representation of the processes occurring in contaminated aquifers. Usage of a first order model outside its range of validity may result either in significant under- or overestimation of the attenuation potential at a site (Bekins et al., 1998). In an extension to this study, therefore a new approach for the estimation of degradation parameters k_{max} and M_C for Michaelis-Menten (MM) kinetics (eq. 22) from the same plume investigation strategy was developed and tested in Beyer et al. (2006 [EP 3]) using the VA method.

In its integral form eq. (22) can be rearranged to

$$\frac{\Delta x}{v_a\left(C_0 - C(x)\right)} = \frac{M_C}{k_{\max}} \frac{\ln\left(\frac{C_0}{C(x)}\right)}{C_0 - C(x)} + \frac{1}{k_{\max}} \quad (25).$$

With the same type of center line investigation data used for the estimation of the first order degradation rate constant (i.e. local concentrations, heads, hydraulic conductivities), eq. (25) can be utilized to estimate the MM parameters k_{max} and M_C by linear regression.

The Monte Carlo scenario definition and site investigation procedure for this study are similar to those explained in section 3.1. Numerical simulations of plume development in homogeneous and heterogeneous aquifers were performed with the GeoSys / Rockflow code. Here, however, the contaminant plumes investigated were generated using MM instead of first order degradation kinetics. The parameters k_{max} and M_C estimated with eq. (25) for the different plume realizations were normalized to the true values used in the numerical simulations and are shown in a 3D-scatterplot versus aquifer heterogeneity (Fig. 12).

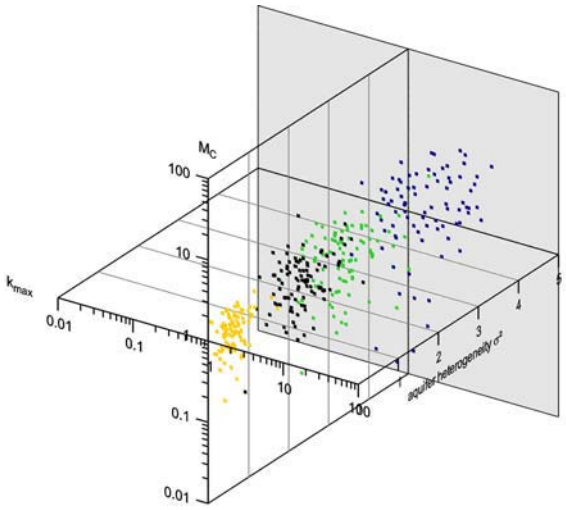

Fig. 12: Normalized Michaelis-Menten parameters (given as overestimation factors) versus aquifer heterogeneity.

In general an overestimation of both k_{max} and M_C is observed, which increases with heterogeneity. An overestimation of k_{max} increases the velocity of contaminant degradation as long as concentrations are much higher than M_C. The simultaneous overestimation of M_C counterbalances this effect because the concentration threshold is raised at which the kinetic begins to show a dependence on concentration and transits from zero to first order and hence decreases the rate of degradation.

To obtain an indicator for the significance of the estimated degradation potential, the MM parameters determined were used in an analytical transport model to estimate the contaminant plume lengths. These then were compared to the respective true plume lengths from the numerical simulations (Fig. 13 (a)). As a consequence of overestimating the degradation parameters, calculated plume lengths for high heterogeneities are estimated to about 75 % of the true length on average and thus are not conservative. For low heterogeneities, however, the suggested regression approach on average yields good estimates of the plume length and the degradation potential.

In addition to the effect of aquifer heterogeneity on estimated MM parameters and the resultant plume length estimates, also the effect of a wrong process identification (compare Fig. 5) is studied in Beyer et al. (2006 [EP 3]). Although it is well known that contaminant degradation in natural aquifers is governed by complex processes and kinetic laws, simple first order models are routinely used at many field sites. This study therefore highlights some of the problems that result from an insufficient wrong process identification. For this end investigation of the plumes following MM degradation kinetics is repeated, assuming the appropriateness of a first order rate law to approximate the contaminant degradation behaviour. Hence the methods of Tab. 1 were used to derive first order rate constants for the multiple plume realizations. As for the estimated MM parameters the estimated first order rate constants were evaluated by analytical transport models to yield estimates of the contaminant plume length. Results for method 1 (Tab. 1) are presented in Fig. 13 (b).

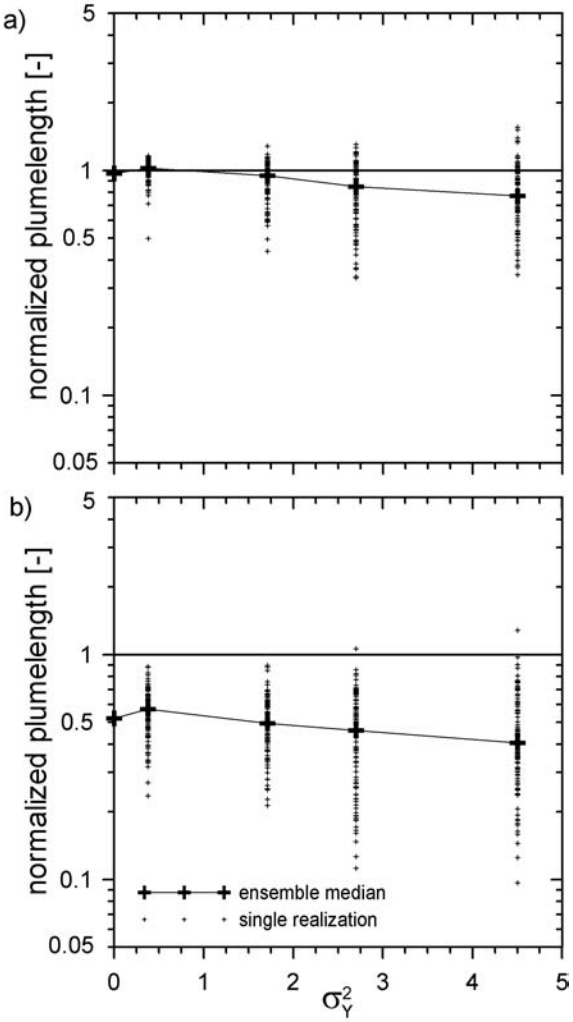

Fig. 13: Plume length overestimation factors versus aquifer heterogeneity (Beyer et al., 2006 [EP 3]). Plume lengths were estimated for plumes following Michaelis-Menten degradation kinetics estimated using the Michaelis-Menten model (a) and assuming validity of a first order rate law (b).

In comparison with Fig. 13 (a) an additional error is introduced which stems from the first order approximation. Uncertainty as well as bias increase significantly, as can be seen by the wider spread of single realization results around the ensemble medians. Estimated plume lengths here are found to be less than 40 % of the true length on average even for mildly heterogeneous aquifers. Plume lengths calculated using the MM parameters in general are significantly closer to the correct length compared to those obtained by a first order approximation. This approach is therefore recommended, if field data collected along the center line of a plume give evidence of MM type degradation kinetics.

3.3. Prognosis of long term contaminant leaching from recycling materials in road constructions

The third application of the numerical models and methods presented in section 2 is focussed on the prognosis of contaminant leaching and transport by seepage water from pollutant loaded recycling materials, which are used in earthworks or road constructions. According to the German federal soil protection decree (BBodSchV, 1999) such a prognosis is required for contaminated sites as well as for constructions or depositions of contaminated materials in order to assess the extent and environmental impact of potential contaminant leaching through the vadose zone to the groundwater. In such a prognosis, the relevant attenuation processes need to be considered and quantified, as significant contaminant attenuation could result in less restrictive utilization criteria without compromising the protection of groundwater resources. For this end, the application of process based numerical transport models is favorable, as complex geometries of the model scenarios and possible process interactions limit the applicability of analytical models or expertise founded “verbal-argumentative” assessments.

In this study, process based type scenario modeling is used as a tool to assess contaminant leaching from recycled demolition waste (DW) material. The type scenarios are based on three different case studies for the utilization of the DW, i.e. recycling as base and subbase layers of a parking lot, a noise protection dam and a road dam (Fig. 14) (Beyer et al., 2007b [EP 6]). Instead of regarding the full spectrum of contaminants typically embodied in DW three model substances are considered in the type scenarios: a conservative tracer

as a representative for highly soluble salts, naphthalene for moderately sorbing and phenanthrene for strongly sorbing organic compounds. Contaminant leaching from the DW to the groundwater surface is studied with six different characteristic subsoil units of Germany (BGR, 2006) to be able to compare the influence of hydraulic and basic physico-chemical soil properties on contaminant attenuation. Fig. 14 presents the conceptual model for the road dam. Here coarse grained DW is used as unbound base / subbase layers below the asphalt surface of the road. According to German road construction regulations, the base / subbase layers are covered by low and high permeable soil layers along the embankment (Fig. 14).

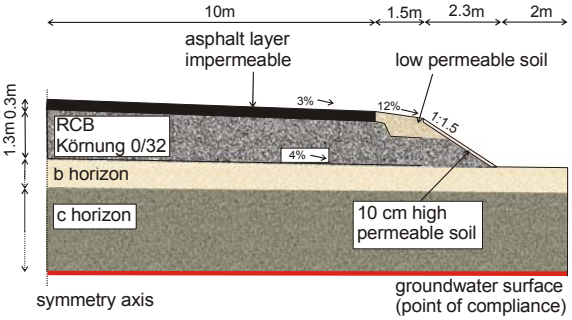

Fig. 14: Road construction with demolition waste recycled in base / subbase layers (Beyer et al., 2007b [EP 6]).

The simulation strategy for this study combines the Eulerian and Lagrangian frameworks of transport modeling. Unsaturated flow, i.e. the hydraulics of the constructions, is modeled with GeoSys / Rockflow using standard FEM. Fig. 15 shows that the two-dimensional scenarios exhibit complex flow patterns under unsaturated conditions. The velocity vectors at the element nodes of the FEM mesh for the road dam presented in Fig. 15 indicate unhindered infiltration of water from the low permeable soil on top of the embankment into the DW material. Along the sloped material boundary with high permeable soil on top of the coarse DW, however, strong capillary barrier effects are observed. These cause a concentration of the water flux on top of the DW and generation of lateral runoff, almost completely bypassing the DW.

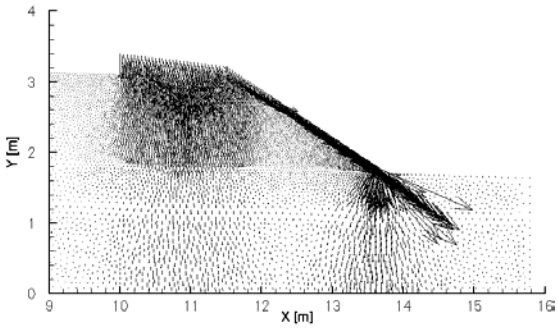

Fig. 15: Element nodes and velocity vectors of unsaturated water flow in a section of the model domain (Beyer et al., 2007b [EP 6]).

Reactive transport of the model compounds is simulated using the stream tube concept of the SMART code, to take full advantage of the reactive process models implemented in SMART (degradation, intraparticle diffusion kinetics, sorption, etc.). Coupling between GeoSys / Rockflow and SMART is achieved through the travel time pdf. These are generated by simulation of conservative tracer breakthrough curves by GeoSys / Rockflow using the FEM. The pdf are used as input for the reactive transport simulations with SMART. The model output of SMART for the three model substances at the groundwater surface represents concentrations integrated along the cross-section of the contaminant transport path only. These breakthrough curves for the tracer in the road dam are displayed in Fig. 16 as grey curves. The three black curves represent the same tracer breakthrough concentrations but are integrated along the groundwater surface of the overall model domain. Hence, they account for dilution by uncontaminated seepage water which bypasses the actual transport path due to the capillary barrier.

Breakthrough curves in relative concentrations C/C_0 [-] are given here for three of the six soils regarded in this study, i.e. for a cambisol, a podzol and a chernozem. Comparing the concentration breakthrough for the transport path (grey curves), it is found that the earliest breakthrough time for the

concentration maximum is for the cambisol, followed by the podzol and the chernozem. In general, however, breakthrough times are very similar for the three soils. Also the maximum concentrations observed are of comparable magnitude. As the tracer is conservative, concentration reductions of about 70 % can be attributed to the dispersion process. Integration of breakthrough concentrations along the overall lower model boundary (black curves) yields a further reduction of concentrations, as about 30 % of the infiltration bypasses the contaminant transport path.

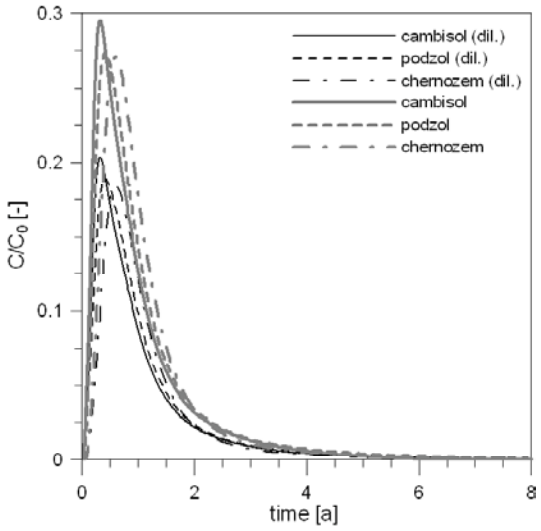

Fig. 16: Tracer breakthrough curves at the groundwater surface below the road dam for three different subsoil types (Beyer et al., 2007b [EP 6]).

For naphthalene and phenanthrene, contaminant transport is regarded with and without degradation. For the cases with degradation, a simple first order kinetics is used. Sorption of both compounds is modeled by a linear isotherm, where the equilibrium sorption coefficient is derived from the soil organic carbon content and the distribution coefficient between organic carbon and the aqueous phase (Beyer et al., 2007b [EP 6]). Sorption kinetics are quantified using the intraparticle diffusion model (eq. 18). Concentration breakthroughs are presented in Fig. 17. For the moderately sorbing naphthalene without decay the influence of soil organic carbon C_{org} is clearly visible. The cambisol, which is almost free of C_{org} (0.01 %), shows the earliest breakthrough of the three soils. For the podzol with a little higher C_{org} (0.21 %), the maximum concentration breakthrough is slightly retarded. The latest breakthrough time is observed for the chernozem, which is the soil with the highest C_{org} (0.88 %) regarded here. For the strongly sorbing phenanthrene this behaviour is even more characteristic. For the chernozem, the maximum concentration breakthrough is not yet observed within 275 a of simulated contaminant leaching. In contrast to the tracer, for which source concentrations are depleted within a few years, retardation within the DW causes naphthalene and phenanthrene leachate concentrations to stay on an almost unreduced level throughout the simulation period of 275 a (Beyer et al., 2007b [EP 6]). As high contaminant concentrations are constantly delivered from the source material, dispersive concentration reductions remain ineffective. Hence for the transport path maximum concentration breakthrough between 70 and 90 % of C_0 is observed. As for the tracer, these are reduced by about 30 % when integrated along the overall lower model boundary.

In comparison to the other type scenarios (parking lot, noise protection dam) studied in Beyer et al. (2007b [EP 6]), the contaminant residence times in the road dam are rather short, as high amounts of runoff water from the road asphalt which infiltrate along the embankment result in comparably high flow velocities. The short residence times reduce the effectiveness of degradation. Hence, naphthalene and phenanthrene concentrations are reduced by factors between 2.5 and 5, respectively, while for the other two type scenarios concentration reductions by factors between 10 and 150 were observed. From this type scenario modeling study the relevant transport and attenuation processes for contaminant leachate from DW used in road constructions could be identified and quantified for the assumed model structure.

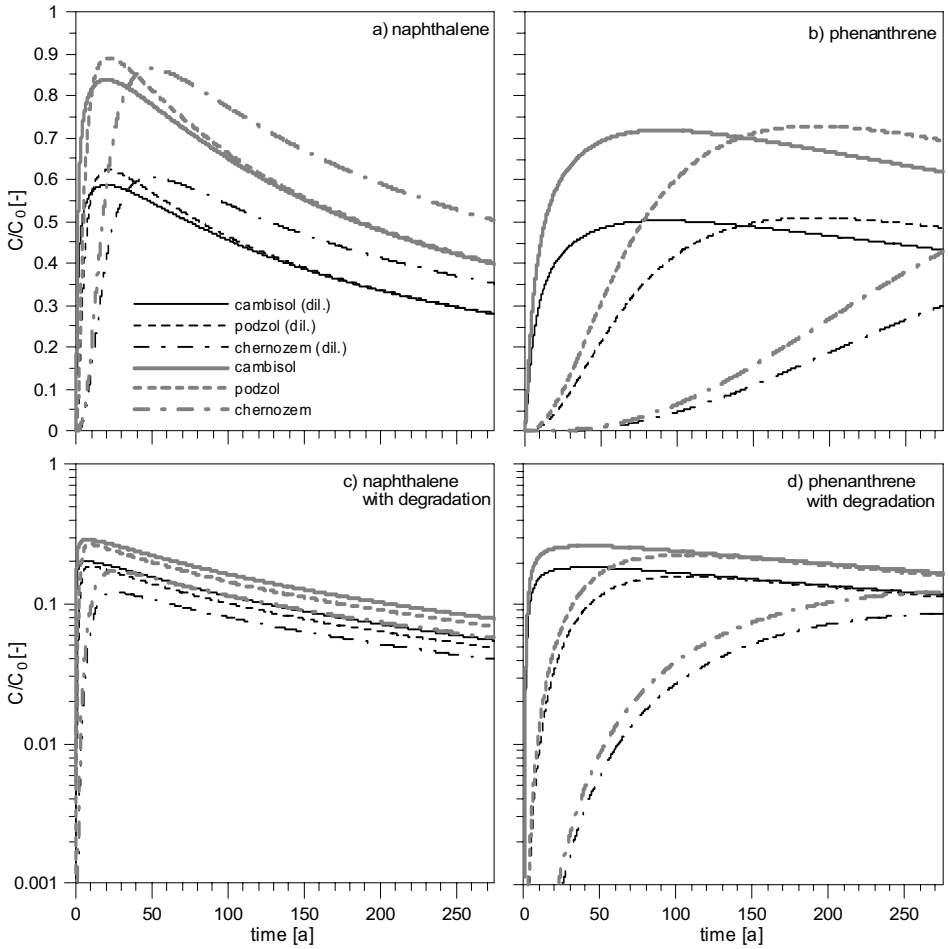

Fig. 17: Concentration breakthrough curves at the groundwater surface below the road dam for three different subsoil types showing naphthalene without (a) and with degradation (c), and phenanthrene without (b) and with degradation (d) (Beyer et al., 2007b [EP 6]).

The results allow important conclusions on mechanisms (e.g. capillary barrier effects) and complementary design criteria for road constructions, which can be used to reduce contaminant leaching to groundwater.

4. Conclusions and outlook

In this thesis, the utilization of process based numerical models of saturated / unsaturated flow and reactive contaminant transport is demonstrated for two different fields of application.

The Virtual Aquifer (VA) concept is introduced, which uses numerical modeling as a tool for the computer based evaluation of investigation and remediation strategies for contaminated soils and aquifers. In the application examples presented, the VA concept proves its usefulness for assessing the uncertainty involved in the investigation of heterogeneous sites and the parameterization of degradation process models. Moreover, the VA concept is successfully applied to test a newly developed approach for the inference of biodegradation parameters from data typically collected during site investigation. Both applications exemplify the importance but also the pitfalls of a careful and accurate collection of investigation data, if these are to be used for prognosis of the contaminant behaviour at a site. The main advantage of the VA is, that individual factors, such as hydraulic heterogeneity or conceptual model errors can be studied in detail at low costs and without high effort, either individually or in combination and under otherwise ideal and controlled conditions. As the sum of these

possibilities can not be provided neither by large scale field experiments nor in the laboratory, the VA concept can be considered a valuable contribution complementing state of the art experimental methods. Future applications of the VA concept will incorporate more realistic degradation kinetics and structures of aquifer heterogeneity, in order to study the influence of flow and transport channelling on the effectiveness of natural contaminant attenuation processes.

In the second field of interest regarded here, numerical models are applied for an assessment of environmental impact of recycling materials used in road constructions. In this study, the reactive streamtube model SMART is used for the first time in combination with the finite element model GeoSys / Rockflow to simulate the extent of contaminant leaching from contaminated demolition waste within road structures to the groundwater surface. The coupling between GeoSys / Rockflow and SMART combines the Eulerian and Langrangian frameworks of flow and transport. In so doing, the complex hydraulic behaviour of the two-dimensional model geometries are successfully modeled by travel time probability density functions, which allows to take full advantage of the process models implemented in the SMART code. For the assessment of contaminant leaching consequences on groundwater recharge quality, type scenario modeling is used. The relevant transport and attenuation processes in road constructions are identified. The study allows important conclusions on how these mechanisms could be used or enhanced to further reduce contaminant leaching to groundwater. As an example, hydraulic processes like capillary barrier formation from layered composition of granular base / subbase materials in a road dam could be exploited to reduce water fluxes through contaminant loaded recycling materials. This study demonstrates that process based numerical models can provide valuable tools for optimizing design and construction with regard to both functionality and environmental impacts.

In as much as the application of numerical models provides preeminent and cost effective means of assessment and prognosis, their value and credibility relies on a thorough collection and preparation of the required parameters and input data. Only if utmost care is taken in the stage of setting up the model, reliable results can be expected. As the data and parameter acquisition is of fundamental importance to a successful modeling of hydrogeosystems - be it by direct measurements in laboratory and field experiments, research in literature and databases or utilization of expert knowledge - both processes are closely related and therefore should, if possible, go hand in hand.

References

Altfelder, S., Streck, T. (2006): Capability and limitations of first-order and diffusion approaches to describe long-term sorption of chlortoluron in soil. J. Contam. Hydrol., 86, 279-298, 10.1016/j.jconhyd.2006.04.002.

Anderson, M., Woesner, W. (1992): Applied groundwater modeling. Simulation of flow and advective transport. Academic Press, New York, 381 p.

Baker, A.J. (1983): Finite Element Computational Fluid Mechanics McGraw-Hill Publ., / Hemisphere, New York, 1983, 544 p.

Ball, W.P., Roberts, P.V. (1991): Long-term sorption of halogenated organic chemicals by aquifer material: 2. Intraparticle diffusion. Environ. Sci. Technol. 25, 1237–1249, 10.1021/es00019a003.

Bauer, S., Kolditz, O. (2006): Assessing contaminant mass flow rates by the integral groundwater investigation method by using the virtual aquifer approach. In: Bierkens, M.F.P., Gehrels, J.C., Kovar, K. (eds.), Calibration and Reliability in Groundwater Modelling: From Uncertainty to Decision Making. Proceedings of ModelCARE'2005, The Hague, The Netherlands, June 2005. IAHS Publ. 304, 123–129.

Bauer, S., Beyer, C., Kolditz, O. (2005): Assessing measurements of first order degradation rates by using the virtual aquifer approach. In: Thomson, N.R. (ed.), GQ2004, Bringing Groundwater Quality Research to the Watershed Scale. Proceedings of a Symposium held at Waterloo, Canada, July 2004. IAHS Publ. 297, 274–281.

Bauer, S., Beyer, C., Kolditz, O. (2006a): Assessing measurement uncertainty of first-order degradation rates in heterogeneous aquifers. Water Resour. Res., 42, W01420, 10.1029/2004WR003878.

Bauer, S., Beyer, C., Kolditz, O. (2007): Einfluss von Heterogenität und Messfehler auf die Bestimmung von Abbauraten erster Ordnung - eine Virtueller Aquifer Szenarioanalyse. (Influence of heterogeneity and measurement error on the determination of first order degradation rates by us1ing the virtual aquifer approach.), Grundwasser, 12, 3–14, 10.1007/s00767-007-0019-8

Bauer, S., Beyer, C., Chen, C., Gronewold, J., Kolditz, O., (2006b): Virtueller Aquifer (VA) - Computergestützte Bewertung von Erkundungs-, Sanierungs- und Monitoringstrategien im Hinblick auf das "Natural Attenuation" (NA) und "Enhanced Natural Attenuation" (ENA) - Potenzial kontaminierter Böden und Grundwässer. Statusseminar des KORA-TV 7, 8.6.2006, Dresden. Gemeinsame Mitteilungen des DGFZ e.V. und seiner Partner, 3/2006, Dresden, 93-113.

Baveye, P., Valocchi, A. (1989): An evaluation of mathematical models of the transport of biologically reacting solutes in saturated soils and aquifers. Water Resour. Res., 25, 1413–1421, 10.1029/89WR00367.

Bear, J. (1972): Dynamics of Fluids in Porous Media. American Elsevier Publishing Co., New York, 761 p.

Bear, J. (1979) Hydraulics of Groundwater. McGraw-Hill Book Co., London 567 p.

Bear, J., Bachmat, Y. (1990): Introduction to Modeling of Transport Phenomena in Porous Media. Kluwer Academic Publ., 554 p.

BBodSchV (1999): Bundes-Bodenschutz- und Altlastenverordnung vom 16. Juli 1999. Bundesgesetzblatt Jahrgang 1999, Teil I Nr. 36, 1554-1682.

Bekins, B.A., Warren, E., Godsy, E.M. (1998): A comparison of zero-order, first-order, and Monod biotransformation models. Ground Water, 36, 261-268.

Beyer, C., Bauer, S., Kolditz, O. (2006): Uncertainty Assessment of Contaminant Plume Length Estimates in Heterogeneous Aquifers. J. Contam. Hydrol., 87, 73-95, 10.1016/j.jconhyd.2006.04.006.

Beyer, C., Chen, C., Gronewold, J., Kolditz, O., Bauer, S. (2007a): Determination of first order degradation rate constants from monitoring networks. (accepted by Ground Water.).

Beyer, C., Konrad, W., Park, C.H., Bauer, S., Rügner, H., Liedl, R., Grathwohl, P. (2007b): Modellbasierte Sickerwasserprognose für die Verwertung von Recycling-Baustoff in

technischen Bauwerken. (Model based prognosis of contaminant leaching for reuse of demolition waste in construction projects.) (accepted by Grundwasser and published online via SpringerLink), 10.1007/s00767-007-0025-x.

BGR (Bundesanstalt für Geowissenschaften und Rohstoffe) (2006): Nutzungsdifferenzierte Bodenübersichtskarte der Bundesrepublik Deutschland 1:1.000.000 (BÜK 1000 N2.3). Auszugskarten Acker, Grünland, Wald; Digit. Archiv FISBo BGR; Hannover und Berlin.

Bitterlich, S., Durner, W., Iden, S.C., Knabner, P. (2004): Inverse Estimation of the Unsaturated Soil Hydraulic Properties from Column Outflow Experiments Using Free-Form Parameterizations, Vadose Zone J., 3, 971-981.

Brooks, R.H., Corey, A.T. (1966): Properties of porous media affecting fluid flow. Proc. Amer. Soc. Civ. Eng., 92 [IR2], 61–87.

Brusseau, M.L., Rao, P.S.C. (1989): Sorption nonideality during organic contaminant transport in porous media. Crit. Rev. Environ. Control, 19, 33–99.

Buscheck, T.E., Alcantar, C.M. (1995): Regression techniques and analytical solutions to demonstrate intrinsic bioremediation. In Hinchee, R.E., Wilson, T.J., Downey, D. (Eds.), Intrinsic Bioremediation. Battelle Press, Columbus, OH, 109-116.

Carrayrou, J., Mosé, R., Behra, P. (2004): Operator-splitting procedures for reactive transport and comparison of mass balance errors. J. Contam. Hydrol., 68: 239-268, 10.1016/S0169-7722(03)00141-4.

Celia, M., Russel, T., Herrera, I. Ewing, R. (1990): An Eulerian-Lagrangian localized adjoint method for the advection-diffusion equation. Adv. Water Resour., 13, 187-206, 10.1016/0309-1708(90)90041-2

Cvetkovic, V., Dagan, G. (1996): Reactive transport and immiscible flow in geological media. 2 Applications.- Proc. Royal Soc. London A, 452, 303-328.

Dagan, G. (1989): Flow and Transport in Porous Formations. Springer, Heidelberg. 465 p.

Du, Y., Wang, W. Kolditz, O. (2005): Benchmarking of Richards Model. GeoSys – Preprint [2005-12], GeoSystemsResearch, Center for Applied Geosciences, University of Tübingen.

Durner, W. (1994): Hydraulic conductivity estimation for soils with heterogeneous pore structure, Water Resour. Res., 30, 211-223, 10.1029/93WR02676.

Durner, W., Flühler, H. (2005): Chapter 74: Soil Hydraulic Properties, in: Anderson M.G. and J. J. McDonnell (eds.), Encyclopedia of Hydrological Sciences, John Wiley & Sons, Ltd., Chapter 74, 1103-1120,

Fetter, C.W. (1993): Contaminant Hydrogeology, Prentice Hall, New Jersey, 500 p.

Finkel, M., Liedl, R., Teutsch, G. (1998): Modelling surfactant-enhanced remediation of polycyclic aromatic hydrocarbons. J. Environ. Modelling & Software, 14, 203-211. 10.1016/S1364-8152(98)00071-1.

Freeze, R.A., Cherry, J.A. (1979): Groundwater. Prentice Hall, Englewood Cliffs, New Jersey, 604 p.

Grathwohl, P. (1998): Diffusion in Natural Porous Media: Contaminant Transport, Sorption/Desorption and Dissolution Kinetics. Kluwer Academic Publishers, 224 p.

Haverkamp, R., Vaclin, M., Touma, J., Wierenga, P.J., Vachaud, G. (1977): A comparison of numerical simulation models for one-dimensional infiltration. Soil Sci. Soc. Am. J., 41, 285-294.

Helmig, R. (1997): Multiphase Flow and Transport Processes in the Subsurface: A Contribution to the Modeling of Hydrosystems. Springer, Berlin, Heidelberg, 255 p.

Huyakorn, P.S., Pinder, G.F. (1983): Computational Methods in Subsurface Flow. Academic Press, New York, 473 p.

Islam, J., Naresh, S., O'Sullivan, M., (2001): Modeling biogeochemical processes in leachate-contaminated soils: A review. Transp. Porous Media, 43, 407-440, 10.1023/A:1010737825232.

Jäger, R., Liedl, R. (2000): Prognose der Sorptionskinetik organischer Schadstoffe in heterogenem Aquifermaterial. Grundwasser, 2, 57-66.

Jury, W.A., Gardner, W.R., Gardner, W.H. (1991): Soil Physics. John Wiley & Sons, New York, 328 p.

Kinzelbach, W. (1983): Analytische Lösungen der Schadstofftransportgleichung und ihre Anwendung auf Schadensfälle mit flüchtigen Chlorkohlenwasserstoffen. In: Methoden zur rechnerischen

Erfassung und hydraulischen Sanierung von Grundwasserkontaminationen, Mitteilungen des Instituts für Wasserbau, Universität Stuttgart, Heft 54, 115-199.

Kinzelbach, W., Schäfer, W., Herzer, J. (1991): Numerical modeling of natural and enhanced denitrification processes in aquifers. Water Resour. Res., 27, 1123-1136, 10.1029/91WR00474.

Knabner, P., Schneid, E. (2002): Adaptive Hybrid Mixed Finite Element Discretization of Instationary Variably Saturated Flow in Porous Media. In: Breuer, M.,. et al., (eds.), High Performance Scientific and Engineering Computing, Springer Verlag, Berlin, 37-44.

Korsawe, J., Starke, G., Wang, W., Kolditz, O. (2006): Finite Element Analysis of Poro-Elastic Consolidation in Porous Media: Standard and Mixed Approaches. Comput. Methods Appl. Mech. Engrg., 195, 1096-1115, 10.1016/j.cma.2005.04.011

Kolditz, O. (2002): Computational methods in environmental fluid dynamics. Springer, Heidelberg, 400 p.

Kolditz, O., Bauer, S. (2004): A process-oriented approach to computing multi-field problems in porous media. J. Hydroinf., 6, 225-244.

Kolditz, O., Xie, M., Kalbacher, T., Bauer, S., Wang, W., McDermott, C., Chen, C., Beyer, C., Gronewold, J., Kemmler, D., Walsh, R., Du, Y., Park, C.H., Hess, M., Amanidis, P. (2006): GeoSys/Rockflow version 4.4.03 - Theory and users manual, Center for Applied Geoscience, University of Tübingen.

Ma, L., Selim, H.M. (1994): Predicting atrazine adsorption–desorption in soils: a modified second-order kinetic model. Water Resour. Res., 30, 447–456. 10.1029/93WR02478

Morris, B., Lawrence, A., Chilton, P., Adams, B., Calow, R., Klinck, B. (2003): Groundwater and its susceptibility to degradation: a global assessment of the problem and options for management. Nairobi: United Nations Environmental Programme, 140 p.

Mualem, Y. (1976): A New model for predicting the hydraulic conductivity of unsaturated porous media, Water Resour. Res., 12, 513 - 522.

Neuman, S. (1981): An Eulerian-Lagrangian numerical scheme for the dispersion convection equation using conjugate space time grids, J. Comput. Phys. 41, 270-285.

Newell, C.J., Rifai, H.S., Wilson, J.T., Connor, J.A., Aziz, J.A., Suarez, M.P. (2002): Calculation and use of first-order rate constants for monitored natural attenuation studies. U.S. EPA Ground Water Issue, U.S. EPA/540/S-02/500.

Olsen, S.R., Kemper, W.D. (1968): Movement of nutrients to plant roots. Adv. Agronomy, 30, 91-151.

Park, C.H., Beyer, C., Bauer, S., Kolditz, O. (2006): An effcient method of random walk particle tracking: accuracy and resolution. (submitted to Adv. Water Resour.)

Pinder, G.F., Gray, W.G. (1977): Finite element simulation in surface and subsurface hydrology. Academic Press, New York, 295 p.

Rittmann, B., VanBriesen, J.M. (1996): Microbiological processes in reactive modeling. In: Lichtner, P., Steefel, C., Oelkers, E. (eds.), Reactive Transport in Porous Media. Reviews in Mineralogy, 34, Mineralogical Society of America, Washington, DC, 311-334.

Rügner, H., Kleineidam, S., Grathwohl, P. (1999): Long term sorption kinetics of phenanthrene in aquifer materials. Environ. Sci. Technol., 33, 1645–1651, 10.1021/es980664x

Rubin, Y. (1983): Transport of reacting solutes in porous media: Relationship between mathematical nature of problem formulation and chemical nature of reactions. Water Res. Resour., 19, 1231-1252.

Schäfer, D., Schäfer, W., Kinzelbach, W. (1998): Simulation of Reactive Processes Related to Biodegradation in Aquifers. 1. Structure of the 3D Reactive Transport Model, J. Contam. Hydrol., 31, 167-186, 10.1016/S0169-7722(97)00060-0

Schäfer, D., Schlenz, B. Dahmke, A. (2004): Evaluation of exploration and monitoring methods for verification of natural attenuation using the virtual aquifer approach. Biodegradation, 15, 453-465, 10.1023/B:BIOD.0000044600.81216.00.

Schäfer, D., Schlenz, B., Dahmke A. (2006a): Virtuelle Aquifere – ein Werkzeug zur Simulation von Natural Attenuation und zur Bewertung von Monitoringstrategien. Statusseminar des KORA-TV 7, 8.6.2006, Dresden. Gemeinsame Mitteilungen des DGFZ e.V. und seiner Partner, 3/2006, Dresden, 115-139.

Schäfer, D., Dahmke, A., Kolditz, O., Teutsch, G. (2002): "Virtual Aquifers": A concept for evaluation of exploration, remediation and monitoring strategies. In: Kovar, K., Hrkal, Z. (eds.), Calibration and Reliability in Groundwater Modelling: A Few Steps Closer to Reality. Proceedings of the ModelCARE 2002 Conference, Prague, Czech Republic, June 2002. IAHS Publication 277, 52-59.

Schäfer, D., Hornbruch, G. Schlenz, B., Dahmke A. (2006b): Schadstoffausbreitung unter Annahme verschiedener kinetischer Ansätze zur Modellierung mikrobiellen Abbaus. Grundwasser (in print).

Scheidleder, A., Grath, J., Winkler, G., Stärk., U, Koreimann., C, Gmeiner, C., Nixon, S., Casillas, J., Gravesen, P., Leonard, J., Elvira, M. (1999): Groundwater quality and quantity in Europe. European Environment Agency, Copenhagen, 123 p.

Simkins, S., Alexander, M. (1984): Models for mineralization kinetics with variables of substrate concentration and population density. Appl. Envir. Microbiol., 47, 1299-1306.

Starke, G. (2000): Least-squares mixed finite element solution of variably saturated subsurface flow problems. SIAM J. Sci. Comput. 21, 1869-1885, 10.1137/S1064827598339384

Stenback, G.A., Ong, S.K., Rogers, S.W., Kjartanson, B.H. (2004): Impact of transverse and longitudinal dispersion on first-order degradation rate constant estimation. J. Contam. Hydrol., 73, 3-14, 10.1016/j.jconhyd.2003.11.004.

Streck, T., Poletika, N.N., Jury, W.A. Farmer, W.J. (1995): Description of simazine transport with rate-limited, two-stage linear and nonlinear sorption. Water Resour. Res., 31, 811-822, 10.1029/94WR02822

Thorenz, C. (1999): Model Adaptive Simulation of Multiphase and Density Driven Flow in Fractured and Porous Media. Dissertation, Institut für Strömungsmechanik, Universität Hannover, Bericht Nr. 62/2001.

Van Genuchten, M.T. (1980): A closed form equation for predicting the hydraulic conductivity of unsaturated soils. Soil Sci. Soc. Am. J., 44, 892-898.

Van Genuchten, M.T., Alves, W.J. (1982): Analytical solutions of the one-dimensional convective dispersive solute transport equation. USDA ARS Technical Bulletin Number 1661. U.S. Salinity Laboratory, 4500 Glenwood Drive, Riverside, CA 92501.

Wang, W., Datcheva, M., Schanz, T., Kolditz, O. (2006): A sub-stepping approach for elasto-plasticity with rotational hardening. Computational Mechanics. (in print). 10.1007/s00466-005-0710-5

Wiedemeier, T.H., Swanson, M.A., Wilson, J.T., Kampbell, D.H., Miller, R.N., Hansen, J.E. (1996): Approximation of biodegradation rate constants for monoaromatic hydrocarbons (BTEX) in ground water. Ground Water Monit. Remed., 16 (3),186-194.

Wiedemeier, T.H., Rifai, H.S., Newell, C.J., Wilson, J.T. (1999): Natural Attenuation of Fuels and Chlorinated Solvents in the Subsurface. John Wiley and Sons, New York, 632 p.

Wilson, R.D., Thornton, S.F., Mackay, D.M. (2004): Challenges in monitoring the natural attenuation of spatially variable plumes, Biodegradation, 15, 459-469, 10.1023/B:BIOD.0000044591.45542.a9

Xie, M., Bauer, S., Kolditz, O., Nowak, T., Shao, H. (2006): Numerical simulation of reactive processes in an experiment with partially saturated bentonite, J. Contam. Hydrol., 83, 122-147. 10.1016/j.jconhyd.2005.11.003

Zhang, Y.-K., Heathcote, R.C. (2003): An improved method for estimation of biodegradation rate with field data. Ground Water Monit. Remed., 23 (3), 112-116.

Zheng, C., Bennett, G.D., (1995): Applied Contaminant Transport Modeling: Theory and Practice. Van Nostrand Reinhold, New York, 440 p.

Zienkiewicz, O.C., Taylor, R. (1991): The Finite Element Method, Vol. 1, 2 (4th edition). McGraw-Hill, London, 459 p.

Enclosed publications

[EP 1] Bauer, S., **Beyer, C.,** Kolditz, O., (2005): Assessing measurements of first order degradation rates by using the Virtual Aquifer approach. In: Thomson, N.R. (Ed.), GQ2004, Bringing Groundwater Quality Research to the Watershed Scale. Proceedings of a Symposium held at Waterloo, Canada, July 2004. IAHS Publication 297, IAHS Press, Wallingford, 274-281.

[EP 2] Bauer, S., **Beyer, C.,** Kolditz, O. (2006a): Assessing measurement uncertainty of first-order degradation rates in heterogeneous aquifers. Water Resour. Res., 42, W01420, 10.1029/2004WR003878.

[EP 3] **Beyer, C.,** Bauer, S., Kolditz, O. (2006): Uncertainty assessment of contaminant plume length estimates in heterogeneous aquifers. J. Contam. Hydrol., 87, 73-95, 10.1016/j.jconhyd.2006.04.006.

[EP 4] Bauer, S., **Beyer, C.,** Kolditz, O. (2007): Einfluss von Heterogenität und Messfehler auf die Bestimmung von Abbauraten erster Ordnung - eine Virtueller Aquifer Szenarioanalyse. (Influence of heterogeneity and measurement error on the determination of first order degradation rates by us1ing the virtual aquifer approach.), Grundwasser, 12, 3–14, 10.1007/s00767-007-0019-8.

[EP 5] **Beyer, C.,** Chen, C., Gronewold, J., Kolditz, O., Bauer, S. (2007a): Determination of first order degradation rate constants from monitoring networks. (accepted by Ground Water.).

[EP 6] **Beyer, C.,** Konrad, W., Park, C.H., Bauer, S., Rügner, H., Liedl, R., Grathwohl, P. (2007b): Modellbasierte Sickerwasserprognose für die Verwertung von Recycling-Baustoff in technischen Bauwerken. (Model based prognosis of contaminant leaching for reuse of demolition waste in construction projects.) (accepted by Grundwasser and published online via SpringerLink), 10.1007/s00767-007-0025-x.

Enclosed Publication 1

Bauer, S., Beyer, C., Kolditz, O. (2005): Assessing measurements of first order degradation rates by using the Virtual Aquifer approach. In: Thomson, N.R. (Ed.), GQ2004, Bringing Groundwater Quality Research to the Watershed Scale. Waterloo, Canada, July 2004. IAHS Publication 297, IAHS Press, Wallingford, 274-281.

Bringing Groundwater Quality Research to the Watershed Scale (Proceedings of GQ2004, the 4th International Groundwater Quality Conference, held at Waterloo, Canada, July 2004). IAHS Publ. 297, 2005.

Assessing measurements of first-order degradation rates through the virtual aquifer approach

SEBASTIAN BAUER, CHRISTOF BEYER & OLAF KOLDITZ

Center for Applied Geoscience, University of Tübingen, Sigwartstrasse 10, D 72076 Tübingen, Germany

sebastian.bauer@uni-tuebingen.de

Abstract The principal idea behind the "virtual aquifer" is to simulate and evaluate investigation strategies for contaminated sites by modelling typical contamination scenarios. In this paper, first-order degradation rates using various methods were the focus of study. A virtual reality of a contaminated aquifer was generated by simulating the spreading of a plume, originating from a defined source zone, subject to first-order degradation. This plume was investigated through monitoring wells placed along the plume centre-line. Using information such as head measurements, concentration and hydraulic conductivity, first-order degradation rates were calculated and compared to the true predefined value. This comparison was conducted for varying degrees of heterogeneity, represented by $\ln(K_F)$, randomly distributed conductivity fields. It was found that when heterogeneity was increased, "measured" degradation rates overestimated the true degradation rate by several orders of magnitude. The range of degradation rates obtained roughly corresponds to the range stated in literature values.

Key words first-order degradation; modelling; natural attenuation; virtual reality

INTRODUCTION

At a real contaminated site, the true hydrogeological properties (e.g. conductivity, porosity, recharge rates, source position, degradation rates, etc.) are generally unknown (spatially). The basic idea behind the "virtual aquifer" is to produce a "virtual" contaminated site, where the spatial distribution of parameters is exactly known. By using a process-based flow and transport model, the fate of contaminants in the subsurface can be simulated, including plume development. The second step for creating a virtually contaminated site is to examine the virtual aquifer properties using standard investigative procedures (e.g. interpolating hydraulic head and contaminant concentrations measured at monitoring wells). The result of this virtual investigation can be compared to the true hydrogeological property distribution of the virtual aquifer because, contrary to an actual contaminated site, the exact distribution is known. The investigation techniques used can thus be tested and evaluated with respect to certain influences, i.e. sensitivity to aquifer heterogeneity or variation of other parameters. When the virtual plume is examined, only the data obtained by these investigation techniques are used, i.e. only the data that would also be measured at a real field site. Data such as hydraulic head and contaminant concentrations are "measured" in the virtual aquifer by "reading" the model output. The "virtual aquifer" approach offers the ability to test and evaluate site investigation techniques, which cannot be performed in the real world. In this paper, four methods for determining first-order degradation rate constants, all based on the plume centre-line method, are examined by the "Virtual Aquifer" approach.

METHODS

Virtual aquifers were produced by generating random fields of hydraulic conductivity for the model area (dimensions: 184 × 64 m, Fig. 1). Flow direction was from left to right, with a mean hydraulic gradient of 0.003. For this application, a mean hydraulic conductivity of 7.2×10^{-5} m s^{-1} was assumed, with $\ln(K_F)$ variances of 0.38, 1.71, 2.7 and 4.5; the variances were chosen to simulate different degrees of heterogeneity. An exponential variogram model, with an integral scale of 2.33 m, was used to describe spatial correlation. A virtual contaminant source zone of widths 4, 8 and 16 m was introduced into the aquifer, emitting a contaminant which was subject to a first-order degradation constant, λ, of 1 $year^{-1}$. A conservative tracer was also released. By using first order degradation kinetics for the reactive contaminant, the plume evolving corresponds to the methods used to estimate the first order degradation rate. This is certainly not true in reality, where the degradation of a contaminant follows changing and more complex kinetics. The plume was simulated using a process-based numerical flow and transport model, assuming longitudinal and transverse dispersivities of 0.25 and 0.05, respectively. Thus, the virtual contaminated aquifer was generated. In the second step, the plume's properties were examined using the centre-line approach. For this investigation, not the full data of the model is used but only the values which are obtained by the centreline approach. There were three initial observation wells; one was directly in the source zone, while the other two were outside of the source (Fig. 1). At these three wells, the hydraulic heads were measured by reading the model output. A hydrogeological triangle was constructed and the direction of groundwater flow was thus determined. Along the estimated direction of groundwater flow, new observation wells were installed at every 10 m. These wells were then used to measure (arrows in Fig. 1) hydraulic head, contaminant concentrations, tracer concentrations and local hydraulic conductivity. From the hydraulic head difference, the true porosity and the well positions the respective groundwater flow velocities are calculated. Together with the concentration data, this allows the determination of the degradation rate constant

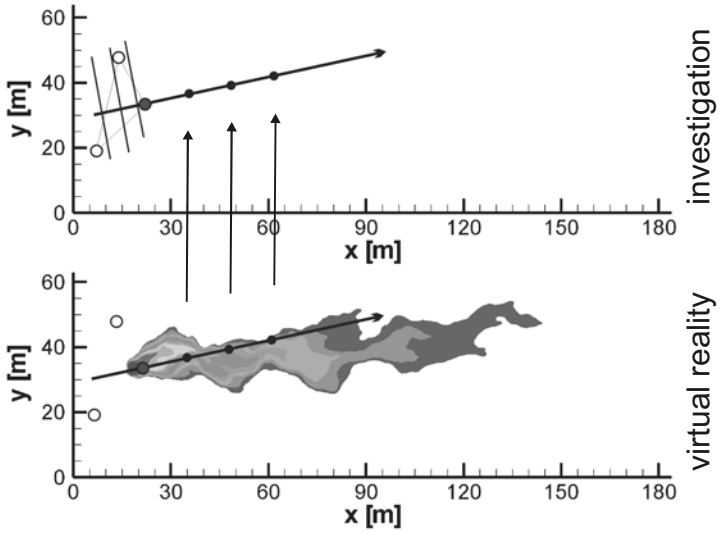

Fig. 1 Method used to obtain plume centreline concentrations. The upper graph depicts the investigation procedure and the lower graph is the virtual site.

Table 1 Methods used for calculating first-order rate constants λ. v_a is the transport velocity, Δx is the observation well distance, $C(x)$ is the downstream concentration and C_0 the source concentration, while α_L and α_T are the longitudinal and transverse dispersivities, W_S is the source width and *erf* is the error function.

Method	Formula for degradation rate	Description
1	$\lambda_1 = -\frac{v_a}{\Delta x}\ln\left(\frac{C(x)}{C_0}\right)$	Analytical solution to 0-D transport equation (batch reactor)
2	$\lambda_2 = -\frac{v_a}{\Delta x}\ln\left(\frac{C(x)}{C_0}\frac{C_0^*}{C(x)^*}\right)$	Concentration normalized to a non-degrading co-contaminant, thus accounting for dilution and dispersion
3	$\lambda_3 = \frac{v_a}{4\alpha_L}\left(1 - 2\alpha_L\frac{\ln(C(x)/C_0)}{\Delta x}\right)^2 - 1\right)$	Analytical solution to the 1-D transport equation. Accounts for longitudinal dispersion.
4	$\lambda_3 = \frac{v_a}{4\alpha_L}\left(1 - 2\alpha_L\frac{\ln(C(x)/(C_0\beta))}{\Delta x}\right)^2 - 1\right)$ with: $\beta = erf\left(\frac{W_S}{4\sqrt{\alpha_T\Delta x}}\right)$	Analytical solution to the 2-D transport equation. Accounts for longitudinal as well as transverse dispersion and a finite source width.

first-order degradation; modelling; natural attenuation; virtual reality. The setup is thus designed to resemble ideal conditions for the application of the four methods for estimating the degradation rate constant. The only uncertainty and variability is introduced by the aquifer heterogeneity. The data used for the centreline method is thus only the data which can be measured at the three initial and the three downstream wells. Thus neither the mean hydraulic conductivity nor the variance or correlation length is known.

The four centre-line methods used are provided in Table 1. Method 1 (Wiedemeier *et al.*, 1996) is the batch solution to a first-order degradation (i.e. no transport is included). Method 2 was proposed by Wilson *et al.* (1994) (see also Wiedemeier *et al.*, 1996) and is similar to Method 1, except amended concentrations are used. The measured concentrations for the reactive contaminant are corrected by using the ratio of the conservative co-contaminant at the observation well. This method corrects for dispersion and measurements taken outside of the plume centre-line at the three new observation wells. Method 3 was proposed by Buscheck & Alcantar (1995) and is based on the solution of a one-dimensional (1-D) transport equation with a first-order decay constant. This method accounts explicitly for longitudinal dispersion of the plume. To account for transverse dispersion (Method 4), Stenback *et al*. (2004) suggest using the analytical solution for a 2-D transport equation with first-order decay. In order to carry out Methods 3 and 4, it is required that the longitudinal and the transverse dispersivities be known. The following dispersivities were used according to Wiedemeier *et al.* (1999): 0.1 of the plume length for the longitudinal dispersivity, and 0.33 of longitudinal dispersivity for the transverse dispersivity. For each of the four approaches, first-order degradation rates were calculated and compared to the value used in generating the plume. For each degree of heterogeneity, 100 realizations were evaluated to obtain a statistical measure of the error introduced by the heterogeneity of

the hydraulic conductivity. For each realization, the procedures described above were followed and a degradation rate was calculated for each method, at each downstream well and for every source width.

RESULTS AND DISCUSSION

Figure 2 illustrates the results for the calculated first-order rate constants. Calculated rate constants were reported as normalized rate constants (i.e. the calculated rate constant was divided by the true rate constant used in the numerical simulation). The normalized rate constant can thus be interpreted as an overestimated factor or an underestimated factor. Inspection of Fig. 2 yields that most calculated rates are higher than one (i.e. the degradation rate is overestimated). This conclusion is quite concerning for single realizations, where overestimations can be of several orders of magnitude. On the left-hand side of Fig. 2(a), the variation of the calculated normalized rate with the source zone width is illustrated. It is clear that for Method 1, the calculated rates improve when the source zone width is increased; this is because Method 1 does not account for dilution, dispersion or measurements outside of the plume. These factors become less relevant with increasing source width since the basic assumptions inherent in Method 1 are better fulfilled, and the overestimation factor drops accordingly. On the right-hand side of Fig. 2(a), the dependence of the calculated rate on the degree of heterogeneity (given as variance) is shown. It is obvious that an increase of $\sigma^2\ln(K_F)$ leads to an overestimation of the calculated degradation rate. Furthermore, the standard deviation of the mean calculated degradation rate increases, leading to greater uncertainty in the calculated rate. For the smallest degree of heterogeneity the mean overestimation is a factor a bit smaller than 2, which increases to values between 3 and 5 for medium to high heterogeneity, and 10 for very high heterogeneity.

Figure 2(b) shows the results for Method 2. Degradation rates for this method were also overestimated. However, when comparing this method to Method 1, the over-estimation factor and standard deviation are generally smaller (i.e. both the error and the uncertainty are lower compared to Method 1). When examining the left-hand side of Fig. 2(b), the calculated rates show no dependence on source width. This effect is inherent to the method, since Method 2 accounts for dispersion, dilution and measurements taken outside of the plume. Method 3 depicts results similar to Method 1 regarding the rate dependence on source width and on the degree of heterogeneity (Fig. 2(c)). However, the normalized degradation rates for Method 3 are higher than for Method 1 (and also higher than Method 2); this is due to the dispersivity term. In comparison to Method 1, a portion of the concentration reduction from the source observation well to the downstream observation well is attributed to dispersion and corrected for, and thus a higher degradation rate is estimated. Method 4 (Fig. 2(d)) displays behaviour similar to Method 3, except that the rate values are slightly lower. Lower rate values are attributed to the additional term in the rate equation, which accounts for transverse dispersion. It should also be noted that at the lowest degree of heterogeneity, the normalized degradation rates were actually underestimated; this is due to an "over correction" of the effects for transverse dispersion. To effectively illustrate the over and underestimation of the degradation rates for all four methods, the degradation rates where calculated (for a homogeneous hydraulic conductivity) and

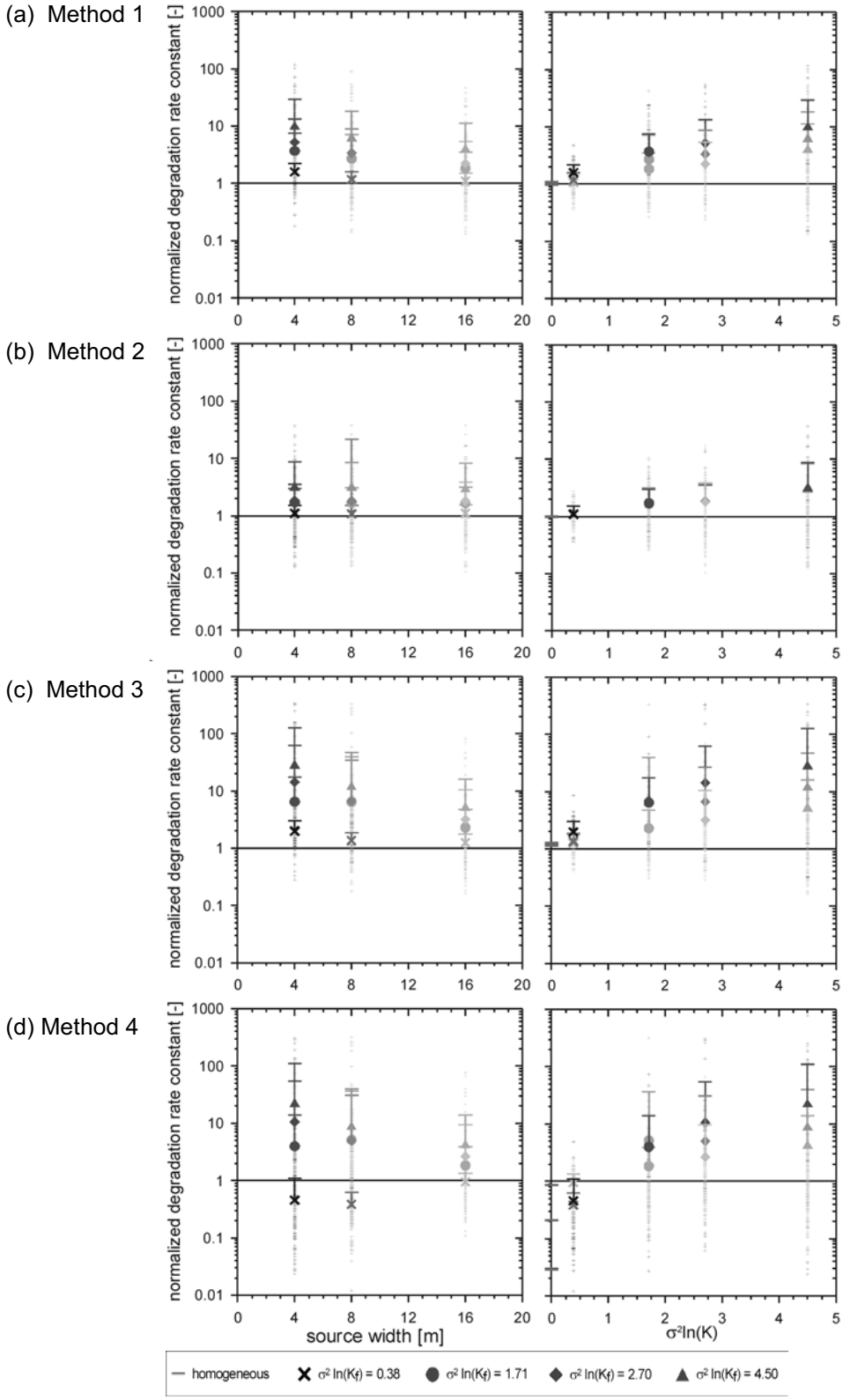

Fig. 2 "Measured" first-order degradation rate constants normalized to the true degradation rate constant *vs* source width (left) and degree of heterogeneity (right) for (a) Method 1, (b) Method 2, (c) Method 3 and (d) Method 4. All figures show results for all observations (small symbols) as well as their mean value (large symbols) and the corresponding standard deviations (error bars).

plotted as small horizontal bars for $\sigma^2\ln(K_F)$ of 0 on the right-hand side graphs of Fig. 2. It is obvious that for Method 1 and Method 2, the normalized degradation rate is exactly 1 for the homogeneous case (i.e. these methods yield the correct result). Method 3 shows a slight overestimation, while Method 4 yields very small, normalized degradation rates. The smallest rate, from Method 4, was obtained for the smallest source width, as then the correction is largest (compare Method 4 in Table 1). For large source widths, the argument of the error function of method 4 approaches 1.

As mean and standard deviations are true for the ensemble mean, but not for single observations, an alternative method was chosen for comparing the four methods. The four methods were contrasted by plotting the probability of success against the error factor; the results are illustrated in Fig. 3. An error factor of 10 corresponds to an interval of 0.1 to 10 for normalized degradation rates, i.e. the interval that is obtained by multiplying 1 with the error factor and dividing 1 by the error factor ("within one order of magnitude"). An error factor of 5 thus corresponds to an interval of 0.2 to 5. These plots illustrate the probability that the measured degradation rate is within the interval of the corresponding error factor. Figure 3(a) represents the lowest degree of heterogeneity and shows that the probability of calculating the degradation rate with an error factor of less than 2 (i.e. "within a factor of 2") is about 0.7 for Method 1, 0.9 for Method 2, 0.55 for Method 3 and 0.3 for Method 4. When increasing the error factor

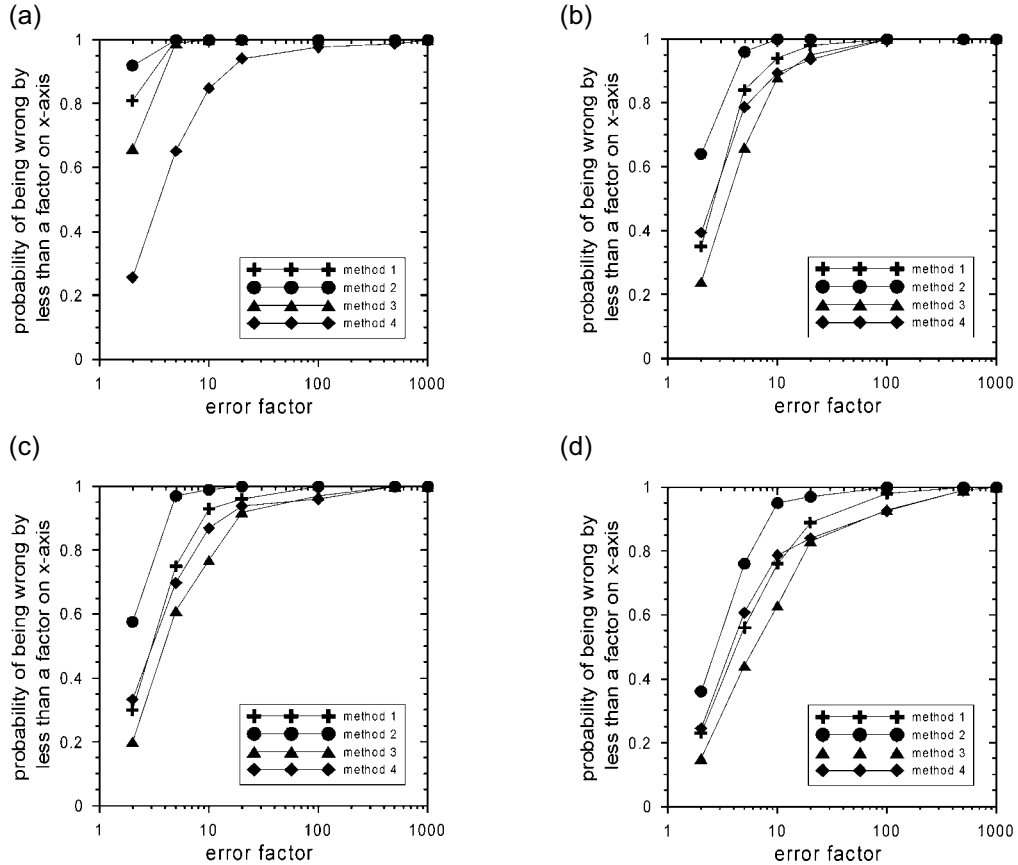

Fig. 3 Probability plots for all methods for $\sigma^2\ln(K_F)$ of: (a) 0.38, (b) 1.71, (c) 2.7 and (d) 4.5, resembling the four degrees of heterogeneity, shown for a source width of 4 m. The probability of method success is plotted against the error factor.

to 5, Methods 1, 2 and 3 show a success probability of about 1, while Method 4 yields a probability of 0.7. Figure 3 also illustrates that all methods exhibit a decreasing probability of success when the degree of heterogeneity is increased. An error factor of 5 yields a success probability of about 1 for the lowest degree of heterogeneity (0.38) for Method 1; this probability decreases to 0.7, 0.5 and 0.35 for a $\sigma^2\ln(K_F)$ of 1.71, 2.7 and 4.5, respectively. For Method 2 the corresponding success probabilities are 1.0, 0.9, 0.8 and 0.6; Method 3 yields values of 1.0, 0.55, 0.35 and 0.25; and Method 4 0.7, 0.7, 0.6 and 0.4.

To achieve the degradation rate within a factor of 10 of the correct degradation rate (for high hydraulic heterogeneity, Fig. 3(c)), the success probabilities were found to be 0.8, 0.95, 0.8 and 0.6 for Methods 1 through 4, respectively. For all degrees of heterogeneity, Method 2 yielded the highest probability for achieving the correct degradation rate. For medium to very high heterogeneity, Method 4 was second best, and was the worst for aquifers that were only slightly heterogeneous (Fig. 3(a)). Method 1, although the simplest method, yielded similar probabilities as Method 4, except Method 1 works well for aquifers of low heterogeneity. Method 3 yielded the lowest success probabilities, with the exception of an aquifer of low heterogeneity.

CONCLUSIONS

From the study presented, it can be concluded that the four methods for examining decay coefficients behave differently when heterogeneity is increased. All methods show a decrease in success probability with increasing heterogeneity. Figure 2 illustrated that the decrease in success probability is attributed to an overestimation of the degradation rate constant. The overestimation was largest for Method 3, yielding the lowest success probability. Method 2 was the least affected by an increase in heterogeneity and was also the method that depicted the lowest overestimation of degradation rates. Methods 3 and 4, the most realistic since they are based on the 1-D and 2-D transport equations, illustrated low success probabilities and high over-estimation of degradation rates, Method 3 being the worst. Methods 3 and 4 were prone to errors due to the introduction of longitudinal and transverse dispersivities, which were required to calculate the degradation rate constant. Method 1, the simplest method, yielded results comparable to Method 4.

It can be concluded from this study, that Method 2 (using a non-reactive co-contaminant) is the preferred method for field investigations, where first-order degradation rates are to be estimated. If this co-contaminant is not available, then Method 1 is preferred as then no uncertainty regarding the dispersivities is introduced. Although widely used and published in the literature, the method of Buscheck & Alcantar (1995), Method 3, yielded the worst results in this study.

Acknowledgements This work is funded by the German Ministry of Education and Research as part of the KORA priority programme, sub-project 7.2.

REFERENCES

Buscheck, T. E. & Alcantar, C. M. (1995) Regression techniques and analytical solutions to demonstrate intrinsic bioremediation, In: *Intrinsic Bioremediation* (ed. by R. E. Hinchee, T. J. Wilson, & D. Downey), 109–116. Batelle Press, Columbus, Ohio, USA.

Stenback, G. A., Ong, S. K., Rogers, S. W. & Kjartonson, B. H. (2004) Impact of transverse and longitudinal dispersion on first-order degradation rate constant estimation. *J. Contam. Hydrol.* **73**, 3–14.

Wiedemeier, T. H., Swanson, M. A., Wilson, J. T., Kampbell, D. H., Miller, R. N. & Hansen, J. E. (1996) Approximation of biodegradation rate constants for monoaromatic hydrocarbons (BTEX) in ground water. *Ground Water Monitoring Remed.* **16**(3), 186–194.

Wiedemeier, T. H., Rifai, H. S., Wilson, J. T. & Newell, C. (1999) *Natural Attenuation of Fuels and Chlorinated Solvents in the Subsurface*. Wiley, New York, USA.

Wilson, J. T., Pfeffer, F. M., Weaver, J. W., Kampbell, D. H., Wiedemeier, T. H., Hansen, J. E., & Miller, R. N. (1994) Intrinsic bioremediation of JP-4 jet fuel. In: *Symposium on Intrinsic Bioremediation of Ground Water* (Denver, Colorado, USA), 60–72. US-EPA/540 R-94/515, Washington DC, USA.

Enclosed Publication 2

Bauer, S., Beyer, C., Kolditz, O. (2006a): Assessing measurement uncertainty of first-order degradation rates in heterogeneous aquifers, Water Resour. Res., 42, W01420, doi:10.1029/2004WR003878.

Assessing measurement uncertainty of first-order degradation rates in heterogeneous aquifers

Sebastian Bauer, Christof Beyer, and Olaf Kolditz

Center for Applied Geoscience, University of Tübingen, Tübingen, Germany

Received 7 December 2004; revised 7 October 2005; accepted 18 October 2005; published 31 January 2006.

[1] The principal idea of this paper is to simulate and evaluate the determination of first-order degradation rate constants at heterogeneous contaminated sites under realistic conditions. First, a set of heterogeneous and contaminated synthetic aquifers is generated; second, the spreading of a solute plume subject to first-order degradation is simulated. Third, this plume is investigated using ''monitoring wells'' placed along the presumed plume center line. Using only piezometric heads, concentrations and hydraulic conductivities obtained at these monitoring wells, first-order degradation rate constants are calculated by methods typically used in field applications. The estimated rate constants are compared to the ''real'' value known from the simulations. This comparison is conducted for different degrees of heterogeneity, represented by lognormally distributed random conductivity fields. The results indicate that, with increasing degree of heterogeneity, ''measured'' degradation rate constants become uncertain with a high variability around the true constant. Measured rate constants tend to overestimate the true constant by up to one order of magnitude. A sensitivity analysis of the influences of source width, transport velocity, and dispersivity shows that (1) with increasing source width, measured rate constants decrease their relative error and increase their accuracy; (2) the choice of dispersivity can produce both over- and under-estimation of the true rate constant; and (3) that large-scale measurements of hydraulic conductivity yield better estimates of flow velocities as compared to local scale measurements. These results explain in part the high variability of field measured degradation rate constants reported in the literature.

Citation: Bauer, S., C. Beyer, and O. Kolditz (2006), Assessing measurement uncertainty of first-order degradation rates in heterogeneous aquifers, *Water Resour. Res.*, *42*, W01420, doi:10.1029/2004WR003878.

1. Introduction

[2] This work studies the uncertainty involved in estimating first order degradation rate constants by the plume center line method for the assessment of natural attenuation at contaminated groundwater sites. Natural attenuation, also known as intrinsic bioremediation, refers to the observed reduction in contaminant concentration via natural processes as contaminants migrate from the source into environmental media [*U.S. Environmental Protection Agency* (*EPA*), 1999; *Wiedemeier et al.*, 1999]. The processes contributing to natural attenuation include dilution, dispersion, sorption, volatilization and biodegradation, where biodegradation is the only process that decreases the total contaminant mass. The relative efficiencies of the attenuation processes active at a contaminated site must be carefully assessed before natural attenuation can be adopted as a cleanup remedy or risk reduction strategy. Thus degradation rates of the contaminants under consideration may play an important role in decision making and site management, when natural attenuation is considered as a remedial alternative or a remedial step in contaminated site management. Degradation rate constants can be used to estimate (1) the total overall natural attenuation potential of an aquifer, (2) contaminant plume lengths and (3) downstream concentrations. They can also be used for identifying potential receptors and exposure levels in case of a risk analysis.

[3] Several approaches for estimating biodegradation rates in ground water in the field are commonly used, including mass balances, in situ microcosm studies and the use of concentration-distance relations obtained along the plume center line [*Chapelle et al.*, 1996; *Wiedemeier et al.*, 1999]. The latter include a batch-reaction solution [*Wiedemeier et al.*, 1996], normalization to a recalcitrant co-contaminant [*Wiedemeier et al.*, 1996, 1999] and the method of *Buscheck and Alcantar* [1995]. The method of *Buscheck and Alcantar* [1995] utilizes contaminant concentrations measured along the plume center line, which are evaluated by an analytical solution to the one-dimensional transport equation with first-order degradation. The first-order degradation rate is calculated from the concentrations and an assumed longitudinal dispersivity. An additional requirement is, that the plume has reached steady state. This approach has been used by a number of authors, e.g., *Chapelle et al.* [1996], *Wiedemeier et al.* [1996], *Zamfirescu and Grathwohl* [2001], *Suarez and Rifai* [2002] or *Bockelmann et al.* [2003]. Recently, two- and three-dimensional approaches were suggested [*Zhang and Heathcote*, 2003; *Stenback et al.*, 2004] as extensions to the

0043-1397/06/2004WR003878$09.00

method by *Buscheck and Alcantar* [1995], which are based on analytical solutions for transport in two and three dimensions and account for finite source widths as well as transverse dispersion. By a method comparison with the original data *Zhang and Heathcote* [2003] showed that the method of *Buscheck and Alcantar* [1995] overestimates the degradation rate by 21% and 65% in case of a two- and three-dimensional plume, respectively. *McNab and Dooher* [1998] reported that the method by *Buscheck and Alcantar* [1995] is easily subject to misinterpretation, as transverse dispersivities and temporal effects can produce center line concentration profiles which resemble a degrading contaminant, even in the absence of degradation.

[4] The spatial variability of aquifer properties has a significant influence on the distribution of contaminants and plume development. As a consequence, the methods for the estimation of degradation rates presented above are prone to effects of hydraulic heterogeneity, as they rely on concentration samples along the (presumed) plume center line as well as on estimations of site specific dispersivity. As *Wilson et al.* [2004] point out, the center line of a plume can easily be missed by monitoring wells installed based on assumed, but incorrect, groundwater flow directions. Moreover, contaminant plumes may wander in all three dimensions due to macroscale heterogeneities [*Wilson et al.*, 2004]. However, so far no study has been reported in literature which investigates these effects. Aim of this work is therefore to assess the influence of spatially heterogeneous hydraulic conductivities on the determination of first-order degradation rates using sets of synthetic aquifer models.

[5] Owing to the limited accessibility of the subsurface, measurements of piezometric heads and contaminant concentrations at contaminated sites are sparse and may not be representative of the heterogeneous hydrogeologic conditions. Therefore site investigation is subject to uncertainty, reflecting the limited knowledge on the aquifer properties and the extent of the contamination. Owing to this uncertainty, field investigation methods for plume screening or measuring hydraulic conductivity or degradation rates can neither be tested nor verified in the field. The only way of assessing the performance and reliability of field investigation methods is by studying them in synthetic aquifers within a Monte Carlo framework. By applying the investigation method under consideration in the synthetic contaminated and heterogeneous aquifer, the method results can be compared to the true values. These are known from the synthetic aquifer, unlike in reality, where the true values are unknown.

[6] This approach uses synthetic aquifer models, which are generated as the first step based on statistical properties of real aquifers and have a defined source of contamination. A reactive transport model is then used to simulate the spreading of the plume, resulting in realistic concentration distributions in the synthetic aquifer. In comparison to the "real world," the unique advantage of the synthetic aquifer is that the spatial distribution of all physical and geochemical properties and parameters as well as the contaminant concentrations are exactly known. In the second step, the synthetic aquifer is investigated by standard monitoring and investigation techniques. In this step, only the data obtained by the investigation methods, i.e., heads and concentrations at the observation wells, is used, because in case of a real site investigation the true parameter distribution is unknown. In the third step, the results from the investigation are compared to the true values, which allows to test and evaluate the investigation method used. Using synthetic aquifers offers furthermore the possibility to single out the influence of different parameters, such that sources of uncertainty and error for the investigation method can be studied individually. Owing to this possibility of extensive and detailed scenario analysis and visualization, this approach is well suited to explore the uncertainty involved in hydrogeologic investigation and management. It has been applied under the term "virtual aquifer" by *Schäfer et al.* [2002, 2004], *Bauer et al.* [2005] and *Bauer and Kolditz* [2006].

[7] This paper uses synthetic heterogeneous and contaminated aquifers in a Monte Carlo approach to assess for the first time the influence of spatially heterogeneous hydraulic conductivities on the determination of first-order degradation rates. To this end, plumes formed by contaminants degrading according to a first-order degradation rate in aquifers of different degrees of heterogeneity are investigated by the center line approach. By comparison of the estimated degradation rate constant with the true degradation rate constant the methods are tested and evaluated. This is performed by individually studying the influence of aquifer heterogeneity, source width, flow velocity and dispersivity on the estimated rate constant.

2. Methods

2.1. Model Domain

[8] The model domain used for the numerical investigation is a two-dimensional aquifer with 184 m length and 64 m width (Figure 1). Flow is from left to right, with a mean hydraulic gradient of 0.003, which is induced by fixed head boundary conditions on the left and the right hand side of the model domain. No flow boundary conditions are assigned to all other sides of the model domain. The model domain is discretized with a grid density of 0.5 m in both directions. A contaminant source is emplaced 11.5 m downstream of the inflow boundary in the center of the aquifer, emitting a contaminant subject to first-order degradation with a degradation rate constant λ of 1 a^{-1} (one per year). The contaminant source is represented by a fixed concentration boundary condition at the source position. Neither sorption, i.e., retardation, nor volatilization or dilution by recharge are accounted for. Additionally, a conservative compound is emitted from the source. The model setup is thus designed to provide ideal conditions for the application of the four center line methods to be studied. This is certainly not the case in nature, where the reaction kinetics will follow more complicated laws and may be spatially dependent, or influences from sorption and dilution have to be accounted for. However, these assumptions are used here to be able to study the standard methods closely and evaluate individually the influence of heterogeneity of the hydraulic conductivity. Further studies will use model setups which incorporate, e.g., different degradation kinetics.

[9] A plume is generated using a process based numerical flow and reactive transport model. The simulation code

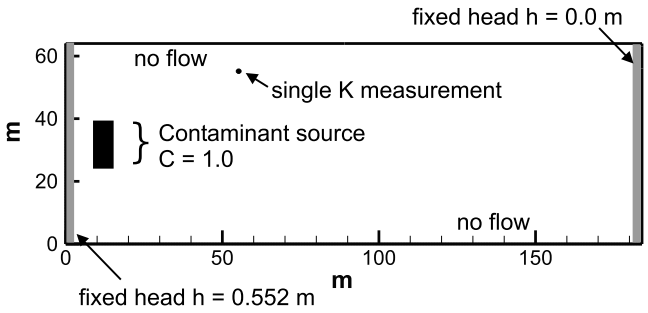

Figure 1. Model area of the synthetic aquifer and boundary conditions applied.

GeoSys/RockFlow [*Kolditz*, 2002; *Kolditz et al.*, 2004] is used here, which solves the flow and transport equations by standard Galerkin finite element methods [e.g., *Huyakorn and Pinder*, 1983] and using implicit Euler time stepping. The governing equations are given as [e.g., *Bear*, 1972]:

$$S\frac{\partial h}{\partial t} = \nabla(K\nabla h) + q \tag{1}$$

and

$$\frac{\partial C}{\partial t} = -v_a\nabla C + \nabla(D\nabla C) - \lambda C \tag{2}$$

where S is the storage coefficient, h is the piezometric head, K is the tensor of hydraulic conductivity, q are sources and sinks of water, C is concentration, v_a is the transport velocity, D is the dispersion tensor, λ is the first order degradation rate constant and t is time. The model parameters used in this study are given in Table 1. Details on numerical and software issues can be found in the work of *Kolditz* [2002] and *Kolditz and Bauer* [2004]. The simulation code has been used for ground water flow and transport simulations by *Kolditz et al.* [1998], *Diersch and Kolditz* [1998, 2002], *Thorenz et al.* [2002] and *Beinhorn et al.* [2005].

[10] To study the effects of spatially variable hydraulic conductivity, K is regarded as a random variable following a lognormal distribution with an expected value of $E[Y = \ln(K)] = -9.54$. This corresponds to an effective hydraulic conductivity K_{ef} of 7.2 10^{-5} m s^{-1} using the geometric mean [*Rubin*, 2003]. Using a porosity n of 0.33, the mean transport velocity is given by 6.5 10^{-7} m s^{-1}. The spatial correlation structure is characterized by an isotropic exponential covariance function $C_Y = \sigma_Y^2\exp(-\Delta h/l_Y)$, with an integral scale of l_Y = 2.67 m and the variance σ_Y^2. Four different cases of increasing heterogeneity with ln(K) variances σ_Y^2 of 0.38, 1.71, 2.70 and 4.50 are considered, representing mildly to highly heterogeneous conductivity fields. The value of $\sigma_Y^2 = 0.38$ as well as the integral scale l_Y is taken from the Borden field site [*Sudicky*, 1986]. The value of 1.71 stems from an alluvial valley aquifer in southern Germany [*Herfort*, 2000]. The values of 2.70 and 4.50 were reported for the Columbus Air Force Base site [*Rehfeldt et al.*, 1992]. The geostatistical software tool gstat2.4 [*Pebesma and Wesseling*, 1998] is used to generate 100 realizations of the random field for each value of σ_Y^2 by unconditional sequential Gaussian simulation. The random K values are generated over a two-dimensional grid of density 0.5 m, exactly matching the numerical grid. Thus, following a rule of thumb of *Ababou et al.* [1989], a sufficient resolution of $5.33 > 1 + \sigma_Y^2$ grid nodes per integral scale is ensured.

[11] To generate steady state plumes, as required by the methods under consideration, a stationary flow field is assumed. The time development of the plume is calculated, until the plume has reached steady state. A local longitudinal dispersivity α_L = 0.25 m and a local transversal dispersivity of α_T = 0.05 m are used for the numerical simulations (compare Table 1).

2.2. Center Line Method

[12] Four methods for the determination of first-order degradation rate constants are investigated here, which are all based on the plume center line method. Method 1 is based on the one-dimensional transport equation, considering advection and first-order degradation only. The steady state solution for the concentration profile can be rearranged to yield the first-order degradation rate constant for method 1, i.e., λ_1 [T^{-1}] as:

$$\lambda_1 = -\frac{v_a}{\Delta x}\ln\left(\frac{C(x)}{C_0}\right) \tag{3}$$

where v_a [L T^{-1}] is the transport velocity, Δx [L] is the distance between the observation wells, and C_0 and $C(x)$ [M L^{-3}] are the upstream and downstream contaminant concentrations at the observation wells. In this formulation, all concentration changes resulting from processes other than degradation, i.e., diffusion, dispersion and dilution, are attributed to degradation. Therefore the rate constant λ_1 determined with method 1 can be considered rather an overall (or bulk) attenuation rate than a degradation rate constant [*Newell et al.*, 2002]. Also, if the downstream observation well is not placed on the plume center line, the measured concentration is smaller than on the plume center line and the degradation rate constant is overestimated.

[13] Method 2 was proposed by *Wiedemeier et al.* [1996] and is based on the same transport equation as method 1. However, to overcome the above mentioned drawbacks, amended concentrations are used: The measured concentrations of the reactive contaminant are corrected by the ratio of upgradient concentration C_0^* to downgradient concentration $C(x)^*$ [M L^{-3}] of a nondegrading co-contaminant at the same observation wells. Thus the method corrects for dispersion of the plume or for the effects of unintended measurements off the plume center line. The degradation

Table 1. Model Parameters Used in the Simulations

Parameter	Value
K_{ef}	7.2 10^{-5} m s^{-1}
l_Y	2.67 m
σ_y^2	0, 0.38, 1.71, 2.7, 4.5
n	0.33
λ	1 a^{-1}
S, q	0
α_L	0.25 m
α_T	0.05 m

rate constant for method 2 is then calculated as [*Wiedemeier et al.*, 1996]:

$$\lambda_2 = -\frac{v_a}{\Delta x}\ln\left(\frac{C(x)}{C_0}\frac{C_0^*}{C^*(x)}\right) \quad (4)$$

A prerequisite for the application of method 2 is that physicochemical properties of degradable and recalcitrant compounds like Henry's Law constants and sorption coefficients must be comparable. A group of substances that has been proven to be well suited for the normalization of downgradient concentrations in BTEX plumes under anaerobic conditions are several trimethylbenzene (TMB) isomers [*EPA*, 1998; *Wiedemeier et al.*, 1996, 1999]. When TMB is subject to biodegradation the estimated rate constant will be less than the actual value. For chlorinated solvent plumes, inorganic compounds like chloride may be appropriate substances for the normalization. Reductive dechlorination results in the production of chloride along the flow path, which by means of a mass balance can be used to derive the correction factor [*EPA*, 1998].

[14] The third method investigated here was proposed by *Buscheck and Alcantar* [1995]. It is based on the steady state solution to the one-dimensional transport equation, accounting for advection, dispersion and first-order degradation. In comparison to method 1, method 3 accounts additionally for effects of longitudinal dispersion and thus requires an estimate of the longitudinal dispersivity α_L [m]. The degradation rate constant for method 3 is given by *Buscheck and Alcantar* [1995]:

$$\lambda_3 = -\frac{v_a}{4\alpha_L}\left(\left(1-2\alpha_L\frac{\ln\left(\frac{C(x)}{C_0}\right)}{\Delta x}\right)^2 - 1\right) \quad (5)$$

Method 4 used here is the modified method of *Buscheck and Alcantar* [1995], as proposed by *Zhang and Heathcote* [2003]. Since in this study a two-dimensional synthetic aquifer is used to assess the different approaches, for method 4 the analytical solution to the two-dimensional transport equation including first order decay [*Domenico*, 1987] is adopted. Method 4 accounts for a finite source width as well as longitudinal and transverse dispersion. Therefore longitudinal and transverse dispersivities α_L [m] and α_T [m] as well as the source width W_S [m] perpendicular to the average flow direction have to be known or estimated. Given these prerequisites, the degradation rate constant is given as [*Zhang and Heathcote*, 2003]:

$$\lambda_4 = -\frac{v_a}{4\alpha_L}\left(\left(1-2\alpha_L\frac{\ln\left(\frac{C(x)}{C_0\beta}\right)}{\Delta x}\right)^2 - 1\right)$$
$$\beta = erf\left(\frac{W_S}{4\sqrt{\alpha_T\Delta x}}\right) \quad (6)$$

2.3. Investigation Scenario

[15] The site investigation mimicked in this study is depicted in Figure 2, where a steady state plume has evolved from a contaminant source. This plume is investigated by the center line approach. Figure 2a shows the initial situation, where three observation wells are present in the aquifer. One of these wells (solid circle) is in the source and concentrations are high, while the other two show no concentration. This situation is the starting point for the investigation scenario for all realizations and represents the initial knowledge on the site. In the first investigation step, the flow direction is determined (Figure 2b). Hydraulic heads are measured in the three wells (by reading the model output at the well positions), a hydrogeologic triangle is constructed and the hydraulic gradient is calculated. In the second investigation step, three new observation wells are installed every 10 m along the estimated direction of flow (Figure 2c). These wells are then used to obtain hydraulic heads and concentrations of the contaminant and the nonreactive co-contaminant as well as local hydraulic conductivities at the observation wells by using the model input for hydraulic conductivity at the corresponding location. From the head difference, the true porosity and the well positions the respective groundwater flow velocities are calculated. An effective conductivity K_{ef} between each upstream and downstream well is estimated by calculating the geometric mean of the local conductivities. Together with the concentration data, this information allows for the determination of

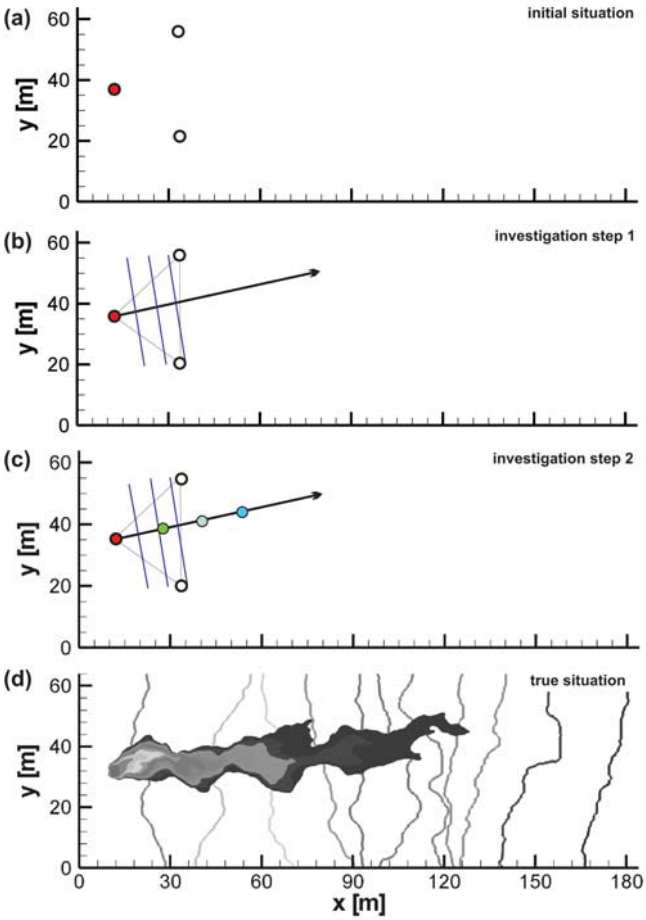

Figure 2. Representation of the investigation method to obtain plume center line concentrations: (a) initial situation, (b) estimation of flow direction by application of a hydrogeologic triangle, (c) measured concentrations on the inferred center line, and (d) comparison to true concentrations and heads.

the first-order degradation rate constants by the four methods presented above. The investigation setup is designed to resemble ideal conditions for the application of the four methods for estimating the degradation rate constant. All measurements are assumed to be exact, which means that there is no measurement error involved. The only uncertainty and variability is introduced by the heterogeneity of hydraulic conductivity. For methods 3 and 4, additionally α_L and α_T have to be known. These are estimated following *Wiedemeier et al.* [1999] as 0.1 of the plume length for α_L, with α_T being about 0.33 of the longitudinal dispersivity. As plume length the maximum distance covered by the observation wells, i.e., 30 m, is used. As the plumes are generally longer, this assumption yields rather low dispersivities. Thus α_L and α_T are estimated to be 3.0 and 1.0 m, respectively. These estimates of dispersivities are not optimal, as they are not based on the heterogeneity of the hydraulic conductivity. However, dispersivities based on results from stochastic hydrogeology are difficult to obtain, as for most field sites structure and degree of heterogeneity are not well known. Also, the four samples taken in this investigation scenario do not allow for an estimation of the correlation length or the ln(K) variances. Both the correct source width and the correct porosity are used. In the last step, by each of the four approaches the corresponding first-order degradation rate constants λ_1 through λ_4 are calculated. These values can be compared to the value used to generate the plume ($\lambda = 1\ a^{-1}$). For each realization, the investigation procedure described above is followed and a degradation rate is calculated for each method, each downstream well and for each source width. For each of the four classes of heterogeneity used in this study (ln(K) variances σ_Y^2 of 0.38, 1.71, 2.70 and 4.50) a minimum of 100 realizations is evaluated. Thus statistical measures of the errors and uncertainties introduced by the heterogeneity of the hydraulic conductivity are obtained. Additionally, also the impact of the width of the source zone is studied. Here it is expected, that for increasing source width the one-dimensional methods yield better results, as then the investigated situation corresponds better to the assumptions of the method. Source widths W_S of 4 m, 8 m and 16 m are used, corresponding to 1.5, 3 and 6 integral scales l_Y. Then methods for estimating the flow velocity are elucidated for the different degrees of heterogeneity. This is because the goodness of the calculated value for lambda is directly related to estimated transport velocity accuracy. Finally the influence of estimated longitudinal and transversal dispersivities on results by methods 3 and 4 is studied in a sensitivity analysis.

2.4. Numerical Tests

[16] Convergence of the Monte Carlo simulation with regard to the sample size N of estimated degradation rate constants was tested by a procedure following *Goovaerts* [1999]. The test is only conducted for the highest degree of heterogeneity used in this study ($\sigma_Y^2 = 4.5$) and the smallest source width of 4 m, as this is the case of highest variability. A total of 1000 realizations of the random conductivity field was generated. For each realization, plume development was simulated and the degradation rate constant λ_1 was calculated using method 1. The resulting set of 1000 degradation rates is assumed to be sufficiently large to represent the global population. The global population of λ_1 was randomly sampled with a sample size of $N = 2$, yielding a subset of two λ_1. For this subset the mean degradation rate as well as the standard deviation were calculated. Random sampling was repeated 999 times, resulting in 1000 subsets of $N = 2$. From these subsets, the average subset mean $\overline{\lambda_1}$, the standard deviation of subset means $\sigma_{\overline{\lambda_1}}$ and the average standard deviation of the subset population $\overline{\sigma_{\lambda_1}}$ are calculated. Random sampling was repeated with increasing subset sizes $N = 3, 4, \ldots, 1000$, resulting in 999 triplets of the statistics, one for each subset size. Dependence of the three statistics on N is shown in Figure 3.

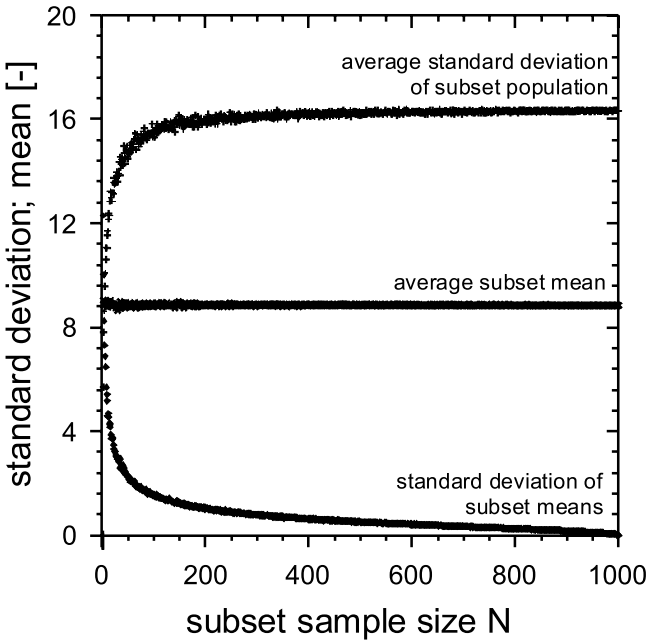

Figure 3. Influence of Monte Carlo sample size N on the average subset mean ($\overline{\lambda_1}$), the standard deviation of subset means ($\sigma_{\overline{\lambda_1}}$), and the average standard deviation of the subset population ($\overline{\sigma_{\lambda_1}}$) for the highest degree of heterogeneity (σ_Y^2).

[17] The middle curve in Figure 3 displays the average subset mean $\overline{\lambda_1}$, which shows almost no dependence on N and yields values very close to the global mean of 8.9. The standard deviation of the subset means ($\sigma_{\overline{\lambda_1}}$, lower curve) shows a strong decrease from 12.3 ($N = 2$) to 2.2 ($N = 50$) and 1.5 ($N = 100$), with a significantly reduced decrease for larger subset sizes. In relation to the global mean of 8.9, the variation among the subsets is therefore small for $N \geq 100$. The upper curve in Figure 3 shows the average standard deviation of the random sample subsets $\overline{\sigma_{\lambda_1}}$, which strongly increases with subset size for small N, but with a much smaller increase for $N > 50$. For $N = 100$ a value of 15.5 is found, which is 95% of the standard deviation of the global population, as obtained for $N = 1000$. The observed reduction in increase of $\overline{\sigma_{\lambda_1}}$ with N indicates the redundancy of additional realizations with regard to the subset variability. As the rate of decrease of $\sigma_{\overline{\lambda_1}}$ as well as the rate of increase of $\overline{\sigma_{\lambda_1}}$ becomes small for more than 100 realizations, we feel confident that a sample size of $N = 100$ is sufficient to yield stable ensemble averaged rate coefficients. Since the analysis was conducted for the largest degree of heterogeneity,

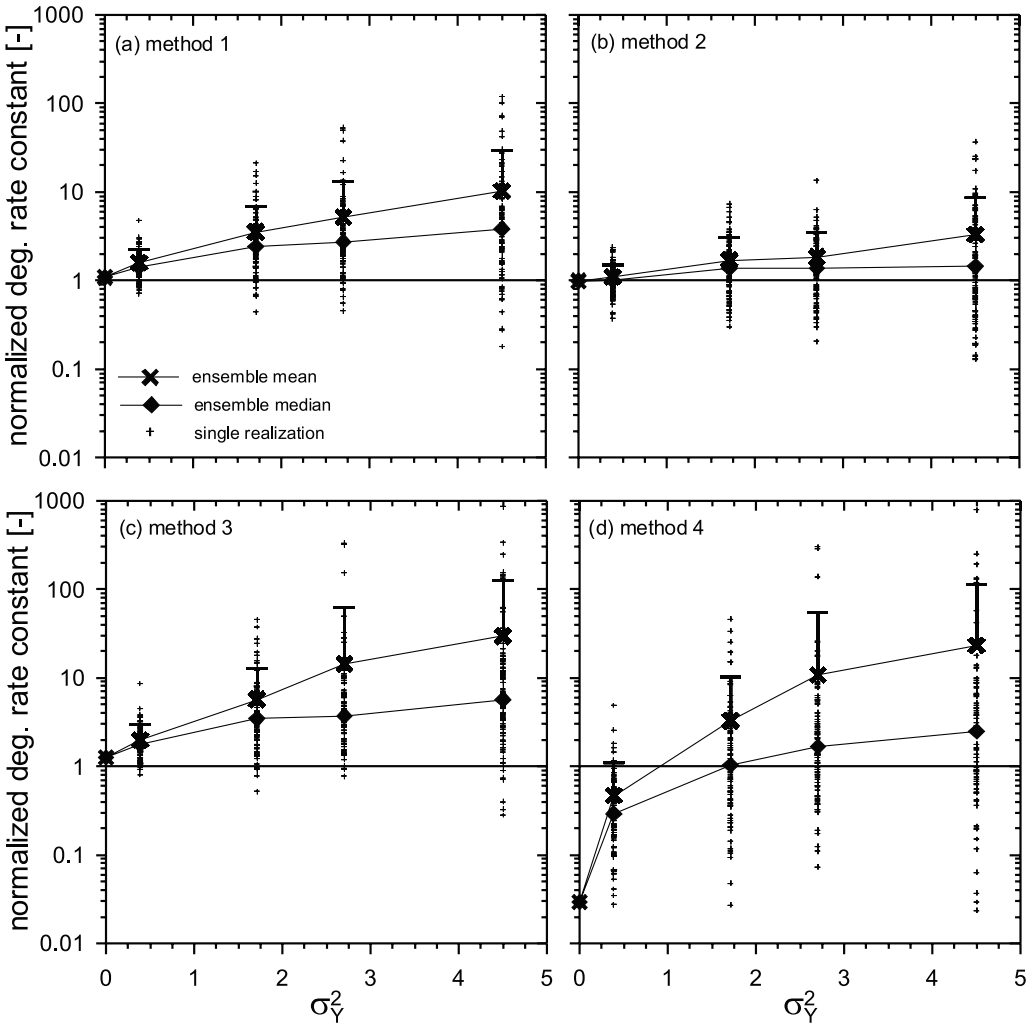

Figure 4. Estimated first-order degradation rate constants Λ_i (normalized to the true rate constant λ) versus degree of heterogeneity σ_Y^2 for (a) method 1, (b) method 2, (c) method 3, (d) and method 4. All figures show results for all single realizations (small symbols) as well as their ensemble means (large crosses) with their corresponding standard deviations (error bars) and ensemble medians (large diamonds). The reference rate constant used in the numerical simulations is indicated by the horizontal line.

for lower values of σ_Y^2 convergence can be expected already at lower sample sizes.

[18] Another check was performed concerning the mean flux over the flow domain. Although deviations between single realizations are quite distinct and increase with σ_Y^2, the ensemble averages for each σ_Y^2 match the theoretical value with less than a 1% error. Furthermore, the correct operation of the investigation methods was verified by applying the investigation procedure for a source of infinite width, i.e., a width equal to the model area, and by assuming the aquifer is homogeneous. Then all methods reduce to the one-dimensional method and yield the correct degradation rate constant. This result was obtained and thus the correct operation verified.

3. Results and Discussion

3.1. Influence of Heterogeneous Conductivity

[19] To examine the influence of heterogeneity on the estimation of the rate constants, a contaminant source of width $W_S = 4$ m perpendicular to the average flow direction is emplaced in the synthetic aquifer and flow as well as reactive transport are simulated. With the investigation scenario described in section 2.3 applied to a single realization, each of the four methods yields differing rate constants, λ_i, for each of the three center line observation wells (10 m, 20 m, and 30 m distance from the source). For the assessment of the four methods, these rate constants $\lambda_{i,10}$, $\lambda_{i,20}$ and $\lambda_{i,30}$ are averaged to yield one single estimated λ_i for each method. This procedure is repeated for all realizations. Figure 4 presents results of the calculated rate constants λ_i versus the degree of heterogeneity (given as ln conductivity variance σ_Y^2). Calculated rates λ_i are reported as normalized rates Λ_i, i.e., the calculated rate λ_i is divided by the true rate λ used in the numerical simulation. The normalized rate constants Λ_i thus can be interpreted as over- or under-estimation factors. The homogeneous case ($\sigma_Y^2 = 0$) is included for reference.

[20] Figure 4a presents the results for method 1, i.e., based on the one-dimensional advection-degradation solution

(equation (3)). It can be clearly seen, that an increase of σ_Y^2 leads to an increase in spread of the single realizations. Quite a number of realizations exhibit normalized rate constants Λ_1 of more than 10 up to about 100, i.e., the true rate constant is severely overestimated by a factor of 10 to 100. Also, Λ_1 increases with increasing σ_Y^2 as well as the standard deviations of the ensemble means. This points to an increase in uncertainty and reflects the spread of the single realizations. Mean overestimation increases from a factor of about 1.6 for $\sigma_Y^2 = 0.38$ to about 10.2 in the case of $\sigma_Y^2 = 4.50$. In the homogeneous case ($\sigma_Y^2 = 0$), method 1 yields the correct result. Although on average λ is overestimated, even for high values of σ_Y^2 in single realizations λ may actually be underestimated by Λ_1. For the highest degree of heterogeneity, the Λ_1 of the single realizations span about three orders of magnitude. Comparison of ensemble means with the corresponding medians shows that in all cases the medians are significantly lower. The populations of estimated λ_1 are positively skewed as some exceedingly large values of λ_1 shift the means to high values. However, the general trend of increasing overestimation with heterogeneity is also distinct for the medians.

[21] Figure 4b shows the corresponding results obtained with method 2, i.e., using the one dimensional advection-degradation equation with normalization to a recalcitrant co-contaminant (equation (4)) [*Wiedemeier et al.*, 1996]. As for method 1, the spread of the single realizations increases with increasing σ_Y^2. Compared to method 1, however, the spread is smaller and more equally distributed about $\Lambda_2 = 1$. Therefore the average overestimation factors as well as the standard deviations are much smaller than for method 1 and both the error and the uncertainty are lower. Average rate constants Λ_2 are 1.1 for $\sigma_Y^2 = 0.38$, increasing to 3.3 for $\sigma_Y^2 = 4.50$. For homogeneous conditions, also method 2 yields the correct result, i.e., $\Lambda_2 = 1$ for $\sigma_Y^2 = 0$. Ensemble medians are just slightly above the true λ, i.e., deviating less than a factor of 2.

[22] Degradation rate constants calculated with method 3, i.e., the one-dimensional method introduced by *Buscheck and Alcantar* [1995] (equation (5)), are displayed in Figure 4c. They exhibit a similar general behavior as found with method 1, i.e., increasing spread and increasing overestimation of the true rate constant for higher σ_Y^2. However, mean Λ_3 are significantly higher than the corresponding Λ_1, with ensemble means of 2.0 for $\sigma_Y^2 = 0.38$ increasing to 29.4 for $\sigma_Y^2 = 4.50$. In the homogeneous case, the true rate constant is slightly overestimated, i.e., $\Lambda_3 = 1.25$ for $\sigma_Y^2 = 0$. Spread in the single realizations is higher compared to method 1, now spanning nearly four orders of magnitude for the largest variance value of σ_Y^2.

[23] Results for method 4, i.e., the two-dimensional solution (equation (6)) suggested by *Zhang and Heathcote* [2003], are depicted in Figure 4d. Compared to the other methods, method 4 displays the largest spread of calculated Λ_4 around the mean values. For the highest degree of heterogeneity, the spread of the single realizations covers nearly five orders of magnitude. Ensemble means of Λ_4 increase from 0.6 for $\sigma_Y^2 = 0.38$ to about 23.0 for $\sigma_Y^2 = 4.5$, i.e., for low σ_Y^2 the normalized rate constant Λ_4 is actually underestimated in most realizations, while for larger variances the ensemble averages approach the results of method 3. In the homogeneous case ($\sigma_Y^2 = 0$), the estimated rate constant λ_4 is about two orders of magnitude lower than the true rate constant λ. Ensemble medians for method 4 show a similar behavior as the ensemble means, with their values closer to the true rate constant than for methods 1 and 3 for large heterogeneities ($\sigma_Y^2 = 1.71$). This reflects the fact, that the spread of the single realizations is distributed symmetrically around $\Lambda_4 = 1$, however, the spread of the populations and thus the uncertainty is significantly larger than for methods 1 and 3.

[24] Method 1 is based on the one-dimensional solution to first-order biodegradation and advection. Therefore it is expected that rate constants estimated with method 1 overestimate the true rate constant due to two effects. Firstly, method 1 does not account for measuring off the center line. So if an observation well is placed off the plume center line, concentrations sampled there will be smaller than on the center line and therefore the degradation rate constant will be estimated too high. Secondly, as method 1 is based on a one-dimensional solution of the transport equation, it does not account for transverse dispersion, which lowers concentrations on the plume center line. This second effect also causes an overestimation of the rate constant. Both effects together cause the overestimation of the rate constant as shown in Figure 4a. Method 2 tries to overcome these two problems by normalization to a conservative tracer. Both above effects also determine the concentration of the nonreactive component, and are thus corrected for by the normalization. As is shown in Figure 4b, results of method 2 are considerably better than of method 1, both considering spread and ensemble averages. However, as can be seen from Figure 4b, method 2 does not correct for all effects, as overestimation is observed with increasing σ_Y^2. Effects of dispersion and measuring off the center line are accounted for by method 2, so the deviation seen for method 2 has to have a hydraulic cause. This deviation is introduced by the determination of the average flow velocity between the observation wells, which is calculated using an averaged value of the hydraulic conductivity at the two observation wells. This averaged value may not be representative of the flow path between the two wells and bias may be introduced into the calculation of degradation rate constants. This effects is studied closely below in section 3.3.

[25] Method 3 is based on the one-dimensional transport equation including advection, degradation and longitudinal dispersion. Results from method 3, as shown in Figure 4c, display a higher spread and higher ensemble averages compared to method 1. Because method 3 includes longitudinal dispersion, it should be closer to reality and advantageous over method 1. The differences in estimated rate constants between method 1 and 3 are therefore due to the longitudinal dispersivity α_L in method 3. With the one-dimensional transport model used, pronounced longitudinal dispersion of a degrading contaminant results in a stronger spreading of the solute downstream and thus in higher concentrations along the plume center line compared to an advection only case. Therefore a larger rate constant is calculated to accomplish a given concentration decrease between the upgradient and the downgradient observation well. λ_3 grows linearly with α_L and is always larger than λ_1,

as can be seen by expanding the squared brackets in equation (3) and using $C(x) \leq C_0$:

$$\lambda_3 = v_a\left(\alpha_L\left(\frac{\ln(C(x)/C_0}{\Delta x}\right)^2 - \frac{\ln(C(x)/C_0)}{\Delta x}\right) \geq v_a\left(-\frac{\ln(C(x)/C_0}{\Delta x}\right) = \lambda_1 \quad (7)$$

[26] If $\alpha_L = 0$, method 3 reduces to the advection only case, i.e., method 1. Method 3 still does not account for transverse dispersion, which is the process causing smaller concentrations on the plume center line. Method 4 is based on a two-dimensional solution to the transport equation including advection, longitudinal and transverse dispersion and first-order degradation. Results from method 4 (Figure 4d) show an underestimation of the true rate constant for homogeneous or slightly heterogeneous conditions ($\sigma_Y^2 \leq 1.71$), while for high degrees of heterogeneity ($\sigma_Y^2 \geq 2.7$), the ensemble averages of the estimated rate constants approach the respective values obtained with method 3. The underestimation for low heterogeneities is a consequence of the correction for transverse dispersion, represented by the error function β in equation (4). The effect of lower concentrations along the plume center line due to transverse dispersion is strong for small source widths, large transversal dispersivities and large well spacings. β is always less than 1 and asymptotically approaches unity for arguments of the error function larger than 2, i.e., λ_4 converges toward λ_3 for small α_T or large W_S. For arguments <2, method 4 always yields rate constants smaller than those derived by method 3. Since W_S is only 4 m in the scenario considered here, the argument of the error function is small. The underestimation of Λ_4 for low degrees of heterogeneity with method 4 is thus due to an "over correction" for the effects of transverse dispersion. Obviously a value of $\alpha_T = 1$ m is too large for $\sigma_Y^2 \leq 1.71$, yielding the small values of Λ_4. Method 4 thus may yield rate constants which are too high as well as rate constants which are too low. Effects of choosing dispersivity values are studied in more detail in section 3.4.

3.2. Influence of Source Width

[27] To study the sensitivity of the four methods compared in this study on the source width perpendicular to the average flow direction, reactive transport simulations and estimation of the degradation rate constants is performed for all realizations with source widths W_S of 4 m, 8 m and 16 m. Results of these simulations with regard to aquifer heterogeneity are presented in Figures 5a–5d. For the sake of clearness only ensemble means (solid lines) and standard deviations (dashed lines) are illustrated here. For method 1, increasing W_S improves the estimation of Λ_1 significantly. In the case of $\sigma_Y^2 = 4.50$, the ensemble mean Λ_1 decreases from 10.2 ($W_S = 4$ m) to 4.1 ($W_S = 16$ m). Also the standard deviation decreases, indicating that the spread of the single realizations is reduced considerably by increasing W_S. The standard deviation decreases by about a factor of 3 from 18.9 at $W_S = 4$ m to 7.2 at $W_S = 16$ m. With increasing source width W_S, the basic assumption of one-dimensionality of method 1 is better fulfilled as effects of transverse dispersion become smaller. Furthermore, it is less likely to measure off the plume center line in a wide plume. For an infinite source width, therefore, method 1 would yield the same results as method 2. As can be seen in Figure 5b, Λ_2 shows no dependence on W_S. This effect is inherent to method 2, as it accounts for the above mentioned effects by the normalization procedure. Also the standard deviations do not change with increasing source width. Estimated Λ_3 again display an explicit improvement, when W_S is increased from 4 to 8 and to 16 m (Figure 5c). The reason for this improvement is the same as for method 1 mentioned above. Standard deviation decreases by about one order of magnitude, when W_S is increased from 4 to 16 m, i.e., spread of the single realizations is reduced considerably, but is still higher than for method 1. Also for method 4, mean overestimation as well as spread are reduced with W_S. Worth noticing is that the underestimation of Λ_4 for low heterogeneities is drastically reduced, when W_S is increased. For $\sigma_Y^2 = 0.38$ and $W_S = 16$ m, the ensemble mean of $\Lambda_4 = 0.96$ nearly matches the true rate constant. This improvement is a consequence of the explicit consideration of W_S in the correction term β in (4). The smallest rates are obtained for the smallest source width, as then the correction is largest. As mentioned before, Λ_4 converges toward Λ_3 for large W_S and small α_T. However, with the macrodispersion coefficients estimated ($\alpha_T = 1$ m, see section 2.3), Δx being between 10 and 30 m and a maximum W_S of 16 m, the arguments of the error function β are always clearly below 2 and therefore Λ_4 must always be smaller than the corresponding Λ_3. These results show that performance of all methods improves with source width. The smallest W_S used here corresponds to 1.5 l_Y, the largest to 6 l_Y. Therefore, for sources on the order or even smaller than about one l_Y, a much higher uncertainty and bias has to be expected than for sources which have dimensions of about 6 l_Y and thus already average some of the effects of hydraulic heterogeneity. This result is in accordance with findings by *Zhang* [2003], who found that with increasing source width perpendicular to the mean flow direction plumes become ergodic and longitudinal macrodispersivity approaches an asymptotic value, which depends on the source width.

3.3. Influence of the Estimation of Transport Velocity

[28] As outlined in the previous sections, errors made in the determination of the transport velocity v_a are directly propagated into the estimated rate constant, as λ is linearly related to v_a. In a heterogeneous system v_a can be calculated by the help of Darcy's law using an effective conductivity K_{ef} and the porosity. In a statistically homogeneous domain, the arithmetic mean conductivity K_a constitutes an upper bound for K_{ef}, whereas the harmonic mean K_h is its lower bound [*Dagan*, 1989]. Exact calculation of K_{ef} is possible for a stationary isotropic domain with a Gaussian probability density function (pdf) of $Y = \ln(K)$. K_{ef} is then given by:

$$K_{ef} = K_g \exp\left[\left(\frac{1}{2} - \frac{1}{m}\right)\sigma_Y^2\right] \quad (8)$$

with m being the dimensionality of the domain [*Rubin*, 2003]. For two dimensions, i.e., m = 2, (8) reduces to the geometric mean K_g. *Dykaar and Kitanidis* [1992] showed that (8) is accurate for m = 3 and conductivity variances of up to $\sigma_Y^2 = 6$. However, for many "real world" field sites, data on the site-specific spatial structure of K is insufficient to allow the inference of the pdf.

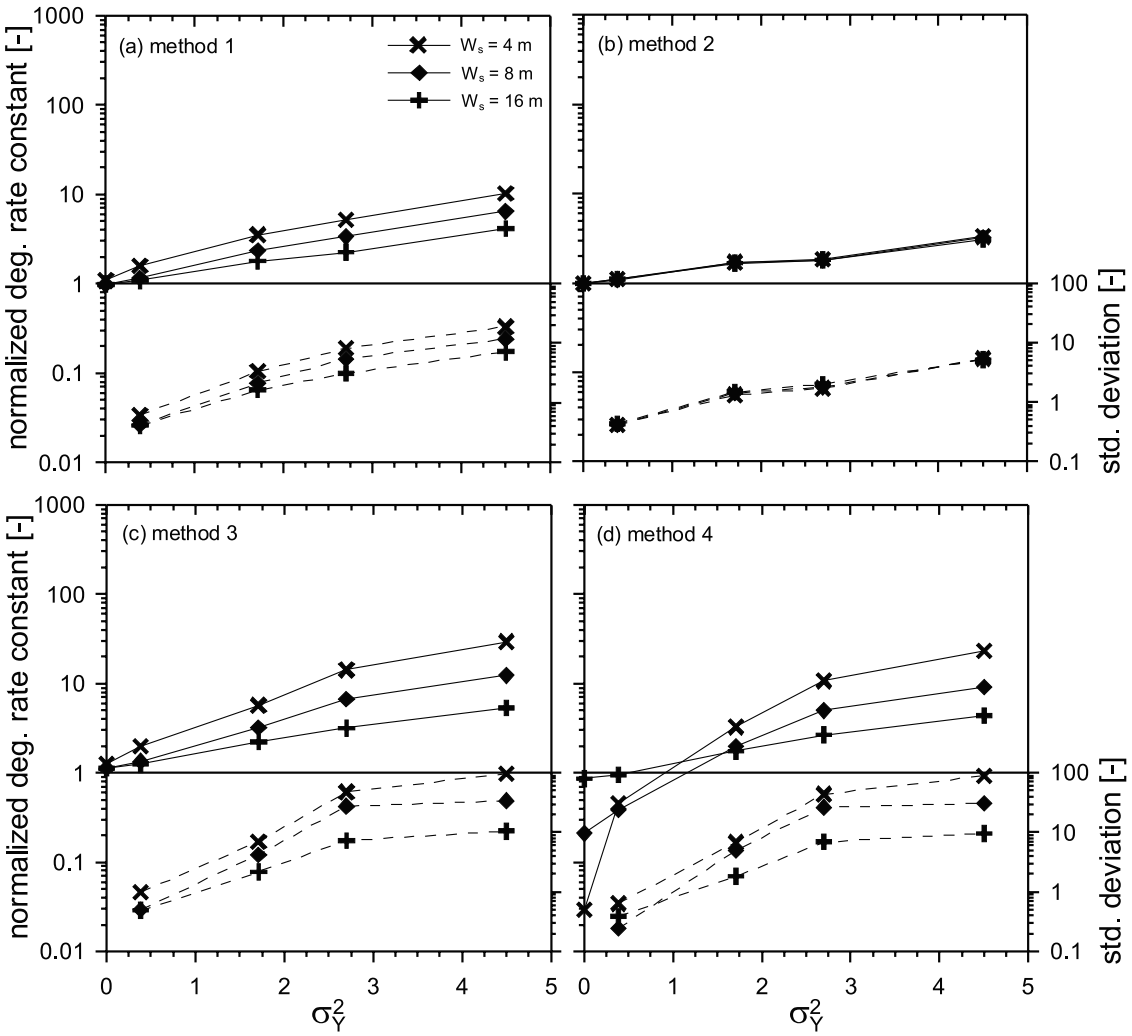

Figure 5. Estimated first-order degradation rate constants versus degree of heterogeneity σ_Y^2 for (a) method 1, (b) method 2, (c) method 3, and (d) method 4 and source widths W_S of 4, 8, and 16 m, respectively. Solid lines show ensemble means normalized to the true degradation rate constant (left axis), dashed lines show the corresponding standard deviations (right axis).

[29] In the following, the influence of different approaches for estimating K (and thus v_a) on the determination of λ_i is analyzed. As the plume samples only part of the full domain, the hydraulic conductivity needed is not the effective conductivity for the complete domain, but an equivalent hydraulic conductivity valid for the flow path along the center line wells. This equivalent hydraulic conductivity may differ from the global effective value. During the field investigation by the center line method, only the local hydraulic conductivities measured at the observation wells placed along the inferred plume center line or only the global effective hydraulic conductivity are known. Neither the underlying statistical parameters nor the complete conductivity field are known. The first approach represents the situation, where local hydraulic conductivities have been obtained in the observation wells, e.g., by slug tests or sieve analysis, and are averaged to obtain an estimate of the equivalent hydraulic conductivity between the two observation wells used for rate determination. In addition to the geometric mean K_g, as used so far, also the arithmetic mean K_a and the harmonic mean K_h are used, as they present upper and lower limits for K_{ef} [e.g., *Renard and de Marsily*, 1997]. As hydraulic conductivity data is available only at four wells, a full characterization of the conductivity field is not possible. Often at a real site, values of hydraulic conductivity are not available at the locations of the observation wells at the plume center line, but only from a single well not on the plume center line and thus not used for rate determination. This case is simulated by using a value K_S of hydraulic conductivity from a well at point [55.10 m, 55.20 m] (see Figure 1). In the last approach, the true global effective conductivity K_G of the synthetic aquifer is known, i.e., from a large-scale pumping test, and K_G is used as an estimator for the local equivalent hydraulic conductivity at the observation wells.

[30] Figure 6 shows the ensemble averages (Figure 6a) and medians (Figure 6b) of the degradation rate constants estimated using the above five approaches. Only results for method 2 and W_S = 16 m are presented here, because method 2 is only affected by the hydraulic error due to a wrong estimation of flow velocity. Inspection of Figure 6a shows that all approaches lead to an overestimation of the

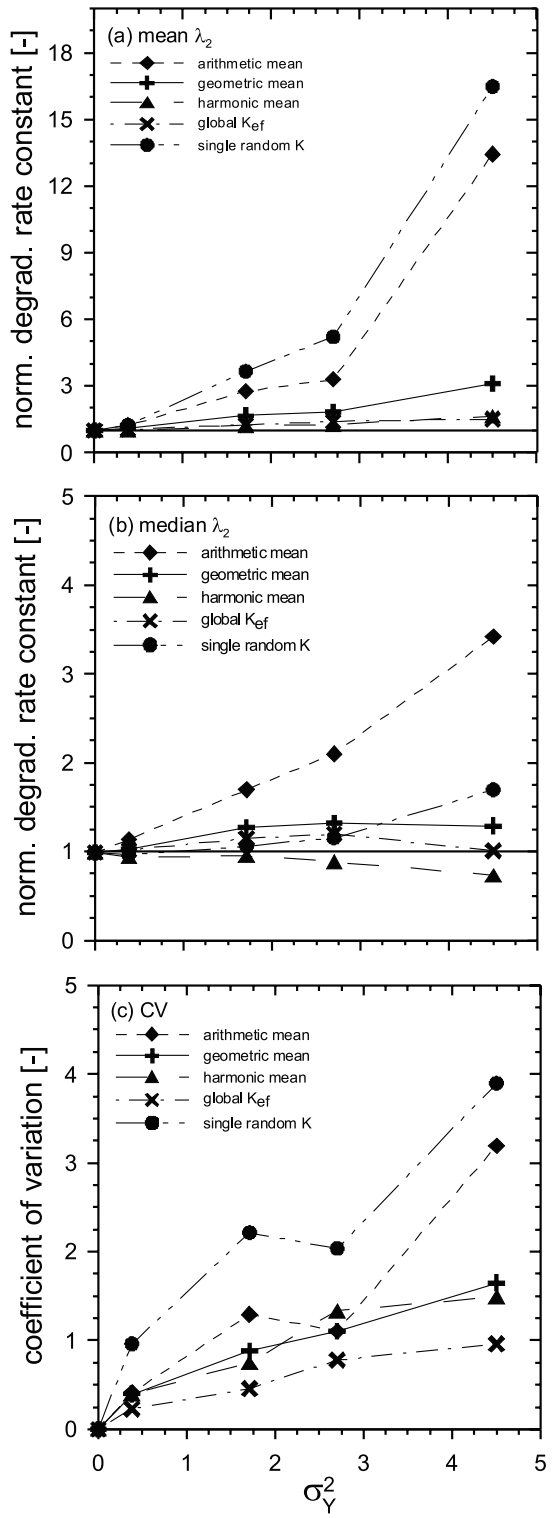

Figure 6. Ensemble (a) means and (b) medians of calculated Λ_2 for the different approaches of average flow velocity estimation and (c) the corresponding coefficients of variation.

ensemble averaged Λ_2, which increases with σ_Y^2. This increase is most pronounced for K_a and K_S. For $\sigma_Y^2 = 4.50$ the average Λ_{2,K_a} is about 4.3 times larger than Λ_{2,K_g}, whereas for single realizations the difference may reach a factor of 70 (not shown here). If only the single K_S value is used, overestimation is even larger for all degrees of heterogeneity. In comparison to the geometric average, using the harmonic average K_h or the true global effective conductivity K_G reduces the overestimation of Λ_2 considerably. Both approaches result in nearly identical ensemble averages. However, inspecting ensemble medians as shown in Figure 6b, harmonic averaging of K measurements results in an underestimation of Λ_2 in more than 50% of all realizations. Taking this into account, usage of the global K_G seems to be the best approach for the estimation of the local average flow velocity between two observation wells along the plume center line. This finding is supported by Figure 6c, which shows coefficients of variation (CV) of Λ_2 as a measure of uncertainty. Using K_G yields the smallest spread. Comparison of all five approaches yields: $CV_{K_G} < CV_{K_g} \approx CV_{K_h} < CV_{K_a} < CV_{K_S}$ for all σ_Y^2. These findings indicate that for the conditions given in this work the best estimate of local flow velocities and of the degradation rate constant is given by the global geometric average of the hydraulic conductivity. This result is expected for large well distances, as then ergodic conditions have been reached. Our results show that also for nonergodic conditions due to small well distances of just a few integral scales the global geometric average yields better estimates of local flow velocity compared to using locally measured hydraulic conductivities. The spread observed in Figure 6 is thus due to the nonergodic conditions of single realizations, i.e., the fact that the plume has sampled only a part of the domain. Thus for a field case, a single large-scale pumping test would be preferable to small-scale local information obtained directly at the sampling wells.

3.4. Influence of Dispersivity Parameterization

[31] As demonstrated in the previous sections, the parameterization of macrodispersivities α_L and α_T solely based on the scale of the contaminant plume according to *Wiedemeier et al.* [1999] using 0.1 of the assumed plume length for α_L and $\alpha_T = \alpha_L/3$ introduces a significant additional error when rate constants are estimated with methods 3 or 4. For method 3, this error is always toward higher rate constants, while for method 4 errors in both directions may occur. It is known that α_L and α_T do not only depend on plume scale, because the variability of flow velocity resulting from the heterogeneity of hydraulic conductivity is also important for the spreading during solute transport. If additional information on the spatial distribution and variability of hydraulic conductivity is available, i.e., from an geologically analogous aquifer, where these parameters have been determined, this information can be used to obtain estimates of the dispersivity values based on aquifer heterogeneity. So far in the manuscript, only estimates based on plume length have been used.

[32] In a two-dimensional isotropic domain with zero local dispersivity and for ergodic conditions, the asymptotic large time longitudinal dispersivity is given by $\alpha_L = \sigma_Y^2 l_Y$, whereas the asymptotic limit of α_T is 0 [*Dagan*, 1989; *Rubin*, 2003]. For the two-dimensional model setup investigated in this manuscript and the values of σ_Y^2 (0.38, 1,71, 2.7, 4.5) and l_Y (2.67) m, the corresponding values for the asymptotic limit of α_L are 1.02, 4.57, 7.21 and 12.02 m, respectively. Close to the source, i.e., in the preasymptotic

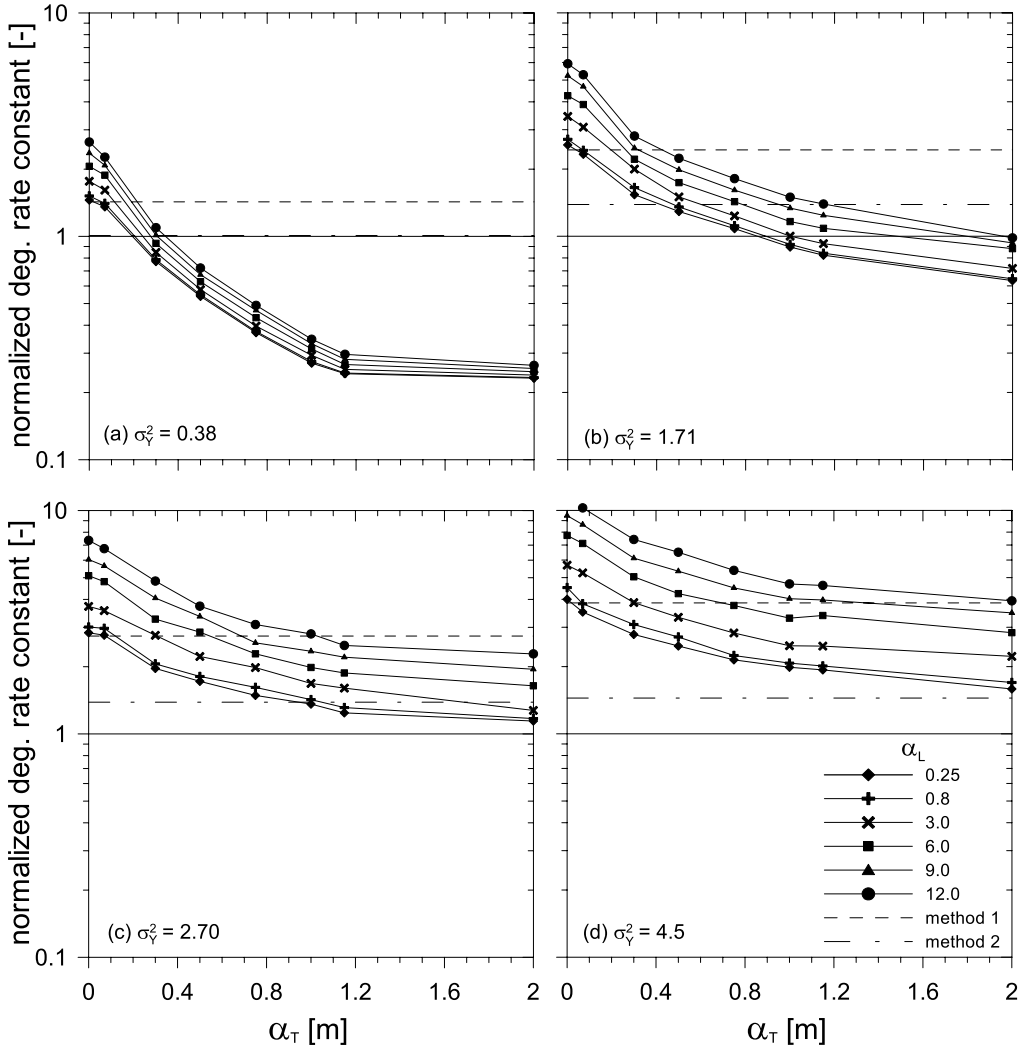

Figure 7. Ensemble medians of estimated first-order rate constants Λ_4 for (a) $\sigma_Y^2 = 0.38$, (b) 1.71, (c) 2.7, and (d) 4.5 for different values of α_L versus α_T. Values for method 3 are obtained using $\Lambda_3(\alpha_L) = \Lambda_4(\alpha_L, \alpha_T = 0)$. Medians for Λ_1 and Λ_2 are depicted in each diagram by dashed and dash-dotted horizontal lines for reference.

region, α_L will show lower values. α_T grows with travel distance until α_T reaches peak values at about 2.5 l_Y of 0.1, 0.44, 0.69 and 1.15 m, respectively. The asymptotic limit of α_T is 0. For nonzero but small local dispersivities ($\alpha_{L,T}$ $l_Y^{-1} \ll 1$), α_L is unaffected or slightly reduced, while α_T increases and a non zero long time limit will establish [*Zhang and Neuman*, 1996]. As the observation wells used for the investigation of the plumes are located within 3.8 to 11.2 l_Y from the contaminant source, it is expected, that the asymptotic limits of α_L and α_T are not yet reached. Thus for methods 3 and 4, α_L values below those listed above should be used. Similarly, α_T values in the range between the peak values and the asymptotic limit should be used for method 4. As this rough estimation already shows, applying the stochastically derived values in a real field case may introduce uncertainty, as the local conditions are generally not known exactly.

[33] To study the influence of dispersivity parameterization on rate constants estimated with methods 3 and 4, the sensitivity of Λ_3 and Λ_4 on different values of α_L and α_T is investigated. Because in a real field application these values will be always uncertain, this investigation is performed as a sensitivity analysis, which allows to cover a wider range of values for α_L and α_T. For α_L values of 12, 9, 6, 3, 0.8 and 0.25 m are used, while for α_T values of 2, 1.15, 1, 0.75, 0.5, 0.3, 0.07 and 0 m are used. Thus the range of reasonable values of α_L and α_T up to the maximum values for each σ_Y^2 is well represented. Figure 7 presents for each σ_Y^2 the medians of estimated rate constants Λ_3, using $\Lambda_3(\alpha_L) = \Lambda_4(\alpha_L, \alpha_T = 0)$, and $\Lambda_4(\alpha_L, \alpha_T)$ in dependence on α_T for the different values of α_L. For reference, also medians for Λ_1 and Λ_2 (compare Figure 4) are included. Because method 2 corrects for dispersion as well as for measuring off the plume center line, but not for errors in the estimated transport velocity, and the same value of the transport velocity is used for all four methods, Λ_2 can be seen as the optimal lower limit for methods 3 and 4. Method 1 involves no correction for longitudinal and transverse dispersion or measuring off the center line. Thus a good parameterization of α_L and α_T for method 4 should result in rate constant estimates $\Lambda_4 < \Lambda_1$. However, $\Lambda_4 < \Lambda_2$ would indicate over correction for transverse dispersion.

[34] Results of the sensitivity study are presented in Figure 7. For all degrees of heterogeneity, decreasing median degradation rates are found with increasing α_T. Differences between the different α_L are most distinct for low values of α_T. Considering method 3, it is clearly shown that $\Lambda_3 = \Lambda_1$ only for $\alpha_L = 0$, and $\Lambda_3 > \Lambda_1$ for $\alpha_L > 0$. This demonstrates again that method 3 always yields higher estimated degradation rate constants as compared to method 1 (compare equation (7)). Considering that generally λ is overestimated in our study, accounting only for α_L by using method 3 aggravates this problem.

[35] For method 4 it is found that for low and medium heterogeneity values for α_L and α_T exist, which allow for an optimal estimation of the degradation rate constant, i.e., $\Lambda_4 = 1$, and thus $\Lambda_4 \leq \Lambda_2$. For $\sigma_Y^2 = 2.70$, $\Lambda_4 > 1.0$ always, but $\Lambda_4 < \Lambda_2$ can be achieved for large values of α_T and small values of α_L. However, for the highest degree of heterogeneity, $\Lambda_4 > \Lambda_2 > 1$ always. For small values of α_T, the degradation rate is overestimated for all degrees of heterogeneity, while for low and medium heterogeneity $\Lambda_4 < 1$ is possible for large values of α_T.

[36] For $\sigma_Y^2 = 0.38$ and $\alpha_T = 0.07$ m, all medians are larger than Λ_1 (when $\alpha_L > 0.8$), at $\alpha_T = 0.3$ all medians are $<\Lambda_2$ (except for $\alpha_L = 12$ m), demonstrating that the rate coefficient is underestimated when too large values for α_T are used (Figure 7a). These findings indicate that using $\alpha_L \approx 0.8$ m and α_T in the range of 0.07–0.2 m for $\sigma_Y^2 = 0.38$ would be appropriate for method 4. For medium heterogeneity ($\sigma_Y^2 = 1.71$, Figure 7b), $\alpha_L \approx 3$ m and α_T between 0.2 and 0.6 m would yield estimates of Λ_4 in between Λ_1 and Λ_2. For $\sigma_Y^2 = 2.7$ with $\alpha_L \approx 6$ m, medians of $\Lambda_4 < \Lambda_1$ are only obtained when $\alpha_T > 0.5$ m (Figure 7c). However, even for an unrealistically large α_T of 2 m, Λ_4 is still significantly larger than Λ_2. A similar behavior is found for $\sigma_Y^2 = 4.5$ (Figure 7d), where only using $\alpha_L = 9$ m and $\alpha_T > 1.15$ m will result in Λ_4 being closer to the true rate constant than the corresponding Λ_1.

[37] These results show, that a wide range of dispersivities can and must be used to obtain better estimates using method 4 than using method 1 or method 2. It is also found that the theoretical values (as given above) lead only for the case of low heterogeneity to considerably better estimates than using method 1. Therefore a large fraction of the observed overestimation must result from off center line measurements, as it cannot be corrected for by reasonable values of α_T. Especially for the cases of high heterogeneity, the effects of dispersion seem to be minor in comparison to the effect of missing the center line.

[38] As shown above, method 4 could yield estimated rate coefficients that are as close or even closer to the true rate constant than rate coefficients estimated with method 2, regardless of the degree of heterogeneity. However, this requires unreasonably low values for α_L and very high values for α_T, as these parameters would have to correct for the off center line measurement errors. In this case, α_L and α_T would no longer represent the actual dispersivities, but are lumped fitting parameters. As the magnitude of bias introduced by missing the center line as well as the exact values of σ_Y^2 or λ_Y are usually not known at a real field site, choosing dispersivities is highly uncertain and may cause over- as well as under-estimation of the degradation rate constant. Thus estimation of dispersivity introduces an additional error into the estimation of degradation rate constants using methods 3 or 4. Only for aquifers of low heterogeneity method 4 yields better estimates than method 1. Better estimates than using method 2 are only possible by assuming unphysical dispersivity values.

4. Summary and Conclusions

[39] In this paper the performance of four different methods for the estimation of degradation rate constants in an aquifer with a heterogeneous distribution of the hydraulic conductivity is studied. All four methods are based on the center line approach. The results demonstrate that a heterogeneous distribution of the hydraulic conductivity may lead to severe overestimation of the ensemble averaged degradation rate constant. Furthermore, the single realizations show a large spread and a large standard deviation, indicating that results obtained from any one estimation are highly uncertain. Mean overestimation as well as spread increase with degree of aquifer heterogeneity. By method comparison, the main reasons are identified as "measuring off the plume center line" and effects of transverse dispersion. Best method performance is observed for method 2, which is based on the one-dimensional transport equation including advection and first order degradation. By normalizing the measured concentrations of the degrading contaminant to a nonreactive co-contaminant emitted by the same source, the above mentioned effects are corrected for. Method 2 thus shows the lowest spread and the lowest overestimation of estimated degradation rate constants of all four methods. However, the presence of the recalcitrant co-contaminant needed for the normalization approach may not always be given at a site. Second best performance is observed for method 1, which yields consistently higher spread and degradation rate constant overestimation as compared to method 2. Methods 3 and 4, although more realistic in the sense that they base on the one-dimensional and two-dimensional transport equation, respectively, show higher spread and larger overestimation. Both methods are prone to errors introduced by estimating longitudinal and transverse dispersivities. The choice of these values introduces additional uncertainty without yielding substantially better results than methods 1 or 2. The ensemble averaged degradation rate constant is highest for method 3, due to the longitudinal dispersivity term in equation (3), while performance of method 4 crucially depends on the choice of an appropriate transverse dispersivity value α_T. If α_T is chosen too small with respect to the real macrodispersivity at the field site under consideration, the degradation rate constant may be overestimated. If α_T is chosen too large, the degradation rate may be underestimated. For all methods, a high spread of the results from the single realizations is found, causing a high uncertainty of the estimated degradation rate constant for all methods. For a single realization, the estimated degradation rate may deviate by one or even two orders of magnitude from the correct value. This deviation is caused only by the heterogeneity of the hydraulic conductivity. The spread observed here may contribute to the spread observed in degradation rate constants observed in the field. *Wiedemeier et al.* [1999] and *Aronson and Howard* [1997] report measured degradation rate constants for PCE ranging over two orders of

magnitude from 0.07 a^{-1} to 1.2 a^{-1} and for TCE ranging from 0.05 a^{-1} to 4.75 a^{-1}. For benzene, toluene and xylene rate constants of 0.07–3.0 a^{-1}, 0.36–21.0 a^{-1} and 0.32–76.0 a^{-1}, respectively, are reported [*Wiedemeier et al.*, 1999]. Method performance increases with increasing source width for all methods. For sources very wide with respect to the integral scale of the hydraulic conductivity field, all methods yield reasonable results. In reality, however, when sources are heterogeneous or formed by a complex combination of a number of zones, the total source width may be difficult to estimate. If degradation rates are used for assessing the NA potential at a contaminated site, overestimation of the degradation rates is a critical point. Overestimation of the degradation rate constant leads to an overestimation of the overall natural attenuation potential. If plume lengths are calculated with too high degradation rate constants, then estimated plume lengths are too short. Remediation times as well as downgradient concentrations may be underestimated. The results presented show that determination of degradation rate constants suffers from two main sources of error, i.e., sampling off the plume center line and an incorrect estimate of the average transport velocity. The first can be overcome by using method 2, the second can be resolved by conducting tracer tests or additional measurements of the hydraulic conductivity. A tracer test would furthermore prove, that the observation wells under consideration are sampling the same flow path. Further work on this subject will include the effects of measurement error on the estimated degradation rates, both in measuring hydraulic head and contaminant concentration. Also effects of different formulations of the kinetic reactions used to simulate the plume will be investigated.

[40] **Acknowledgments.** This work is funded by the German Ministry of Education and Research as part of the KORA priority program, subproject 7.1 Virtual Aquifer. We would like to acknowledge the thoughtful reviews of three anonymous reviewers. Their comments have greatly improved this manuscript.

References

Ababou, R., D. McLaughlin, A. L. Gutjahr, and A. F. B. Tompson (1989), Numerical simulation of three-dimensional saturated flow in randomly heterogeneous porous media, *Transp. Porous Media*, *4*, 549–565.

Aronson, D., and P. H. Howard (1997), Anaerobic biodegradation of organic chemicals in groundwater: A summary of field and laboratory studies, *SRC TR-97-0223F, Sci. Cent. Rep.*, Syracuse Res. Corp., New York.

Bauer, S., and O. Kolditz (2006), Assessing contaminant mass flow rates obtained by the integral groundwater investigation method by using the virtual aquifer approach, *IAHS Publ.*, in press.

Bauer, S., C. Beyer, and O. Kolditz (2005), Assessing measurements of first order degradation rates by using the Virtual Aquifer approach, *IAHS Publ.*, *297*, 274–281.

Bear, J. (1972), *Dynamics of fluids in Porous Media*, Elsevier, New York.

Beinhorn, M., O. Kolditz, and P. Dietrich (2005), 3-D numerical evaluation of density effects on tracer tests, *J. Contam. Hydrol.*, *81*, 89–105, doi:10.1016/j.jconhyd.2005.08.001.

Bockelmann, A., D. Zamfirescu, T. Ptak, P. Grathwohl, and G. Teutsch (2003), Quantification of mass fluxes and natural attenuation rates at an industrial site with a limited monitoring network: A case study, *J. Contam. Hydrol.*, *60*, 97–121, doi:10.1016/S0169-7722(02)00060-8.

Buscheck, T. E., and C. M. Alcantar (1995), Regression techniques and analytical solutions to demonstrate intrinsic bioremediation, in *Intrinsic Bioremediation*, edited by R. E. Hinchee, T. J. Wilson, and D. Downey, pp. 109–116, Battelle Press, Columbus, Ohio.

Chapelle, F. H., P. M. Bradley, D. R. Lovley, and D. A. Vroblesky (1996), Measuring rates of biodegradation in a contaminated aquifer using field and laboratory methods, *Ground Water*, *34*(4), 691–698.

Dagan, G. (1989), *Flow and Transport in Porous Formations*, Springer, New York.

Diersch, H.-J., and O. Kolditz (1998), Coupled groundwater flow and transport: 2. Thermohaline and 3-D convection processes, *Adv. Water Resour.*, *21*(5), 401–425.

Diersch, H.-J., and O. Kolditz (2002), Variable-density flow and transport in porous media: Approaches and challenges, *Adv. Water Resour.*, *25*(8–12), 899–944.

Domenico, P. A. (1987), An analytical model for multidimensional transport of a decaying contaminant species, *J. Hydrol.*, *91*, 49–59.

Dykaar, B. B., and P. K. Kitanidis (1992), Determination of the effective hydraulic conductivity for heterogeneous porous media using a numerical spectral approach: 2. Results, *Water Resour. Res.*, *28*(4), 1167–1178.

Goovaerts, P. (1999), Impact of the simulation algorithm, magnitude of ergodic fluctuations and number of realizations on the spaces of uncertainty of flow properties, *Stochastic Environ. Res. Risk Assess.*, *13*(3), 161–182, doi:10.1007/s004770050037.

Herfort, M. (2000), Reactive transport of organic compounds within a heterogeneous porous aquifer, *Tübinger Geowiss. Arbeiten*, Univ. of Tübingen, Tübingen.

Huyakorn, P. S., and G. F. Pinder (1983), *Computational Methods in Subsurface Flow*, Academic, San Diego, Calif.

Kolditz, O. (2002), *Computational Methods in Environmental Fluid Dynamics*, Springer, New York.

Kolditz, O., and S. Bauer (2004), A process-oriented approach to computing multi-field problems in porous media, *J. Hydroinf.*, *6*(3), 225–244.

Kolditz, O., R. Ratke, H.-J. Diersch, and W. Zielke (1998), Coupled groundwater flow and transport: 1. Verification of variable density flow and transport models, *Adv. Water Resour.*, *21*(1), 27–46.

Kolditz, O., et al. (2004), *GeoSys—Theory and users Manual, Release 4.1*. GeoSystems Res., Cent. for Appl. Geosci., Univ. of Tübingen, Tübingen. (Available at http://www.uni-tuebingen.de/zag/geohydrology.)

McNab, W. W., and B. P. Dooher (1998), A critique of a steady-state analytical method for estimating contaminant degradation rates, *Ground Water*, *36*(6), 983–987.

Newell, C. J., H. S. Rifai, J. T. Wilson, J. A. Connor, J. A. Aziz, and M. P. Suarez (2002), Calculation and use of first-order rate constants for monitored natural attenuation studies, *U.S. EPA Ground Water Issue, EPA/540/S-02/500*, U.S. Environ. Protect. Ag., Washington, D. C.

Pebesma, E. J., and C. G. Wesseling (1998), Gstat: A program for geostatistical modeling, prediction and simulation, *Comput. Geosci.*, *24*(1), 17–31, doi:10.1016/S0098-3004(97)00082-4.

Rehfeldt, K. R., J. M. Boggs, and L. W. Gelhar (1992), Field study of dispersion in a heterogeneous aquifer: 3. Geostatistical analysis of hydraulic conductivity, *Water Resour. Res.*, *28*(12), 3309–3324.

Renard, P., and G. de Marsily (1997), Calculating equivalent permeability: A review, *Adv. Water Resour.*, *20*(5–6), 253–278.

Rubin, Y. (2003), *Applied Stochastic Hydrogeology*, Oxford Univ. Press, New York.

Schäfer, D., A. Dahmke, O. Kolditz, and G. Teutsch (2002), "Virtual Aquifers": A concept for evaluation of exploration, remediation and monitoring strategies, *IAHS Publ.*, *277*, 52–59.

Schäfer, D., B. Schlenz, and A. Dahmke (2004), Evaluation of exploration and monitoring methods for verification of natural attenuation using the virtual aquifer approach, *Biodegradation J.*, *15*(6), 453–465, doi:10.1023/b:biod.0000044600.81216.00.

Stenback, G. A., S. K. Ong, S. W. Rogers, and B. H. Kjartonson (2004), Impact of transverse and longitudinal dispersion on first-order degradation rate constant estimation, *J. Contam. Hydrol.*, *73*, 3–14, doi:10.1016/j.jconhyd.2003.11.004.

Suarez, M. P., and H. S. Rifai (2002), Evaluation of BTEX remediation by natural attenuation at a coastal facility, *Ground Water Monit. Remed.*, *22*(1), 62–77.

Sudicky, E. A. (1986), A natural gradient experiment on solute transport in a sand aquifer: Spatial variability of hydraulic conductivity and its role in the dispersion process, *Water Resour. Res.*, *22*(13), 2069–2082.

Thorenz, C., G. Kosakowski, O. Kolditz, and B. Berkowitz (2002), An experimental and numerical investigation of saltwater movement in coupled saturated-partially saturated systems, *Water Resour. Res.*, *38*(6), 1069, doi:10.1029/2001WR000364.

U.S. Environmental Protection Agency (EPA) (1998), Technical protocol for evaluating natural attenuation of chlorinated solvents in groundwater, *Rep. EPA/600/R/128*, Washington, D. C.

U.S. Environmental Protection Agency (EPA) (1999), Use of monitoring natural attenuation at Superfund, RCRA Corrective Action, and Underground Storage Tank Sites, *Office of Solid Waste and Emergency Response Directive 9200.4-17*, Washington, D. C.

Wiedemeier, T. H., M. A. Swanson, J. T. Wilson, D. H. Kampbell, R. N. Miller, and J. E. Hansen (1996), Approximation of biodegradation rate constants for monoaromatic hydrocarbons (BTEX) in ground water, *Ground Water Monit. Remed.*, *16*(3), 186–194.

Wiedemeier, T. H., H. S. Rifai, T. J. Wilson, and C. Newell (1999), *Natural Attenuation of Fuels and Chlorinated Solvents in the Subsurface*, John Wiley, Hoboken, N. J.

Wilson, R. D., S. F. Thornton, and D. M. Mackay (2004), Challenges in monitoring the natural attenuation of spatially variable plumes, *Biodegradation J.*, *15*(6), 459–469, doi:10.1023/b:biod.0000044591. 45542.a9.

Zamfirescu, D., and P. Grathwohl (2001), Occurrence and attenuation of specific organic compounds in the groundwater plume at a former gasworks site, *J. Contam. Hydrol.*, *53*, 407–427, doi:10.1016/S0169-7722(01)00176-0.

Zhang, D., and S. P. Neuman (1996), Effect of local dispersion on solute transport in randomly heterogeneous media, *Water Resour. Res.*, *32*, 2715–2723.

Zhang, Y.-K. (2003), Non-ergodic solute transport in physically and chemically heterogeneous porous media, *Water Resour. Res.*, *39*(7), 1197, doi:10.1029/2003WR002116.

Zhang, Y.-K., and R. C. Heathcote (2003), An improved method for estimation of biodegradation rate with field data, *Ground Water Monit. Remed.*, *23*(3), 112–116.

S. Bauer, C. Beyer, and O. Kolditz, Center for Applied Geoscience, University of Tübingen, Sigwartstr. 10, D-72076 Tübingen, Germany. (sebastian.bauer@uni-tuebingen.de; christof.beyer@uni-tuebingen.de; kolditz@uni-tuebingen.de)

Enclosed Publication 3

Beyer, C., Bauer, S., Kolditz, O. (2006): Uncertainty Assessment of Contaminant Plume Length Estimates in Heterogeneous Aquifers. J. Contam. Hydrol., 87, 73-95, doi: 10.1016/j.jconhyd.2006.04.006.

Available online at www.sciencedirect.com
ScienceDirect
Journal of Contaminant Hydrology 87 (2006) 73–95
JOURNAL OF Contaminant Hydrology
www.elsevier.com/locate/jconhyd

Uncertainty assessment of contaminant plume length estimates in heterogeneous aquifers

Christof Beyer *, Sebastian Bauer, Olaf Kolditz

Center for Applied Geoscience, University of Tübingen, Sigwartstraße 10, D 72076 Tübingen, Germany

Received 4 November 2005; received in revised form 14 April 2006; accepted 25 April 2006
Available online 16 June 2006

Abstract

The Virtual Aquifer approach is used in this study to assess the uncertainty involved in the estimation of contaminant plume lengths in heterogeneous aquifers. Contaminant plumes in heterogeneous two-dimensional conductivity fields and subject to first order and Michaelis–Menten (MM) degradation kinetics are investigated by the center line method. First order degradation rates and plume lengths are estimated from point information obtained along the plume center line. Results from a Monte-Carlo investigation show that the estimated rate constant is highly uncertain and biased towards overly high values. Uncertainty and bias amplify with increasing heterogeneity up to maximum values of one order of magnitude. Calculated plume lengths reflect this uncertainty and bias. On average, plume lengths are estimated to about 50% of the true plume length. When plumes subject to MM degradation kinetics are investigated by using a first order rate law, an additional error is introduced and uncertainty as well as bias increase, causing plume length estimates to be less than 40% of the true length. For plumes with MM degradation kinetics, therefore, a regression approach is used which allows the determination of the MM parameters from center line data. Rate parameters are overestimated by a factor of two on average, while plume length estimates are about 80% of the true length. Plume lengths calculated using the MM parameters are thus closer to the correct length, as compared to the first order approximation. This approach is therefore recommended if field data collected along the center line of a plume give evidence of MM kinetics.

Keywords: Natural Attenuation; Heterogeneity; Plume length; Center line method; Uncertainty analysis; Monte-Carlo; Numerical modelling

* Corresponding author. Tel.: +49 7071 29 73176; fax: +49 7071 5059.
E-mail address: christof.beyer@uni-tuebingen.de (C. Beyer).

0169-7722/$ - see front matter © 2006 Elsevier B.V. All rights reserved.
doi:10.1016/j.jconhyd.2006.04.006

1. Introduction

One major requirement for the implementation of natural attenuation (NA) as a remedial and risk reduction strategy for contaminated aquifers is an assessment of the dimensions of contaminant plumes and to predict their fate. Down gradient contaminant concentrations, i.e. plume lengths, must be calculated or estimated to identify potential receptors and predict exposure levels. For this purpose analytical and numerical solute transport models (e.g. Bioscreen (Newell et al., 1996), Biochlor (Aziz et al., 2000), Bioplume III (Rifai et al., 1998)) are routinely used. The rate of contaminant removal through biodegradation is a key parameter, as concentrations and the modeled plume lengths are highly sensitive to the degradation rate (McNab, 2001; Suarez and Rifai, 2004). Although very detailed mathematical descriptions of contaminant degradation in the subsurface are available (Baveye and Valocchi, 1989; Rittmann and VanBriesen, 1996; Wiedemeier et al., 1999; Islam et al., 2001), for applications in the field, usually simplified approaches are used because the identification of a large number of parameters and processes from field data is often impossible. Due to its mathematical simplicity, its ease of implementation into transport models and the necessity of determining only a single parameter, the most frequently used degradation model is first order kinetics (Wiedemeier et al., 1999). Field methods for the determination of biodegradation rates in ground water include mass balance calculations, in-situ microcosm studies and the center line method (Chapelle et al., 1996; Wiedemeier et al., 1999). The latter is frequently used for plume monitoring and degradation rate evaluation (e.g. Chapelle et al., 1996; Wiedemeier et al., 1996; Zamfirescu and Grathwohl, 2001; Suarez and Rifai, 2002; Wilson and Kolhatkar, 2002; Bockelmann et al., 2003), and is based on contaminant concentrations measured in observation wells installed along the presumed center line of a plume. This approach, however, is only applicable for plumes that have reached a (quasi-) steady state, i.e. the plume is neither shrinking nor expanding and the measured concentrations do not change with time. The concentration-distance relations thus obtained for a steady state plume can be used to estimate the first order rate constant λ. This parameter can then be used with an appropriate transport model to estimate the contaminant distribution in the aquifer. However, as the spatial variability of aquifer properties has a substantial influence on the distribution of contaminants and plume development, also the results of such an assessment are affected. Wilson et al. (2004) point out that the approach is prone to errors because the center line of a plume may be missed by monitoring wells if the inferred ground water flow direction is incorrect or the contaminant plume meanders in all three dimensions due to macro-scale heterogeneities. McNab and Dooher (1998) demonstrated that, even in a homogeneous aquifer, transverse dispersion can produce center line concentration profiles of recalcitrant compounds that exhibit characteristics consistent with first order degradation; this can easily lead to misinterpretation of the monitoring data. The result of these complicating factors is that the degradation potential may be severely overestimated, causing underestimation of plume length or contaminant mass and an over optimistic prognosis of down gradient concentrations and exposure levels. Moreover, it is well known that the use of first order kinetics may be problematic in some situations, as it is a poor representation of the processes occurring in contaminated aquifers. Usage of a first order model outside its range of validity may result either in significant under- or overestimation of the attenuation potential at a site (Bekins et al., 1998). In a numerical experiment, Schäfer et al. (2004a) demonstrated that for specific points in time, first order kinetics may be able to approximately reproduce mass and dimensions of contaminant plumes that follow from a far more complex degradation model. For a long term prognosis, however, the first order approximation proved inappropriate, resulting in an underestimation of plume length and contaminant mass. Recently, Bauer et al. (2006) performed a sensitivity study on the influences of aquifer heterogeneity on first

order degradation rate constants estimated from using the center line method. This study demonstrated that aquifer heterogeneity introduces significant uncertainty in the estimated rate constants and may cause a severe overestimation of the degradation potential.

Since the determination of degradation rates is usually only an intermediate step for the characterization of contaminated sites, the present paper takes the approach of Bauer et al. (2006) one step further. Here, the uncertainty involved in the estimation of contaminant plume lengths in heterogeneous aquifers is evaluated using the Virtual Aquifer concept. Three different scenarios are studied in detail. In case A, synthetic contaminant plumes following first order degradation kinetics are investigated. First order rate constants are estimated by methods typically used in field applications. The rate constants are then used to calculate the corresponding contaminant plume lengths with analytical transport models. As the first order degradation model results in theoretically infinite plumes, a relative concentration contour line is defined as the plume length here. Results are analysed with regard to errors and uncertainty in the rate constants and their propagation to the plume length estimates. In case B, the additional error is studied that arises when a first order approximation is used although degradation kinetics deviate from a first order rate law. Here the attenuation potential for plumes following Michaelis–Menten (MM) degradation kinetics is assessed using the same first order methods employed in case A. In case C, a regression approach is used to estimate the MM parameters and plume lengths for the plumes with MM degradation kinetics. Results are compared to cases A and B to allow conclusions about potentials and limitations of this approach.

2. Virtual Aquifer concept

Due to the limited accessibility of the subsurface, measurements of piezometric heads and pollutant concentrations at contaminated sites are sparse and may not be representative of the heterogeneous hydrogeologic conditions. Any site investigation is thus subject to uncertainty, reflecting the limited knowledge of the aquifer properties and the extent of the contamination. Due to this uncertainty, field investigation methods for plume screening and measuring of hydraulic conductivity or degradation rates can neither be tested nor verified in the field. One appropriate method of assessing the performance and reliability of field investigation methods is by studying them in heterogeneous synthetic (virtual) aquifers. With this approach the results of a particular method can be compared to the "true" values, as these values are known from the synthetic aquifer.

The "Virtual Aquifer" concept is a combination of different methodologies, tools and techniques, particularly aimed at this type of problem. Its two key components are (1) a flexible and efficient modelling system, allowing the numerical simulation of reactive multi-component transport in the subsurface, and (2) an extensive database, containing statistical information, physical and (bio-) geochemical data from a large number of well investigated sites and aquifers. Moreover, the concept comprises a collection of analytical and numerical methods, that are commonly used for the investigation of contaminated sites and aquifers or the interpretation of measured data. The synthesis of both, the database and the simulation system allows a proper definition and computer based evaluation of scenarios and case studies, focussed on investigation strategies, redevelopment and monitoring at contaminated sites.

As a first step for such an analysis, synthetic aquifer models are generated based on the statistical properties of real aquifers. Thus, to a certain degree, these aquifer models represent realistic analogues of existing sites. A defined source of contamination is then introduced and a reactive transport model is used to simulate the evolution of the plume, resulting in realistic concentration distributions in the synthetic aquifer. In comparison to the "real world", the unique advantage of the synthetic aquifer is that the spatial distribution of all physical and geochemical properties and parameters as well as the

contaminant concentrations are exactly known. In the second step, the synthetic aquifer is investigated by standard monitoring and investigation techniques. Although the parameter distribution of the synthetic aquifer is known a priori, only the data "measured" at the observation wells (i.e. hydraulic heads and concentrations) are used and interpreted. This is done because in a real site investigation also only a limited amount of measured data would be available, with the amount of information depending on investigation intensity and project finances. In the third step, the investigation results are compared to the "true" values, allowing an evaluation of the accuracy of the investigation method. In addition, the use of synthetic aquifers offers the possibility to assess the influence of different parameters, such that sources of uncertainty and error for the investigation method can be considered individually and the sensitivity of investigation results on these can be studied. Stochastic simulation techniques like the Monte-Carlo method are applied to study the propagation of parameter variability and uncertainty into the investigation results. Due to the ability to perform extensive and detailed scenario analysis and visualization, this approach is well suited to the exploration of the uncertainty involved in hydrogeologic investigation and management. The methodology has been applied under the term "Virtual Aquifer" by Schäfer et al. (2002, 2004b), Bauer and Kolditz (2005) and Bauer et al. (2005, 2006).

3. Scenario definition

In this study, the Virtual Aquifer concept is used in a Monte-Carlo framework to assess the influence of spatially heterogeneous hydraulic conductivities on the estimation of degradation rates and contaminant plume lengths. Multiple plume realizations of contaminants degrading according to a first order degradation kinetics or Michaelis–Menten kinetics in aquifers with different degrees of heterogeneity are investigated using the center line approach. By comparison of the estimated degradation rates and plume lengths with the respective virtual reality data the investigation methods are tested and evaluated. Three different cases are studied in detail:

In case A, four different standard methods for the determination of the first order rate constant λ are applied to concentration vs. distance data obtained from investigation of synthetic contaminant plumes following first order degradation kinetics. Accordingly, four different rate constants are estimated for each plume realization. For each λ the length of the contaminant plume is estimated using an analytical transport model. The four methods and the corresponding analytical transport models are introduced in Sections 4.1 and 4.2. The main objectives of case A are to test the applicability and performance of the four different methods of determining the first order degradation rate constant in heterogeneous aquifers and to analyse the propagation of errors and uncertainty from the rate constant to the plume length estimate.

In case B, the same four methods are evaluated with regard to their ability to approximate the degradation potential and estimate the plume length, when the true degradation kinetics deviate from first order. Here plumes following MM degradation kinetics are investigated in an analogous manner to case A. The additional error that arises from the first order approximation is studied. The motivation behind this scenario is that although it is well known that contaminant degradation in natural aquifers may follow far more complicated processes and kinetic laws than a simple first order model, the latter is routinely used at many field sites. Therefore, this scenario highlights some of the problems that result from this discrepance.

In case C, a regression approach is studied which allows the estimation of MM kinetic parameters from plume center line data. This method is developed in Section 4.1 and tested under the influence of aquifer heterogeneity in case C. Here the plumes following MM degradation kinetics are investigated. As for cases A and B the propagation of errors and uncertainty from the estimated MM

Table 1
Overview of scenarios studied

Case	Contaminant plume following	Degradation rate determined with	Plume length determined with	Results in section
A	First order kinetics	First order kinetics (Eqs. (1)–(4))	First order kinetics (Eqs. (7)–(9))	6.1
B	Michaelis–Menten kinetics	First order kinetics (Eqs. (1)–(4))	First order kinetics (Eqs. (7)–(9))	6.2
C	Michaelis–Menten kinetics	Michaelis–Menten kinetics (Eq. (5))	Michaelis–Menten kinetics (Eq. (10))	6.3

parameters to the plume lengths is analysed. Results are set in relation to cases A and B to discuss advantages and disadvantages, potentials and limitations of the MM parameter estimation approach. An overview of the three different cases is given in Table 1.

4. Methods

4.1. Estimation of degradation rate constants

Four different standard methods for the determination of the first order degradation rate constant λ (Table 2, Eqs. (1)–(4)) are compared in this study. Each of the four methods requires concentration-distance relations obtained by measuring contaminant concentrations in several observation wells along the center line of a steady state plume. The degradation rate constant λ is estimated by fitting a linear function to the logarithms of concentration vs. distance from the source by linear regression. Methods 1–4 are introduced only briefly here, more details are given in Bauer et al. (2006). Furthermore, a regression approach that allows the estimation of MM kinetics parameters from center line data is developed and tested as method 5 (Table 2, equation (5)).

Method 1 (Table 2, equation (1)) is based on the one dimensional transport equation, considering advection and first order degradation only. Rate constants determined with method 1 can be considered rather an overall or bulk attenuation rate than a degradation rate constant (Newell et al., 2002) as all concentration changes that result from processes other than degradation, such as diffusion, dispersion, volatilization and dilution, are attributed to the degradation process. Method 2 (Table 2, equation (2); Buscheck and Alcantar, 1995) is based on the steady state solution to the one dimensional transport equation considering advection, longitudinal dispersion and first order degradation. Method 2 thus requires an estimate of longitudinal dispersivity α_L [m]. Method 3 (Table 2, equation (3)) was proposed by Zhang and Heathcote (2003) and represents a two-dimensional modification of method 2. A correction term derived from the analytical solution of the two-dimensional transport equation including first order decay (Domenico, 1987) is used to account for lateral spreading and the width of the source zone. A similar approach, which also allows the inclusion of measurements off the plume center line was presented by Stenback et al. (2004). Method 4 (Table 2, equation (4); Wilson et al., 1994; Wiedemeier et al., 1996) is based on the same transport equation as method 1. However, measured concentrations of the reactive contaminant are scaled by up and down gradient concentration C_0^* and $C(x)^*$ [$M\,L^{-3}$] of a non-degrading conservative solute spreading from the same source. Since dispersion and measuring off the center line also affect the measured concentrations of non-reactive solutes, this procedure allows a correction for both effects. Method 5 (Table 2, equation (5)) is valid for contaminant plumes following Michaelis–Menten (MM) degradation kinetics (Beyer et al., 2005). When the

Table 2
Estimation of first order degradation rate constants (methods 1–4) and Michaelis–Menten degradation kinetics parameters (method 5) from center line data

Method (equation)	Formula	Description	Parameter estimated
(1)	$\lambda_1 = -\frac{v_a}{\Delta x}\ln\left(\frac{C(x)}{C_0}\right)$	1D transport equation with advection and first order degradation; advective velocity, v_a, source concentration C_0, down gradient concentration, $C(x)$, first order degradation rate constant, λ, distance, x	λ
(2)	$\lambda_2 = \frac{v_a}{4\alpha_L}\left(\left(1-2\alpha_L\frac{\ln(C(x)/C_0)}{\Delta x}\right)^2-1\right)$	1D transport equation with advection, longitudinal dispersion and first order degradation; longitudinal dispersivity, α_L	λ
(3)	$\lambda_3 = \frac{v_a}{4\alpha_L}\left(\left(1-2\alpha_L\frac{\ln(C(x)/(C_0\beta))}{\Delta x}\right)^2-1\right)$ with $\beta = \mathrm{erf}\left(\frac{W_S}{4\sqrt{\alpha_T\Delta x}}\right)$	2D transport equation with advection, longitudinal and transverse dispersion, source width and first order degradation; transverse dispersivity, α_T, source area width, W_S	λ
(4)	$\lambda_4 = -\frac{v_a}{\Delta x}\ln\left(\frac{C(x)}{C_0}\frac{C_0^*}{C(x)^*}\right)$	Same as method 1; contaminant concentrations normalized with regard to conservative solute concentrations, C_0^*, $C(x)^*$	λ
(5)	$\frac{\Delta x}{v_a(C_0-C(x))} = \frac{M_C}{k_{max}}\frac{\ln(C_0/C(x))}{C_0-C(x)}+\frac{1}{k_{max}}$	1D transport equation with advection and Michaelis–Menten degradation kinetics; maximum degradation rate, k_{max}, half saturation concentration, M_C	k_{max}, M_C

Table 3
Calculation of contaminant plume lengths for first order and Michaelis–Menten degradation kinetics

Method	Formula	Equation
1	$L_1 = \Delta x = -\frac{v_a}{\lambda}\ln(C(x)/C_0)$	(7)
2	$L_2 = \Delta x = 2\alpha_L \frac{\ln(C(x)/C_0)}{1-(1+4\lambda\alpha_L/v_a)^{0.5}}$	(8)
3, 4	$L_{3,4} = \Delta x_i$, for $\frac{C(x)}{C_0} - \exp\left\{\frac{\Delta x_i}{2\alpha_L}\left[1-\sqrt{1+\frac{4\lambda\alpha_L}{v_a}}\right]\right\}\mathrm{erf}\left(\frac{W_S}{4\sqrt{\alpha_T \Delta x_i}}\right) = 0$	(9)
5	$L_{MM} = \Delta x = \frac{v_a}{k_{max}}\left[M_C \ln\left(\frac{C_0}{C(x)}\right) + C_0 - C(x)\right]$	(10)

degradation of a contaminant is not limited by electron acceptor availability and the microbial density is assumed to be constant with time, Eq. (6) applies (Simkins and Alexander, 1984):

$$\frac{dC}{dt} = -k_{max}\frac{C}{C+M_C} \tag{6}$$

where k_{max} is the maximum degradation rate [$M\,L^{-3}\,T^{-1}$] and M_C is the MM half-saturation concentration [$M\,L^{-3}$]. This approximation may be applicable when aquifer sediments have been exposed to contaminants for several years (Bekins et al., 1998). The integral form of Eq. (6) can be rearranged to yield equation (5) of Table 2. According to Robinson (1985), equation (5) is the most reliable of several different formulations of the integrated MM model for estimation of k_{max} and M_C. Both parameters are estimated by a linear least squares fit of $\Delta x/[v_a(C_0 - C(x))]$ vs. $\ln(C_0/C(x))/(C_0 - C(x))$. Thus k_{max} is obtained as the reciprocal of the intercept of the linear function and M_C as its slope multiplied by k_{max}. Application of method 5 assumes advective transport only (see also Parlange et al., 1984). As Robinson (1985) points out, application of a linearized integrated MM model for least squares estimation of its parameters may be problematic, because measured concentrations $C(x)$ appear in the dependent as well as in the independent variable. A preliminary examination of several nonlinear least squares approaches for fitting the MM parameters to the concentration vs. distance data showed that the parameters determined by method 5 were on average more accurate than those obtained by other methods.

4.2. Estimation of contaminant plume lengths

Given a first order degradation rate constant λ (by estimation with one of the four center line methods presented above), equations (1)–(3) (Table 2) can be rearranged to calculate the length of the steady state contaminant plume (see Table 3). The plume length here is defined as the largest distance between the source and the concentration isoline for concentration C_{PL} [$M\,L^{-3}$]. Equation (7) gives this distance for the purely advective case of method 1, equations (8) and (9) correspond with methods 2 and 3, respectively. As the rate constant estimated with method 4 is corrected for dispersion, this process has to be accounted for when the plume length is calculated. Therefore equation (9) is also used for calculation of plume lengths based on λ_4. A steady state plume length can also be calculated using the MM parameters estimated using method 5. Rearrangement of equation (5) of Table 2 yields equation (10) and gives the distance L_{MM} at which concentrations fall

below C_{PL}. To define the plume length for this study, the 1% relative concentration contour line of the contaminants is used, i.e. $C_{PL}=C(x)/C_0=0.01$.

4.3. Numerical Monte-Carlo simulations

To study the influence of heterogeneous hydraulic conductivity on the investigation results two-dimensional virtual aquifers are used. The model domain has dimensions of 184 m length and 64 m width (Fig. 1). A mean hydraulic gradient I of 0.053 is induced by fixed head boundary conditions on the left and the right hand side of the model domain. No flow boundary conditions are assigned to all other sides. Flow conditions are at steady state.

The model domain is discretized with a grid density of 0.5 m in both directions. A contaminant source of 3 m × 8 m, represented by a fixed concentration boundary condition, is centered at [11.5 m; 32.0 m] down stream of the inflow boundary. The source emits two reactive contaminants and a conservative compound, each with a unit concentration of 1. The first reactive contaminant is degraded by first order kinetics with a rate constant $\lambda=5.87\cdot10^{-7}$ s^{-1}. Degradation of the second reactive contaminant follows MM kinetics. MM parameters are taken from Bekins et al. (1998) ($k_{max}=3.9\cdot10^{-9}$ g L^{-1} s^{-1} and $M_C=1.33\cdot10^{-3}$ g L). Using the source concentration of $2.68\cdot10^{-2}$ g L^{-1} given in Bekins et al. (1998) these parameters were scaled to a dimensionless source concentration of 1.0, as used here, yielding relative values (in normalized units) of $k_{max}=1.45\cdot10^{-7}$ s^{-1} and $M_C=4.97\cdot10^{-2}$. Thus the first order and MM plume lengths for both compounds are equal in a two-dimensional homogeneous aquifer for $C_{PL}=C(x)/C_0=0.01$. Neither growth of microorganisms nor limitation or inhibition of degradation by other substances is considered here. All compounds are not retarded and show no volatilization. The conceptual model used in this study is a rigorous simplification of the processes observed in natural aquifer systems, where degradation follows more complicated laws and is spatially dependent. The model setup is thus designed to provide ideal conditions for the application of the center line methods to be studied. This is certainly not the case in nature, where the reaction kinetics will follow more complicated laws, may be spatially dependent, be steered by the availability of electron donors and acceptors, or additional influences from transient effects and dilution have to be accounted for. However, these simplifying assumptions are used here to be able to study the standard methods closely and evaluate individually the influence of heterogeneity of the hydraulic conductivity and the influence of degradation kinetics on the performance of the methods under otherwise ideal conditions. Case B (Table 1) is the case were we study the combination of errors stemming from hydraulics and from reaction kinetics.

The hydraulic conductivity K of the virtual aquifers is regarded as a spatial random variable, following a lognormal distribution with an expected value of $E[Y=\ln(K)]=-9.54$, which corresponds to an effective conductivity K_{ef} of $7.19\cdot10^{-5}$ m s^{-1} using the geometric mean. An isotropic exponential covariance function with an integral scale l_Y of 2.67 m is used for the spatial correlation

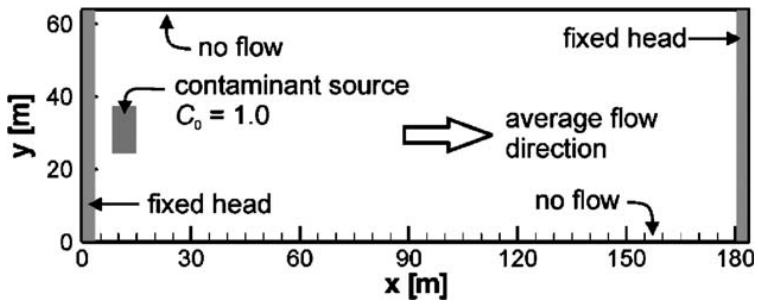

Fig. 1. Virtual Aquifer model domain and boundary conditions.

structure. Four different cases with increasing heterogeneity, i.e. ln(K) variances σ_Y^2 of 0.38, 1.71, 2.7 and 4.5, respectively, are considered in this study, representing mildly to highly heterogeneous conductivity fields. The parameters l_Y and σ_Y^2=0.38 are taken from the Borden field site (Sudicky, 1986); the value of 1.71 was found at the Testfeld Süd in southern Germany (Herfort, 2000); the values of 2.7 and 4.5 were reported for the Columbus Air Force Base site (Rehfeldt et al., 1992). A constant porosity n of 0.33 is used, resulting in a mean flow velocity v_a of $1.16 \cdot 10^{-5}$ m s^{-1}. For each of the four degrees of heterogeneity, ensembles of 100 realizations of the random field are generated by unconditional Gaussian simulation. The Monte-Carlo strategy is chosen in order to obtain statistical measures of the errors and uncertainties introduced by the heterogeneity of K. Plumes of the three compounds are generated in each virtual aquifer using a process based numerical flow and reactive transport model. The GeoSys/RockFlow simulation code (Kolditz et al., 2004) is used here, which solves the flow and transport equations by finite element methods. The governing equations are given as (e.g. Bear, 1972; Kolditz, 2002):

$$\nabla(K\nabla h) = 0 \tag{11}$$

$$\frac{\partial C}{\partial t} = -v_a \nabla C + \nabla(D\nabla C) - \Gamma \tag{12}$$

with h as the piezometric height, K the tensor of hydraulic conductivity, C concentration, D the dispersion tensor, t time and Γ a sink term representing first order or MM degradation kinetics. For local dispersivities α_L and α_T values of 0.25 m and 0.05 m were used. Details of numerical and software issues can be found in Kolditz (2002) and Kolditz and Bauer (2004). All model parameters are summarized in Table 4.

5. Investigation of the synthetic plumes

The steady state contaminant plumes in each virtual aquifer are investigated by the center line method (see Fig. 2). Initially three observation wells are present in the aquifer (Fig. 2 (a)), one being located directly in the source in the center of the aquifer (full circle) at [13.0 m; 32.0 m], showing high concentrations. This setup is the starting point for the investigation of all realizations. The initial knowledge on the site comprises only the hydraulic heads at the three wells. The full concentration,

Table 4
Model parameters used in the numerical simulations

Parameter		Value
K_{ef}	Effective conductivity	$7.19 \cdot 10^{-5}$ m s^{-1}
σ_Y^2	ln(K)-variance	0, 0.38, 1.71, 2.7, 4.5
l_Y	Integral scale	2.67 m
n	Porosity	0.33
I	Hydraulic gradient	0.053
α_L	Longitudinal dispersivity	0.25 m
α_T	Transverse dispersivity	0.05 m
λ	First order degradation rate constant	$5.87 \cdot 10^{-7}$ s^{-1}
k_{max}	Maximum degradation velocity [a]	$1.45 \cdot 10^{-7}$ s^{-1}
M_C	Half saturation concentration [a]	0.0497

[a] In normalized units, see explanation in the text.

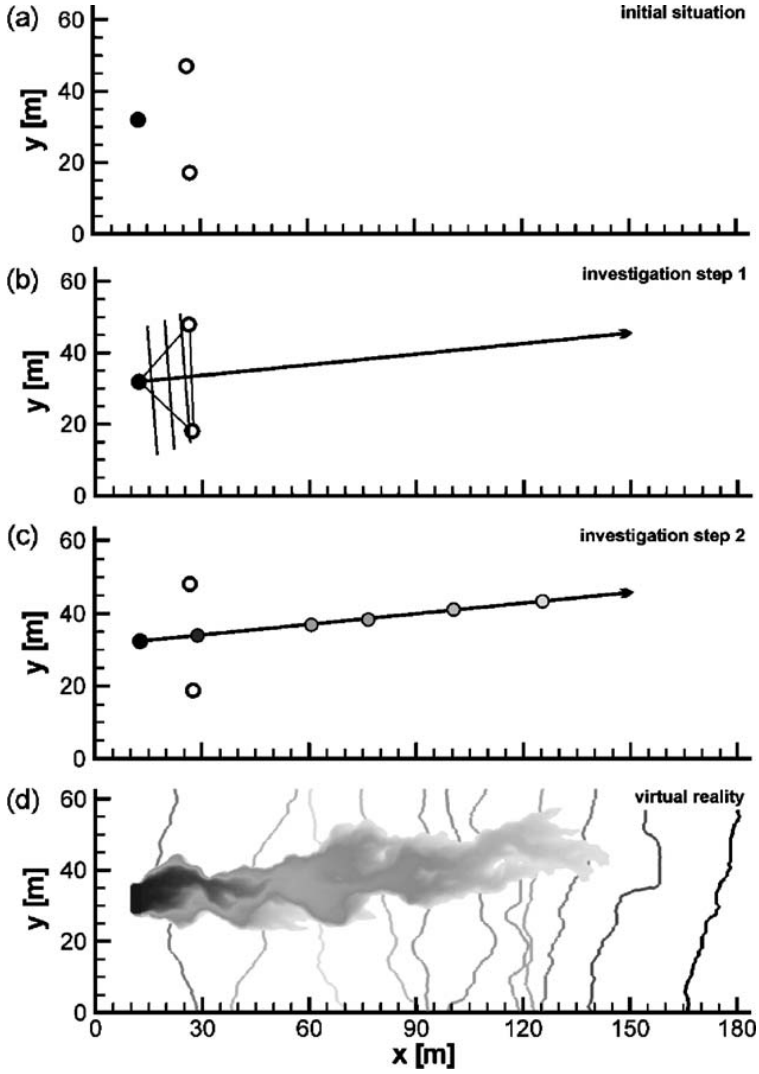

Fig. 2. Investigation of a virtual plume by the center line approach: (a) initial situation, (b) estimation of flow direction by application of a hydrogeologic triangle, (c) observation wells on the inferred center line, (d) comparison to virtual reality (concentration and heads).

head and conductivity distributions of the virtual sites are assumed unknown. In the first investigation step, the flow direction is determined (Fig. 2 (b)). A hydrogeologic triangle is constructed and the hydraulic gradient is calculated using the heads measured at the three wells. After this, five new observation wells are installed along the estimated flow direction with distances of 15, 50, 75, 100 and 125 m from the source (Fig. 2 (c)). At these and at the well at the source hydraulic heads and concentrations of the three compounds are measured. Additionally, local hydraulic conductivities are determined (e.g. by a slug test). The geometric mean of these six K values is used as an estimator for the effective conductivity K_{ef} along the flow path. From the head difference, the true porosity and K_{ef} an average v_a is calculated. For methods 3 and 4, estimates of dispersivities α_L and α_T are required. Following Wiedemeier et al. (1999) α_L is taken as 0.1 of the plume length and α_T is assumed to be 0.1 of α_L. As the true plume length is unknown at this stage of the site investigation, the maximum distance covered by the observation wells, i.e. 125 m, is used. Consequently, α_L and α_T are estimated to be 12.5 and 1.25 m, respectively. Of course, such rather rough estimates of α_L and α_T are not optimal, as they are not based on the heterogeneity structure of the aquifer. In practice, however, dispersivities based on results from stochastic hydrogeology are difficult to obtain, as for most field sites structure and degree of heterogeneity are not well characterized. Also with this scenario, the

samples taken at all eight wells do not allow for an estimation of l_Y and σ_Y^2, which would be required to derive α_L and α_T. A detailed study on the effects of dispersivity parameterization on the performance of methods 2 and 3 is presented in Bauer et al. (2006).

The information obtained by the site investigation allows the application of the five methods for estimation of the degradation kinetic parameters and the subsequent calculation of contaminant plume lengths as presented in Sections 4.1 and 4.2. The investigation setup is designed to resemble ideal conditions for this purpose. All measurements are assumed to be exact, i.e. without measurement error, and are obtained by reading the model output at the respective well positions. The only uncertainty and variability is introduced by the heterogeneity of the hydraulic conductivity.

6. Results and discussion

As outlined in Section 3, three different cases A, B and C are investigated here (see Table 1). The next three Sections 6.1, 6.2 and 6.3 present detailed results and discussions for each case studied. A detailed comparison and discussion of the performance of the different approaches is given in Section 6.4.

6.1. Case A: estimation of first order degradation rate constants and plume lengths for plumes following a first order degradation kinetics

6.1.1. Estimation of rate constants

In case A methods 1–4 are tested and compared based on their ability to estimate the first order degradation rate constant λ and the contaminant plume length in heterogeneous aquifers. Therefore, plumes following first order degradation kinetics are investigated here. The four estimated rate constants λ_i are divided by the true rate constant to yield corresponding normalized Λ_i, which can be interpreted as an over- or underestimation factor. Fig. 3 presents ensemble means with corresponding standard deviations as error bars, medians, coefficients of variation and the single realization results for methods 1–4 against the aquifer heterogeneity σ_Y^2.

Results for method 1 (Fig. 3 (a)) show that $\Lambda_1 = 1$ in the homogeneous case ($\sigma_Y^2 = 0$), thus in this case the true rate is obtained. However, already for the lowest degree of heterogeneity ($\sigma_Y^2 = 0.38$), about 77% of the rate constants estimated fall above the reference line which indicates the true rate constant, overestimating λ up to factors of 4.79 in the worst case. In the remaining realizations λ is underestimated. The spread of the ensemble of 100 realizations covers about one order of magnitude. When σ_Y^2 is further increased, spread and standard deviation also increase. For $\sigma_Y^2 = 4.5$ the Λ_1 cover almost two orders of magnitude with single realizations showing overestimation factors > 10. Mean Λ_1 is 3.3 with standard deviation and coefficient of variation of 3.65 and 1.11, respectively. Increasing the heterogeneity of the aquifer thus results in a higher uncertainty of λ and increases the probability of a significant overestimation. For method 2 normalized rate constants Λ_2 are shown in Fig. 3 (b). As seen for method 1 a systematic overestimation of λ can be observed, increasing with σ_Y^2. However, the Λ_2 are significantly larger than the corresponding Λ_1. In the homogeneous case method 2 yields $\Lambda_2 = 1.7$, increasing to 9.38 for $\sigma_Y^2 = 4.50$. In extreme cases, overestimation of λ is larger than a factor of 50. Also spread and standard deviations are larger than for Λ_1. Estimated rate constants Λ_3 obtained by method 3 (Fig. 3 (c)) are only slightly lower than those of method 2, ranging from 1.17 in the homogeneous case to 7.39 for $\sigma_Y^2 = 4.5$. Method 4 (Fig. 3(d)) yields the true rate for homogeneous conditions, i.e. $\Lambda_4 = 1$. As for the other methods, spread and uncertainty increase with σ_Y^2. Compared to methods 1–3 the spread is smaller and balanced around the true rate constant. For $\sigma_Y^2 \leq 2.7$ the ensemble averages and medians match the true rate constant well. For $\sigma_Y^2 = 4.50$ the average Λ_4 reaches 1.73.

The overestimation observed for the different Λ_i results from a combination of several effects. Method 1, which is the simplest approach used in this study, is based on the one dimensional transport equation only accounting for advection and degradation. Concentration reductions on the plume center line caused by transverse dispersion therefore are incorrectly attributed to the degradation process and Λ_1 is overestimated. Moreover, when the inferred center line deviates from the true center line, concentrations measured are too low, which further increases rate overestimation. A third source of error is the estimate of v_a (see Section 5), which may not be representative for the flow path. Overestimation is caused if v_a is estimated too high, while a too low value of v_a causes underestimation of the rate constant. All three error types are also relevant for method 2. The additional bias of method 2 towards too large rate constants in comparison with method 1 is a consequence of accounting for α_L in equation (2) of Table 2. Longitudinal dispersion of a degrading contaminant results in a stronger spreading of the solute down stream and consequently in higher concentrations along the center line of a steady state plume. Equation (2) can be rearranged to show that $\lambda_2 = \lambda_1 + \alpha_L v_a (\ln(C(x)/C_0)/\Delta x)^2$, i.e. λ_2 grows linearly with α_L and is always larger than λ_1 for $\alpha_L > 0$. Method 3 is affected by errors in v_a and off center line measurements. By accounting for transverse dispersion, rate constant estimates are improved compared to method 2, because $\beta < 1.0$ in equation (4) and thus $\Lambda_3 < \Lambda_2$ always. Because β approaches unity for arguments > 2, Λ_3 converges with Λ_2 for small α_T, short transport distances Δx

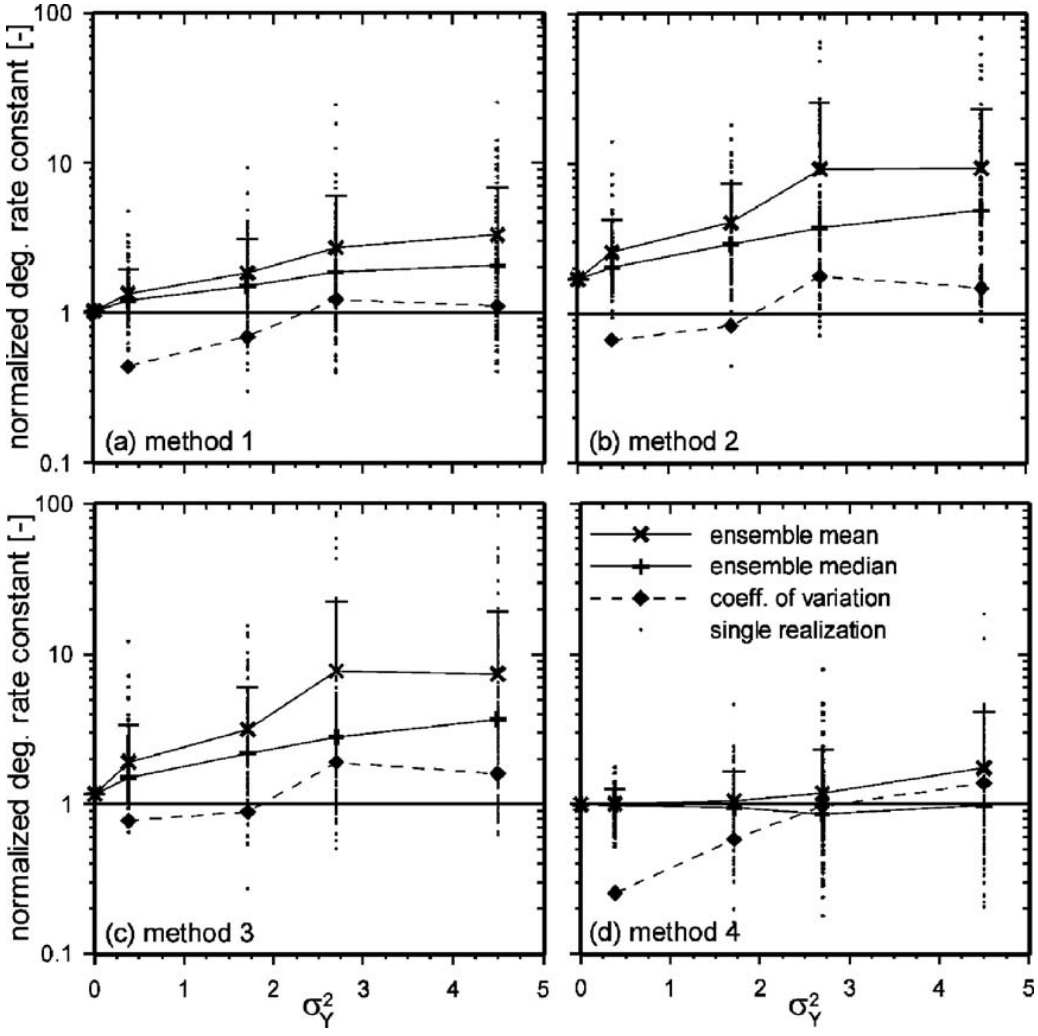

Fig. 3. Estimated first order degradation rate constants Λ_i (normalized to the true rate constant λ, indicated by the horizontal line) vs. heterogeneity of the aquifer σ_Y^2 for methods 1 (a), 2 (b), 3 (c) and 4 (d) for case A.

and large source widths W_S. A surprising result is that method 1, despite its simplicity, yields closer estimates of the true rate constant than the more comprehensive description by method 3. Since method 3 depends on longitudinal and transverse dispersivities, an adequate parameterization is crucial for its success. From stochastic hydrogeology it is known that α_L as well as α_T strongly depends on travel time and distance as well as on the correlation structure of hydraulic conductivity and flow velocity (e.g. Dagan, 1989). Consequently, a uniform parameterization solely based on the scale of the contaminant problem as used in this study (and with many field applications) is not adequate. A detailed sensitivity study on the influence of dispersivity parameterization on the performance of methods 2 and 3 is presented in Bauer et al. (2006). It is found that for method 2 no value of α_L and for method 3 only very high and thus unphysical values of α_T yield the correct degradation rate constant. The required values, however, cannot be deduced from aquifer heterogeneity σ_Y^2 alone, as the other errors also influence the estimated degradation rate constant.

Method 4 circumvents this problem and corrects for transverse dispersion as well as for measuring off the center line by normalizing concentrations to a conservative tracer. The bias towards too large degradation rate constants observed for the other methods is significantly reduced yielding the closest estimates of λ of the four methods. The remaining deviation from the true rate constant is due to the hydraulic error introduced by the approximation of v_a. For low heterogeneities there is no evidence for a systematic bias towards either too high or too low rate constants. A prerequisite which may limit the applicability of method 4 is the presence of a suited normalization compound. A discussion of potential normalization compounds is provided in U.S. EPA (1998) and Wiedemeier et al. (1996, 1999).

6.1.2. Estimation of plume lengths

During site characterization, estimating degradation rate constants rarely is a goal per se. Here, the kinetics of contaminant degradation are quantified to be used for prediction of the steady state length of the plumes. In site assessment, such information could be used to identify potential receptors and exposure levels. Rate constants λ_1, λ_2 and λ_3 are evaluated using the respective corresponding equations (7), (8) and (9) of Table 3 yielding plume length estimates L_1, L_2 and L_3. For λ_4 also equation (9) is used yielding L_4. To be able to compare the results of all realizations, the L_i are normalized by the respective true length L read from the model output. Resulting over- respectively underestimation factors against aquifer heterogeneity σ_Y^2 are presented in Fig. 4 (single realization results, ensemble means with standard deviations as error bars, medians, coefficients of variation).

Plume lengths L_1 and L_2, calculated from λ_1 and λ_2, show exactly identical results, although the λ_2 show a stronger overestimation than the corresponding λ_1 for all realizations. The reason for the equivalence of L_1 and L_2 is that the bias introduced by estimating λ_2 with a one dimensional model accounting for longitudinal dispersion only is reversed by using the same transport equation to calculate the plume length. While for homogeneous conditions the true plume length is obtained, L is underestimated in most realizations for all degrees of heterogeneity. Mean L_1 and L_2 decrease to 0.59 for σ_Y^2=4.5. As for λ, spread and uncertainty of L increase with σ_Y^2. The overestimation of the degradation rate constant is thus reflected in an underestimation of the plume length.

Plume lengths L_3 calculated with the two-dimensional transport equation on average are lower than the corresponding L_1 and L_2. This is a consequence of the β term in equation (5) (Table 2), which is used to correct down gradient concentrations for transverse dispersion. When estimating the rate constant with method 3, each down gradient concentration $C(x)$ is scaled by a different value β, as the correction factor is dependent on the distance from the source. This scaling is not fully reversed when the plume length is calculated using equation (9) (Table 3), as then only one single Δx is used.

As shown before, degradation rate constants λ_4 in general are significantly better estimated than those obtained by the other three approaches. This is also reflected in plume lengths L_4 (Fig. 4 (c)). For all σ_Y^2 the ensemble means almost perfectly match the true L. Of all four approaches the L_4 consistently show the lowest coefficients of variation, indicating the lowest spread and thus the lowest uncertainty.

The plume length results presented for case A demonstrate that the determination of degradation rate constants using the center line method as well as the subsequent calculation of contaminant plume lengths both are subject to uncertainty induced by the heterogeneity of the medium. However, the uncertainty observed for the rate constants is only partially transferred to the calculated plume lengths. For all approaches the observed spread of the ensembles of estimated plume lengths is smaller than for the corresponding rate constants. This is most obvious for the L_4, which also show the best agreement with the true plume lengths. Moreover, the L_4 are unbiased, showing equal amounts of under- as well as overestimation. However, both types of error are undesirable. Underestimation of the contaminant plume length, i.e. a "non-conservative" result, may pose a threat to down gradient receptors. On the other hand, a "conservative" result, i.e. an overestimation of plume dimensions, might result in wrong decisions regarding the necessity and dimensioning of engineered remediation measures with unnecessary financial expenses. In

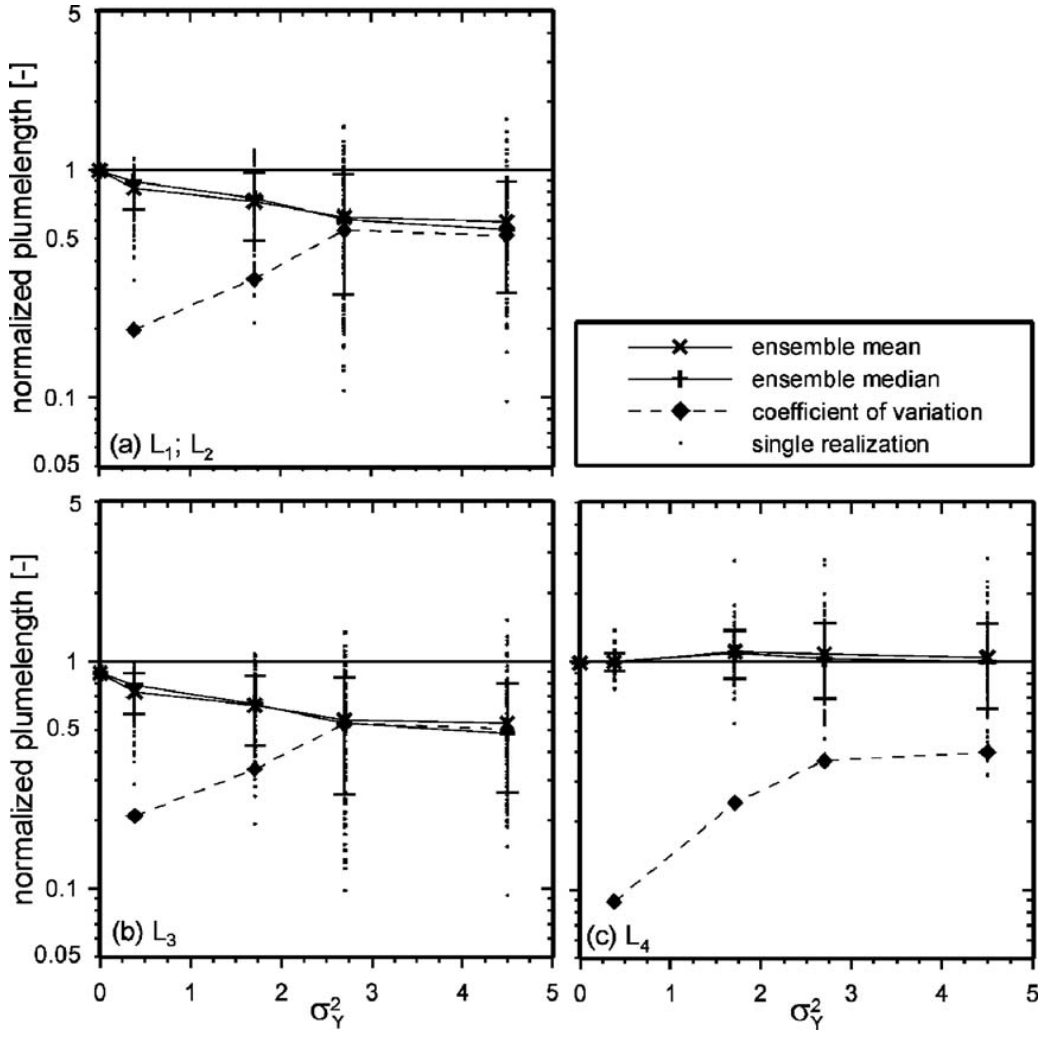

Fig. 4. Plume lengths L_i calculated with degradation rate constants λ_1 through λ_4. The L_i are normalized by the true plume length L (indicated by the horizontal line) for case A.

contrast to L_4, plume lengths L_1, L_2 and L_3 show a clear tendency of underestimation, demonstrating the non-conservativeness of too large rate constants. Comparing methods 1, 2 and 3, differences in calculated plume lengths are not as pronounced as for the rate constants. Thus it can be concluded, that the same underlying equation should be used for rate constant and plume length estimation. However, if e.g. a rate constant estimated with method 2 is used in a two- or three-dimensional (numerical) transport model, results are susceptible to the bias in method 2, resulting in a significantly stronger underestimation of the plume length.

6.2. Case B: estimation of first order degradation rate constants and plume lengths for plumes following Michaelis–Menten degradation kinetics

In case B the additional error is studied, that arises when the four methods for the estimation of first order degradation rate constants (Table 2, equations (1)–(4)) and the respective equations for plume lengths (Table 3, equations (7)–(9)) are used for plumes with a degradation kinetics deviating from first order but following MM degradation kinetics instead (see Table 1).

Since a direct comparison of estimated rate constants λ_1 through λ_4 with the MM parameters k_{max} and M_C used in the numerical simulations is not possible, the evaluation here is based on calculated

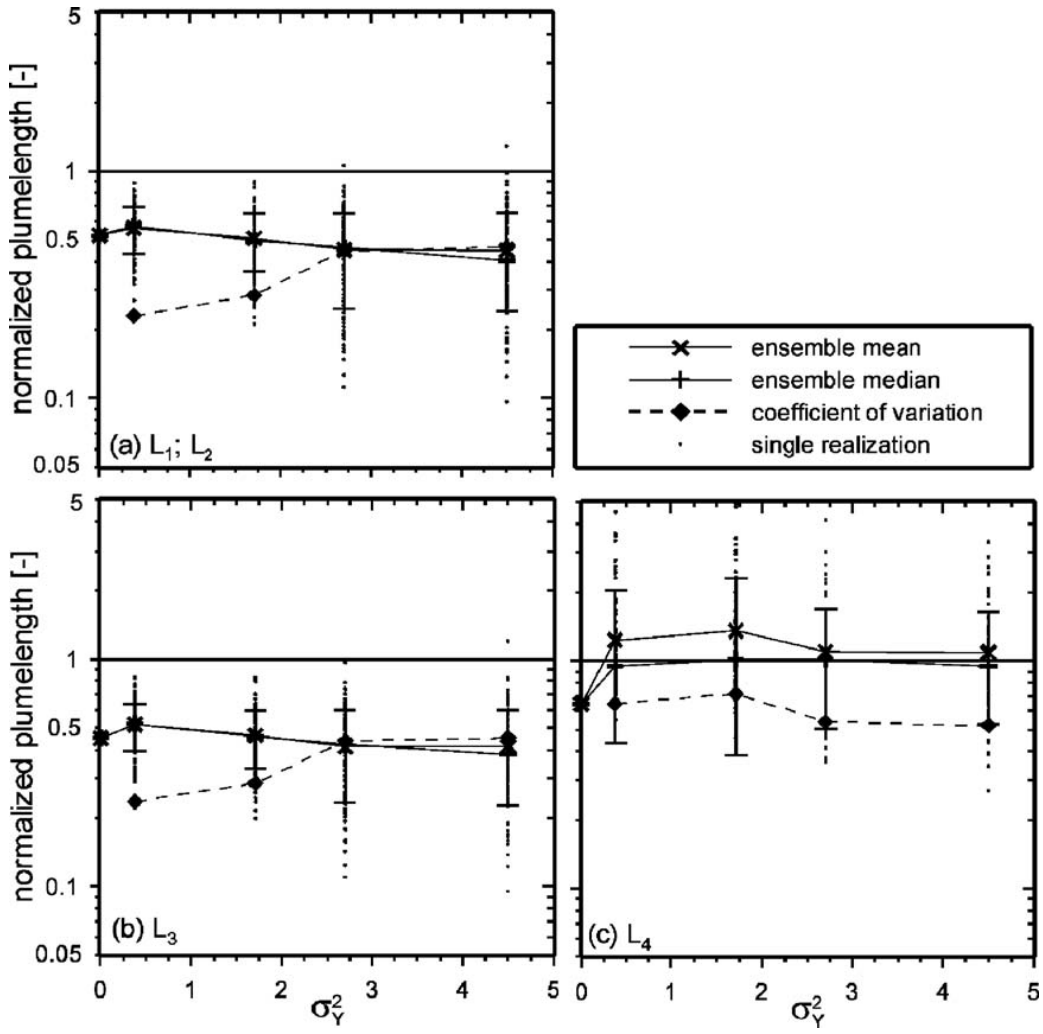

Fig. 5. Normalized plume lengths L_i calculated with degradation rate constants λ_1 through λ_4 for the contaminant plumes following Michaelis–Menten degradation kinetics.

plume lengths only. The estimated contaminant plume lengths L_i are displayed in Fig. 5 (single realization results, ensemble means with standard deviations as error bars, medians, coefficients of variation). As for case A, L_1 and L_2 (Fig. 5 (a)) yield very similar results. However, in comparison to case A, underestimation is clearly increased. This is most obvious for homogeneous conditions, where L_1 and L_2 are only about 50% of the true length and thus no longer yield the correct result. Underestimation of L increases with heterogeneity, yielding mean values of L_1 and L_2 of 0.45 for σ_Y^2=4.5. Spread is about 0.75 orders of magnitude for low heterogeneity and one order of magnitude for high heterogeneities, which is similar to case A. Plume lengths L_3 (Fig. 5 (b)) show the same general behaviour as the L_1 and L_2, with mean values being slightly lower. In contrast to this, L is overestimated for most realizations by L_4 (Fig. 5 (c)). While for homogeneous conditions a too short L_4 of 0.65 is obtained, L_4 increases to values larger than one for higher degrees of heterogeneity. Spread of single realizations is significantly increased in comparison to case A (compare Figs. 4 (c) and 5(c)), as a spread of about one order of magnitude can be observed for all degrees of heterogeneity.

The additional error introduced by using methods 1 through 4 for plumes following Michaelis–Menten kinetics degradation is most pronounced for low heterogeneities. Compared to case A, plume lengths are underestimated to a larger extent, as can be seen by the lower mean values and

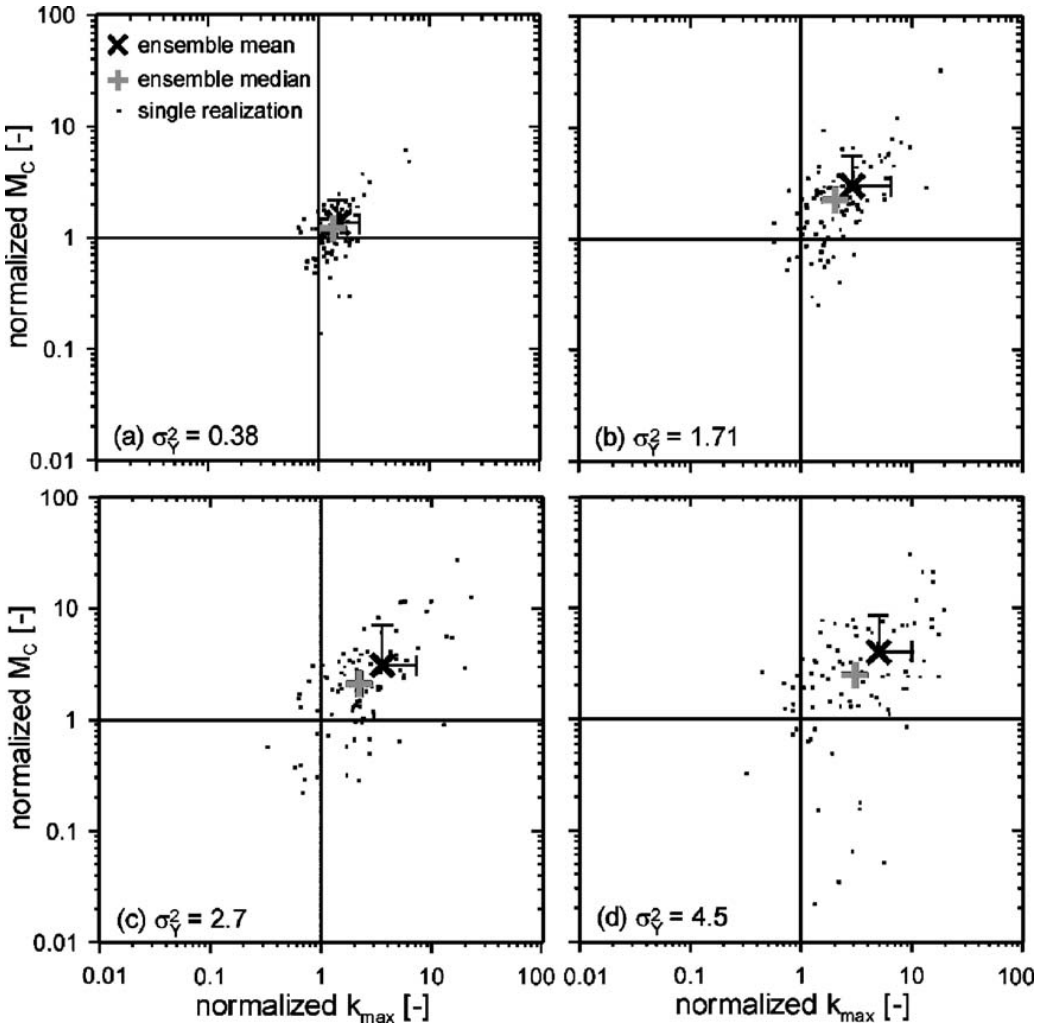

Fig. 6. Normalized Michaelis–Menten kinetics parameters k_{max} vs. M_C estimated for σ_Y^2=0.38 (a), 1.71 (b), 2.7 (c) and 4.5 (d), respectively.

medians. Only for L_4 plume length overestimation is observed and uncertainty is increased in comparison to case A.

6.3. Case C: estimation of Michaelis–Menten kinetics parameters and plume lengths for plumes following Michaelis–Menten degradation kinetics

6.3.1. Estimation of rate parameters

As demonstrated in case B, using a first order kinetics approximation for plumes following MM degradation kinetics introduces an additional error, yielding less conservative estimates of plume lengths ($L_1 - L_3$) as well as higher uncertainty (L_4). Therefore, method 5 for the estimation of the MM parameters is tested by application to the contaminant plumes following MM degradation kinetics (see Table 1). Using the same concentration vs. distance data as in Section 6.2, MM parameters k_{max} and M_C are estimated by a linear fit as explained in Section 4.1. These parameters then are used to calculate the length of the contaminant plumes L_{MM} by equation (10) (Table 3).

Fig. 6 presents the results of the parameter estimation in single diagrams for each σ_Y^2 (results for single realizations, ensemble means with corresponding standard deviations as error bars, medians). Since for each realization the maximum degradation rate k_{max} and half-saturation concentration M_C are estimated simultaneously, the parameters are shown in scatter plots. For the homogeneous case (not shown), k_{max} is slightly overestimated with a value of 1.06, while for M_C an underestimation is observed with $M_C = 0.91$. This error results from neglecting the dispersion process. Fig. 6 shows that normalized k_{max} and M_C are increasingly overestimated with increasing σ_Y^2. Also uncertainty increases with σ_Y^2. This is a similar behaviour as found for the first order rate constants in case A. Approximate orientation of the data points along a diagonal axis with positive slope gives evidence of a weak positive correlation between k_{max} and M_C. An overestimation of k_{max} increases the degradation rate as long as concentrations are higher than M_C. However, overestimation of M_C raises the concentration threshold at which kinetic degradation transits from zeroth to slower first order, which counter-balances the effects of the k_{max} overestimation.

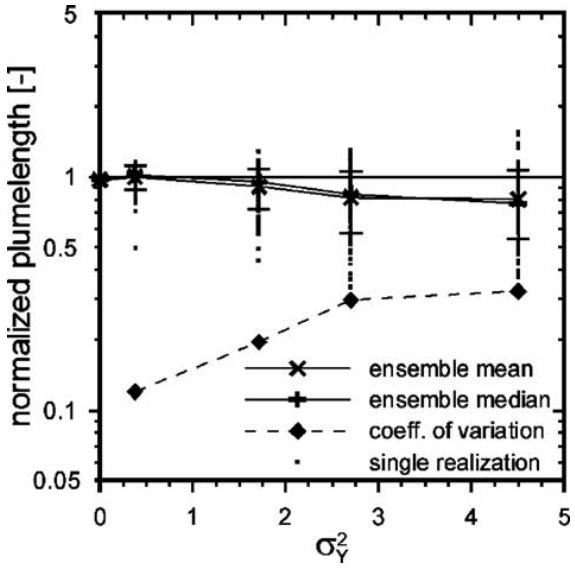

Fig. 7. Normalized plume lengths L_{MM} calculated with Eq. (10) based on estimated Michaelis–Menten kinetics parameters k_{max} and M_C.

6.3.2. Estimation of plume lengths

For the determination of contaminant plume lengths, the estimated parameters k_{max} and M_C are evaluated with equation (10) (Table 3). Normalized plume lengths L_{MM} are presented in Fig. 7 (single realization results, ensemble means with corresponding standard deviations as error bars, medians, coefficients of variation). For the homogeneous case the estimated and true plume lengths agree well with L_{MM}=0.97. Also for σ_Y^2=0.38 the mean yields the correct result with L_{MM}=1.0 and spread is about 0.5 orders of magnitude. For higher heterogeneities, however, plume lengths again tend to be underestimated with L_{MM} decreasing to 0.80 for σ_Y^2=4.5. Spread for all degrees of heterogeneity is smaller than one order of magnitude. When the spread of estimated k_{max} and M_C values is compared to the spread of calculated MM plume lengths, it is found – as for case A – that the uncertainty in MM parameters is not fully propagated to the plume lengths. Comparing MM plume lengths with those determined for the plumes subject to first order degradation in case A (see Fig. 4), the L_{MM} outperform L_1, L_2 or L_3 with regard to accuracy as well as uncertainty. Only the L_4 are closer to the true lengths on average, while the spread of single realizations is comparable. It is thus found in this study that the proposed method of estimating MM kinetics parameters is adequate and performs better than the methods for estimating first order rate constants.

6.4. Comparison and discussion of cases B and C

In this section the plume lengths L_{MM} calculated in case C using the MM model (Table 3, equation (10)) are compared to the L_1-L_4 of case B, where plume lengths were calculated using the first order kinetics approximations of equations (7) through (9) of Table 3. Table 5 compares the accuracy of calculated plume lengths using MM parameters estimated by method 5 with the four different first order approaches. Given are the percentages of realizations for which L_{MM} constitutes a closer estimate of L than L_1, L_2, L_3, or L_4. In comparison to L_1, L_2 and L_3 it is found that L_{MM} is the closer estimate for 93 up to 99% of all realizations, depending on the degree of heterogeneity and the first order method used. In comparison with L_4 L_{MM} constitutes the closer estimate still for 53 up to 72% of all realizations.

As a more quantitative criterion, plume length error factors EF are calculated for each realization and all five estimation methods:

$$\mathrm{EF} = \left(\frac{L*}{L}\right)^a \text{ with } \begin{cases} a = -1 | L* < L \\ a = +1 | L* \geq L \end{cases} \tag{13}$$

where L_* and L are the estimated and true plume lengths, respectively, and the exponent a is used to obtain a standardized measure for over- as well as for underestimation. Hence, EF gives the degree of accuracy of the plume length estimate L_*. For each ensemble of L_i and L_{MM} cumulative empirical

Table 5
Percentage of realizations for which L_{MM} is a closer estimate of L than L_1-L_4

σ_Y^2	L_{MM} vs. L_1, L_2 %	L_{MM} vs. L_3 %	L_{MM} vs. L_4 %
0.38	97	99	72
1.71	99	99	57
2.7	98	99	59
4.5	94	93	53

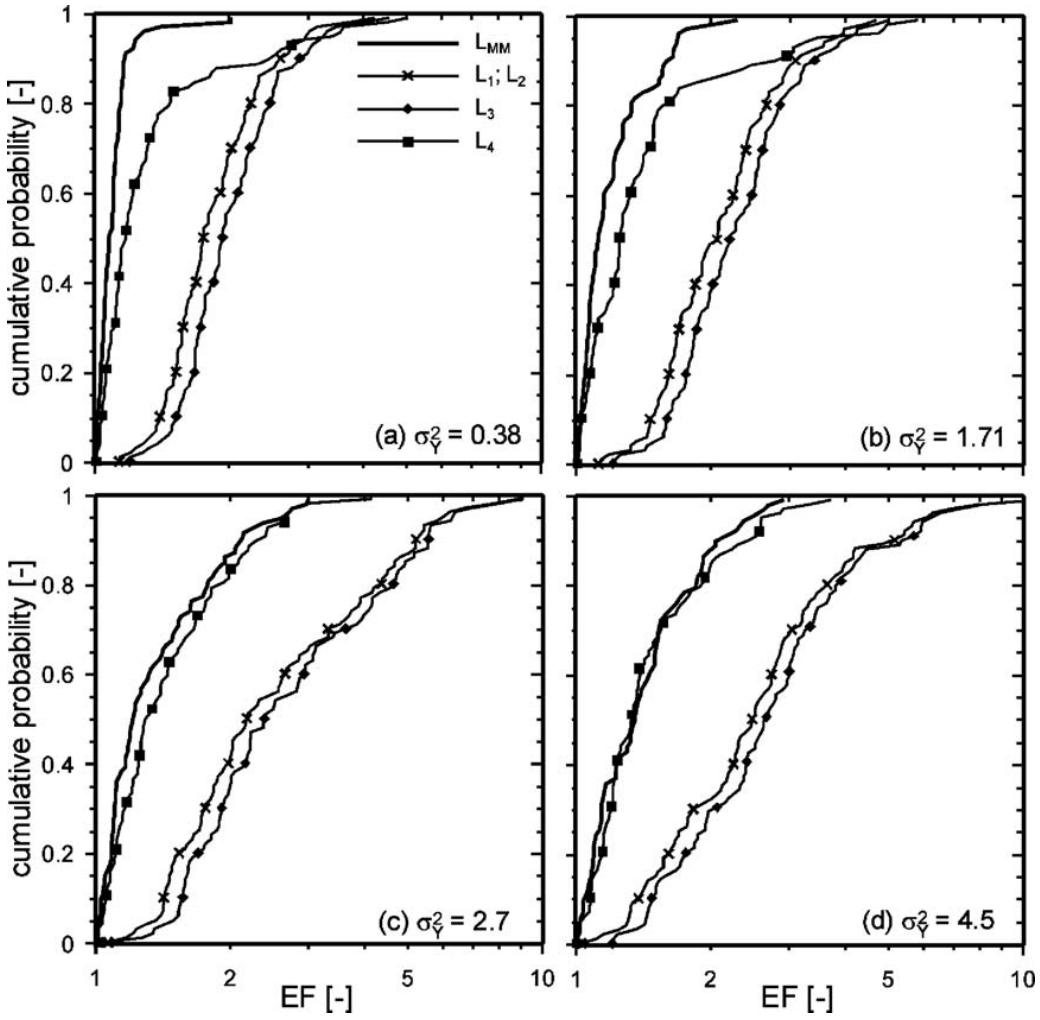

Fig. 8. Cumulative empirical distribution functions of plume length error factors for estimated plume lengths L_1 through L_4 and L_{MM} and aquifer heterogeneities σ_Y^2 of 0.38 (a), 1.71 (b), 2.7 (c) and 4.5 (d). The diagrams yield the probability of obtaining an estimate of the plume length L with an accuracy (EF) as given on the abscissa.

distribution functions (edf) of the EF were calculated. These are presented in Fig. 8 (a) through (d) for each degree of heterogeneity. The edf give the probability of obtaining an estimate of the plume length with an EF less than or equal to the associated quantile on the abscissa. In Fig. 8 (a) with σ_Y^2=0.38, for example, the probability of estimating L by L_{MM}, given an accuracy of factor 2, i.e. allowing a maximum underestimation by 50% or overestimation by 100%, is about 0.98. In contrast to this, the probability of obtaining L_1 (=L_2) or L_3 as accurate as a factor of 2 is only 0.68 and 0.55, respectively, while for L_4 the probability is approximately 0.89. When aquifer heterogeneity increases, the probabilities are reduced, as can be seen by the shift towards higher EF and the flattening of the slopes (note the logarithmic scale of the abscissa). Moreover, differences between L_{MM} and L_4 diminish. Thus for σ_Y^2=4.5 (Fig. 8 (d)) edf for both approaches almost coincide and show the same degree of accuracy. However, L_{MM} still yields significantly higher probabilities for a given EF than L_1, L_2 or L_3.

The results obtained in this comparison clearly support that for plumes following MM degradation kinetics usage of the MM parameter estimation approach allows a distinct improvement of plume length estimates over those obtained using a first order approximation, especially when aquifer heterogeneity is not too high. For the majority of realizations investigated in this study, L_{MM}

constitutes a more accurate estimate of the true plume length than any of the first order methods used. Only when aquifer heterogeneity is very high, L_4 is able to yield plume length estimates of almost comparable accuracy. This is mainly, because increased transverse dispersion produces concentration profiles that allow a log-linear fit of a first order rate constant.

7. Summary and conclusions

In this study the Virtual Aquifer concept is used to assess the uncertainty involved in estimating down stream contaminant concentrations and plume lengths in heterogeneous aquifers. For such an analysis a key element is the quantification of the degradation rate at the site under study. Therefore, the main focus of this work is on the influence of this parameter on the estimated plume lengths. Three different scenarios are analysed.

In case A, four different standard field methods based on the center line investigation strategy are tested and compared with regard to their capability of estimating first order degradation rate constants and the contaminant plume length in heterogeneous aquifers. The four methods are applied to plumes following first order degradation kinetics. It is found that both, the estimated degradation rate constants and the calculated plume lengths, are subject to high uncertainty. On average, estimated rate constants exceed the true degradation rate constant, causing calculated plume lengths that are too short. Both bias and uncertainty of estimated degradation rate constants increase with the degree of heterogeneity to about a factor in the order of a magnitude, respectively. However, the uncertainty observed in the rate constants does not fully propagate to the plume length estimates. On average plume lengths are underestimated by about 50% of the true plume length, and up to a factor of ten in the worst cases. Of the four different methods, the approach of Wiedemeier et al. (1996) using concentrations normalized to a conservative tracer yields the best results for the rate constants and for the plume lengths. Consequently, this method should preferably be used. However, the presence of a suitable recalcitrant compound may not always be given. In this case, the most simple of the four approaches, which is based on the advection equation and neglects dispersive processes should be used to determine the degradation potential, as this method yields closer estimates of the first order rate constant than the approaches using the one- (Buscheck and Alcantar, 1995) and two-dimensional advection dispersion equations (Zhang and Heathcote, 2003).

The non-conservative plume length estimates might cause threats to down stream receptors, as the risk of contamination could be underrated. The high uncertainty when estimating plume dimensions could result in incorrect decisions regarding the necessity and dimensioning of engineered remediation measures or when considering the applicability of natural attenuation. All four methods are only applicable to steady state plumes. In reality, however, contaminant plumes often show temporal variations in extent and orientation as the plume expands, the source slowly depletes, or the flow regime changes over time. For expanding plumes, application of methods 1–4 would result in an overestimation of the rate constant, and thus in underestimation of the plume length at steady state. This is because the down stream transient contaminant concentrations are lower than those at steady state, causing a higher concentration decrease along the center line, which would be falsely attributed to the degradation process. For the same reason rate constants would also be overestimated for shrinking plumes. An examination of the current state of the plume is necessary, when one of the four methods is to be applied at a site. An overview of techniques for this purpose is given by Newell et al. (2002).

Case B analyses the additional error that results from application of the four methods, although the true degradation kinetics deviate from first order. Here plumes following Michaelis–Menten degradation kinetics are investigated. Results show that for the three approaches without correction of concentrations to a conservative tracer, an additional underestimation occurs which

is largest for low heterogeneities. For the approach using the tracer correction, the estimated plume lengths still match the true lengths on average. However, the uncertainty of the plume lengths is significantly increased as compared to case A.

In case C, a regression approach is introduced to estimate the parameters of the MM kinetics and to calculate the plume lengths for the same plumes as investigated in case B. Since longitudinal and transverse dispersion are neglected in this method, the MM parameters are overestimated on average. Overestimation increases from less than a factor of two for low degrees of heterogeneity to a factor of roughly four for high heterogeneity. Consequently an underestimation of the corresponding plume lengths is observed for most realizations. For low heterogeneity, the plume length is estimated precisely with low uncertainty, for high heterogeneity the average estimated plume length is about 80% of the true plume length, with estimates as low as 40–35% in the worst cases. However, in comparison with the first order approximation investigated in case B the error resulting from this approach is significantly reduced, with the uncertainty of the plume length estimates being reduced by a factor of three. Therefore, if field data collected along the center line of a plume gives evidence of MM kinetics (linear behaviour of concentrations vs. distance in a linear plot, concave down behaviour in a semi-logarithmic plot (Bekins et al., 1998)), this approach is recommended.

Generally, the Virtual Aquifer concept has proven useful in assessing the performance of methods for investigating first order rate constants and plume lengths from plume center line measurements. The main advantage is, that individual factors, as here the hydraulic heterogeneity and the assumption of a wrong plume kinetics, can be studied either individually in detail or in combination and under otherwise ideal conditions. However, the restrictions from the simplified setup of the model scenario have to be kept in mind when drawing conclusions for field applications. In reality, contaminant degradation follows more complicated rate laws, depending e.g. on electron acceptor and donor availability, may include transient effects, or dilution and phase changes to the unsaturated zone. Further studies will thus incorporate more realistic degradation kinetics as well as influences from e.g. measurement errors.

Acknowledgements

This work is funded by the German Ministry of Education and Research (BMBF) under grant 033 05 12/033 05 13 as part of the KORA priority program, sub-project 7.2. We wish to thank Robert Walsh for his helpful comments on the manuscript. We also wish to thank our project partners at the Christian-Albrechts-University Kiel Andreas Dahmke and Dirk Schäfer for their support in our research. We acknowledge Uwe Wittmann, Iris Bernhardt and Ludwig Luckner for coordination of the project work. Furthermore we would like to acknowledge the thoughtful reviews of the anonymous reviewers and the Editor. Their comments have greatly improved the manuscript.

References

Aziz, C.E., Newell, C.J., Gonzales, A.R., Haas, P., Clement, T.P., Sun, Y., 2000. BIOCHLOR Natural Attenuation Decision Support System User's Manual. U.S. EPA, Office of Research and Development, EPA/600/R-00/008, Washington D.C.

Bauer, S., Kolditz, O., 2005. Assessing contaminant mass flow rates by the integral groundwater investigation method by using the virtual aquifer approach. In: ModelCARE 2005, Fifth International Conference on Calibration and Reliability in Groundwater Modelling. From Uncertainty to Decision Making. Pre-published Proceedings, The Hague (Scheveningen), The Netherlands, June 2005, pp.301–307.

Bauer, S., Beyer, C., Kolditz, O., 2005. Assessing measurements of first order degradation rates by using the virtual aquifer approach. In: Thomson, N.R. (Ed.), GQ2004, Bringing Groundwater Quality Research to the Watershed Scale. Proceedings of a Symposium held at Waterloo, Canada, July 2004. IAHS Publication, vol. 297. IAHS Press, Wallingford, pp. 274–281.

Bauer, S., Beyer, C., Kolditz, O., 2006. Assessing measurement uncertainty of first-order degradation rates in heterogeneous aquifers. Water Resour. Res. 42, W01420. doi:10.1029/2004WR003878.

Baveye, P., Valocchi, A., 1989. An evaluation of mathematical models of the transport of biologically reacting solutes in saturated soils and aquifers. Water Resour. Res. 25 (6), 1413–1421.

Bear, J., 1972. Dynamics of Fluids in Porous Media. Elsevier, Amsterdam. 784 pp.

Bekins, B.A., Warren, E., Godsy, E.M., 1998. A comparison of zero-order, first-order, and Monod biotransformation models. Ground Water 36 (2), 261–268.

Beyer, C., Bauer, S., Kolditz, O., 2005. Uncertainty assessment of degradation rate measurements in heterogeneous media using the virtual aquifer approach. In: Kolditz, O., Bauer, S., Gronewold, J. (Eds.), Proceedings of the 5th Workshop "Porous Media", Blaubeuren, Germany, December 2004. ZAG Publisher, Tübingen.

Bockelmann, A., Zamfirescu, D., Ptak, T., Grathwohl, P., Teutsch, G., 2003. Quantification of mass fluxes and natural attenuation rates at an industrial site with a limited monitoring network: a case study. J. Contam. Hydrol. 60 (1–2), 97–121.

Buscheck, T.E., Alcantar, C.M., 1995. Regression techniques and analytical solutions to demonstrate intrinsic bioremediation. In: Hinchee, R.E., Wilson, T.J., Downey, D. (Eds.), Intrinsic Bioremediation. Battelle Press, Columbus, OH, pp. 109–116.

Chapelle, F.H., Bradley, P.M., Lovley, D.R., Vroblesky, D.A., 1996. Measuring rates of biodegradation in a contaminated aquifer using field and laboratory methods. Ground Water 34 (4), 691–698.

Dagan, G., 1989. Flow and Transport in Porous Formations. Springer, Heidelberg. 465 pp.

Domenico, P.A., 1987. An analytical model for multidimensional transport of a decaying contaminant species. J. Hydrol. 91 (1–2), 49–59.

Islam, J., Naresh, S., O'Sullivan, M., 2001. Modeling biogeochemical processes in leachate-contaminated soils: a review. Transp. Porous Media 43 (3), 407–440.

Herfort, M., 2000. Reactive Transport of Organic Compounds Within a Heterogeneous Porous Aquifer, PhD Thesis, University of Tübingen, Tübinger Geowissenschaftliche Arbeiten (TGA), 54, Tübingen. 76 pp.

Kolditz, O., 2002. Computational Methods in Environmental Fluid Dynamics. Springer, Heidelberg. 400 pp.

Kolditz, O., Bauer, S., 2004. A process-oriented approach to computing multifield problems in porous media. J. Hydroinform. 6 (3), 225–244.

Kolditz, O., de Jonge, J., Beinhorn, M., Xie, M., Kalbacher, T., Wang, W., Bauer, S., McDermott, C., Chen, C., Beyer, C., Gronewold, J., Kemmler, D., Manabe, T., Legeida, D., Adamidis, P., 2004. GeoSys- Theory and users manual. release 4.1. GeoSystems Research, Center for Applied Geoscience, University of Tübingen, http://www.uni-tuebingen.de/zag/geohydrology, Tübingen.

McNab Jr., W.W., 2001. A Monte Carlo simulation method for assessing biotransformation effects on groundwater fuel hydrocarbon plume lengths. Comput. Geosci. 27 (1), 31–42.

McNab Jr., W.W., Dooher, B.P., 1998. A critique of a steady-state analytical method for estimating contaminant degradation rates. Ground Water 36 (6), 983–987.

Newell, C.J., McLeod, R.K., Gonzales, J.R., 1996. BIOSCREEN Natural Attenuation Decision Support System User's Manual. Version 1.3. U.S. EPA, Office of Research and Development, EPA/600/R-96/087, Washington D.C.

Newell, C.J., Rifai, H.S., Wilson, J.T., Connor, J.A., Aziz, J.A., Suarez, M.P., 2002. Calculation and use of first-order rate constants for monitored natural attenuation studies. U.S. EPA Ground Water Issue, U.S. EPA, Office of Research and Development, EPA/540/S-02/500, Washington D.C.

Parlange, J.-Y., Starr, J.L., Barry, D.A., Braddock, R.D., 1984. Some approximate solutions of the transport equation with irreversible reactions. Soil Sci. 137, 434–442.

Rehfeldt, K.R., Boggs, J.M., Gelhar, L.W., 1992. Field study of dispersion in a heterogeneous aquifer, 3, geostatistical analysis of hydraulic conductivity. Water Resour. Res. 28 (12), 3309–3324.

Rifai, H.S., Newell, C.J., Gonzales, J.R., Dendrou, S., Kennedy, L., Wilson, J.T., 1998. BIOPLUME III Natural Attenuation Decision Support System Version 1.0 User's Manual. U.S. EPA, Office of Research and Development, EPA/600/R-98/010, Washington D.C.

Rittmann, B., VanBriesen, J.M., 1996. Microbiological processes in reactive modeling. In: Lichtner, P., Steefel, C., Oelkers, E. (Eds.), Reactive Transport in Porous Media. Reviews in Mineralogy, vol. 34. Mineralogical Society of America, Washington, DC, pp. 311–334.

Robinson, J.A., 1985. Determining microbial kinetic parameters using nonlinear regression analysis. Adv. Microb. Ecol. 8, 61–114.

Schäfer, D., Dahmke, A., Kolditz, O., Teutsch, G., 2002. "Virtual Aquifers": a concept for evaluation of exploration, remediation and monitoring strategies. In: Kovar, K., Hrkal, Z. (Eds.), Calibration and Reliability in Groundwater Modelling: A Few Steps Closer to Reality. Proceedings of the ModelCARE 2002 Conference, Prague, Czech Republic, June 2002. IAHS Publication, vol. 277. IAHS Press, Oxfordshire, pp. 52–59.

Schäfer, D., Manconi, A., Dahmke, A., 2004a. Identification and consequences of different kinetic approaches for simulation of microbial degradation. In: Aagaard, P., Bedbur, E., Bidoglio, G., Candela, L., Nuetzmann, G., Trevisan, M., Vanclooster, M., Viotti, P. (Eds.), Proceedings of the International Workshop: Saturated and Unsaturated Zone, Integration of Process Knowledge into Effective Models. University of Rome La Sapienza", Rome, Italy, May 2004, pp. 291–296.

Schäfer, D., Schlenz, B., Dahmke, A., 2004b. Evaluation of exploration and monitoring methods for verification of natural attenuation using the virtual aquifer approach. Biodegradation 15 (6), 453–465.

Simkins, S., Alexander, M., 1984. Models for mineralization kinetics with variables of substrate concentration and population density. Appl. Environ. Microbiol. 47 (6), 1299–1306.

Stenback, G.A., Ong, S.K., Rogers, S.W., Kjartanson, B.H., 2004. Impact of transverse and longitudinal dispersion on first-order degradation rate constant estimation. J. Contam. Hydrol. 73, 3–14.

Suarez, M.P., Rifai, H.S., 2002. Evaluation of BTEX remediation by natural attenuation at a coastal facility. Ground Water Monit. Remediat. 22 (1), 62–77.

Suarez, M.P., Rifai, H.S., 2004. Modeling natural attenuation of total BTEX and benzene plumes with different kinetics. Ground Water Monit. Remediat. 24 (3), 53–68.

Sudicky, E.A., 1986. A natural gradient experiment on solute transport in a sand aquifer: spatial variability of hydraulic conductivity and its role in the dispersion process. Water Resour. Res. 22 (13), 2069–2082.

U.S. EPA, 1998. Technical protocol for evaluating natural attenuation of chlorinated solvents in groundwater, U.S. EPA, Office of Research and Development, EPA/600/R/128, Washington, D.C.

Wiedemeier, T.H., Swanson, M.A., Wilson, J.T., Kampbell, D.H., Miller, R.N., Hansen, J.E., 1996. Approximation of biodegradation rate constants for monoaromatic hydrocarbons (BTEX) in ground water. Ground Water Monit. Remediat. 16 (3), 186–194.

Wiedemeier, T.H., Rifai, H.S., Wilson, T.J., Newell, C., 1999. Natural Attenuation of Fuels and Chlorinated Solvents in the Subsurface. Wiley, New York. 632 pp.

Wilson, J.T., Kolhatkar, R., 2002. Role of natural attenuation in life cycle of MTBE plumes. J. Environ. Eng. 128 (9), 876–882.

Wilson, J.T., Pfeffer, F.M., Weaver, J.W., Kampbell, D.H., Wiedemeier, T.H., Hansen, J.E., Miller, R.N., 1994. Intrinsic bioremediation of JP-4 jet fuel. Symposium on Intrinsic Bioremediation of Ground Water, Denver, Colorado, EPA/540/R-94/515, pp. 60–72.

Wilson, R.D., Thornton, S.F., Mackay, D.M., 2004. Challenges in monitoring the natural attenuation of spatially variable plumes. Biodegradation 15 (6), 459–469.

Zamfirescu, D., Grathwohl, P., 2001. Occurrence and attenuation of specific organic compounds in the groundwater plume at a former gasworks site. J. Contam. Hydrol. 53 (1–2), 407–427.

Zhang, Y.-K., Heathcote, R.C., 2003. An improved method for estimation of biodegradation rate with field data. Ground Water Monit. Remediat. 23 (3), 112–116.

Enclosed Publication 4

Bauer, S., Beyer, C., Kolditz, O. (2007): Einfluss von Heterogenität und Messfehler auf die Bestimmung von Abbauraten erster Ordnung - eine Virtueller Aquifer Szenarioanalyse. (Influence of heterogeneity and measurement error on the determination of first order degradation rates by us1ing the virtual aquifer approach.), Grundwasser, 12, 3–14, doi: 10.1007/s00767-007-0019-8

Einfluss von Heterogenität und Messfehler auf die Bestimmung von Abbauraten erster Ordnung – eine Virtueller Aquifer Szenarioanalyse*

Influence of heterogeneity and measurement error on the determination of first order degradation rates - a virtual aquifer scenario analysis

Sebastian Bauer, Christof Beyer, Olaf Kolditz

Zentrum für Angewandte Geowissenschaften, Universität Tübingen, Sigwartstraße 10,
D 72076 Tübingen. Tel: 07071-2973171. Fax: 07071 5059
e-mail: sebastian.bauer@uni-tuebingen.de, christof.beyer@uni-tuebingen.de, kolditz@uni-tuebingen.de

Kurzfassung

Die grundlegende Idee des Virtuellen Aquifers ist, durch numerische Modellierung von typischen Schadensfällen Erkundungsstrategien zu simulieren und zu bewerten. In diesem Beitrag wird die Bestimmung von Abbauraten erster Ordnung untersucht. Eine Schadensquelle wird dabei in einen virtuellen Aquifer eingebracht und die stationäre Schadstofffahne unter der Annahme einer Abbaukinetik erster Ordnung simuliert. Diese Fahne wird dann durch Beobachtungspegel entlang der Zentrallinie der Fahne untersucht. Anhand von vier typischen Methoden werden Abbauraten erster Ordnung berechnet und mit dem vorgegebenen Wert verglichen. Dieser Vergleich wird für unterschiedlich stark ausgeprägte hydraulische Heterogenitäten durchgeführt. Dabei zeigt sich, dass mit zunehmender Heterogenität die ermittelten Abbauraten die tatsächliche Abbaurate um Größenordnungen überschätzen können und sie somit sehr unsicher sind. Bei der Untersuchung der Messfehler wurden Abweichungen bei der Bestimmung der Piezometerhöhe und der Konzentration angenommen. Hierbei ergibt sich, dass Messfehler ebenfalls zu einer hohen Unsicherheit der Ratenkonstante führen können, wobei Messfehler der Piezometerhöhe einen stärkeren Einfluss haben.

Abstract

The principal idea of the Virtual Aquifer is to simulate and evaluate monitoring strategies and remediation options for contaminated sites by modelling of typical contamination scenarios. Here the determination of first order degradation rates is studied. A virtual reality is generated by simulating the spreading of a plume, originating from a defined source and subject to first order degradation. This plume is investigated using monitoring wells placed along the plume center line. From the information thus obtained first order degradation rates are calculated by methods typically used and are then compared to the predefined value. This comparison is conducted for different degrees of heterogeneity. It is found that with increasing heterogeneity degradation rates overestimate the real degradation rate by up to orders of magnitude and show a high uncertainty. Then measurement errors are introduced for piezometric head and concentration measurements. It is found that deviations of the estimated first order rate constant from the true one of up to orders of magnitude can occur, with errors of the piezometric head measurement causing the dominant uncertainty.

Keywords: natural attenuation, heterogeneity, first-order degradation rate, virtual aquifer, scenario analysis

* Bauer, S., Beyer, C., Kolditz, O. (2007): Einfluss von Heterogenität und Messfehler auf die Bestimmung von Abbauraten erster Ordnung - eine Virtueller Aquifer Szenarioanalyse. (Influence of heterogeneity and measurement error on the determination of first order degradation rates by us1ing the virtual aquifer approach.), Grundwasser, 12, 3–14, doi: 10.1007/s00767-007-0019-8.

Einführung

In dieser Arbeit wird eine „Virtueller Aquifer“ Szenarioanalyse verwendet, um die Unsicherheit bei der Bestimmung von Abbauratenkonstanten erster Ordnung anhand von Messstellen auf der Zentrallinie der Schadstofffahne („Center line method“) im Kontext von Natural Attenuation zu untersuchen und zu quantifizieren. Natural Attenuation (NA), auch als Bioremediation bekannt, bezieht sich auf die Abnahme von Schadstoffkonzentrationen durch natürliche Abbauprozesse mit zunehmendem Abstand von der Quelle (US-EPA, 1999; WIEDEMEIER et al., 1999). Dabei werden Dispersion, Verdünnung, Sorption, Ausgasung und Bioabbau betrachtet, wobei der Bioabbau der einzige Prozess ist, der zu einer Verringerung der Schadstoffmasse führt. Die an einem Standort ablaufenden Prozesse müssen sorgfältig charakterisiert werden, um Aussagen über NA treffen zu können. Hierbei können insbesondere die Abbauraten der betrachteten Schadstoffe für mögliche Sanierungen und das Standortmanagement eine Rolle spielen. Die Abbauraten werden verwendet, um das gesamte NA-Potential am Standort zu charakterisieren, um die Länge von Schadstofffahnen in der Zukunft zu prognostizieren und um unterstromige Konzentrationen zu berechnen, die für eine Auswirkungsprognose benötigt werden (WIEDEMEIER et al., 1999).

Zur Bestimmung von Abbauraten im Feld stehen derzeit mehrere Methoden zur Verfügung, wie z.B. Massenbilanzen, in-situ Mikrokosmosstudien oder die Verwendung von Konzentrations-Abstands-Beziehungen, die auf der Fahnenzentrallinie einer stationären Schadstofffahne ermittelt wurden (CHAPELLE, 1996). Für letztere sind in der Literatur vier unterschiedliche Methoden beschrieben. Die erste beruht auf der eindimensionalen Transportgleichung mit Advektion und Abbau erster Ordnung (WIEDEMEIER et al., 1996). Die zweite Methode ist eine Erweiterung der ersten, indem die Konzentrationen des betrachteten Schadstoffes auf die Konzentrationen eines nichtreaktiven Mitkontaminanden normiert werden (WIEDEMEIER et al., 1996, 1999; WILSON et. al., 1994). Die dritte Methode, von BUSCHECK & ALCANTAR (1995) vorgeschlagen, beruht auf der eindimensionalen Transportgleichung mit Advektion, Dispersion und Abbau erster Ordnung und wurde bereits an einigen Standorten eingesetzt (CHAPELLE et al., 1996; WIEDEMEIER et al., 1996; ZAMFIRESCU & GRATHWOHL, 2001; SUAREZ & RIFAI, 2002; BOCKELMANN et al., 2003). In letzter Zeit wurden als Erweiterung zur Methode von BUSCHECK & ALCANTAR (1995) zwei- und dreidimensionale Methoden entwickelt (ZHANG & HEATHCOTE, 2003; STENBACK et al., 2004). ZHANG & HEATHCOTE (2003) konnten zeigen, dass die eindimensionale Methode durch Vernachlässigung der Querdispersion die Abbauraten um 21% im Vergleich zum zweidimensionalen und um 65% im Vergleich zum dreidimensionalen Fall überschätzt. MCNAB Jr. & DOOHER (1998) beschrieben, wie transversale Dispersion und instationäre Strömungszustände Konzentrationsverteilungen erzeugen können, die durch die Methode von BUSCHECK & ALCANTAR (1995) dann fälschlich als Bioabbau klassifiziert werden können, obwohl am Standort kein Abbau stattfindet.

Aufgrund der eingeschränkten Zugänglichkeit des Untergrundes sind Beobachtungen an kontaminierten Standorten nur an einzelnen räumlichen Punkten möglich. Die aus einzelnen Messpunkten abgeleiteten Ergebnisse und Aussagen sind daher immer mit Unsicherheit behaftet, die das eingeschränkte und punktuelle Wissen über den Standort widerspiegelt. Eine „Virtuelle Aquifer“ Szenarioanalyse kann verwendet werden, um diese Unsicherheit näher zu betrachten und zu quantifizieren (SCHÄFER et al., 2002; SCHÄFER et al., 2004; BAUER et al., 2006; BEYER et al., 2005a; BAUER & KOLDITZ, 2005). Eine Untersuchung des Einflusses der Parametrisierung der Abbaukinetik auf die prognostizierte Fahnenlänge wird in SCHÄFER et al. (2005) durchgeführt. Dabei werden numerische synthetische Modelle typischer Aquifere generiert. Mithilfe eines reaktiven Transportmodells können dann typische Schadensszenarien, wie beispielsweise die Ausbreitung einer Schadstofffahne ausgehend von einer Schadstoffquelle, simuliert werden. Der große Vorteil der Virtuellen Aquifere ist, dass die so erhaltene realistische räumliche Verteilung aller Parameter, wie z.B. Piezometerhöhe oder Konzentration, exakt bekannt ist. Die virtuelle Schadstoffahne wird dann in einem zweiten Schritt durch typische Erkundungsstrategien (hier: Zentrallinienmethode) untersucht. Eine Messung im virtuellen Aquifer bedeutet, die entsprechenden Werte aus der Modellausgabedatei zu lesen. Bei dieser Erkundung der virtuellen Schadstofffahne werden nur die Messwerte (hier: Piezometerhöhe, Konzentration) berücksichtigt, die auch an einem echten Standort erhalten werden können. Ausgehend von diesen (virtuellen) Messwerten werden dann weitere Parameter ermittelt (hier: hydraulische Durchlässigkeiten, Abbauraten). Bei diesem zweiten Schritt ist also die richtige Parameterverteilung nicht bekannt. Indem das Ergebnis der virtuellen Erkundung im dritten Schritt mit der wahren Parameterverteilung (hier: Abbauratenkoeffizient) verglichen wird, können die verwendeten Untersuchungsmethoden getestet und bewertet werden.

Die räumliche Heterogenität von Aquiferparametern hat einen erheblichen Einfluss auf die Fahnenentwicklung und die resultierende Konzentrationsverteilung eines Schadstoffes im Aquifer. Die

oben erwähnten Methoden zur Bestimmung von Abbauratenkonstanten erster Ordnung unterliegen daher dem Einfluss der Heterogenität, da sie auf Messdaten entlang der vermuteten Fahnenzentrallinie und auf Abschätzungen der Dispersivität beruhen. Wird die Grundwasserfließrichtung falsch abgeschätzt, kann die Fahnenzentrallinie leicht verfehlt werden (WILSON et al., 2004). Bisher existiert in der Literatur keine Studie, die den Einfluss der Heterogenität auf die Ermittlung von Abbauratenkonstanten erster Ordnung untersucht. Bei der Probenahme im realen Fall können darüber hinaus noch Messfehler auftreten, die ebenfalls die Ratenkonstanten beeinflussen. Diese können sowohl bei der Pegeleinmessung, bei der Bestimmung der hydraulischen Leitfähigkeit, bei Wasserstandsmessungen und insbesondere bei Konzentrationsmessungen auftreten. Auch hierzu existieren noch keine Untersuchungen in der Literatur. Ziel dieser Arbeit ist daher a) die Genauigkeit von Abbauraten, wie sie aus Feldmessungen gewonnen werden, zu ermitteln, und b) die verschiedenen Methoden zu Bestimmung von Abbauraten zu bewerten. Dazu wird der Einfluss von hydraulischer Heterogenität und Messfehlern anhand einer „Virtueller Aquifer" Szenarioanalyse untersucht. Hierzu werden in einem synthetischen Aquifer mit unterschiedlich stark ausgeprägter Heterogenität virtuelle stationäre Fahnen simuliert, die einer Abbaukinetik erster Ordnung unterliegen. Die anhand der oben genannten vier Methoden bestimmten Abbauratenkonstanten erster Ordnung werden mit dem wahren Wert verglichen und so Aussagen über die Zuverlässigkeit und Unsicherheit der Methoden und der resultierenden Ratenkonstanten abgeleitet. Bei der Untersuchung des Einflusses des Messfehlers auf die Ratenkonstante wird anschließend von einem homogenen Aquifer ausgegangen. Der Einfluss von Messfehlern bei der Bestimmung der Piezometerhöhe und bei der Konzentrationsmessung wird separat untersucht und quantifiziert.

Methodik

Das verwendete Modellgebiet ist zweidimensional und misst 184 m auf 64 m (vergl. Abb. 1). Das Grundwasser strömt von links nach rechts, der mittlere hydraulische Gradient beträgt 0.003 und wird durch Festpotentialrandbedingungen am linken und rechten Modellrand erzeugt. Alle anderen Ränder sind undurchlässig. Das Modellgebiet ist mit einer Gitterweite von 0.5 m regelmäßig diskretisiert. 11.5 m vom oberstromigen Rand ist eine Schadstoffquelle, durch eine Festkonzentrationsrandbedingung dargestellt, eingebracht, die einen Schadstoff emittiert, der einer Abbaukinetik erster Ordnung folgend mit einer Ratenkonstanten λ abgebaut wird. Zusätzlich wird ein nichtreaktiver Stoff aus der Quelle freigesetzt. Es werden Quellbreiten von 4, 8 und 16 m betrachtet. Weder Sorption noch Ausgasung werden berücksichtigt. Der Schadstoff verhält sich also genau so, wie es von den Methoden zur Bestimmung der Abbaurate angenommen wird – eine Annahme, die in der Realität nur annähernd erfüllt ist, da die Abbauraten komplexeren Gesetzmäßigkeiten folgen. Diese Abstraktion ist hier notwendig, um die vier Methoden möglichst genau untersuchen zu können. Als longitudinale und transversale Dispersionslängen werden im Modell 0.25 m und 0.05 m angenommen. Diese stellen die lokale Dispersion dar, in die effektive Dispersion geht noch die Heterogenität der hydraulischen Durchlässigkeit ein, die hier im Modell explizit dargestellt wird. Mit Hilfe des Programms GeoSys (KOLDITZ et al., 2005) wird dann eine stationäre Schadstofffahne erzeugt. Um den Einfluss räumlicher Heterogenität untersuchen zu können, wird die hydraulische Durchlässigkeit K als eine ln – normalverteilte Zufallsvariable aufgefasst mit einem Erwartungswert von ln(K) = -9.54, was einer mittleren hydraulischen Durchlässigkeit von 7.2 10^{-5} m s^{-1} entspricht. Mit der verwendeten Porosität von 0.33 ergibt sich so eine mittlere Transportgeschwindigkeit von $6.5 \cdot 10^{-7}$ m s^{-1}. Die räumliche Struktur wird durch ein isotropes exponentielles Covarianzmodell $C_{ln(K)} = \sigma^2 exp\,(-\Delta h/l)$ abgebildet, wobei eine integrale Länge von l = 2.67 m verwendet wird, was einer Korrelationslänge von 8.0 m entspricht (RUBIN, 2003). Vier Klassen von hydraulischer Heterogenität werden betrachtet, die durch ln(K)-Varianzen σ^2 von 0.38, 1.71, 2.70 und 4.50 gegeben sind und das Spektrum von wenig bis stark heterogenen Bedingungen abdecken. Der Wert σ^2 = 0.38, das Covarianzmodell, die mittlere hydraulische Durchlässigkeit und Porosität als auch die integrale Länge l entsprechen dem Standort Borden (SUDICKY, 1986). Der Wert 1.71 wurde in einem alluvialen Aquifer in Süddeutschland bestimmt (HERFORT, 2000), während die Werte 2.70 und 4.50 von Untersuchungen der Columbus Air Force Base stammen (REHFELDT et al., 1992). Die geostatistische Software gstats2.4 (PEBESMA & WESSELING, 1998) wurde zur Generierung der Zufallsverteilungen der hydraulischen Durchlässigkeit durch unkonditionierte Gauss'sche Simulation verwendet.

Die so erzeugten Fahnen werden nun anhand der Zentrallinien-Methode untersucht. Dabei sind anfänglich drei Beobachtungsbrunnen vorgegeben, von denen einer direkt in der Schadstoffquelle liegt, während die anderen keine Kontamination zeigen (Abb.1 a). An diesen drei Brunnen werden nun die Piezometerhöhen „gemessen", indem die Modellausgabe gelesen wird. Durch Konstruktion eines hydrogeologischen Dreiecks wird die lokale Fließrichtung an der Schadensquelle bestimmt (Abb.1b).

Entlang der so bestimmten Grundwasserfließrichtung werden nun drei neue Messstellen im Abstand von je 10 m installiert. An diesen Messstellen werden dann Piezometerhöhen, Konzentrationen des reaktiven und des nichtreaktiven Schadstoffes und die lokale hydraulische Durchlässigkeit „gemessen“ (Abb. 1c). Aus der Differenz der Piezometerhöhen, den hydraulischen Durchlässigkeiten und der wahren, d.h. der auch im Modell verwendeten, Porosität wird die Grundwasserfließgeschwindigkeit bestimmt. Zusammen mit den gemessenen Schadstoffkonzentrationen können dann Abbauraten erster Ordnung anhand von vier Methoden berechnet werden. Der Virtuelle Aquifer und das Messszenario sind so ausgelegt, dass optimale Bedingungen für eine Bestimmung der Abbauraten vorliegen. Die einzige Unsicherheit wird durch die heterogene Verteilung der hydraulischen Durchlässigkeit erzeugt.

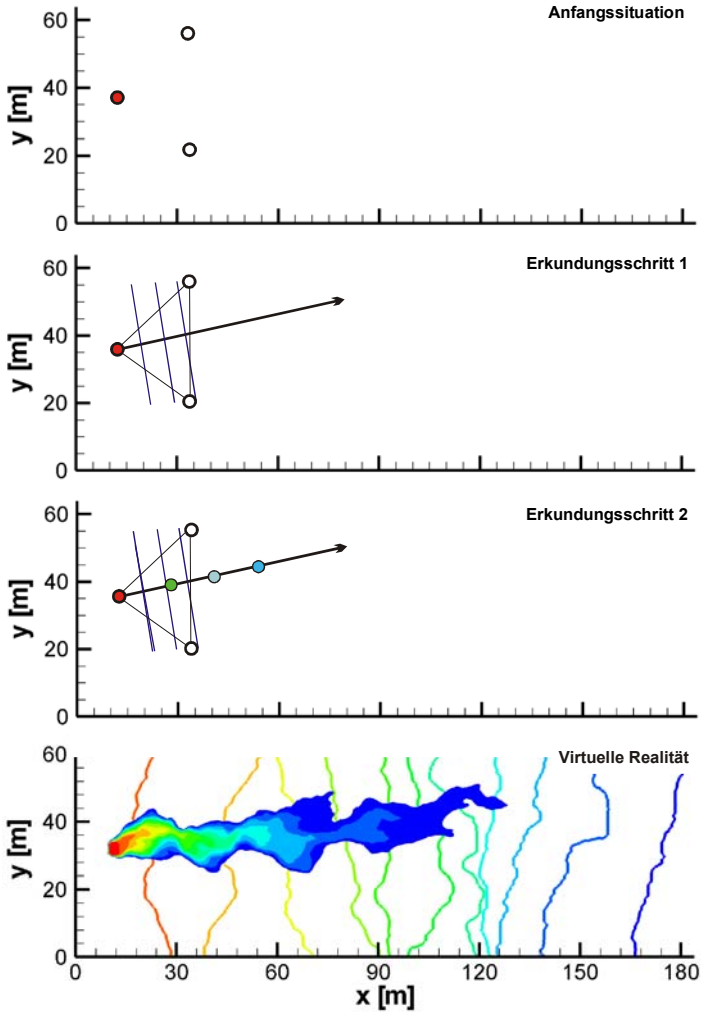

Abb. 1 *Verwendete Methodik, um Konzentrationen von der Zentrallinie der Fahne zu erhalten: a) Anfangszustand, b) Abschätzung der Fließrichtung anhand des hydrogeologischen Dreiecks, c) „gemessene“ Konzentrationen auf der ermittelten Zentrallinie, d) Vergleich mit der Virtuellen Realität (Piezometerhöhen und Fahne).*

Für den zweiten Teil dieses Beitrags, in dem der Einfluss von Messfehlern untersucht wird, wird der Aquifer als homogen angenommen. Die Unsicherheit wird nun also nicht durch das heterogene Fließfeld erzeugt, sondern durch fehlerhaftes „Messen“ von Piezometerhöhe und Schadstoffkonzentration. Im Falle der Piezometerhöhe lautet das Fehlermodell:

$$[1] \qquad h' = h + z\Delta h_{\max}$$

wobei h’ die fehlerbehaftete, hh die wahre Piezometerhöhe und Δh_{max} der maximale Messfehler für die Piezometerhöhe ist. z ist eine gleichverteilte Zufallszahl aus dem Intervall [-1, 1], mit der Δh_{max}

multipliziert wird, um einen fehlerbehafteten Messwert für die Piezometerhöhe aus dem Intervall [h-Δh_{max}, h+Δh_{max}] zu erhalten. Die fehlerbehafteten Messwerte streuen also symmetrisch um den wahren Wert. Δh_{max} wird zwischen 0 und 5 cm variiert. Bei der Ermittlung der Ratenkonstante wird nun bei der Probenahme für die Piezometerhöhe ein Messfehler gemäß des vorgestellten Fehlermodells berücksichtigt. Die gesamte Auswertung wird einhundert mal durchgeführt, um statistisch repräsentative Aussagen über den Einfluss des Messfehlers auf die Ratenkonstante zu erlangen.

Da für die Messung von Konzentrationen ein höherer Messfehlerbereich zu erwarten ist, wurde das Fehlermodell angepasst:

$$[2] \qquad c' = c(z\Delta c_{\max})^a$$

wobei c' die fehlerbehaftete, ch die wahre Konzentration und Δc_{max} der maximale Messfehlerfaktor für die Konzentration ist. Der Exponent a ist –1 oder 1 und wird zufällig bestimmt, z ist eine gleichverteilte Zufallszahl aus dem Intervall [0, 1], mit der Δc_{max} multipliziert wird. Man erhält so einen fehlerbehaftet Messwert für die Konzentration aus dem Intervall [c/Δc_{max}, cΔc_{max}]. Δc_{max} wird zwischen 1 und 100 variiert. Dieses Verfahren ist ähnlich zu dem für die Piezometerhöhe angewendeten Verfahren und ein Messfehlerfaktor von 2 entspricht dem umgangsprachlichen „auf einen Faktor 2 genau". Für die Bestimmung des Einflusses von Konzentrationsmessfehlern wurden ein homogenes Strömungsfeld und keine Messfehler für die Piezometerhöhe angenommen. Für den konservativen und den reaktiven Stoff wird dasselbe Messfehlermodell angenommen.

Die vier Methoden, anhand derer die Abbauraten bestimmt werden, sind in Tabelle 1 aufgeführt. Methode 1 stellt die Lösung zur eindimensionalen Advektionsgleichung mit Abbau erster Ordnung dar. Methode 2 wurde von WIEDEMEIER et al. (1996) vorgeschlagen, und baut auf Methode 1 auf. Allerdings werden die Konzentrationen des reaktiven Stoffes auf die Konzentrationen des nicht-reaktiven Stoffes bezogen. Dadurch berücksichtigt Methode 2 Dispersion, Verdünnung und „Aus der Fahne Messen" an Beobachtungspegeln, die nicht genau auf der Zentrallinie der Fahne liegen. Die dritte Methode wurde von BUSCHECK & ALCANTAR (1995) vorgestellt und basiert auf der eindimensionalen Transportgleichung mit Advektion, Dispersion und Abbau erster Ordnung. Diese Methode beinhaltet somit explizit die longitudinale Dispersion. ZHANG & HEATHCOTE (2003) beschrieben die vierte Methode, die auf der analytischen Lösung zur zweidimensionalen Transportgleichung beruht und zusätzlich zur longitudinalen auch die transversale Dispersion berücksichtigt.

Tab. 1 *Methoden zur Bestimmung von Abbauratenkonstanten erster Ordnung λ. v_a ist die Transportgeschwindigkeit, Δx ist der Abstand der verwendeten Beobachtungspegel, C(x) ist die unterstromige und C_0 die Quellkonzentration. α_L und α_T sind die longitudinale und transversale Dispersivität, W_S ist die Quellbreite und erf ist die Fehlerfunktion.*

Methode	**Formel für Abbauratenkonstante**	**Beschreibung**
1	$\lambda_1 = -\frac{v_a}{\Delta x}\ln\left(\frac{C(x)}{C_0}\right)$	Analytische Lösung der 1D Advektionsgleichung mit Abbau erster Ordnung
2	$\lambda_2 = -\frac{v_a}{\Delta x}\ln\left(\frac{C(x)}{C_0}\frac{C_0^*}{C(x)^*}\right)$	Wie Methode 1, aber Konzentration normiert auf einen nichtreaktiven Mitkontaminand, berücksichtigt Verdünnung und Dispersion
3	$\lambda_3 = \frac{v_a}{4\alpha_L}\left(\left(1-2\alpha_L\frac{\ln(C(x)/C_0)}{\Delta x}\right)^2-1\right)$	Analytische Lösung der 1D Transport-gleichung mit longitudinaler Dispersion
4	$\lambda_3 = \frac{v_a}{4\alpha_L}\left(\left(1-2\alpha_L\frac{\ln(C(x)/(C_0\beta))}{\Delta x}\right)^2-1\right)$ mit: $\beta = erf\left(\frac{W_S}{4\sqrt{\alpha_T\Delta x}}\right)$	Analytische Lösung der 2D Transport-gleichung. Berücksichtigt sind longitudinale und transversale Dispersion und die Quellbreite

Für die letztgenannten Methoden müssen die longitudinale und die transversale Dispersivität bekannt sein. Gemäß einem Ansatz in WIEDEMEIER et al. (1999) wurde die longitudinale Dispersivität als 10% der Fahnenlänge angenommen, die transversale Dispersivität beträgt 33% der longitudinalen Dispersivität. Als Fahnenlänge wurde der Abstand von der Quelle zur entferntesten Messstelle angenommen. Dieser Abstand beträgt 30 m, die longitudinale Dispersivität somit 3 m und die Transversale Dispersivität 1 m. Die Dispersivitäten sind damit recht gering geschätzt, eine detaillierte Untersuchung des Einflusses der angenommenen Dispersivitäten ist in BAUER et al. (2005) zu finden. Mithilfe der vier vorgestellten Ansätze werden Abbauraten erster Ordnung ermittelt und mit dem Modelleingabewert verglichen. Für jede Klasse der hydraulischen Heterogenität werden je 100 Realisierungen betrachtet, um ein statistisches Maß für die Unsicherheit zu erhalten, die durch die hydraulische Heterogenität erzeugt wird. Für jede Realisierung wurde die oben beschriebene Auswertung für jede Methode und jede Quellbreite durchgeführt. Dabei wurden jeweils die Abbauraten erster Ordnung ausgehend von der Quelle für die unterstromigen Brunnen im Abstand von 10 m, 20 m und 30 m bestimmt und anschließend arithmetisch gemittelt. Für Methode 4 wird für die Ermittlung der Abbaurate die wahre Quellbreite angenommen.

Ergebnisse und Diskussion

Einfluss der Heterogenität

Abb. 2 zeigt die Ergebnisse der Berechnung der Abbauratenkonstante erster Ordnung. Die Raten werden normalisiert dargestellt, d.h. die berechnete Ratenkonstante wird durch die wahre Ratenkonstante geteilt. Die normalisierte Rate kann so als Überschätzungs- bzw. Unterschätzungsfaktor interpretiert werden. Abb. 2 zeigt, dass die meisten berechneten Ratenkonstanten größer als 1.0 sind, d.h. dass die Ratenkonstante überschätzt wird. Dieser Effekt ist in einzelnen Realisierungen sehr stark, wo Überschätzungen der Ratenkonstante von einigen Größenordnungen auftreten können. Abb. 2a zeigt links die Variation der berechneten normalisierten Ratenkonstante mit der Quellbreite der emittierenden Schadstoffquelle. Es ist deutlich, dass mit zunehmender Quellbreite die berechnete Ratenkonstante sich der wahren Ratenkonstante annähert, d.h. sich dem Wert 1 annähert, was am deutlichsten für große Heterogenitäten sichtbar ist. Dies ist in Methode 1 begründet, die weder Verdünnung noch Dispersion oder „Aus der Fahne messen“ berücksichtigt. Diese Effekte werden mit zunehmender Quellbreite weniger signifikant, da dann die Annahmen zur Anwendung von Methode 1 besser erfüllt sind. Auf der rechten Seite der Abb. 2 ist die Abhängigkeit der berechneten Ratenkonstante von der verwendeten Heterogenitätsklasse, durch die zugehörige Varianz $\sigma^2\ln(K)$ bezeichnet, dargestellt. Es ist zu erkennen, dass eine Erhöhung von $\sigma^2\ln(K)$ im Mittel zu einer Überschätzung der Ratenkonstante führt. Zusätzlich zu diesem Trend nimmt auch die Standardabweichung der berechneten Ratenkonstanten zu, was die Zunahme der Spanne der ermittelten Ratenkonstanten wiederspiegelt. Diese Zunahme der Spanne kann als Zunahme der Unsicherheit der berechneten Ratenkonstante verstanden werden. Die Überschätzung beträgt im Mittel ca. 2 für geringe Heterogenität, steigt jedoch auf Werte von 4 bis 10 für mittlere und hohe Heterogenität und erreicht einen Wert von ca. 100 im Falle der sehr hohen hydraulischen Heterogenität.

Abb. 2b stellt die Ergebnisse für Methode 2 dar. Auch anhand von Methode 2 werden die Ratenkonstanten überschätzt, jedoch sind, verglichen mit Methode 1, die Überschätzungen als auch die Standardabweichung generell geringer. Methode 2 liefert also bessere und mit weniger Unsicherheit behaftete Ergebnisse. Wie man an der linken Grafik in Abb. 2b erkennen kann, ergibt sich für Methode 2 keine Abhängigkeit von der Quellbreite. Dies ist in der Methode begründet, da sie Effekte von Dispersion, Verdünnung und „Aus der Fahne messen“ durch die Normierung explizit berücksichtigt. Methode 3 zeigt ein ähnliches Verhalten wie Methode 1, sowohl in Abhängigkeit von der Quellbreite als auch in Abhängigkeit von der Heterogenität (Abb. 2c). Jedoch sind die normalisierten Abbauratenkonstanten höher als für Methode 1, was an der Berücksichtigung der Dispersion in Methode 3 liegt.

Im eindimensionalen Aquifer mit einer Festkonzentration als Randbedingung führt die Berücksichtigung der longitudinalen Dispersion zu höheren Konzentrationen entlang der stationären Fahne, verglichen mit dem Fall ohne Dispersion. Dies wird durch den zusätzlichen dispersiven Massenaustrag aus der Schadstoffquelle verursacht. Um eine gemessene Konzentrationsabnahme zwischen Quelle und unterstromigen Brunnen mit Methode 3 erklären zu können ist also eine höhere Abbauratenkonstante notwendig als mit Methode 1. Methode 4 (Abb. 2d) schließlich zeigt ein sehr ähnliches Bild wie Methode 3. Aufgrund der in Methode 4 berücksichtigten Querdispersivität sind die bestimmten Abbauratenkonstanten etwas geringer als bei Methode 3. Für geringe Heterogenität wird die Ratenkonstante durch Methode 4 sogar unterschätzt. Dies liegt an einer zu hohen Korrektur durch

den Querdispersionsterm, der die Effekte der Querdispersion für geringe Heterogenität überschätzt. Für den Fall geringer oder keiner Heterogenität sind die hier gewählten und in Methode 4 verwendeten Dispersivitäten zu groß.

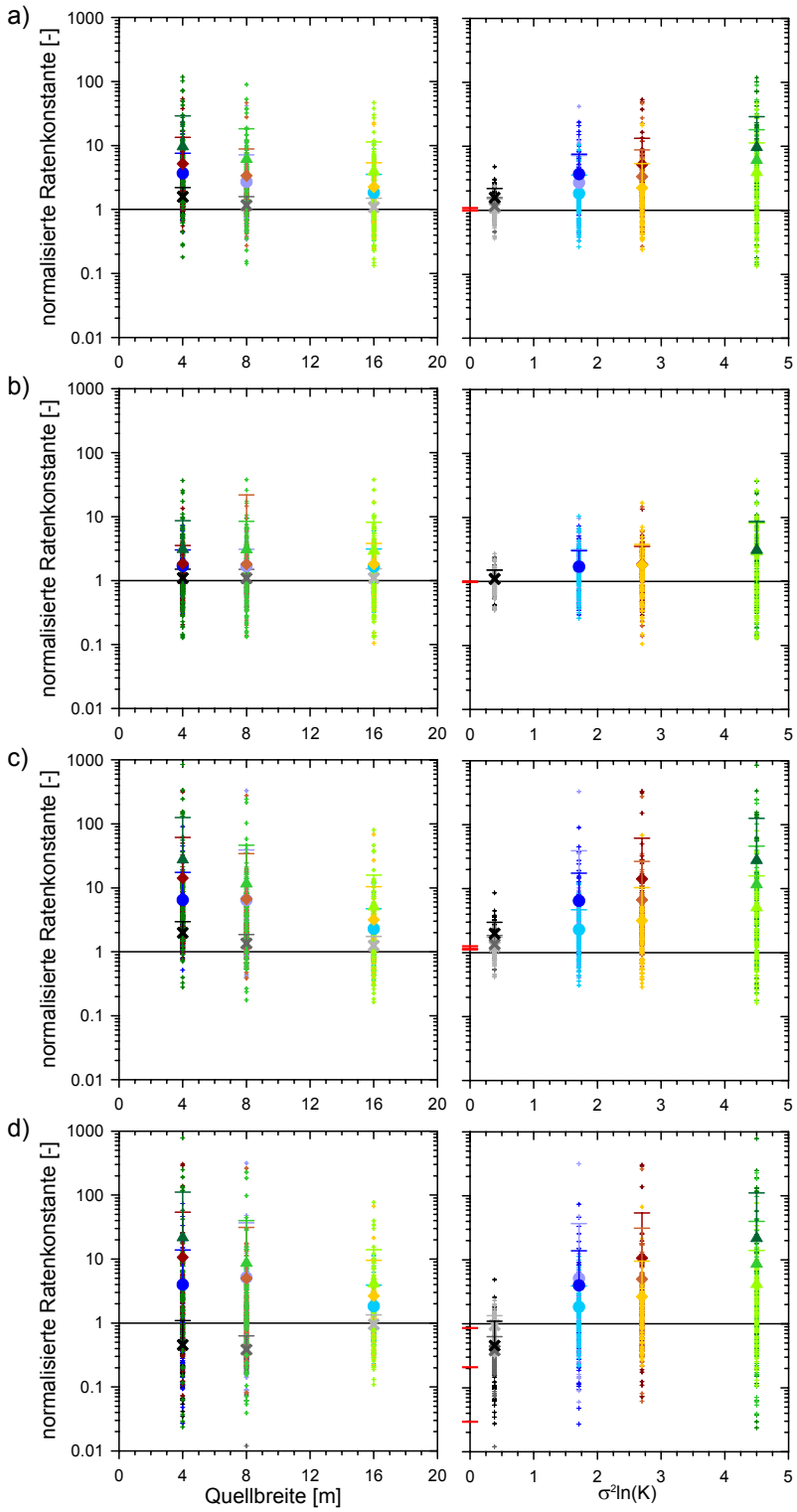

Abb. 2 *"Gemessene" Abbauratenkonstanten erster Ordnung, normalisiert auf die wahre Abbauratenkonstante, aufgetragen gegen Quellbreite (links) und Heterogenität (rechts). a) Methode 1, b) Methode 2, c) Methode 3 und d) Methode 4. Alle Abbildungen zeigen die Einzelergebnisse aller Realisierungen (kleine Symbole), ihren Mittelwert (große Symbole) und die zugehörige Standardabweichung (Fehlerbalken). Unterschiedliche Grautöne geben die Quellbreite, unterschiedliche Symbole die verwendeten $\sigma^2 ln(K)$ an.*

Um diesen Effekt zu verdeutlichen sind in Abb. 2 für alle Methoden noch die für den homogenen Fall bestimmten Ratenkonstanten eingetragen. Die Ergebnisse sind für $\sigma^2 \ln(K) = 0$ in den Abbildungen rechter Hand als kleine horizontale Balken dargestellt. Für Methode 1 und Methode 2 beträgt die normalisierte Ratenkonstante im homogenen Fall genau 1.0, d.h. diese Methoden liefern exakt die wahre Ratenkonstante. Mit Methode 3 ergibt sich eine geringe Überschätzung, mit Methode 4 eine deutliche Unterschätzung der wahren Ratenkonstante. Die geringste Ratenkonstante wird für die geringste Quellbreite ermittelt, da hier die Korrektur durch β am größten ist (vergl. Tab 1).

Da die bisher gezeigten Mittelwerte und Standardabweichungen repräsentativ für das Ensemblemittel sind, nicht jedoch für die einzelnen Realisierungen, wurde ein weiteres Maß zum Vergleich der anhand der vier Methoden bestimmten Ratenkonstanten entwickelt. Abb. 3 zeigt die Wahrscheinlichkeit, mit der eine Methode zum Erfolg führen kann, worunter hier verstanden wird, dass die Abbaurate anhand der Methode mit einer gewünschten Genauigkeit ermittelt wird. Die gewünschte Genauigkeit wird als sogenannten Fehlerfaktor angegeben. Ein Fehlerfaktor von 10 entspricht dem Intervall 0.1 bis 10 der normierten Ratenkonstanten, wobei dieses Intervall durch Division und Multiplikation von 1.0 mit dem Fehlerfaktor (10) ermittelt wird. Dies entspricht somit der umgangssprachlichen Formulierung „... innerhalb einer Größenordnung ...“. Ein Fehlerfaktor von 5 entspricht somit dem Intervall 0.2 bis 5 der normierten Ratenkonstanten. Abb. 3 gibt daher die Wahrscheinlichkeit dafür an, dass eine „gemessene“ Ratenkonstante innerhalb des durch den Fehlerfaktor aufgespannten Intervalls liegt. Abb. 3a zeigt für die geringste Heterogenität, dass die Wahrscheinlichkeit, die Abbauratenkonstante mit einem Fehlerfaktor kleiner als 2.0 zu bestimmen („ ... bis auf einen Faktor zwei ...“), für Methode 1 ca. 70 %, für Methode 2 ca. 90%, für Methode 3 ca. 55% und für Methode 4 ca. 30% beträgt. Wird der Fehlerfaktor auf 5 erhöht, dann erhält man mit Methoden 1 bis 3 eine Erfolgswahrscheinlichkeit von 100%, nur mit Methode 4 beträgt die Erfolgswahrscheinlichkeit ca. 70%. Je geringer die Werte einer Methode in Abb. 3 sind, desto geringer ist die Wahrscheinlichkeit, die Abbauratenkonstante mit der gewünschten Genauigkeit bestimmen zu können. Wie Abb. 3 zeigt, sinkt für alle Methoden die Erfolgswahrscheinlichkeit mit zunehmender Heterogenität. Beträgt die Erfolgswahrscheinlichkeit von Methode 1 für einen Fehlerfaktor von 5 noch ca. 100% für die geringste Heterogenität, so sinkt diese Wahrscheinlichkeit auf 70%, 50% und schließlich 35% für die höheren Heterogenitätsklassen. Für Methoden 2 bis 4 sind die Werte analog Abbildung 3 zu entnehmen.

Abb. 3 erlaubt daher einen direkten Vergleich der in dieser Arbeit untersuchten vier Methoden. Wird die Ratenkonstante in einem stark heterogenen Aquifer beispielsweise auf einen Faktor zehn genau benötigt, betragen die Erfolgswahrscheinlichkeiten ca. 80%, 95%, 80% und 60% für Methoden 1 bis 4 (Abb. 3c). Für alle Heterogenitätsklassen liefert Methode 2 die höchste Wahrscheinlichkeit, das richtige Ergebnis zu bekommen. Für mittlere bis hohe Heterogenitäten folgt Methode 4 an zweiter Stelle, während diese Methode für geringe Heterogenität die schlechtesten Erfolgswahrscheinlichkeiten aufweist. Obwohl Methode 1 die einfachste Methode ist, liefert sie sehr ähnliche Ergebnisse wie Methode 4. Für geringe Heterogenitäten ergeben sich mit Methode 1 sogar die besseren Abschätzungen der Ratenkonstante. Methode 3 zeigt – bis auf geringe Heterogenität – immer die geringste Erfolgswahrscheinlichkeit.

Für größere Quellbreiten ergeben sich qualitativ dieselben Ergebnisse. Methode 2 ist unabhängig von der Quellbreite, daher ist auch für Quellbreiten von 8 m oder 16 m die Erfolgswahrscheinlichkeit von Methode 2 dieselbe wie im Falle von 4 m. Für die anderen Methoden ergeben sich mit zunehmender Quellbreite höhere Erfolgswahrscheinlichkeiten. So steigt z.B. die Erfolgswahrscheinlichkeit von Methode 3 für $\sigma^2 \ln(K) = 2.7$ von 35% für eine Quellbreite von 4 m (Abb. 3c) auf 40% für eine Quellbreite von 8 m und ca. 50% für eine Quellbreite von 16 m. Somit steigt die Erfolgswahrscheinlichkeit für Methoden 1, 3 und 4 mit der Quellbreite an, erreichen aber dennoch nicht die Erfolgswahrscheinlichkeit von Methode 2.

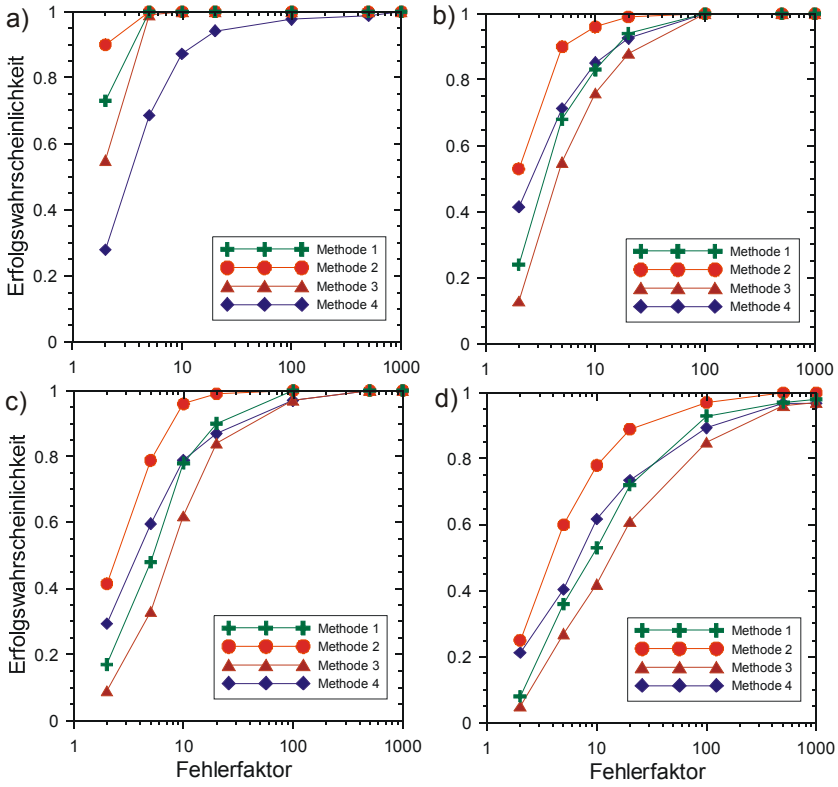

***Abb. 3** Erfolgswahrscheinlichkeit für alle vier Methoden gegen den Fehlerfaktor für $\sigma^2 ln(K)$ a) 0.38, b) 1.71, c) 2.7 and d) 4.5. Die Quellbreite beträgt 4 m.*

Einfluss des Messfehlers

Bei der Untersuchung des Einflusses des Messfehlers wird von einem homogenen Aquifer ausgegangen. Die Unsicherheit wird nun nicht durch das heterogene Fließfeld erzeugt, sondern durch falsches „Messen“ von Piezometerhöhe und Schadstoffkonzentration.

Da in der vorigen Untersuchungen gezeigt wurde, dass Methode 4 mit der gewählten transversalen Dispersivität im homogenen Fall zu kleine Abbauratenkonstanten liefert, wurde die transversale Dispersivität, die für die Auswertung mit Methode 4 (Tabelle 1) verwendet wird, auf 0.15 m verringert. Damit ergibt sich im homogenen Fall die richtige Abbauratenkonstante.

In Abb. 4 ist die auf die wahre Ratenkonstante normierte fehlerbehaftete Ratenkonstante gegen den maximal möglichen Fehler bei der Bestimmung der Piezometerhöhe, Δh_{max}, gesondert für die vier Auswertemethoden aufgetragen. In Abb. 4a erkennt man ein deutliches Ansteigen der normierten Ratenkonstanten mit zunehmendem Δh_{max} für die Auswertung mit Methode 1. Bereits für einen maximalen Messfehler von 1 cm ergibt sich eine mittlere Überschätzung von ca. 2, der für ein Δh_{max} von 5 cm auf ca. 5 steigt. Außerdem ist zu erkennen, dass für einzelne Messungen Überschätzungen der Ratenkonstante von mehr als 10 möglich sind. Generell liegt eine Überschätzung vor, da eine fehlerhaft bestimmte Piezometerhöhe zu einer falschen Abschätzung der Fließrichtung führt. Die neu platzierten unterstromigen Brunnen liegen dann nicht mehr auf der Zentrallinie, d.h. die gemessenen Konzentrationen sind kleiner als auf der Zentrallinie und dies führt zu einer Überschätzung der Ratenkonstanten. Es wird jedoch nicht nur die Fließrichtung falsch ermittelt, sondern auch die Fließgeschwindigkeit entlang der (angenommenen) Zentrallinie, da diese aus den gemessenen Piezometerhöhen, Brunnenabständen und hydraulischen Durchlässigkeiten berechnet wird. Der hieraus resultierende Fehler kann sowohl zu große als auch zu kleine Ratenkonstanten produzieren.

Für Methode 2 (Abb. 4b) ergibt sich ein anderes Bild. Die mittlere Ratenkonstante ist auch für große Δh_{max} sehr nahe bei 1, d.h. es liegt kein Trend zu Über- oder Unterschätzung vor. Die Unsicherheit der bestimmten Abbaurate ist kleiner als bei Methode 1, wie an den Fehlerbalken zu erkennen ist. Da Methode 2 das „aus der Fahne messen“ korrigiert, lässt sich dieser Fehler für Methode 2 nicht beobachten (Abb. 4b). Es kommt sowohl zu einer Über- als auch Unterschätzung der Ratenkonstante, also einem eher symmetrischen Fehler ohne generelle Tendenz, der auf die falsche Abschätzung der Fließgeschwindigkeit zurückzuführen ist. Mit zunehmendem Δh_{max} nimmt auch für Methode 2 die

Unsicherheit zu. Für Methode 3 (Abb. 4c) und Methode 4 (Abb. 4d) ergibt sich – wie schon für die hydraulische Heterogenität – ein sehr ähnliches Bild wie für Methode 1, jedoch mit höheren Überschätzungen und Unsicherheiten als für Methode 1. Für Methode 3 und 4 beträgt die mittlere Überschätzung der Ratenkonstanten für Δh_{max} = 1 cm bereits ca. 5, jeweils verbunden mit einer hohen Unsicherheit.

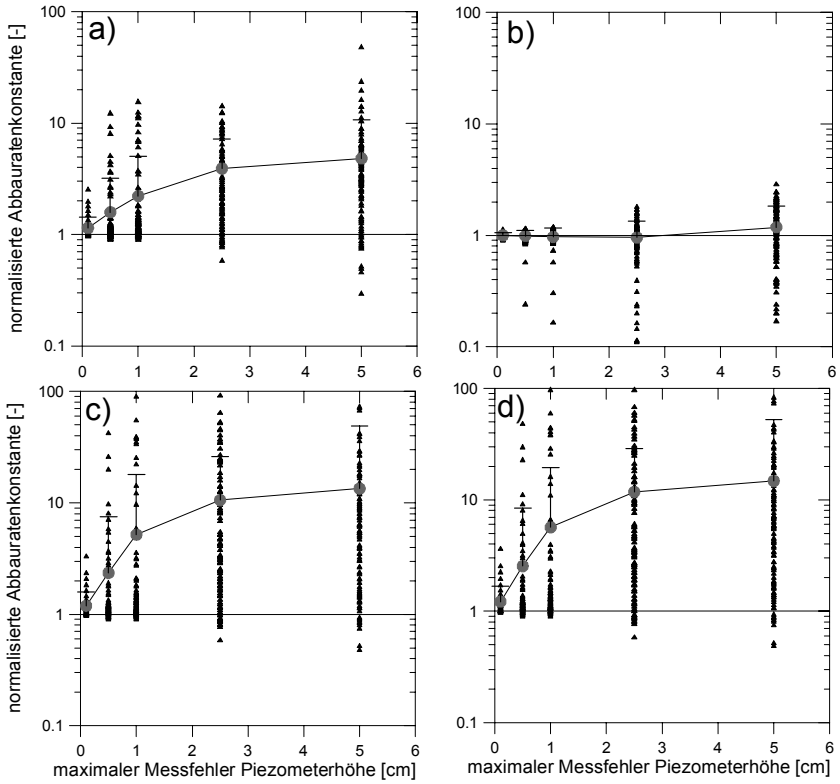

Abb. 4 *Normalisierte Abbauratenkonstante, aufgetragen gegen den maximalen Messfehler bei der Bestimmung der Piezometerhöhe für a) Methode 1, b) Methode 2, c) Methode 3 und d) Methode 4. Dargestellt sind die Einzelergebnisse (kleine Symbole), die Mittelwerte (durch Linie verbundene Punkte) und die zugehörige Standardabweichung (Fehlerbalken).*

Für Konzentrationsmessungen wurde ein höherer Messfehlerfaktor von 100 und eine exakte Messung der Piezometerhöhe angenommen (siehe Kapitel Methodik). Ein Messfehlerfaktor von 100 ist sicherlich sehr hoch gegriffen und wird hier nur zu Demonstrationszwecken eingesetzt. Das Ergebnis für Methode 1 zeigt Abb. 5a, in der die normierte Ratenkonstanten gegen den Fehlerfaktor aufgetragen sind. Man erkennt, dass für geringe Messfehlerfaktoren die Abbaukonstante sehr gut bestimmt werden kann, für einen Messfehlerfaktor von 2 erhält man im Mittel noch das richtige Ergebnis, für einen Messfehlerfaktor von 5 erhält man eine mittlere Überschätzung der Ratenkonstante von ca. 3. Die maximale mittlere Überschätzung der Ratenkonstante von ca. 5 wird bei einem Messfehlerfaktor von ca. 10 erreicht und steigt auch für größere Fehlerfaktoren nicht weiter an. Allerdings nimmt die Unsicherheit, dargestellt als Standardabweichung, mit dem Messfehlerfaktor stark zu und man kann sowohl zu große als auch zu kleine Ratenkonstanten erhalten. Für Methode 2 (Abb. 5b) erhält man generell eine geringere Überschätzung der Ratenkonstante von maximal ca. drei, jedoch eine ähnlich hohe Unsicherheit wie mit Methode 1. Generell werden bei Methode 2 eher kleinere Ratenkonstanten erzeugt als bei Methode 1. Methoden 3 und 4 (Abb 5.c und Abb. 5d) zeigen einen deutlichen Anstieg der ermittelten Überschätzung mit dem Messfehlerfaktor, maximale Werte liegen hier bei etwa 10. Ebenso ist die Unsicherheit dieser Werte sehr hoch.

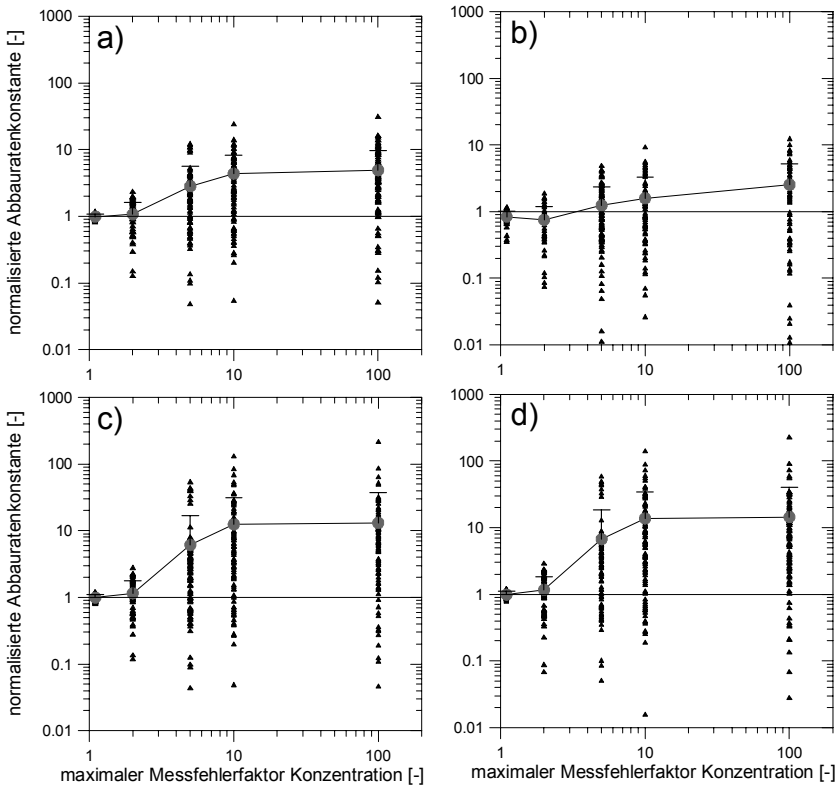

Abb. 5 *Normalisierte Abbauratenkonstante, aufgetragen gegen den maximalen Messfehlerfaktor bei der Bestimmung der Konzentration für a) Methode 1, b) Methode 2, c) Methode 3 und d) Methode 4. Dargestellt sind die Einzelergebnisse (kleine Symbole), die Mittelwerte (durch Linie verbundene Punkte) und die zugehörige Standardabweichung (Fehlerbalken).*

Schlussfolgerungen

Die vorgestellten Ergebnisse zeigen, dass sich die anhand der vier untersuchten Methoden ermittelten Abbauratenkonstanten erster Ordnung sowohl für zunehmende hydraulische Heterogenität als auch für zunehmende Messfehler bezüglich der Piezometerhöhe und der Konzentration unterscheiden. Alle Methoden zeigen geringere Erfolgswahrscheinlichkeiten mit zunehmender Heterogenität (Abb.3) sowie eine erhöhte Unsicherheit (Abb. 2). Aus Abb. 2 ist ersichtlich, dass diese Abnahme der Erfolgswahrscheinlichkeit durch eine generelle Überschätzung der Ratenkonstante verursacht wird. Diese Überschätzung ist am größten für Methode 3. Methode 2 wird dagegen am wenigsten von der hydraulischen Heterogenität beeinflusst und zeigt die geringsten Überschätzungen (Abb. 2) und Unsicherheiten. Obwohl Methoden 3 und 4 realitätsnäher sind, da sie auf der eindimensionalen bzw. zweidimensionalen Transportgleichung beruhen, zeigen sie eine geringere Erfolgswahrscheinlichkeit und eine größere Überschätzung der Ratenkonstanten als Methoden 1 und 2. Beide Methoden sind anfällig für Fehler, die durch die Abschätzung der longitudinalen und transversalen Dispersivitäten erzeugt werden können. Methode 1 als die einfachste Methode, da sie weder die Abschätzung der Dispersivität noch einen nichtreaktiven Mitkontaminanden benötigt, zeigt bessere oder ähnlich gute Ergebnisse wie Methode 4. Sowohl mittlere Überschätzung als auch Unsicherheit steigen mit zunehmender Größe des Messfehlers. Die Untersuchung des Messfehlers der Piezometerhöhe zeigt, dass bereits geringe Messfehler von 1 cm zu deutlicher Überschätzung der Ratenkonstanten und einer erhöhten Unsicherheit führen können. Der Einfluss des Messfehlers der Konzentration auf die Ratenkonstante ist generell geringer. Auch bei der Untersuchung der Messfehler erhält man, wie schon im Falle von hydraulischer Heterogenität, die besten Ergebnisse mit Methode 2. Methoden 3 und 4 zeigen sehr ähnliche Ergebnisse und weisen größere Überschätzungen auf als Methode 2 oder Methode 1.

Insgesamt ergibt sich, dass die Verwendung von Methode 2, die auf der Normierung der Schadstoffkonzentration mit einem nichtreaktiven Mitkontaminanden beruht, zu den besten Ergebnissen bei der Bestimmung von Abbauratenkonstanten erster Ordnung führt. Daher sollte diese Methode, wenn möglich, angewendet werden. Ist kein nichtreaktiver Mitkontaminand vorhanden, sollte Methode 1 verwendet werden, da sie die Abbauratenkonstante besser als Methoden 3 und 4 vorher-

sagt sowie die zusätzliche Problematik des Abschätzens der Dispersivitäten umgeht. In BAUER et al. (2005) wird der Einfluss der geschätzten Dispersivitäten auf die Abbauratenkonstante sowohl für die longitudinale als auch transversale Dispersivität anhand einer Sensitivitätsstudie eingehend untersucht. Es zeigt sich dabei, dass mit Methode 3 nie, mit Methode 4 nur unter Annahme sehr hoher transversaler Dispersivitäten, die nicht mit der Heterogenität (σ^2ln(K)) des Aquifers begründet werden können, die korrekten Abbauraten ermittelt werden. In diesem Aufsatz werden weiterhin der Einfluss der Quellbreite sowie verschiedene Methoden zur Berechnung der Fliessgeschwindigkeit untersucht. Es zeigt sich, dass die Anordnung der Messpegel, abgeleitet aus dem hydraulischen Dreieck, großen Einfluss auf die geschätzte Abbaurate hat, wie er sich auch in Abbildung 1 widerspiegelt. Ebenso ist die Mittelung der an den einzelnen Messpegeln ermittelten hydraulischen Durchlässigkeiten von Bedeutung. Hier ergibt sich, dass eine geometrische Mittelung zu bevorzugen ist (BAUER et al., 2006).

Die gefundene generelle Überschätzung der Ratenkonstante ist im Hinblick auf eine Prognose der Fahnenlänge problematisch, da eine zu hohe Ratenkonstante den Abbau überschätzt und daher zu geringe prognostizierte Fahnenlängen verursacht. Dieser Fehler ist daher nicht konservativ und kann zu einer zu optimistischen Einschätzung der Standortverhältnisse führen. Im Folgenden ist die Fahnenlänge definiert als die Strecke zwischen Schadensquelle und dem Ort auf der Fahnenzentralachse, an dem das Verhältnis C/C_0 einen vorgegebenen Wert erreicht hat (beispielsweise 10^{-3}), wobei C die Konzentration in der Fahne und C_0 die Konzentration in der Quelle ist. Für eindimensionale Lösungen ohne Dispersion ergibt sich, dass Abbaurate und Fahnenlänge umgekehrt proportional zueinander sind und die Fahnenlänge linear mit dem Kehrwert der Abbaurate wächst (Vergleiche Methoden 1 und 2 in Tabelle 1). Eine Überschätzung der Abbaurate um den Faktor 5 verursacht also eine Unterschätzung der Fahnenlänge ebenfalls um den Faktor 5. Im eindimensionalen Fall mit Dispersion sowie im zweidimensionalen Fall ist die Fahnenlänge annähernd umgekehrt proportional zum Kehrwert der Quadratwurzel der Abbaurate, die genauen Werte hängen von den gegebenen Dispersivitäten, der Quellbreite und dem Verhältnis von Abstandsgeschwindigkeit zu Abbaurate ab (vergleiche Methoden 3 und 4 in Tabelle 1). Eine Überschätzung der Fahnenlänge um den Faktor 5 bzw. 10 kann beispielsweise eine Unterschätzung der Fahnenlänge um den Faktor 3 bzw. 5 verursachen. Der Einfluss der Dispersion verringert die Sensitivität der Fahnenlänge auf die Abbaurate. Eine genauere Untersuchung des Einflusses der ermittelten Abbaurate auf die prognostizierte Fahnenlänge wurde von BEYER et al., (2005b) durchgeführt. Dabei zeigte sich eine durchschnittliche Unterschätzung der Fahnenlängen um 50 %. Für einzelne Realisierungen ergaben sich zum Teil jedoch erheblich größere Fehler, sodass in ungünstigen Fällen die geschätzte Fahnenlänge lediglich 10% des tatsächlichen Wertes betrug. Dabei zeigt sich, dass die mit Methoden 1, 3 und 4 berechneten Abbauraten prinzipiell zu ähnlichen Abschätzungen der Fahnenlänge führen, wenn diese mit einem mit der Abbaurate korrespondierenden Transportmodell berechnet wird. Die durch Vernachlässigung bzw. falsche Parametrisierung der Längs- und Querdispersion verursachten Fehler in der Abbaurate werden bei der Fahnenlängenprognose teilweise wieder aufgehoben. Als problematisch stellte es sich jedoch heraus, Abbauraten, die mit der eindimensionalen Lösung berechnet wurden, in einem zwei- oder dreidimensionalen Transportmodell zur Prognose der Fahnenlänge zu verwenden (BEYER et al., 2005b).

Danksagung: Der Beitrag entstand im Rahmen des Projekts TV 7.1 „Modellierung und Prognose“ des BMBF- Förderschwerpunktes “Kontrollierter natürlicher Rückhalt und Abbau von Schadstoffen bei der Sanierung kontaminierter Grundwässer und Böden (KORA)“ an den Universitäten Kiel und Tübingen. Den Projektträgern und dem BMBF sei für die hierbei gewährte Unterstützung gedankt.

Literaturangaben

Bauer, S., Beyer, C. , Kolditz, O. (2006): Assessing measurement uncertainty of first order degradation rates in heterogeneous aquifers. - Water Resour. Res., im Druck.

Bauer, S., Beyer, C., Kolditz, O. (2005): Assessing measurements of first order degradation rates by using the Virtual Aquifer approach. - IAHS Publication, 297: 274-281.

Bauer, S., Kolditz, O. (2005): Uncertainty assessment of integral pumping tests in heterogeneous aquifers. - Angenommener Beitrag für eine IAHS Publikation.

Beyer, C., Bauer S., Kolditz, O. (2005a): Uncertainty assessment of degradation rate measurements in heterogeneous media using the virtual aquifer approach. - In: Kolditz, O., Bauer, S., and Gronewold, J. (Eds.): Proceedings of the 5th Workshop “Porous Media”, Blaubeuren, Germany, December 2004,. ZAG Publisher, Tübingen.

Beyer, C., Bauer S., Kolditz, O. (2005b): Using the Virtual Aquifer approach for uncertainty assessment of contaminant plume length estimates. GeoSys Preprint, GeoSystemForschung, Tübingen. http://www.uni-tuebingen.de/zag/geohydrology/index.html

Bockelmann, A., Zamfirescu, D., Ptak, T., Grathwohl, P., Teutsch, G. (2003): Quantification of mass fluxes and natural attenuation rates at an industrial site with a limited monitoring network: A case study. - J. Contam. Hydrol., 60: 97-121.

Buscheck, T.E., Alcantar, C.M. (1995): Regression techniques and analytical solutions to demonstrate intrinsic bioremediation. - In: Proceedings of the 1995 Battelle International Conference on In-Situ and On Site Bioreclamation, Batelle, CA, April 1995. 109-116.

Chapelle, F.H., Bradley, P.M., Lovley, D.R., Vroblesky, D.A. (1996): Measuring rates of biodegradation in a contaminated aquifer using field and laboratory methods. -Ground Water, 34(4): 691-698.

Herfort, M. (2000): Reactive Transport of Organic Compounds Within a Heterogeneous Porous Aquifer. - Tübinger Geowissenschaftliche Arbeiten, 54, Universität Tübingen, Tübingen.

Kolditz, O., de Jonge, J., Beinhorn, M., Xie, M., Kalbacher, M., Wang, W., Bauer, S., McDermott, C., Chen, C., Beyer, C., Gronewold, J., Kemmler, D., Manabe, T., Legeida D., Adamidis, P. (2005): GeoSys - Theory and users manual, release 4.2. GeoHydrology / HydroInformatics, Center for Applied Geoscience, Universität Tübingen, Tübingen.

McNab Jr, W. W., Dooher, B.P. (1998): A critique of a steady-state analytical method for estimating contaminant degradation rates. - Ground Water 36(6): 983–987.

Pebesma, E. J., Wesseling, C. G. (1998): Gstat: A program for geostatistical modeling, prediction and simulation. - Computers & Geosciences, 24(1): 17-31, doi:10.1016/S0098- 3004(97)00082-4.

Rehfeldt, K.R., Boggs, J.M., Gelhar, L.W. (1992): Field study of dispersion in a heterogeneous aquifer, 3, geostatistical analysis of hydraulic conductivity. - Water Resour. Res., 28(12): 3309–3324.

Rubin,Y. (2003): Applied Stochastic Hydrogeology. - 416 S.; Oxford University Press, New York, NY.

Schäfer, D., Dahmke, A., Kolditz, O., Teutsch, G. (2002): "Virtual Aquifers": A concept for evaluation of exploration, remediation and monitoring strategies. - In: Calibration and Reliability in Groundwater Modelling: A Few Steps Closer to Reality (Proceedings of the ModelCARE 2002 Conference held in Prague, Czech Republic, June 2002), edited by K. Kovar & Z. Hrkal, IAHS Publication, 277: 52-59.

Schäfer, D., Schlenz B., Dahmke, A. (2004): Evaluation of exploration and monitoring methods for verification of natural attenuation using the virtual aquifer approach. - Biodegradation Journal 15(6): 453-465.

Schäfer, D., Hornbruch, G., Schlenz B., Dahmke, A. (2005): Untersuchung kinetischer Ansätze zur Modellierung mikrobieller Abbauprozesse mit Hilfe des Virtuelle Aquifere Ansatzes. - Eingereicht bei Grundwasser.

Suarez, M. P., Rifai, H.S. (2002): Evaluation of BTEX remediation by natural attenuation at a coastal facility. - Ground Water Monit. Remed. 22(1): 62-77.

Stenback, G.A., Ong, S.K., Rogers, S.W., Kjartanson, B.H. (2004): Impact of transverse and longitudinal dispersion on first-order degradation rate constant estimation. - J. Cont. Hydrol. 73: 3-14.

Sudicky, E. A. (1986): A natural gradient experiment on solute transport in a sand aquifer: Spatial variability of hydraulic conductivity and its role in the dispersion process. - Water Resour. Res. 22(13): 2069-2082.

U.S. Environmental Protection Agency (1999): Use of monitoring natural attenuation at Superfund, RCRA Corrective Action, and Underground Storage Tank Sites, - Office of Solid Waste and Emergency Response Directive 9200.4-17, Washington, D.C.

Wiedemeier, T.H., Swanson, M.A., Wilson, J.T., Kampbell, D.H., Miller, R.N., Hansen,J.E. (1996): Approximation of biodegradation rate constants for monoaromatic hydrocarbons (BTEX) in ground water. - Ground Water Monit. Remed., 16(3): 186-194.

Wiedemeier, T.H., Rifai, H.S., Wilson, J.T., Newell, C. (1999): Natural Attenuation of Fuels and Chlorinated Solvents in the Subsurface. - 617 S.; Wiley, New York, NY.

Wilson, J. T., Pfeffer, F. M., Weaver, J. W., Kampbell, D. H., Wiedemeier, T. H., Hansen, J. E., Miller, R. N. (1994): Intrinsic Bioremediation of JP-4 Jet Fuel. - In: Symposium on Intrinsic Bioremediation of Ground Water, Denver, Colorado, US-EPA: 60-72.

Wilson, R. D., Thornton, S.F. Mackay, D.M. (2004): Challenges in monitoring the natural attenuation of spatially variable plumes. - Biodegradation Journal 15(6): 459-469.

Zamfirescu, D., Grathwohl, P.(2001): Occurrence and attenuation of specific organic compounds in the groundwater plume at a former gasworks site. - J. Contam. Hydrol. 53: 407-427.

Zhang, Y.-K. , Heathcote, R.C. (2003): An improved method for estimation of biodegradation rate with field data. - Ground Water Monit. Remed., 23(3): 112-116.

Enclosed Publication 5

Beyer, C., Chen, C., Gronewold, J., Kolditz, O., Bauer, S. (2007a): Determination of first order degradation rate constants from monitoring networks. (accepted by Ground Water.).

Determination of first order degradation rate constants from monitoring networks*

Christof Beyer, Cui Chen, Jan Gronewold, Olaf Kolditz, Sebastian Bauer
Center for Applied Geoscience, Eberhard-Karls-University of Tübingen,
Sigwartstraße 10, D 72076 Tübingen, Germany
Tel.: +49 7071 29 73176; Fax: +49 7071 5059. E-mail: christof.beyer@uni-tuebingen.de

Abstract

In this paper different strategies for estimating first order degradation rate constants from measured field data are compared by application to multiple synthetic contaminant plumes. The plumes were generated by numerical simulation of contaminant transport and degradation in virtual heterogeneous aquifers. These sites then were individually and independently investigated on the computer by installation of extensive networks of observation wells. From the data measured at the wells, i.e. contaminant concentrations, hydraulic conductivities and heads, first order degradation rates were estimated by three one-dimensional center line methods, which use only measurements located on the plume axis, and a two-dimensional method, which uses all concentration measurements available downgradient from the contaminant source. Results for both strategies show that the true rate constant used for the numerical simulation of the plumes in general tends to be overestimated. Overestimation is stronger for narrow plumes from small source zones with an average overestimation factor of about 5 and single values ranging from 0.5 to 20, decreasing for wider plumes, with an average overestimation factor of about 2 and similar spread. Reasons for this overestimation are identified in the velocity calculation, the dispersivity parameterization and off-center-line measurements. For narrow plumes the one-dimensional and the two-dimensional strategies show approximately the same amount of overestimation. For wide plumes, however, incorporation of all measurements in the two-dimensional approach reduces the estimation error. No significant relation between the number of observation wells in the monitoring network and the quality of the estimated rate constant is found for the two-dimensional approach.

Introduction

Although detailed mathematical descriptions of contaminant degradation in the subsurface are available (e.g. Rittmann and VanBriesen 1996; Wiedemeier et al. 1999; Islam et al. 2001), in field studies often simplified approaches are used for contaminant transport modeling. This is mainly because the identification of a large number of parameters and processes from field data often is impossible. Due to its mathematical simplicity, its easy implementation into transport models and the necessity of determining only a single parameter, the biodegradation model most frequently used is first order kinetics (Wiedemeier et al. 1999). Field methods for the determination of biodegradation rates in ground water comprise a variety of approaches, including mass balance calculations, in-situ microcosm studies and the so called center line method (Chapelle et al. 1996). With the center line method, only concentration measurements in observation wells located on the plume axis are evaluated and additional information possibly at hand (e.g. well data downgradient from the source but not on the center line) is not explicitly accounted for in the rate estimation. Thus, the center line method is an essentially one-dimensional approach to rate constant estimation, as flow, transport and degradation are only evaluated for a single streamline. Assuming that contaminant biodegradation can be approximated by a first order kinetics, the degradation rate constant can be calculated with analytical transport models to yield the sought for first order rate constant. An overview of common methods for estimating degradation rate constants from field data within the context of monitored natural attenuation is given by Newel et al. (2002). The authors discuss approaches based on (point-) concentration over time data and different concentration vs. distance relations, where dispersion is completely neglected as well as accounted for. Important to note is that the different approaches yield different types of degradation rates that should be used for destined purposes only. Rate constants estimated from concentration vs. time data for single monitoring wells for example represent point decay rates that are typically used to assess source decay or the time required to reach defined remediation goals at a particular location (Newell et al. 2002). Complete neglect of dispersion in the rate estimation procedure for concentration vs. distance data along the center line of the plume yields bulk attenuation rates, which quantify the reduction of contaminant concentrations with distance from the source due to the combined effects of dispersion, dilution (e.g. by recharge) and degradation processes. The frequently used method of Buscheck and Alcantar

* Beyer, C., Chen, C., Gronewold, J., Kolditz, O., Bauer, S. (2007): Determination of first order degradation rate constants from monitoring networks. (accepted by Ground Water.).

(1995) yields a "hybrid" rate constant between a bulk attenuation and a pure biodegradation rate constant, as it accounts for longitudinal dispersion whereas the effects of transverse dispersion are still reflected in the rate constant. A pure biodegradation rate constant can be estimated analytically by normalizing contaminant concentrations to concentrations of a recalcitrant tracer, if such a compound is emitted from the same source zone as the contaminant of concern (Wiedemeier et al. 1996). If this is not the case, an approach of Zhang and Heathcote (2003) may be used, in which the Buscheck and Alcantar (1995) method is extended to account for dispersion in two or three dimensions. Pure biodegradation rate constants exclusive of dispersion or other attenuation processes (and only those) may be used in contaminant transport models for prognoses of plume trends. It is important to note that these center line based rate constant estimation approaches are only applicable to contaminant plumes that have reached steady state conditions, as for still expanding plumes the rate constant would be overestimated.

Although it is known, that biodegradation rate estimates obtained from an investigation of the plume center line are subject to substantial uncertainty, this strategy is frequently used in practice. Even in homogeneous aquifers vertical and horizontal transverse dispersion can produce center line concentration profiles of recalcitrant compounds that could be mistaken as following from first order degradation (McNab Jr. and Dooher 1998). Moreover, the plume axis may easily be missed by monitoring wells when the inferred ground water flow direction is incorrect, changes over time due to transient flow behavior or when the contaminant plume shows large scale meandering due to aquifer heterogeneity (Newell et al. 2002; Wilson et al. 2004). Therefore, biodegradation rate constants obtained from such field data should be taken as rough estimates only (Chapelle et al. 2003). As first order rates calculated from center line data include all effects and processes that lower local contaminant concentrations, the precarious result of the different sources of uncertainty is that the degradation potential may be severely overestimated (Rittmann 2004), causing underestimation of plume length and contaminant mass as well as a too optimistic prognosis of down gradient concentrations and exposure levels. These aspects were recently studied in-depth by Bauer et al. (2006a) and Beyer et al. (2006) by means of numerical experiments in two-dimensional synthetic heterogeneous contaminated aquifers. The numerical experiments were based on coarse monitoring networks with 6 to 8 wells, which were all placed along an inferred plume center line. In reality, however, monitoring networks typically are designed to suit multiple and sometimes conflicting requirements and objectives, which may also change with time, depending on the stage of the site investigation. Objectives in this context are the detection of ground water contamination (e.g. Storck et al. 1997), site characterization and spatial delineation of the contamination (e.g. McGrath and Pinder 2003) or the long term monitoring of the plume behavior (e.g. Wu et al. 2006). These aims require spatially more extensive monitoring networks with larger numbers of wells compared to the relatively simple center line well configurations necessary to estimate a degradation rate constant. Recently, Stenback et al. (2004) demonstrated that additional off center line measurements can be incorporated in the estimation of the degradation rate, when a two-dimensional analytical transport model is fitted to contaminant concentrations of all monitoring wells of an extensive monitoring network downgradient from the source. In a field application example Stenback et al. (2004) showed, that accounting for the additional information on contaminant concentrations and distribution significantly reduced rate constant estimates obtained from the conventional center line approach to about 50 %, pointing out the well known problem of rate constant overestimation with the 1D center line method.

This paper therefore studies the performance of several rate constant estimation approaches based on center line investigation data for sites with extensive monitoring networks and compares the results to the two-dimensional approach of Stenback et al. (2004). Adopting the terminology of Newell et al. (2002) the types of degradation rate constants regarded here comprise bulk attenuation, biodegradation and "hybrid" rate constants. Point decay rates are not addressed in this paper. Both strategies for rate constant estimation, i.e. the investigation of the plume center line and the approach of Stenback et al. (2004), are applied to a set of synthetic sites with extensive monitoring networks, which were independently designed and installed by individual test persons engaged in hydrogeological research and consulting. The networks were installed for a general characterization and quantification of the contaminant plume (Chen et al. 2005; Bauer et al. 2006b), and are used here as a basis for degradation rate estimation. Estimated rate constants for both strategies are compared with regard to magnitude of errors and variability to draw conclusions on their limitations in view of the monitoring network used. Thereby the studies of Bauer et al. (2006a) and Beyer et al. (2006) are considerably extended, as the monitoring networks used in this paper are representative of real field situations by using all installed observation wells, and are not restricted to an one-dimensional plume center line. Moreover, this analysis allows an evaluation of the "human factor" on estimated rate constants resulting from individual notions of "sufficient accuracy" in plume investigation.

Background and Scope

This study is based on a set of synthetic contaminated two-dimensional aquifers, generated by multiple stochastic simulations of heterogeneous hydraulic conductivity fields and subsequent numerical simulation of contaminant spreading from a defined source zone in the synthetic aquifers. The evolved virtual plumes were independently investigated by a number of German scientists engaged in hydrogeological and environmental research using an

interactive plume investigation and mapping software (Chen et al. 2005) with any number of wells considered necessary for a characterization of the synthetic sites and the delineation of the contaminant plume. The plume investigations were performed within a related project (Bauer et al. 2006b) and are described in detail below. The results of these virtual plume investigations yield individually and realistically investigated plumes. The "measured" concentrations, hydraulic heads and conductivities at the observation well networks of the different plumes investigated are used as a basis for the determination of the degradation rate constants. Two different strategies are compared here:

- Strategy A - One-dimensional center line approach: From all observation wells installed the concentration distribution is analyzed and wells along the approximate center line of the contaminant plume are identified (see Figure 1(a)). Concentrations measured in these wells are evaluated using three different methods for the inference of a degradation rate constant (Newell et al. 2002; Buscheck and Alcantar 1995; Zhang and Heathcote 2003). Thus, here only a subset of concentrations measured in the original monitoring network is used for rate constant estimation.
- Strategy B - Two-dimensional evaluation: An approximate solution for the two-dimensional steady state concentration distribution is fitted to concentrations measured in all observation wells of the monitoring network downgradient of the source zone using a residual least squares criterion (Stenback et al. 2004) (Figure 1(b)). Fitting parameters are the first order rate constant and the source concentration.

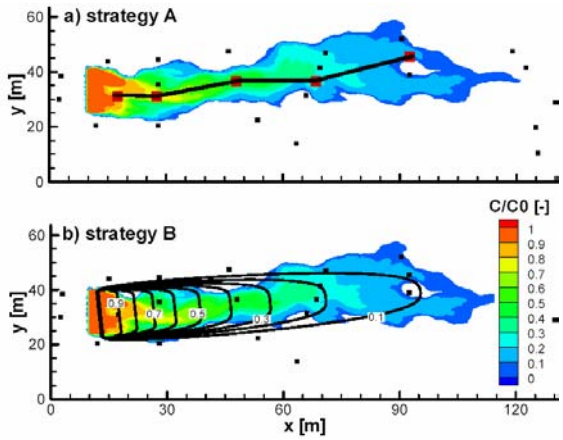

Figure 1: a) Strategy A and b) strategy B for the inference of the degradation rate constant using an existing monitoring network. Shown is the true virtual plume (unknown to the investigator), the monitoring network (small squares) and the identified center line wells (larger squares) (strategy A) as well as an example of a fitted 2D analytical plume (contour lines) (strategy B).

Generation of synthetic sites

The data basis of this study consists of 20 different realizations of heterogeneous steady state contaminant plumes. The plumes were generated by numerical simulation of ground water flow and contaminant transport in 20 different two-dimensional horizontal aquifer realizations with heterogeneous hydraulic conductivity distributions. Into ten of these conductivity fields a source with a width of 4 m perpendicular to the mean flow direction was introduced, for the other 10 aquifer realizations, a source width of 16 m was used. For the numerical simulations the GeoSys/Rockflow code (Kolditz et al. 2006; Kolditz and Bauer 2004) was used, which solves the flow and transport equations by finite element methods. The governing equations for steady state flow conditions are given as (e.g. Bear 1972):

$$\nabla\left(K\nabla h\right)=0 \tag{1}$$

$$\frac{\partial C}{\partial t}=-v_a\nabla C+\nabla\left(D\nabla C\right)-\lambda C \tag{2}$$

with h [L] the hydraulic head, K [L T^{-1}] the tensor of hydraulic conductivity, C [M L^{-3}] concentration, D [L^2 T^{-1}] the dispersion tensor which is calculated acording to Bear (1972), v_a [L T^{-1}] the transport velocity, t [T] time and λ [T^{-1}] representing the first order degradation rate constant. Equation (2) was solved over a two-dimensional numerical grid of 184 m length by 64 m width with node spacing of 0.5 m in both directions and setting the left hand side of equation (2) to 0. This guarantees that the simulated plumes are at steady state. For local dispersivities α_L and α_T values of 0.25 m and 0.05 m are used. A mean hydraulic gradient I of 0.003 is induced by fixed head boundary conditions on the left and the right hand side of the model domain (Figure 2). Flow conditions are at steady state. Hydraulic conductivity K of the virtual aquifers is regarded as a spatial random variable (Figure 2), following a lognormal distribution with an expected value of $E[Y = \ln(K)] = -9.54$, which corresponds to an effective conductivity K_{ef} of $7.19 \cdot 10^{-5}$ m s^{-1} using the geometric mean. As the aquifer models are two-dimensional and horizontal, an isotropic exponential covariance function with an

integral scale l_Y of 2.67 m and ln-conductivity variance σ_Y^2 = 2.7 is used for the spatial correlation structure. K_{ef} and l_Y are taken from the Borden field site (Sudicky 1986), whereas the degree of heterogeneity σ_Y^2 was reported for the Columbus Air Force Base site (Rehfeldt et al. 1992). Porosity n is set to 0.33, resulting in v_a = 6.54 10^{-7} m s^{-1}. For local dispersivities α_L and α_T values of 0.25 m and 0.05 m are used. The contaminant source introduced in the aquifers is of rectangular shape centered at [11.5 m; 32.0 m] downstream of the inflow boundary and has an area of either 3 * 4 m or 3 * 16 m, corresponding to a source width W_S of 1.5 or 6 correlation lengths transverse to the mean flow direction. It emits a contaminant with the contaminant concentration fixed in the source area at C / C_0 = 1.0. The dissolved contaminant is subject to a first order kinetics degradation reaction with a rate constant λ of 1.59·10^{-8} s^{-1} (0.5 a^{-1} = 0.5 yr^{-1}). This value is well within the range of reported / recommended first order degradation rate constants for chlorinated solvents as well as petroleum hydrocarbons under anaerobic conditions listed in Aronson and Howard (1997). The model parameters used are summarized in Table 1.

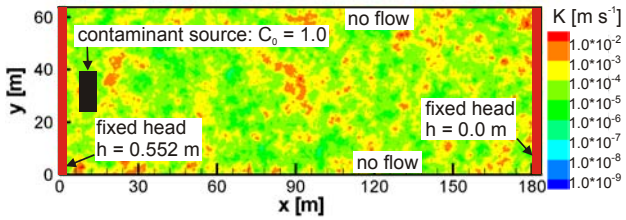

Figure 2: A single realization of the spatially correlated random hydraulic conductivity field and model boundary conditions.

The conceptual model used here is a rigorous simplification of contaminant transport and degradation observed in natural aquifer systems, where biodegradation is a function of electron acceptor and donor availability and the aquifer structure and thus reaction kinetics follow more complicated laws, show spatial dependence and may include transient effects, dilution or phase changes to the unsaturated zone. Furthermore, the contaminant is not retarded and shows no volatilization. However, as the methods assume a uniform rate constant to be valid, only using such simplified representations of reality as virtual test sites allows for a detailed analysis of the influence of heterogeneous hydraulic conductivity on the different methods under otherwise ideal conditions.

Table 1: Model parameters used in the numerical simulations.

parameter	description	value
K_{ef}	effective conductivity	7.19·10^{-5} m s^{-1}
σ_Y^2	ln(K)-variance	2.7
l_Y	integral scale	2.67 m
n	porosity	0.33
α_L	longitudinal dispersivity	0.25 m
α_T	transverse dispersivity	0.05 m
I	hydraulic gradient	0.003
λ	first order degradation rate constant	1.59·10^{-8} s^{-1}

Investigation of synthetic sites

The plumes were independently investigated by 85 different test persons, engaged in hydrogeological and environmental research, consulting or administration. These investigators were confronted with the scenario of contaminant migration downstream from a source zone in a virtual aquifer. A two-dimensional top view of the site, the mean ground water flow direction and the approximate location of the contaminant source were given as the only prior information for the site investigation. Neither the plume nor the hydraulic heads calculated are known at this stage. The task of the investigators was an as exact as possible characterization of the contaminated aquifer by the following procedure:

- Step 1) Emplacing observation wells into the virtual aquifer: Using an interactive graphical user interface, the investigator positions observation wells on the virtual site. At the wells local contaminant concentrations and hydraulic heads are measured.
- Step 2) Regionalization of local measurements: Using different interpolation schemes (e.g. Kriging or Inverse Distance Weighting) the investigator interpolates contaminant concentrations and hydraulic heads measured at the observation wells to the virtual aquifer.

Steps 1 and 2 could be repeated as often as desired by the investigator, until the interpolated contaminant plume was deemed to be investigated accurately enough to properly characterize the contaminant distribution. Thus the interactive site investigation is an iterative procedure and is evaluated by a comparison of the "true" plume with the investigation result. More details on this procedure can be found in Chen et al. (2005).
Using this methodology, a total number of 85 individual investigation results were obtained. 47 of these investigations were conducted for plumes originating from a source of width 4 m, while the plumes with a source width of 16 m were investigated 38 times. Accordingly, the majority of the 20 different plumes were investigated three or four times by different investigators.
The configuration and the number of monitoring wells varies substantially between the different realizations and even for the same realization but different investigators (12 – 93 wells), as the decision about how many wells were needed for an accurate characterization of the site was left to the individual investigators. For two contaminant plumes (one for each source width) the investigation was repeated 13 times. Each investigation was performed by a different investigator. In addition to the general comparison of strategies A and B for the inference of the degradation rate constant, this subset of the whole data set allows for an analysis of estimated rate constant variability for a single site, resulting from different notions of "sufficient accuracy" of the virtual plume investigation.

Rate constant estimation

Using the monitoring networks installed by the investigators of the virtual plumes, first order rate constants were estimated following strategies A and B. Methods A1, A2 and A3 are used in strategy A and are described in detail in Bauer et al. (2006a). Therefore, only a brief description is given here:
Method A1 (equation (3)) is based on the one-dimensional transport equation, considering advection and first order degradation only. The steady state solution for the concentration profile is rearranged to yield λ_{A1}, i.e. the first order degradation rate constant for method A1:

$$\lambda_{A1} = -\frac{v_a}{\Delta x}\ln\left(\frac{C(x)}{C_0}\right) \tag{3}$$

v_a [L T^{-1}] is the transport velocity, Δx [L] the distance between the observation wells and C_0 and $C(x)$ [M L^{-3}] are upstream and downstream contaminant concentrations at the observation wells, respectively. λ_{A1} can be considered rather an overall or bulk attenuation rate than a degradation rate constant (Newell et al. 2002), as all concentration changes due to diffusion, dispersion, volatilization or dilution are attributed to the degradation process.
The method introduced by Buscheck and Alcantar (1995) is the second approach applied in this study (equation (4)). It is based on the steady state solution of the one-dimensional transport equation considering advection, longitudinal dispersion and first order degradation. Method A2 requires an estimate of longitudinal dispersivity α_L [L] and yields a "hybrid" rate constant between a bulk attenuation and a pure biodegradation rate constant, as the effects of transverse dispersion are still reflected in the rate constant estimate λ_{A2}.

$$\lambda_{A2} = \frac{v_a}{4\alpha_L}\left(\left(1 - 2\alpha_L\frac{\ln\left(C(x)/C_0\right)}{\Delta x}\right)^2 - 1\right) \tag{4}$$

Zhang and Heathcote (2003) proposed modifications to the method of Buscheck and Alcantar (1995) to improve the estimation of λ with regard to transverse dispersion. Correction terms derived from analytical solutions to the two- and three-dimensional advection dispersion equations including first order decay are used to account for lateral spreading and the width of the source zone W_S [L] in two and three dimensions, respectively. Therefore information about W_S, α_L and α_T are required for this approach. Method A3 (equation (5)) is the two-dimensional form of the method by Zhang and Heathcote (2003) and yields the biodegradation rate constant estimate λ_{A3}:

$$\lambda_{A3} = \frac{v_a}{4\alpha_L}\left(\left(1 - 2\alpha_L\frac{\ln\left(C(x)/(C_0\beta)\right)}{\Delta x}\right)^2 - 1\right) \quad \text{with} \quad \beta = erf\left(\frac{W_S}{4\sqrt{\alpha_T \Delta x}}\right) \tag{5}$$

For evaluation strategy B, method B (equation (6)) is used, which corresponds to the approach of Stenback et al. (2004). An approximate solution for the steady state concentration distribution derived from the two-dimensional advection-dispersion equation with first order degradation (Domenico and Schwartz 1990) is fitted to measured concentrations:

$$C(x,y) = \frac{C_0}{2}\exp\left\{\left(\frac{x}{2\alpha_L}\right)\left(1 - \sqrt{1 + \frac{4\lambda_B\alpha_L}{v_a}}\right)\right\}\left\{erf\left(\frac{2y + W_S}{4\sqrt{\alpha_T x}}\right) - erf\left(\frac{2y - W_S}{4\sqrt{\alpha_T x}}\right)\right\} \tag{6}$$

The approximate solution employed has the same basis as method 3. Here, however, a real two-dimensional approach is used, as equation (6) is fitted to the concentrations of all observation wells and not only to those measured along the center line.
In strategy A the first step is an analysis of the concentration distribution based on all measurements made at the observation wells of the monitoring network. Starting at the well with the highest measured concentration, those downgradient wells are identified, that best represent the center line of the plume. These then are used to estimate the rate constant. Only locally measured quantities are used here, i.e. local hydraulic conductivities, hydraulic heads and contaminant concentrations are "measured" at these wells by reading the model data at the respective nodes of the numerical grid. The transport velocity v_a between each pair of center line wells is approximated by:

$$v_a = K_{ef} \frac{\Delta h}{n \Delta x} \qquad (7)$$

with K_{ef} the effective conductivity of local hydraulic conductivities at up and down gradient wells, n the porosity, Δh the head difference and Δx the distance between the wells. According to Rubin (2003) in stationary isotropic two-dimensional domains with gaussian probability density functions of $Y = ln(K)$ the effective conductivity K_{ef} can be calculated as the geometric mean (cf. Bauer et al. 2006a). The porosity is assumed to be known correctly. With v_a, λ can then be calculated for each pair of center line wells using methods A1 – A3. For a set of k center line wells thus k-1 rate constants are calculated for one method. These are averaged to yield an estimate of the mean degradation rate constant λ. As an alternative to using only the locally measured conductivities, rate constant estimation is also performed using a global estimate of K_{ef}, which is obtained from the geometric mean value of all hydraulic conductivities measured at all observation wells.
In strategy B, method B (equation (6)) is fitted to measured concentrations of all observation wells of the monitoring network. Both the biodegradation rate constant λ and the source concentration C_0 are varied simultaneously to achieve correspondence of measured and calculated concentrations, as a preliminary analysis (in agreement with results of Stenback et al. (2004)) showed that this procedure on average yields closer estimates of the true rate constant than fitting only λ with a single fixed estimate of the source concentration. A least squares criterion for the concentration residuals is used in the fitting procedure. As in strategy A the flow velocity v_a is approximated using equation (7). K_{ef} is calculated as the geometric mean of hydraulic conductivities measured at all wells of the network. The average hydraulic gradient over the entire site is approximated by fitting a linear trend surface to all head measurements by ordinary least squares regression.
For methods A2, A3 and B estimates of longitudinal and transverse dispersivities are required. Practical guidance on estimating these parameters at the field scale is given e.g. by Wiedemeier et al. (1999), where one suggestion is to use 0.1 times the plume length for α_L and α_T as 0.1 α_L. Here, however, an alternative strategy is employed: Macrodispersivities α_L and α_T are derived from correlation scale, aquifer heterogeneity σ_Y^2 and travel distance (Dagan 1984; Hsu 2003; Rubin et al. 2003). Thus, α_L is taken as 7 m, which roughly corresponds to the large time asymptotic limit for the given conductivity distribution, while α_T is taken as the approximate peak value of transverse macrodispersivity, calculated as 0.7 m (which thus also corresponds to the frequently used relationship as $\alpha_T \approx 0.1\ \alpha_L$). These values are well within the ranges of dispersivities commonly used for the field scale modeling of contaminant transport. The true value of the source width W_S is assumed to be known from the site investigation. These approximations and assumptions were made to ensure that the error introduced in estimated rate constants due to the parameterization of methods A2, A3 and B is as small as possible.

Results and Discussion

Strategy A - One-dimensional center line approach

The rate constants λ_{A1} - λ_{A3} estimated with equations (3) – (5) are divided by the "true" value used in the numerical simulations to yield normalized rate constants Λ_{A1} - Λ_{A3}, which can directly be interpreted as overestimation or underestimation factors. Results in terms of mean values, medians, standard deviations and coefficients of variation (cv) as well as the number of realizations (N) used for strategy A are presented in Table 2 and Figure 3. Comparing methods A1 - A3 for the small source width W_S = 4 m yields that all approaches on average result in a distinct overestimation of λ. For method A1 λ is overestimated on average by a factor of 6.88, while for A2 an mean Λ_{A2} = 8.24 is observed. Hence, method A1 performs better than A2. Method A3 yields a slightly lower mean of Λ_{A3} = 6.82, while the spread of results for A3 is noticeably larger, as can also be seen by the higher cv. Three main error sources for the observed overestimation exist:

- neglect of dispersion by method A1, which thus is attributed to the degradation process (λ_{A1} represents a bulk attenuation rate constant)

- deviation of sampling well locations from the true center line position, which causes the sampling of too low concentrations
- unrepresentative estimates of the local v_a along the flow path, as the estimated λ increases and decreases with v_a (cf. equations (3) – (5)).

These effects are discussed in detail in Bauer et al. (2006a). For method A2 the additional bias towards too large rate constants is a consequence of accounting only for α_L in equation (4), as with a one-dimensional transport model longitudinal dispersion of a degrading contaminant results in a stronger spreading of the solute downstream and consequently in higher concentrations along the center line of a steady state plume compared to an advection only case. Therefore a larger rate constant is needed to fit a given concentration decrease and the "hybrid" rate constant estimate Λ_{A2} is always larger than the bulk attenuation rate constant Λ_{A1} (cf. Bauer et al. 2006a), which appears contradictory.

Table 2: Normalized degradation rate constants estimated with strategy A.

W_S = 4 m			
	method A1	**method A2**	**method A3**
mean	6.88	8.24	6.82
median	4.43	5.50	2.65
stdv.	6.36	7.41	10.09
cv	0.92	0.90	1.48
N	47	47	47
W_S = 16 m			
	method A1	**method A2**	**method A3**
mean	4.46	5.33	4.99
median	2.66	3.23	2.45
stdv.	4.81	6.29	9.59
cv	1.08	1.18	1.92
N	38	38	36

For the source width W_S = 16 m all methods improve (Table 2, Figure 3). Still, method A1 shows the closest estimates of the rate constant and the lowest variability of single realization results in comparison to methods A2 and A3. With method A3 for two out of 38 plumes no reasonable rate constant estimate is obtained. This effect is due to an over-correction for transverse dispersion in the β term of equation (5), which can cause the corrected $C(x)$ to be very close to or even larger than the respective upgradient concentration C_0, yielding very small or even negative λ_{A3}.

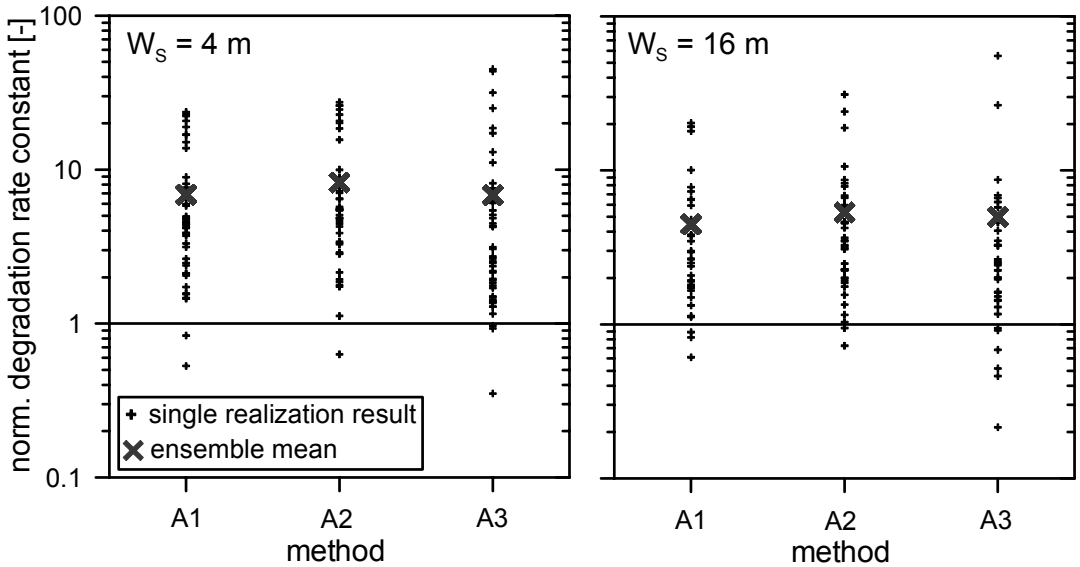

Figure 3: Normalized degradation rate constants estimated with strategy A and methods A1, A2 and A3 for source widths of 4 m (left diagram) and 16 m (right diagram). Small symbols represent results of individual realizations, large symbols the mean of all realizations. K_{ef} used for rate estimation is calculated from measurements at center line wells only.

As Bauer et al. (2006a) demonstrated, the local flow velocity estimate is a crucial parameter for the estimation of the degradation rate constant. In a sensitivity study the authors found that inclusion of field scale information on hydraulic conductivity, which is more representative for the entire site, can improve the accuracy of estimated rate constants over usage of local information only. Therefore the center line data obtained in strategy A are re-evaluated using a field scale estimate of the effective conductivity at the investigated sites: K_{ef} is calculated as the geometric mean of local conductivity values measured at all observation wells of the site and not only using those measured on the center line. Results for this approximation are presented in Table 3 and Figure 4. It is found that consideration of all conductivity measurements available improves the rate constants estimated for all three methods and both source widths. On average all estimates are closer to the true rate than those estimated using only local conductivity information. The average improvement is between a factor of 1.5 for W_S = 4 m and a factor of two for W_S = 16 m. Also the standard deviations from the mean values and the cv are lower. This finding is true for the settings investigated here, i.e. a correlation length smaller than the average distance between observation wells and a stationary K distribution. If the correlation length is on the order or longer than the average observation well distance or K is not stationary, this finding is probably not transferable.

Table 3: Normalized degradation rate constants estimated with strategy A, re-evaluated using a field scale estimate of K_{ef}.

W_S = 4 m			
	method A1	**method A2**	**method A3**
mean	4.75	5.73	4.14
median	4.04	4.67	2.66
stdv.	3.75	4.33	4.06
cv	0.79	0.76	0.98
N	47	47	47
W_S = 16 m			
	method A1	**method A2**	**method A3**
mean	2.16	2.53	2.42
median	1.14	1.50	0.90
stdv.	2.08	2.45	3.98
cv	0.96	0.97	1.64
N	38	38	36

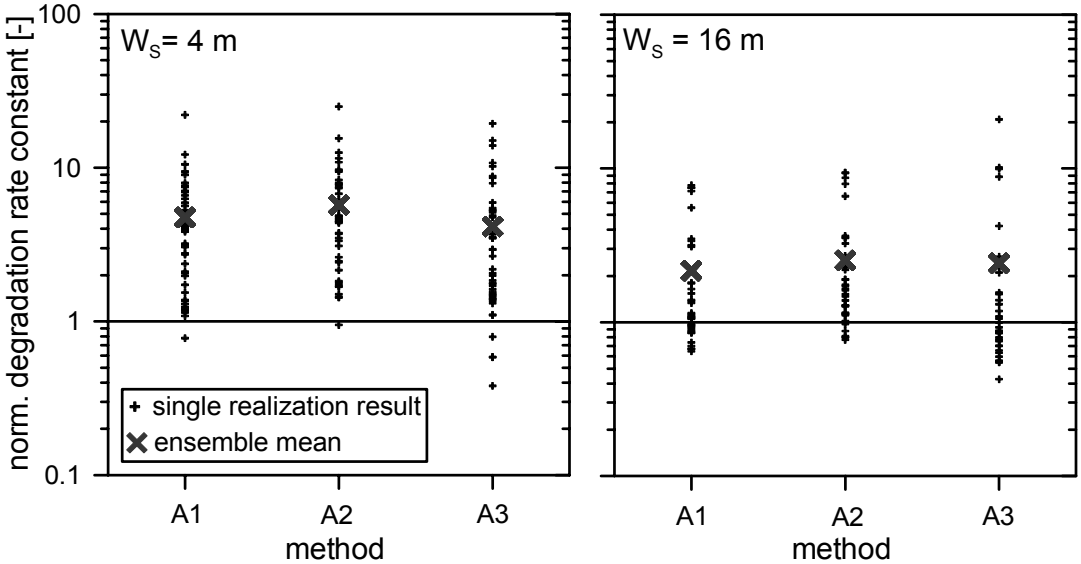

Figure 4: Normalized degradation rate constants estimated with strategy A and methods A1, A2 and A3 for source widths of 4 m (left diagram) and 16 m (right diagram), respectively. K_{ef} used for rate estimation is calculated as a field scale estimate from all monitoring wells available for each investigated plume.

An interesting observation is that the differences between the three methods of strategy A are not as distinct as observed in Bauer et al. (2006a). One explanation for this finding is that due to the larger number of observation wells used for the site investigation in this study, the plume center line positions are better identified on average and concentration samples are taken closer to the true plume axis. Methods A1, A2 and A3 show a different sensitivity on deviations of measurement locations from the plume center line. This is because in method A1, the rate constant estimate is linearly related to $\ln(C(x)/C_0)/\Delta x$, while in method A2 this term appears in linear as well as squared form after rearrangement of equation (4). As a consequence, increasing deviations of observation well locations from the plume center line and thus lower measured contaminant concentrations will result in increasingly stronger overestimation of λ by A2 relative to A1. For method A3, the correction factor β has to be taken into account additionally (cf. equation (5)). For significant deviations from the center line, however, the same effect as for A2 can be shown.

In Figure 5 the degradation rate constants Λ_{A1} estimated with method A1 were plotted against the number of observation wells with relative concentrations $C/C_0 > 0.001$ in the respective monitoring networks. A clear relationship between the number of wells and the accuracy of Λ_{A1} is neither observed for $W_S = 4$ m nor for $W_S = 16$ m. It seems, however, that the spread of estimated rate constants decreases slightly with increasing numbers of wells, but a larger number of samples, especially for numbers of monitoring wells > 30 would be required to derive more meaningful results. For the other methods A2 and A3, the similar observations are made (not shown here).

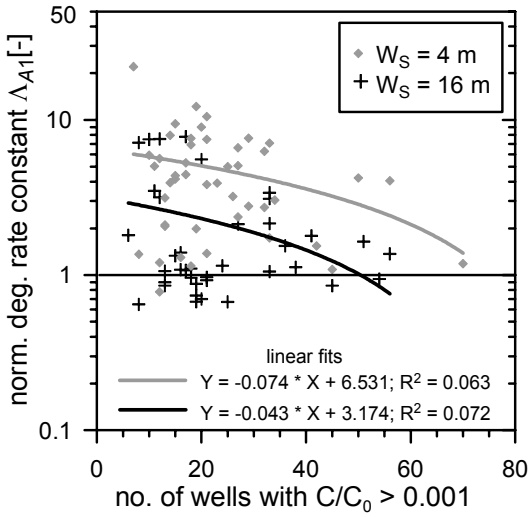

Figure 5: Degradation rate constants Λ_{A1} for source widths of 4 m (grey diamonds) and 16 m (black crosses) versus the number of wells showing relative concentrations $C/C_0 > 0.001$.

Strategy B - Two-dimensional evaluation

Applying method B it is not always possible to obtain a rate constant $\lambda_B > 0$ when minimizing the sum of squared residuals of concentration. The concentration distribution calculated with the analytical model indicates absence of contaminant degradation for the closest fit to the measured data for six out of 47 plumes when $W_S = 4$ m. For the remaining 41 plumes, usage of method B on average yields $\Lambda_B = 4.51$ (Table 4, Figure 6), which is considerably closer to the true rate constant than for methods A1 - A3 with using only local measurements of hydraulic conductivity along the center line (cf. Table 2). The standard deviation for method B, however, is slightly larger than for A1 and A2. With $W_S =$ 16 m for five out of 38 plumes no $\Lambda_B > 0$ is found. Here, the improvement over methods A1 – A3 is even more distinct with the mean $\Lambda_B = 1.92$. Also the spread of single realizations is reduced for the larger source width. However, no definite improvement of Λ_B over those obtained by strategy A using the field scale estimate of K_{ef} (cf. Table 3) is observed. For $W_S = 4$ m the mean Λ_B is slightly lower than the mean Λ_{A1}, but slightly larger than Λ_{A3}. Also the variability of estimated Λ_B is larger than for methods A1 – A3. For $W_S = 16$ m the mean Λ_B is slightly lower than for all methods of strategy A, while the observed spread is only lower in comparison to A3.

In the estimation of λ with method B the source concentration is included as a fitting parameter. On average the true source concentration is overestimated by a factor of three for $W_S = 4$m, while for $W_S = 16$m deviations are lower than 5 %. As for strategy A a distinct relationship between the number of observation wells in the monitoring network and the quality of the degradation rate estimates is not observed.

Table 4: Normalized degradation rate constants estimated with method B.

	W_S = 4 m	W_S = 16 m
mean	4.51	1.92
median	1.96	1.14
stdv.	8.34	2.97
cv	1.85	1.55
N	41	33

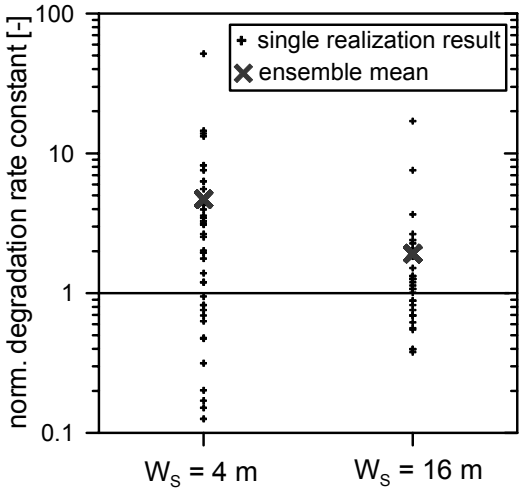

Figure 6: Normalized degradation rate constants estimated with method B for source widths of 4 m and 16 m.

Variability of estimated rate constants for a single site

For each source width, one single plume was repeatedly investigated 13 times by different investigators. For this subset of plumes the variability of estimated rate constants for a single site, resulting from different notions on "sufficient accuracy" of the plume investigation, is studied. As the incorporation of conductivity measurements from all observation wells of the monitoring network significantly improves rate constant estimation with methods A1, A2 and A3, this approach is used in this comparison. Results for strategies A and B are summarized in Table 5 and Figure 7.

For source width W_S = 4 m a slightly stronger overestimation of λ can be observed for strategy A (methods A1 - A3) in comparison to the results for the complete data set. Here, the mean Λ_{A1} resulting from 13 investigations of the single site is 5.26, while Λ_{A1} for the complete data set is 4.75. For methods A2 and A3 the same tendency of increased overestimation is found. The variability among the sets of 13 estimated Λ_{A1}, Λ_{A2} and Λ_{A3}, however, is much smaller. The cv here are only 0.3, 0.34 and 0.68, respectively. With strategy B, i.e. method B, a slightly smaller mean Λ_B = 4.26 is found than for the complete data set and the cv of 0.78 here also is reduced. For a source width of 16 m, all four methods show a much lower mean value of normalized rate constants than for the complete data set. On average, method A1 and A3 yield the correct result for the single investigated site, while method A2 and B show a slight overestimation. Variability of the estimated rate constants in terms of cv is lower than for the complete data set of W_S = 16 m. For strategy B no clear dependence between the precision of the rate constant estimate and the absolute number of wells in the monitoring network nor the number of respective wells showing considerable contaminant concentrations (e.g. $C/C_0 > 0.001$) could be observed. The absence of such an obvious relationship may be due to the low sample size of only 13 investigations of both plume realizations. As described before, it seems, however, that the spread of estimated rate constants decreases slightly with increasing numbers of wells (not shown here).

The stronger overestimation observed for W_S = 4 m as well as the more precise estimation of λ for W_S = 16 m do not allow for any general conclusions regarding the absolute magnitude of errors, as this might probably be an effect of the two individual realizations investigated and their respective plume geometry. The variability observed among the 13 results for each of the two single plumes however shows, that for a single realization of a contaminant plume, substantially different investigation results, in this case degradation rate constants, may be obtained, when investigated by individual persons. For both, the narrow plume with a comparatively small source zone of 4 m width as well as for the wider plume with W_S = 16 m, the variability of investigation results here has a magnitude of 25 % up to 69 % of the variability observed among different realizations of the plume, depending on the method used for rate constant estimation. This clearly shows, that a substantial part of rate constant estimation uncertainty is due to the individual configuration of the monitoring network.

Table 5: Normalized degradation rate constants estimated with methods A1 – A3 and B for two individual plume realizations with different source widths (W_s = 4 m and 16 m). Both plume realizations were independently investigated by 13 individual persons each.

W_S = 4 m				
	method A1	**method A2**	**method A3**	**method B**
mean	5.26	6.25	4.56	4.26
median	5.02	5.88	2.94	3.47
stdv.	1.59	2.11	3.10	3.33
cv	0.30	0.34	0.68	0.78
N	13	13	13	13
W_S = 16 m				
	method A1	**method A2**	**method A3**	**method B**
mean	1.01	1.28	1.00	1.21
median	0.97	1.15	0.87	1.20
stdv.	0.31	0.51	0.48	0.51
cv	0.31	0.40	0.48	0.42
N	13	13	13	13

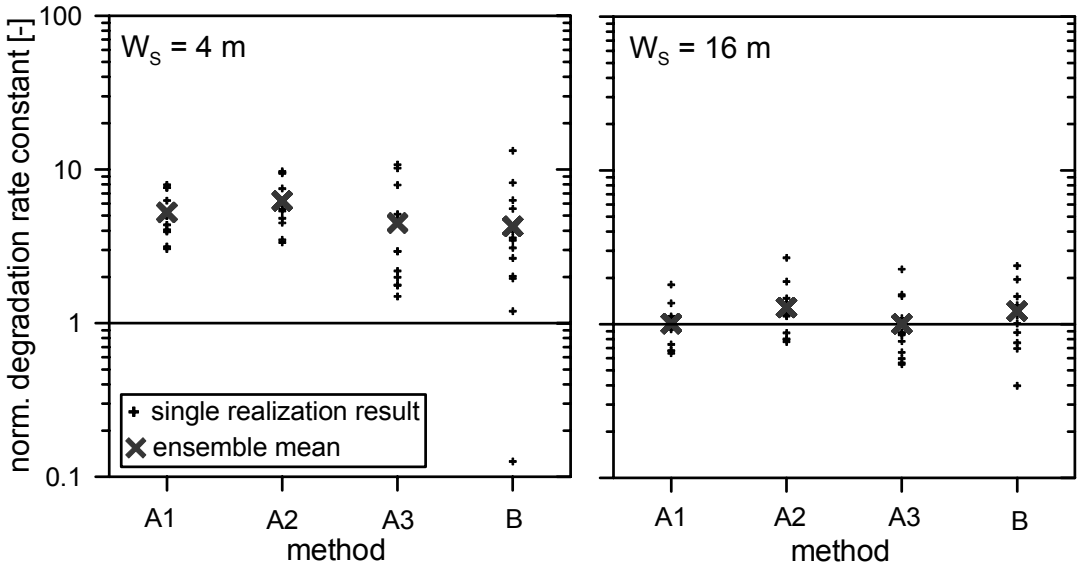

Figure 7: Comparison of normalized degradation rate constants estimated with methods A1 – A3 and B for two single plume realizations with different source widths (W_s = 4 m: left diagram; W_s = 16 m: right diagram). Both plume realizations were repeatedly and independently investigated by 13 individual persons each.

Summary and Conclusions

In this study, the frequently used center line approach for estimation of degradation rate constants is compared to a methodology suggested by Stenback et al. (2004), which uses all concentration measurements downstream of the contaminant source zone to estimate the degradation rate. In a numerical experiment, both strategies are applied to a set of 85 synthetic contaminant plumes, subject to first order degradation, and investigated using extensive monitoring networks. Rate constants are estimated using concentrations, hydraulic heads and conductivities locally measured at the observation wells of the monitoring network.

Results show that rate constants tend to be overestimated in general. Using the center line approach (strategy A) and a simplified observation well set up causes a general overestimation due to three factors:

- biased estimates of the mean flow velocity,
- inadequate parameterizations of longitudinal and transverse dispersivities and
- off center line measurements.

Comparing results for source widths of 4 and 16 m yields, that rate constant estimation improves significantly for wider plumes, as it is less likely, that observation wells are placed off the center line. Estimated rate constants also become more accurate when more than only local information on hydraulic conductivity is used to approximate the effective conductivity along the flow path: Taking K_{ef} as the geometric mean of all measured K values from the monitoring network reduces rate constant overestimation, although wells are not necessarily located on the flow path or even within the contaminant plume.

For the two-dimensional approach (strategy B), sources of error are inadequate parameterizations of longitudinal and transverse dispersivities and an erroneous approximation of the mean flow velocity. As all observation wells downgradient of the source zone are incorporated in the estimation procedure, off center line measurements are not relevant for this strategy. However, when the contaminant plume shows significant meandering, the applicability of strategy B is hampered, as the analytical model which is fitted to the concentration measurements presumes a linear plume axis. This problem is observed for the small source width of 4 m, where overestimation by strategy B is comparable to the one-dimensional approaches using the global estimate of K_{ef}. For larger source widths like the 16 m used in this study, however, strategy B yields closer estimates of the degradation rate constant than strategy A on average.

One drawback of the two-dimensional approach is that source concentration and degradation rate constant have to be fitted simultaneously to obtain accurate estimates of the degradation rate constant. This proves problematic especially for the small source width of 4 m where for some realizations the source concentration is overestimated by up to 300 %. For the source width of 16 m, however, the source concentration is fitted precisely within 5% of the “true” source concentration. These results suggest that incorporation of off center line information in the estimation of the degradation rate can improve results of the plume investigation considerably. Especially for wide plumes, the two-dimensional approach of Stenback et al. (2004) proves superior to the one-dimensional center-line investigation strategy, resulting in more precise estimates of the degradation rate constant.

Studying the variability of estimated degradation rates due to different monitoring network configurations, i.e. the personal factor due to different “site investigators”, it is found that for both source widths the variability of investigation results of one realization ranges from 25 % up to 69 % of the variability observed among different realizations. This demonstrates that the configuration of the monitoring network following from the investigators individual site investigation approach represents a substantial part of the uncertainty of the estimated rate constant.

Overestimation of the degradation rate at a contaminated site is a critical point if monitored natural attenuation is considered as an alternative to conventional engineered remediation measures because the overall NA potential is assessed too positive. As demonstrated by Beyer et al. (2006) plume lengths calculated with biased degradation rates will result in an underestimation of the contaminated regions of the aquifer. Such an application, however, might not be of primary concern, when monitoring networks of sufficient density have already been established over a site. Nonetheless, a too high rate constant could falsely lead to the conclusion, that a plume is at steady state, when the present day length observed fits the calculated steady state plume length. In the assessment of contaminated sites, indication for a steady state plume is an important result, e.g. for the acceptance of NA as a remediation scheme. Also for well investigated sites, a reliable determination of contaminant degradation rates is important, when the rates are to be used as modeling parameters, for comparison with other sites and for comparing and optimizing alternatives of remediation measures.

Acknowledgements: This work is funded by the German Ministry of Education and Research (BMBF) under grant 033 05 12 / 033 05 13 as part of the KORA priority program, sub-project 7.2. We wish to thank our project partners at the Christian-Albrechts-University Kiel Andreas Dahmke and Dirk Schäfer for their support in our research. We acknowledge the support of Uwe Wittmann, Iris Bernhardt and Ludwig Luckner in coordination of the project work. Last but not least we are grateful to Bernie Kueper and two anonymous reviewers for their thoughtful comments and suggestions which considerably improved this paper.

References:

Aronson, D., and P.H. Howard. 1997. Anaerobic biodegradation of organic chemicals in groundwater: A summary of field and laboratory studies, SRC TR-97-0223F, Science Center Report, Syracuse Research Corporation, New York.

Bauer, S., C. Beyer, and O. Kolditz. 2006a. Assessing measurement uncertainty of first-order degradation rates in heterogeneous aquifers. *Water Resources Research* 42, no. 1: W01420. 10.1029/2004WR003878.

Bauer, S., C. Beyer, C. Chen, J. Gronewold, and O. Kolditz. 2006b. Virtueller Aquifer (VA) - Computergestützte Bewertung von Erkundungs-, Sanierungs- und Monitoringstrategien im Hinblick auf das "Natural Attenuation" (NA) und "Enhanced Natural Attenuation" (ENA) -Potenzial kontaminierter Böden und Grundwässer. In *Statusseminar des KORA-TV 7, 8.6.2006, Dresden. Gemeinsame Mitteilungen des DGFZ e.V. und seiner Partner*, vol. 3/2006, 93-113. Dresden.

Bear, J. 1972. *Dynamics of Fluids in porous Media.* Amsterdam: Elsevier.

Beyer, C., S. Bauer, and O. Kolditz. 2006. Uncertainty Assessment of Contaminant Plume Length Estimates in

Heterogeneous Aquifers. *Journal of Contaminant Hydrology* 87, no. 1-2: 73-95. 10.1016/j.jconhyd.2006.04.006.
Buscheck, T.E., and C.M. Alcantar. 1995. Regression techniques and analytical solutions to demonstrate intrinsic bioremediation. In *Intrinsic Bioremediation,* ed. R.E. Hinchee, T.J. Wilson, and D. Downey, 109-116. Columbus OH: Battelle Press.
Chapelle, F.H., P.M. Bradley, D.R. Lovley, and D.A. Vroblesky. 1996. Measuring rates of biodegradation in a contaminated aquifer using field and laboratory methods. *Ground Water* 34, no. 4: 691-698.
Chapelle, F.H., Widdowson, M.A., Brauner, J.S., Mendez, E. and C.C. Casey. 2003. Methodology for estimating times of remediation associated with monitored natural attenuation. USGS Water-Resources Investigations Report 03-4057.
Chen, C., C. Beyer, S. Bauer, and O. Kolditz. 2005. Interactive visual framework to demonstrate the uncertainty of contaminant plume investigation. In *5. Workshop Porous Media, 02.-03.12.2004 Blaubeuren, Workshop Proceedings,* Center for Applied Geosciences, University of Tübingen. http://www.virtual-aquifer.uni-tuebingen.de/pdf/2005_29_chen.pdf
Dagan, G. 1984. Solute transport in heterogeneous porous formations. *Journal of Fluid Mechanics* 145: 151–177.
Domenico, P.A., and F.W. Schwartz. 1990. *Physical and Chemical Hydrogeology*, 2nd ed. New York: John Wiley and Sons.
Hsu, K.-C. 2003. The influence of the log-conductivity autocovariance structure on macrodispersion coefficients. *Journal of Contaminant Hydrology* 65, no. 1-2: 65-77. 10.1016/S0169-7722(02)00231-0.
Islam J., S. Naresh, and M. O'Sullivan. 2001. Modeling biogeochemical processes in leachate-contaminated soils: A review. Transport in Porous Media 43, no. 3: 407 – 440. 10.1023/A:1010737825232.
Kolditz, O., and S. Bauer, 2004. A process-oriented approach to computing multifield problems in porous media. *Journal of Hydroinformatics* 6, no. 3: 225-244.
Kolditz, O., M. Beinhorn, M. Xie, T. Kalbacher, S. Bauer, W. Wang, C. McDermott, C. Chen, C. Beyer, J. Gronewold, D. Kemmler, R. Walsh, Y. Du, C.H. Park, M. Hess, and C. Büurger and J.O. Delfs. 2006. GeoSys/Rockflow version 4.4.03 - Theory and users manual. Center for Applied Geoscience, University of Tübingen.
McGrath, W.A., and G.F. Pinder. 2003. Search strategy for groundwater contaminant plume delineation. *Water Resources Research* 39, no. 10: 1298. 10.1029/2002WR001636.
McNab Jr., W.W., and B.P. Dooher. 1998. A critique of a steady-state analytical method for estimating contaminant degradation rates. *Ground Water* 36, no. 6: 983–987.
Newell, C.J., H.S. Rifai, J.T. Wilson, J.A. Connor, J.A. Aziz, and M.P. Suarez. 2002. Calculation and use of first-order rate constants for monitored natural attenuation studies. U.S. EPA Ground Water Issue, U.S. EPA/540/S-02/500.
Rehfeldt, K.R., J.M. Boggs, and L.W. Gelhar. 1992. Field study of dispersion in a heterogeneous aquifer, 3, geostatistical analysis of hydraulic conductivity. *Water Resources Research* 28, no. 12: 3309–3324. 10.1029/92WR01758.
Rittmann, B.E. 2004. Definition, objectives, and evaluation of natural attenuation. *Biodegradation* 15, no. 6: 349-357. 10.1023/B:BIOD.0000044587.05189.99.
Rittmann, B.E., and J.M. VanBriesen. 1996. Microbiological processes in reactive modeling. In Reactive *Transport in Porous Media. Reviews in Mineralogy*, vol. 34, ed. P. Lichtner, C. Steefel, and E. Oelkers, 311-334. Mineralogical Society of America: Washington DC.
Rubin, Y., A. Bellin, and A.E. Lawrence. 2003. On the use of block-effective macrodispersion for numerical simulations of transport in heterogeneous formations. *Water Resources Research* 39, no. 9: 1242, 10.1029/2002WR001727.
Stenback, G.A., S.K. Ong, S.W. Rogers, and B.H. Kjartanson. 2004. Impact of transverse and longitudinal dispersion on first-order degradation rate constant estimation. *Journal of Contaminant Hydrology* 73, no. 1-4: 3-14. 10.1016/j.jconhyd.2003.11.004
Storck, P., J.W. Eheart, and A.J. Valocchi. 1997. A method for the optimal location of monitoring wells for detection of groundwater contamination in three-dimensional aquifers. *Water Resources Research* 33, no. 9: 2081–2088. 10.1029/97WR01704.
Sudicky, E.A.. 1986. A natural gradient experiment on solute transport in a sand aquifer: Spatial variability of hydraulic conductivity and its role in the dispersion process. *Water Resources Research* 22, no. 13: 2069-2082.
Wiedemeier, T.H., M.A. Swanson, J.T. Wilson, D.H. Kampbell, R.N. Miller, and J.E. Hansen. 1996. Approximation of biodegradation rate constants for monoaromatic hydrocarbons (BTEX) in ground water. *Ground Water Monitoring & Remediation* 16, no. 3: 186-194.
Wiedemeier, T.H., H.S. Rifai, T.J. Wilson, and C. Newell. 1999. *Natural Attenuation of Fuels and Chlorinated Solvents in the Subsurface.* New York: Wiley.
Wilson, R.D., S.F. Thornton, and D.M. Mackay. 2004. Challenges in monitoring the natural attenuation of spatially variable plumes. *Biodegradation* 15, no. 6: 459-469. 10.1023/B:BIOD.0000044591.45542.a9.
Wu, J., C. Zheng, C.C. Chien, and L. Zheng. 2006. A comparative study of Monte Carlo simple genetic algorithm and noisy genetic algorithm for cost-effective sampling network design under uncertainty. *Advances in Water Resources* 29, no. 6: 899–911. 10.1016/j.advwatres.2005.08.005
Zhang, Y.-K., and R.C. Heathcote. 2003. An improved method for estimation of biodegradation rate with field data. Ground Water Monitoring & Remediation 23, no. 3: 112-116.

Enclosed Publication 6

Beyer, C., Konrad, W., Park, C.H., Bauer, S., Rügner, H., Liedl, R., Grathwohl, P. (2007b): Modellbasierte Sickerwasserprognose für die Verwertung von Recycling-Baustoff in technischen Bauwerken. (Model based prognosis of contaminant leaching for reuse of demolition waste in construction projects.) (accepted by Grundwasser and published online via SpringerLink), doi:10.1007/s00767-007-0025-x

Modellbasierte Sickerwasserprognose für die Verwertung von Recycling-Baustoff in technischen Bauwerken*

Model based prognosis of contaminant leaching for reuse of demolition waste in construction projects

Christof Beyer[1], Wilfried Konrad[1], Hermann Rügner[2], Sebastian Bauer[1], Park Chan Hee[1], Rudolf Liedl[3], Peter Grathwohl[1]

[1] *Eberhard-Karls-Universität Tübingen, Zentrum für Angewandte Geowissenschaften (ZAG), Sigwartstraße 10, 72076 Tübingen; Telefon: 07071-29 73176, Telefax: 07071-5059, E-mail: christof.beyer@uni-tuebingen.de*

[2] *Umweltforschungszentrum Leipzig-Halle (UFZ), Permoserstraße 15, 04318 Leipzig*

[3] *TU Dresden, Institut für Grundwasserwirtschaft, 01062 Dresden*

Kurzfassung:

In dieser Studie wird die in der BBodSchV rechtlich etablierte Sickerwasserprognose in Bezug auf die Beurteilung der von Recycling-Baustoff-Verwertungen im Straßenbau ausgehenden Schadstoffeinträge ins Grundwasser weiterentwickelt. Anhand numerischer reaktiver Stofftransportsimulationen für drei praxisrelevante Verwertungsszenarien (Parkplatz, Lärmschutzwall, Straßendamm) sowie eine Auswahl regionaltypischer Unterbodeneinheiten Deutschlands werden zeitliche Konzentrationsverläufe verschiedener Stoffklassen an der Grundwasseroberfläche berechnet. Der Durchbruchszeitpunkt konservativer Tracer wird allein von den hydraulischen Eigenschaften der Unterböden gesteuert, für organische Schadstoffe sind vor allem deren K_{OC}-Werte und die C_{org}-Gehalte der Unterböden ausschlaggebend. Signifikante dispersive Konzentrationsverminderungen ergeben sich nur bei deutlicher Abnahme der Quellstärke vor dem Durchbruch der Konzentrationspeaks. Bei lang anhaltend hohen Quellkonzentrationen relativ zur Transportzeit bleiben die Konzentrationsdurchbrüche unvermindert. Biologischer Schadstoffabbau führt zu deutlich reduzierten Durchbruchskonzentrationen. Für die Szenarien Lärmschutzwall und Straßendamm werden Kapillarsperreneffekte beobachtet, die zu einem teilweisen Umfließen der Schadstoffquelle führen. Bei Berücksichtigung des am Recyclingmaterial vorbeiströmenden Sickerwassers durch Konzentrationsmittelung über die gesamte Bauwerksbreite ergeben sich Konzentrationsminderungen um 30-40%.

Abstract:

In this study contaminant leaching from recycling materials in road constructions to groundwater is assessed by the “Sickerwasserprognose”. Numerical transport simulations for three scenarios (parking lot, noise protection dam, road) and a number of characteristic subsoils of Germany are performed to estimate the breakthrough of different contaminant classes at the groundwater table. Conservative tracer breakthrough times (BTT) primarily depend on subsoil hydraulic properties, for organic pollutants K_{oc} and subsoil *OC* are the controlling parameters. Significant concentration reductions from dispersion only occur when source concentrations decrease prior to contaminant breakthrough. If source concentrations remain high for long periods relative to peak BTT, concentration breakthrough is undamped. Accounting for biodegradation reduces breakthrough concentrations significantly. For the scenarios "noise protection dam" and "road" capillary barrier effects cause the seepage water to partially bypass the recycling material. Accounting for this bypass flow and averaging spatially across the constructions reduces concentrations by about 30-40%.

Keywords: ground water risk assessment; reuse; demolition waste; type-scenarios; road construction; modelling

*Beyer, C., Konrad, W., Park, C.H., Bauer, S., Rügner, H., Liedl, R., Grathwohl, P. (2007b): Modellbasierte Sickerwasserprognose für die Verwertung von Recycling-Baustoff in technischen Bauwerken. (Model based prognosis of contaminant leaching for reuse of demolition waste in construction projects.) (accepted by Grundwasser), doi:10.1007/s00767-007-0025-x

Einleitung und Zielsetzung

In Deutschland fallen jährlich etwa 250 Mio. t mineralischer Abfälle an, die in erheblichem Umfang im Erd-, Straßen- und Verkehrsflächenbau verwertet werden. Recycling-Baustoffe und Rückstände aus der industriellen Produktion (z. B. Hochofenschlacken) oder aus der Abfallbehandlung (z. B. Hausmüllverbrennungsaschen) finden unter anderem in Trag- und Frostschutzschichten beim Straßenbau, zum Bau von Lärmschutzwällen oder als Verfüllmaterial zunehmende Verwendung (Krass et al. 2004a; 2004b). Die Verwertung von Recycling-Baustoffen (RCB) in technischen Bauwerken wird in Deutschland in Übereinstimmung mit der diesbezüglichen Politik der Europäischen Union gegenüber einer Deponierung prinzipiell vorgezogen (KrW-/AbfG 1994). Aufgrund der häufig vorliegenden Belastung von RCB durch organische und anorganische Schadstoffe (z.B. PAK, Salze, Schwermetalle) muss bei der Verwertung in technischen Bauwerken jedoch berücksichtigt werden, dass Inhaltsstoffe durch das Sickerwasser ausgewaschen werden und das Grund- und Oberflächenwasser belasten können. Aus diesem Grund ist eine Bewertung von Verwertungsmaßnahmen hinsichtlich ihrer Umweltauswirkungen notwendig. Das Schadstoffaustragsverhalten technischer Bauwerke ist deshalb ein sowohl auf nationaler als auch auf internationaler Ebene aktuelles und intensiv bearbeitetes Forschungsgebiet. So führten Hjelmar et al. (2007) großskalige Feldstudien an einem Straßenabschnitt in Dänemark durch und beobachteten ein zeitliches Abklingen der Schadstoffquellstärke, welches bei der Umweltwirkungsprognose berücksichtigt werden sollte. Für einige Schadstoffe ergäben sich so weniger konservativen Prognosen, die weniger restriktive Grenzwerte erlauben würden, ohne den Schutz des Grundwassers zu gefährden (Hjelmar et al. 2007). Die Autoren wiesen zudem das Auftreten von Kapillarsperren in Straßendämmen nach, die zu einem Umfließen des Verwertungsmaterials und somit zu reduzierten Wasserflüssen durch die Schadstoffquelle führten. Kapillarsperreneffekte wurden auch von Hansson et al. (2006) bei numerischen Simulationen der Wasserströmung in Straßendämmen beobachtet. Susset (2007) führte Freilandlysimeteruntersuchungen mit RCB über Löss- und geringsorptiven Sandbodenmonolithen durch und stellte einen Rückhalt von PAK über bisher 4 Jahre nach, wobei die Wasserdurchsatzraten übertragen auf Feldbedingungen mehreren Jahrzehnten entsprechen. Sulfatkonzentrationen an der Unterkante des RCB gingen im Beobachtungszeitraum kaum zurück und brachen in voller Höhe durch. Für Chlorid hingegen konnte eine dispersive Verdünnung der Maximalkonzentration beobachtet werden, da die „Lebensdauer“ der Chloridquelle deutlich kleiner als die Transportzeit durch die Lysimeter war. In umfangreichen Säulenexperimenten mit RCB über Böden unter feldnahen Bedingungen zeigten Stieber et al. (2006), dass organische Kontaminanten wie PAK in der ungesättigten Zone effektiv durch mikrobiellen Abbau eliminierbar sind, sofern die dafür physiologisch notwendigen Milieubedingungen nicht durch das Sickerwasser nachteilig verändert werden.

Die Vielzahl der zu berücksichtigenden hydraulischen, geochemischen und mikrobiologischen Prozesse sowie die Komplexität ihrer Interaktionen macht deutlich, dass die Anwendung von prozessbasierten Modellen bei der Bewertung von umweltoffen verwerteten Recyclingmaterialien große Vorteile bietet. Vor diesem Hintergrund untersucht diese Arbeit in Anlehnung an die Methodik der Sickerwasserprognose nach BBodSchV (1999) anhand numerischer reaktiver Stofftransportsimulationen, welche Schadstoffeinträge von im Straßenbau eingesetztem RCB über die ungesättigte Zone ins Grundwasser unter Berücksichtigung möglicher zeitabhängiger Festlegungs- und Abbauprozesse (Sorption, Intrapartikeldiffusion, Bioabbau) erfolgen können. Dazu wird hier erstmals eine Kopplung des Stromröhrenmodells SMART (Finkel 1998, Finkel et al. 1998) mit dem Finite-Elemente-Modell GeoSys/Rockflow (Kolditz & Bauer 2004; Kolditz et al. 2006) eingesetzt. Die Kombination verschiedener repräsentativer Verwertungsszenarien (Parkplatz, Lärmschutzwall, Straßendamm), RCB-typischer Schadstoffklassen und regionaltypischer Unterböden führt zu einem umfangreichen Satz von Typ-Szenarien-Simulationen, deren Ergebnisse es erlauben,

- den aus den Verwertungsszenarien zu erwartenden charakteristischen zeitlichen Verlauf der Schadstoffeinträge in Boden und Grundwasser darzustellen,
- die während des Transports für Schadstoffrückhalt und Konzentrationsminderung relevanten Prozesse zu identifizieren,
- Einflüsse der Unterbodeneigenschaften hinsichtlich des Filter- und Puffervermögens herauszustellen und
- das Potential der modellbasierten Sickerwasserprognose praxisnah zu demonstrieren.

Modellkonzept

Die Berechnung der Schadstoffeinträge aus dem RCB über die ungesättigte Zone ins Grundwasser wird in dieser Studie erstmalig mit Hilfe einer Kopplung zwischen dem Finite-Elemente-Modell GeoSys/Rockflow

und dem stochastischen Stromröhrenmodell SMART durchgeführt. Die Simulationsaufgabe wird hier in die zwei Teilprobleme *Hydraulik/Strömung* und *reaktiver Transport* zerlegt. Diese Vorgehensweise wurde gewählt, um die Auswirkung der räumlich variablen Sickerwasserströmung in den Verwertungsszenarien auf den Schadstofftransport berücksichtigen sowie physikalisch realistische Schadstofffreisetzungsprozesse in der Quelle und die durch Intrapartikeldiffusion zeitabhängige Sorption beim Transport quantifizieren zu können.

Die Kopplung zwischen der Strömungssimulation mit GeoSys/Rockflow und der reaktiven Transportsimulation mit SMART erfolgt über Verteilungsfunktionen (pdf, "probability density function") der Verweilzeiten des Sickerwassers, welche die Einflüsse der hydraulischen Heterogenität auf das Strömungsfeld beschreiben (vgl. Utermann et al. 1990; Bold 2004). Die pdf sind Modellergebnis der Strömungssimulation und werden von SMART als Modelleingabe benötigt, um in der reaktiven Transportsimulation Massendurchbruchskurven an einer unterstromigen Kontrollebene (hier die Grundwasseroberfläche) zu berechnen. Da das SMART-Konzept zwar Transportsimulationen in heterogen zusammengesetzten Materialien erlaubt (Lithokomponenten-Ansatz nach Kleineidam et al. 1999a), entlang der Stromröhre jedoch eine homogene Materialverteilung vorausgesetzt wird, muss für jede Material- bzw. Modellschicht der aus mehreren Baumaterialien und Unterbodenhorizonten bestehenden Typ-Szenarien eine separate SMART-Simulation gerechnet werden. Das Modell ist somit als eine Reihe von hintereinander geschalteten 1D-Stromröhren konzipiert (siehe Abb. 1).

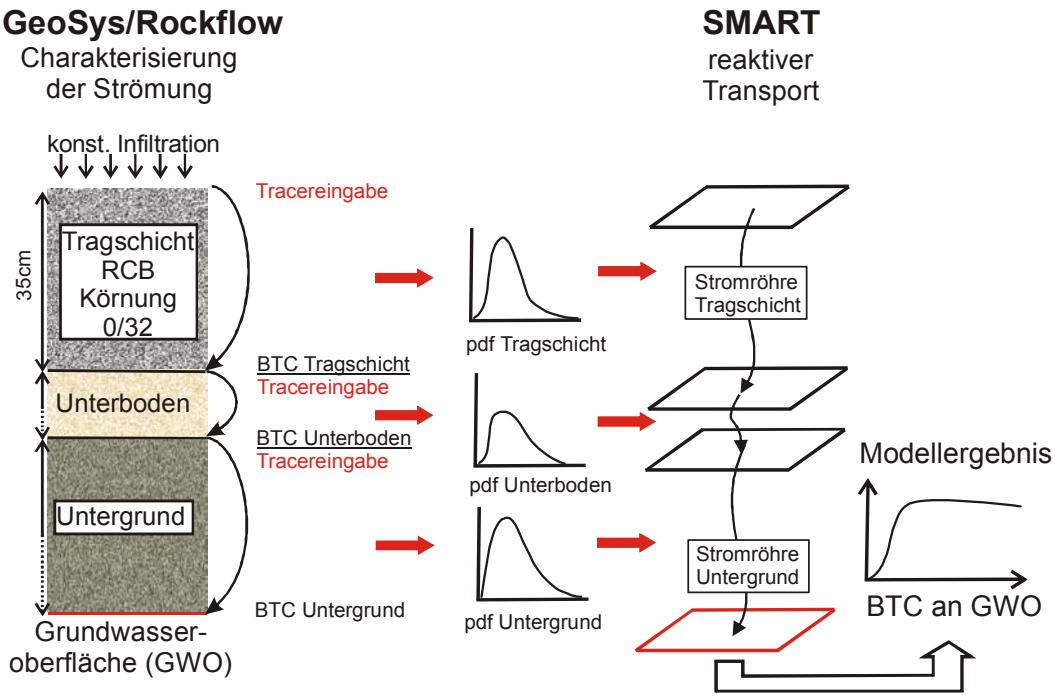

Abb. 1: Veranschaulichung des Modellkonzepts anhand des Parkplatzszenarios: Simulation der Tracerdurchbruchskurven zur Ableitung von Laufzeitverteilungen (pdf) der einzelnen Modellschichten mit GeoSys/Rockflow; reaktive Transportsimulationen mit SMART (BTC = Durchbruchskurve); Kopplung beider Modelle durch die pdf.

Die modellierte Massendurchbruchskurve an der unterstromigen Kontrollebene jeder Stromröhre repräsentiert jeweils die oberstromige zeitabhängige Konzentrationsrandbedingung der nachfolgenden Stromröhre bzw. im Fall der untersten Modellschicht den Schadstoffeintrag ins Grundwasser. Dementsprechend muss für jede Modellschicht eine eigene pdf abgeleitet werden. Aus Gründen der Modellvereinfachung werden die einzelnen pdf als unabhängig voneinander betrachtet (vgl. Vanderborght et al. 2007). Zur Ableitung der pdf wird in GeoSys/Rockflow für jede einzelne Materialschicht an der Schichtobergrenze ein konservativer Tracer mit konstanter Konzentration C_0 in das Strömungsfeld eingegeben und dessen Durchbruch $C(t)$ an der Schichtuntergrenze zeitlich registriert (siehe Abb. 1). Die pdf der Modellschicht ergibt sich als Ableitung der Durchbruchskurve $\mathrm{d}C/\mathrm{d}t$ aufgetragen über die Zeit t.

Die Kopplung beider Simulationsmodelle wurde als sogenannte *lose Kopplung* realisiert, d.h. die Quellcodes wurden nicht kombiniert sondern kommunizieren über Batch-Aufrufe und automatisch generierte Eingabe-/Ausgabedateien während bzw. nach der Programmausführung. Diese Art der Einbindung hat im Hinblick auf

die Anzahl Simulationsläufe den Vorteil, dass pro Kombination aus Verwertungsmaßnahme und Unterbodentyp nur eine Simulation des Strömungsfeldes zur Bestimmung aller pdf notwendig ist und diese jeweils für die darauf folgenden Transportsimulationen der einzelnen Schadstoffklassen mit SMART verwendet werden können.

Numerische Simulation der Strömung und des reaktiven Transports

Die Simulation der ungesättigten Strömung mit GeoSys/Rockflow zur Ableitung der pdf erfolgt auf Grundlage der Richards-Gleichung, zu deren Lösung das Van-Genuchten-Mualem-Modell (van Genuchten 1980; Mualem 1976) verwendet wird (Du et al. 2005). Auf eine umfassende Ausführung der allgemein bekannten Modellgleichung wird hier und im Folgenden verzichtet, eine ausführliche Erläuterung der verwendeten mathematischen Modelle ist in Grathwohl et al. (2006) zu finden. Die Berechnung der Tracerbewegung im ungesättigten Strömungsfeld zur Ableitung der pdf erfolgt auf Grundlage der Konvektions-Dispersionsgleichung. Die Beschreibung des reaktiven Transports mit SMART erfolgt dagegen wie oben beschrieben nicht entlang von Raumkoordinaten sondern in Abhängigkeit der Verweilzeit entlang einer Stromröhre (Finkel, 1998). Die Rückhalteprozesse beim Transport werden durch das in SMART integrierte numerische Modell BESSY (Jäger & Liedl 2000) quantifiziert. Die Berücksichtigung der den Sorptionsprozess zeitlich limitierenden Intrapartikel-Porendiffusion ist insbesondere für Böden mit hohem Kies- oder Skelettanteil notwendig (Grathwohl 1998; Rügner et al. 1997; 1999). Die Sorptionskinetik wird unter Annahme von sphärischen Partikeln durch das 2. Fick´sche Gesetz in Radialkoordinaten beschrieben:

$$\frac{\partial C_w}{\partial t} = D_a\left[\frac{\partial^2 C_w}{\partial r^2} + \frac{2}{r}\frac{\partial C_w}{\partial r}\right] \qquad (1)$$

r [m] bezeichnet den radialen Abstand vom Kornmittelpunkt, C_W [kg m^{-3}] die Konzentration in der wässrigen Phase der Intrapartikelporen und D_a [cm^2 s^{-1}] den scheinbaren Diffusionskoeffizienten, der gegenüber der Diffusion in Wasser (D_{aq}) vermindert ist:

$$D_a = \frac{D_{aq}\varepsilon}{(\varepsilon + K_d \rho_k)\tau_f} \qquad (2)$$

ε [-] bezeichnet die Intrapartikelporosität, τ_f [-] den Tortuositätsfaktor, K_d [m^{-3} kg^{-1}] den Gleichgewichts-Verteilungskoeffizienten und ρ_k [kg m^{-3}] die Partikeldichte gemäß $\rho_k = (1-\varepsilon)\rho$ mit ρ [kg m^{-3}] der Mineraldichte.

Die Verteilung der Schadstoffe zwischen dem in den Intrapartikelporen gelösten und dem sorbierten Anteil wird durch eine lineare Sorptionsisotherme beschrieben, für den Schadstoffabbau im mobilen Porenwasser wird eine Kinetik erster Ordnung angenommen. Somit ergibt sich unter stationären Fließbedingungen ein insgesamt lineares mathematisches Modell für die im Sickerwasser auftretenden Konzentrationen C und eine Proportionalität zwischen C und den anfänglich aus der Schadstoffquelle eluierenden Schadstoff-konzentrationen C_0, bzw. den anfanglich sorbierten Stoffmengen.

Parametrisierung der Typ-Szenarien

Im Rahmen dieser Studie werden drei repräsentative Verwertungsszenarien betrachtet: *Parkplatz* (PP), *Lärmschutzwall* (LSW) und *Straßendamm* (SD). Das in diesen zum Einsatz kommende Verwertungsmaterial besteht aus granularem RCB. Als Schadstoffe werden vier Modellsubstanzen verwendet, die in ihren Eigenschaften für RCB typische Schadstoffe repräsentieren: *Naphthalin* (NAP) und *Phenanthren* (PHE) als schwach bzw. mäßig sorbierende organische Schadstoffe, ein stark sorbierender für das durchschnittliche Verhalten der 15 EPA-PAK repräsentativer *Summenparameter* (Σ15 EPA-PAK) sowie ein konservativer *Tracer* als Beispiel leicht löslicher Salze wie Chlorid. Für die Transportstrecken unterhalb der Quellterme werden sechs regionaltypische Unterbodeneinheiten Deutschlands berücksichtigt, um Charakteristika und Unterschiede hinsichtlich ihrer Filter- und Pufferkapazitäten herauszustellen. Die folgenden Abschnitte erläutern die Parametrisierung der Typ-Szenarien (für detailliertere Ausführungen siehe Grathwohl et al. 2006).

Verwertungsszenarien und -materialien

Das *PP-Szenario* wird als vertikales 1D-Modell betrachtet und orientiert sich am Querschnitt für Verkehrsflächen der Bauklasse VI mit Pflasterdecke und ungebundener Tragschicht auf einer Frostschutzschicht (FSS) nach FGSV (2001). Für Tragschicht und FSS, die im Modell als einheitliche Schicht von 0.35 m betrachtet werden, wird RCB mit einer Körnung der Sieblinie 0/32 (FGSV 2004) eingesetzt. Das Pflaster selbst wird nicht berücksichtigt, da die geforderte Versickerungsleistung von $2.7*10^{-5}$ m s^{-1} (FGSV 1998) deutlich über den hier angenommenen Infiltrationsraten liegt (s.u.). Abb. 1 zeigt neben dem Modellkonzept auch den für die Modellierung vereinfachten PP-Aufbau.

Die Szenarien LSW und SD werden als 2D-Vertikalschnitte betrachtet, bei denen die Simulationen aus Symmetriegründen nur für jeweils eine Hälfte des Querschnitts durchgeführt wurden. Das *LSW*-Modell (Abb. 2) orientiert sich an einem von Mesters (1993) experimentell untersuchten LSW. Als Bodenabdeckung des Wallkerns aus RCB wird ein Lehmboden verwendet.

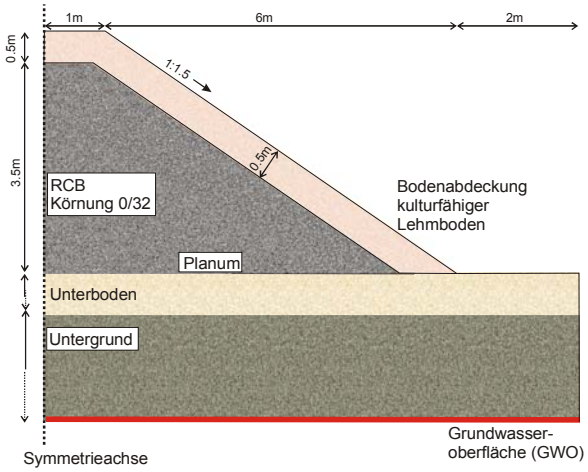

Abb. 2: Lärmschutzwall mit Wallkern aus Recycling-Baustoff (RCB).

Das *SD*-Modell (Abb. 3) orientiert sich am Regelquerschnitt RQ 26 für vierstreifige Autobahnen (FGSV 1996). Das Bankett wird nach FGSV (2005) als schwach durchlässiger Boden SŪ* ausgeführt (entspr. Bodenart Su3), die Bodenabdeckung der Böschung als stark durchlässiger Sand (entspr. Bodenart Ss). Die hydraulischen Eigenschaften der für Bankett und Böschung verwendeten Böden sind in Tab. 1 aufgeführt. Unterhalb der Asphaltdeckschicht schließt sich eine ungebundene Tragschicht an, für die wie für den darunter liegenden Dammkern RCB der Sieblinie 0/32 angenommen wird.

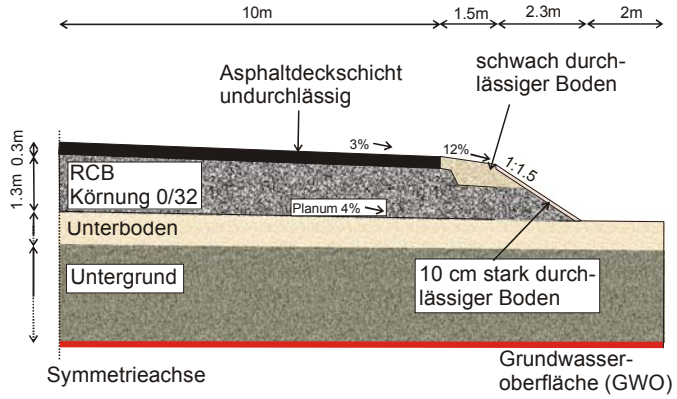

Abb. 3: Straßendamm mit Frostschutzschicht/Tragschicht aus Recycling-Baustoff (RCB).

Zu den ungesättigten hydraulischen Eigenschaften von Recyclingmaterialien im Straßenbau finden sich in der Literatur kaum experimentelle Angaben. Deshalb wurden die Van-Genuchten-Parameter für den RCB in den einzelnen Verwertungsszenarien mit einem Ansatz von Arya & Paris (1981) bzw. Mishra et al. (1989) auf

Grundlage des Korngrößenspektrums der 0/32-Siebline, der Lagerungsdichte $\rho_b = (V \cdot \rho_p)$ und der Porosität $\eta = (1 - \rho_b / \rho)$ abgeleitet. V [-] ist der Verdichtungsgrad und ρ_p die Proctordichte [g cm^{-3}] (siehe Tab. 1). Dieser Ansatz wurde für natürliche Böden entwickelt, sollte nach Hansson et al. (2006) jedoch auch für relativ grobkörnige Materialien wie Tragschichtschotter im Straßenbau geeignet sein. Für die gesättigte Leitfähigkeit K_s von Tragschichten wird ein Mindestwert von 5.4*10^{-5} m s^{-1} gefordert (FGSV 1998). Aufgrund der großen Spannbreite experimentell in Labor und in-situ bestimmter Durchlässigkeiten (z.B. Wörner et al. 2001; Stoppka 2002; Kellermann 2003) wird dieser Wert hier in allen Verwertungsszenarien für den RCB angenommen. Abb. 4 zeigt die θ-ψ- sowie die θ-K-Beziehungen des RCB für PP, LSW und SD. Die Kurvenverläufe sind durchweg sehr ähnlich und durch sehr geringe Kapillarität gekennzeichnet, was zu einer schnellen Drainage der Tragschichten erforderlich ist.

Tab. 1: Hydraulische Eigenschaften der Baumaterialien für Parkplatz, Lärmschutzwall und Straßendamm

	Parkplatz	**Lärmschutzwall**		**Straßendamm**		
	RCB	**RCB**	**Böschung**[‡]	**RCB**	**Bankett**[†]	**Böschung**[†]
θ_s	0.27	0.31	0.43	0.25	0.36	0.37
θ_r	0.00	0.00	0.08	0.00	0.00	0.04
n	1.29	1.29	1.56	1.29	1.28	1.57
α [m^{-1}]	166	154	3.60	146	2.64	8.74
l	0.50	0.50	0.50	0.50	0.50	0.50
ρ [g cm^{-3}][¶]	2.66	2.66	2.65	2.66	2.65	2.65
ρ_b [g cm^{-3}]	1.94	1.84	1.51	2.00	1.69	1.67
ρ_p [g cm^{-3}][¶]	1.94	1.94	-	1.94	-	-
V [-][§]	1	0.95	-	1.03	-	-
K_s [m s^{-1}]	5.40*10^{-5}	5.40*10^{-5}	1.00*10^{-6}	5.40*10^{-5}	1.00*10^{-6}	2.90*10^{-6}

[‡]: Carsell & Parish 1988; [†]: Hennings 2000;

[§]: FGSV 2002 (PP), 1997 (LSW), 2004 (SD); [¶]: Kellermann 2003

α, n, l: empirische Van-Genuchten-Parameter

θ_r, θ_s: residualer und gesättigter Wassergehalt

ρ, ρ_b, ρ_p: Mineral-, Lagerungs- und Proctordichte

V: Verdichtungsgrad; K_s: gesättigte hydraulische Leitfähigkeit

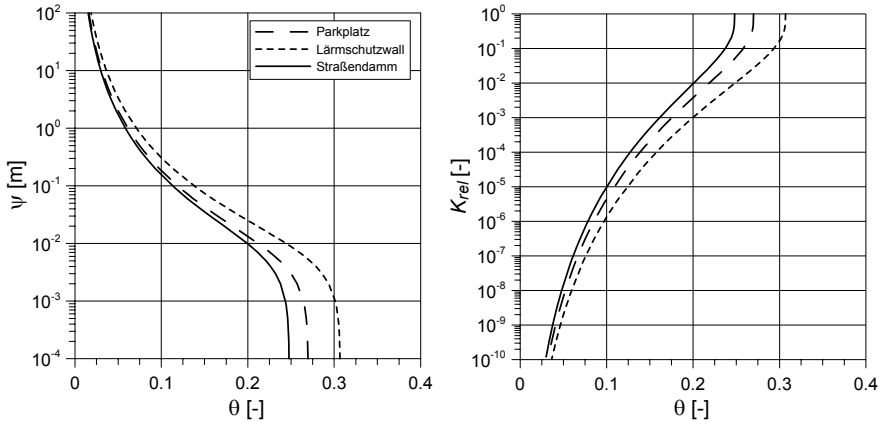

Abb. 4: Wassergehalts-SAugspannungs- (links) sowie Wassergehalts-Leitfähigkeits-Beziehungen (rechts) für Recycling-Baustoff in den drei Verwertungsszenarien (ψ = Matrixpotential, K_{rel} = relative Leitfähigkeit, θ = Wassergehalt).

Die K_d-Werte von NAP, PHE und Σ15 EPA-PAK im RCB von 106, 496 bzw. 1333 l kg^{-1} sowie die Intrapartikelporosität ε = 0.015 wurden von Henzler (2004) experimentell bestimmt. D_{aq} für PHE und NAP wurde mit 7.86*10^{-10} bzw. 9.15*10^{-10} m² s^{-1} nach Hayduk & Laudie (1974) abgeschätzt. Die heterogene Zusammensetzung des RCB aus verschiedenen Korngrößenfraktionen wurde durch den Lithokomponenten-Ansatz nach Kleineidam et al. (1999a) berücksichtigt. Wegen sehr langer Rechenzeiten wird der RCB durch zwei Korngrößenklassen modelliert (siehe auch Rügner et al. 2005), für die die kinetische Sorption jeweils separat berechnet wird. Auf die Fein- und Grobfraktion entfallen Anteile von 32.8 % bzw. 67.2 % mit „effektiven" Kornradien von a = 0.25 mm bzw. a = 8 mm (siehe Henzler (2004)).

Auswahl und Klassifizierung der Unterbodenprofile

Die Charakterisierung der Unterbodenprofile erfolgte auf Basis der nutzungsdifferenzierten Bodenübersichtskarte 1:1.000.000 (BÜK1000; BGR 2006). Aus deren 672 Referenzprofilen wurden sechs Profile nach Flächenrepräsentanz und dem zu erwartenden charakteristischen Transportverhalten für die numerischen Simulationen des reaktiven Stofftransports ausgewählt (Braunerde und Podsol aus Sand, Fahlerde aus Geschiebelehm, Schwarzerde und Parabraunerde aus Löss, Pelosol aus verwittertem Mergel- und Tonstein). Zur Vereinfachung der Simulationen wurde eine Reduktion der vertikalen Profildifferenzierung durch Zusammenfassung mehrerer Horizonte vorgenommen, soweit eine einheitliche Betrachtung nach bodenkundlichen und geologischen Aspekten möglich schien. Bei allen Profilen wurden somit Daten aus verschiedenen Horizonten nach deren Mächtigkeit gewichtet gemittelt (Tab. 2). Als zu berechnende Profiltiefe wurde für die Böden die in der BÜK1000 (BGR 2006) beschriebene Profiltiefe ohne den Oberboden angesetzt, da dieser bei der Bebauung abgetragen wird. Die resultierenden Profiltiefen (Tab. 2) sind im Sinne von Mindesttiefen zu verstehen, da die in der Praxis relevanten Grundwasserflurabstände häufig deutlich größer sein dürften.

Zur Festlegung der K_s-Werte und Van-Genuchten-Parameter wurden Pedotransferfunktionen von Wösten et al. (1998) angewendet. Der Sättigungswassergehalt θ_s wurde für alle Bodenschichten der Porosität gleichgesetzt. K_s bezieht sich auf den Feinbodenanteil (< 2 mm) und wurden bei höheren Skelettgehalten um die Reduktion der Leitfähigkeit durch den Skelettanteil mit einem Verfahren von Brakensiek & Rawls (1994) korrigiert. Für die Simulation der Tracerversuche in GeoSys/Rockflow zur Ableitung der pdf wurden die Dispersivitäten mit α_L = 0.1 m und α_T = 0.01 m festgelegt.

Die K_d–Werte wurden aus dem Gehalt an organischem Kohlenstoff f_{oc} [-] (= 0.01 C_{org}; vgl. Tab. 2) und dem auf den C_{org}-Gehalt normierten Verteilungskoeffizienten K_{OC} [l kg^{-1}] durch $K_d = K_{OC} f_{oc}$ abgeschätzt. Für Horizonte, die nach BÜK1000 (BGR 2006) als „humusfrei" ausgewiesen sind, wurde als konservative Annahme für den Feinboden ein minimaler C_{org} von 0.01 % angenommen. Zur Abschätzung des K_{OC} wurde die auf der Wasserlöslichkeit S [mol l^{-1}] beruhende Korrelation von Seth et al. (1999) verwendet (für vergleichbare Ansätze siehe auch Allen-King et al. 2002):

$$\log K_{OC} = -0.88 \log S + 0.07 \qquad (3)$$

S beträgt für PHE 3.46*10^{-5}, für NAP 8.74*10^{-4} mol l^{-1}. Für Σ15 EPA-PAK wurde S über ein mittleres Molgewicht von 202 g mol^{-1} und einer effektiven Wasserlöslichkeit von 2.5 g l^{-1} (Grathwohl 2004) mit 1.14 *10^{-5} mol l^{-1} abgeschätzt. Für die verschiedenen Böden ergeben sich so K_d-Werte für NAP zwischen 0.06 und 5.10 l kg^{-1}, für PHE zwischen 0.99 und 87.2 l kg^{-1} sowie für Σ15 EPA-PAK zwischen 2.45 und 217 l kg^{-1} Für die Skelettanteile wurden K_{OC}-Werte von 4.0 l kg^{-1} (NAP), 5.2 l kg^{-1} (PHE) und 5.7 l kg^{-1} (Σ15 EPA-PAK) angenommen (Rügner et al. 2005). Mit diesen vergleichsweise hohen Werten wird berücksichtigt, dass es sich beim C_{org} dieser Komponenten idR. um gealtertes Material mit höherer Sorptionskapazität handelt (Kleineidam et al. 1999b). Der f_{oc} wurde mit 0.0005 angesetzt (Kleineidam et al. 1999b).

Die Sorptionskapazität und -kinetik für den Feinboden wird vor allem durch das partikuläre organische Material bestimmt. Es wurden folgende effektive Parameter zugrunde gelegt: a = 11.7 µm, ε = 0.00175, ρ = 2.65 g cm^{-3} und die Tortuosität $\tau_f = 1/\varepsilon$ (Grathwohl, 1992; Rügner et al. 1999). Für die Grobfraktion (> 2 mm) wurden a = 1 cm und ε = 0.01 angenommen (Rügner et al. 1999; Kleineidam et al. 1999a).

Die Transportsimulationen für NAP, PHE und Σ15 EPA-PAK wurden jeweils mit und ohne Berücksichtigung von Bioabbau durchgeführt, wobei nur die in Lösung vorliegenden Anteile als abbaubar betrachtet wurden. Zur Beurteilung der langfristigen Filterwirkung des Bodens bedarf es repräsentativer Langzeit-Ratenkonstanten (Henzler et al. 2006), deren quantitative Abschätzung in der ungesättigten Zone jedoch durch die Komplexität der Wechselwirkungen zwischen schadstoffspezifischen Eigenschaften, klimatischen und geochemischen Randbedingungen (Grathwohl et al. 2003, Höhener et al. 2006) bisher kaum möglich ist. Aus diesem Grund wurde ein relativ niedriger Wert von 1.15*10^{-7} s^{-1} (Halbwertzeit = 70 d) angenommen.

Dies ist als konservative Abschätzung zu betrachten, da viele Schadstoffe in der ungesättigten Zone unter Feldbedingungen deutlich schneller abgebaut werden können (Maier & Grathwohl 2005, Rügner et al. 2005).

Tab. 2: Bodeneigenschaften der sechs betrachteten Unterböden aus der BÜK1000 (BGR 2006). Für vertikal aggregierte Horizonte wurden die Parameter über die Mächtigkeit der einzelnen Horizonte gewichtet gemittelt.

Bodentyp	**Braunerde**	**Podsol**	**Fahlerde**		**Schwarz-erde**	**Para-braunerde**	**Pelosol**
Fläche [km²]	1672	7237	6933		3455	14428	5614
Einteilung	Unterboden	Unterboden	Unterboden	Untergrund	Unterboden	Unterboden	Unterboden
von - bis [m]	0.00-1.70	0.00-1.70	0.00-0.90	0.90-1.70	0.00-1.70	0.00-1.70	0.00-1.75
Ton [%]	3.82	10.40	31.85	31.85	19.69	19.78	39.88
Schluff [%]	14.54	20.48	20.48	20.48	69.40	70.28	37.00
Sand [%]	57.41	63.21	38.68	38.68	8.44	8.43	16.48
Skelett [%]	24.24	5.91	9.00	9.00	2.47	1.50	6.64
C_{org} **[%]**	0.01‡	0.21	0.01‡	0.01‡	0.88	0.01‡	0.03
ρ_b **[g cm^{-3}]**	1.71	1.61	1.62	1.75	1.42	1.63	1.60
θ_s	0.29	0.36	0.35	0.34	0.45	0.38	0.39
θ_r†	0.01	0.01	0.01	0.01	0.01	0.01	0.01
n†	1.34	1.26	1.17	1.08	1.15	1.13	1.16
α† **[m^{-1}]**	5.93	5.98	6.21	4.95	1.76	1.24	2.73
l†	1.77	-0.30	-0.66	-3.57	-1.91	-0.32	-2.75
K_s† **[m s^{-1}]**	$1.52*10^{-6}$	$3.37*10^{-6}$	$3.09*10^{-6}$	$8.46*10^{-7}$	$3.83*10^{-6}$	$1.38*10^{-6}$	$9.48*10^{-7}$

‡: 0.00 nach BÜK1000; Annahme eines minimalen C_{org}-Gehaltes des Feinbodens von 0.01%

†: abgeleitet nach Wösten et al. (1998); K_s korrigiert um Skelettanteil nach Brakensieck & Rawls (1994)

θ_r, θ_s: residualer und gesättigter Wassergehalt; ρ_b: Lagerungsdichte

α, n, l: empirische Van-Genuchten-Parameter; K_s: gesättigte hydraulische Leitfähigkeit

Abschätzung der Sickerwasserrate

Für eine langfristige Beurteilung der Schadstoffverlagerung ist es sinnvoll und zulässig von vereinfachten Fließverhältnissen auszugehen (Grathwohl & Susset 2001; Henzler et al. 2006). Aus diesem Grund wird eine stationäre ungesättigte Strömung angenommen. Die jährlichen mittleren Infiltrationsraten I [mm a^{-1}] der Verwertungsszenarien wurden als Mittelwerte für Deutschland abgeschätzt. Hierzu wurde das BAGLUVA-Verfahren (Glugla et al. 2003) angewendet. Als mittlerer korrigierter Niederschlag N_{jahr} wurde ein Wert von 859 mm a^{-1} angenommen (BMU 2000). I ergibt sich als Differenz von N_{jahr} und der Jahressumme der Evapotranspiration ET. Diese wird als Funktion der maximalen ET und standortspezifischer Parameter bestimmt. Für den PP wurde I so mit 583 mm a^{-1} abgeschätzt, was im oberen Bereich für sickerfähige Pflasterdecken liegt (Richter 2003). Die Annahme wird jedoch durch Freilandlysimeter-Untersuchungen von Flöter (2006) gestützt, in denen der Anteil von I am Niederschlag über 4 a im Mittel rund 80 % betrug. Für den LSW wurde I mit 313 mm a^{-1} abgeschätzt. Für den SD ergibt sich die zu infiltrierende Wassermenge als Summe des Oberflächenabflusses der Asphaltdecke (Abflussbeiwert = 0.9; FGSV 2005) und des auf Bankett und Böschung fallenden Niederschlags abzüglich der ET. Für die räumliche Verteilung der Infiltration mussten vereinfachende Annahmen getroffen werden, da der SD-Querschnitt eine neue Bauweise nach FGSV (2005) darstellt, bei der der Straßenabfluss zu größeren Teilen über die Böschung infiltrieren soll, bisher jedoch keine experimentellen Daten dazu vorliegen. Aus diesem Grund wurde angenommen, dass die Versickerung gleichmäßig über Bankett und Böschung erfolgt. Auf den Querschnitt bezogen ergibt sich I mit 2318 mm a^{-1}. Für den Böschungsfuß wurden wie für den LSW I = 313 mm a^{-1} angenommen.

Ergebnisse und Diskussion

Die im Folgenden vorgestellten zeitlichen Konzentrationsverläufe der Modellsubstanzen an der GWO stellen über den unteren Modellrand integrierte Durchbruchskurven dar. Dabei ist für das LSW- und SD-Szenario zwischen den mit SMART berechneten, auf den Transportpfad bezogenen (graue dicke Kurven, Abb. 5, 8, 9) und den über den gesamten Querschnitt gemittelten Konzentrationen (schwarze dünne Kurven, Abb. 5, 8, 9) zu unterscheiden (siehe auch Abb. 6).

Die Tracer-Durchbruchskurven an der GWO für die drei Szenarien PP, LSW und SD sind in Abb. 5 (a)-(c) dargestellt. Für den PP erfolgt der Durchbruch des Tracers am frühesten bei Braunerde und Podsol, später bei Pelosol, Parabraunerde und Schwarzerde (Abb. 5 (a)), die eine geringere Porenwasserfließgeschwindigkeit als die Sandböden aufweisen. Dispersion führt zu Verminderungen der Durchbruchskonzentrationen auf C/C_0 zwischen 0.23 (Braunerde) und 0.16 (Schwarzerde). Die hier betrachteten Transportstrecken von bis zu 1.75 m ab der RCB-Unterkante dürften idR. kürzer als die in vielen Praxisfällen relevanten Grundwasserflurabstände sein, wodurch unter Umständen eine stärkere dispersive Konzentrationsreduktion möglich wäre.

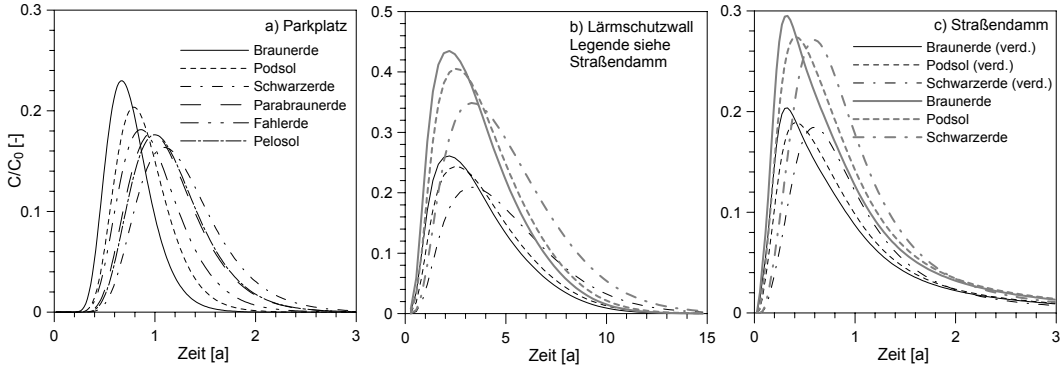

Abb. 5: Durchbruchskurven des Tracers an der Grundwasseroberfläche für (a) Parkplatz-, (b) Lärmschutzwall- und (c) Straßendamm-Szenario. Gezeigt werden Durchbruchskurven für den Schadstofftransportpfad ((b) und (c), graue dicke Kurven) bzw. auf das Gesamtbauwerk bezogene Durchbruchskurven unter Berücksichtigung der Verdünnung durch nicht belastetes Sickerwasser ((b) und (c), schwarze dünne Kurven).

Die über den unteren Modellrand integrierten Tracer-Durchbruchskurven für das LSW-Szenario (Abb. 5 (b)) zeigen im Vergleich zum PP ein stärkeres Tailing und über längere Zeiträume anhaltende hohe Konzentrationen C/C_0. Aus Anschaulichkeitsgründen werden die Ergebnisse hier nur für Braunerde, Podsol und Schwarzerde vorgestellt. Das ausgeprägte Tailing resultiert aus der geringeren Infiltrationsrate sowie aus der Geometrie des LSW. Die Überdeckung des grobkörnigen RCB mit einem feinkörnigen Lehm führt an der Böschung zu einer Kapillarsperre, welche die Infiltration in den RCB vermindert und ein Umströmen des Wallkerns verursacht (siehe Abb. 6 (a)).

Die Kapillarsperre bildet sich aus, da der RCB aufgrund geringer Kapillarität bereits bei geringen Saugspannungen einen Großteil des Porenwassers verliert (siehe Abb. 4) und die hydraulische Leitfähigkeit gegenüber dem Lehm deutlich stärker abnimmt. Das Sickerwasser kann so entlang der geneigten Materialgrenze in dem nun besser wasserleitenden Lehmboden abfließen. Mit zunehmender Distanz von der Wallkrone erhöhen sich die Wasserflüsse im Lehm, sodass in Abhängigkeit der Druckverhältnisse zunehmend Wasser infiltrieren kann (Ross 1990). Die räumliche Variabilität der Sickerwasserströmung führt zu Bereichen mit stark reduzierten Fließgeschwindigkeiten und so zu einem langsameren Auswaschen des Tracers aus dem RCB. Die Maximalkonzentrationen erreichen die GWO nach etwa 2 (Braunerde) bis 3.5 a (Schwarzerde) (Abb. 5 (b)). Im Vergleich zum PP kommt es zudem zu höheren Peakkonzentrationen C/C_0 für den Transportpfad (Braunerde: 0.43, Schwarzerde: 0.35), da zum Zeitpunkt des Peak-Durchbruchs an der GWO die Eluatkonzentrationen der Quelle noch deutlich höher als beim PP sind (siehe Abb. 7 (a)) und so die dispersive Konzentrationsminderung weniger effektiv ist. Der länger anhaltende hohen Eluatkonzentrationen resultieren aus den geringeren Sickerwassermengen, der Reduktion der Infiltration in den RCB durch Kapillarsperren und der größere Mächtigkeit des RCB gegenüber dem PP. Auf das gesamte Bauwerk bzw. auf die gesamte infiltrierende Wassermenge bezogen reduzieren sich die Maximalkonzentrationen durch kleinräumige Mittelung jeweils um ca. 40 %. Zu beachten ist in diesem Zusammenhang, dass die Ausprägung und Effektivität einer Kapillarsperre von einer Reihe von

Randbedingungen abhängig ist. Aus diesem Grund sind die berechneten Verdünnungsfaktoren nur für die hier betrachteten Geometrien, Infiltrationsraten und Materialkombinationen quantitativ gültig.

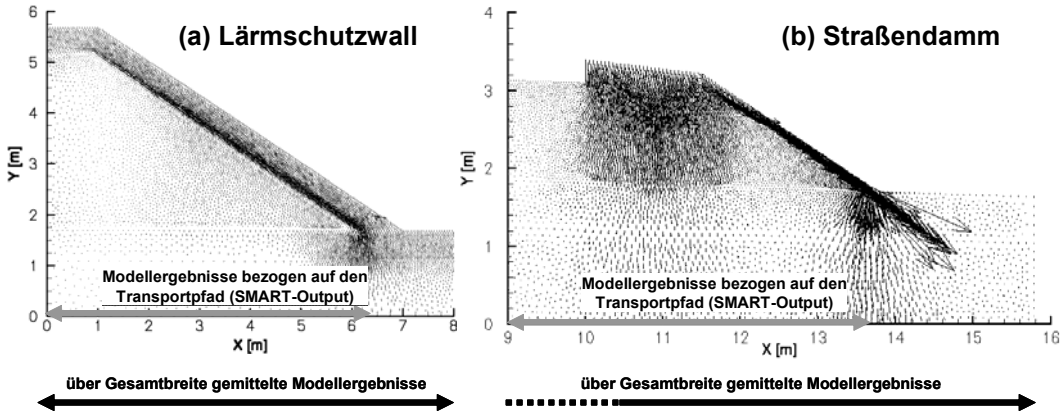

Abb. 6: Geschwindigkeitsvektoren der ungesättigten Strömung an allen Elementknoten im Lärmschutzwall (a) und in einem Ausschnitt des Straßendammes (b). Die Konzentration des Flusses in den Bodendeckschichten ist Resultat des Kapillarsperreneffektes, wird durch die feinere Netzdiskretisierung jedoch überzeichnet.

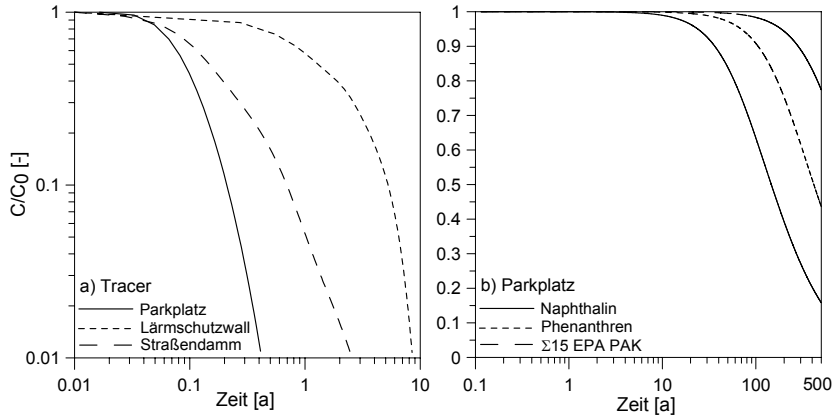

Abb. 7: Zeitliche Entwicklung der aus der Schadstoffquelle eluierenden Konzentrationen an der Recycling-Baustoff-Unterkante (RCB) für ausgewählte Schadstoff-Verwertungsszenario-Kombinationen: (a) konservativer Tracer für Parkplatz-, Lärmschutzwall- und Straßendammszenario; (b) Naphthalin, Phenanthren und Σ15 EPA-PAK für das Parkplatzszenario.

Auch für das SD-Szenario ist ein Kapillarsperreneffekt zu beobachten (Abb. 6(b)). Während sich im Bankettbereich eine relativ gleichförmige Verteilung der Sickerwasserströmung zeigt, strömt in der Bodenabdeckung der Böschung ein Teil des Sickerwassers am RCB vorbei und infiltriert konzentriert am Böschungsfuß. Bei kleinräumiger Mittelung der Durchbruchskonzentrationen ergibt sich eine Verdünnung um ca. 31 %. Die Durchbruchskurven des Tracers (Abb. 5 (c)) zeigen ein steileres Ansteigen als beim LSW und fallen innerhalb von fünf Jahren auch deutlich schneller ab. Die maximalen Durchbruchskonzentrationen C/C_0 liegen im kleinräumigen Mittel zwischen 0.20 (Braunerde) und 0.18 (Schwarzerde).

Abb. 8 zeigt die Durchbruchskurven für NAP, PHE und Σ15 EPA-PAK jedoch ohne Abbau. Für das PP-Szenario zeigt sich in Abb. 8 (a)-(c) deutlich der Effekt der vom C_{org} des Unterbodens abhängigen Sorption. Während für die C_{org}-armen Böden NAP bereits nach kurzer Zeit durchbricht, wird es beim mäßig C_{org}-haltigen Podsol leicht, bei der C_{org}-reichen Schwarzerde stärker retardiert (Abb. 8 (a)). Für PHE und Σ15 EPA-PAK (Abb. 8 (b) und (c)) zeigen auch die C_{org}-armen Böden eine deutliche Retardation. Der flachere Verlauf der Durchbruchskurven für Braunerde im oberen Konzentrationsbereich deutet zudem auf einen Einfluss der langsamen Sorptionskinetik des Skelettanteils hin. Für alle Böden bis auf die Schwarzerde wird innerhalb der Simulationszeit der Durchbruch der PHE-Peaks mit C/C_0 zwischen 0.70 und 0.96 und eine

anschließende Konzentrationsabnahme auf Grund der zeitlichen Abnahme der Quellstärke (siehe Abb. 7 (b)) beobachtet. Für die Schwarzerde steigt C/C_0 nach 500 a noch deutlich an.

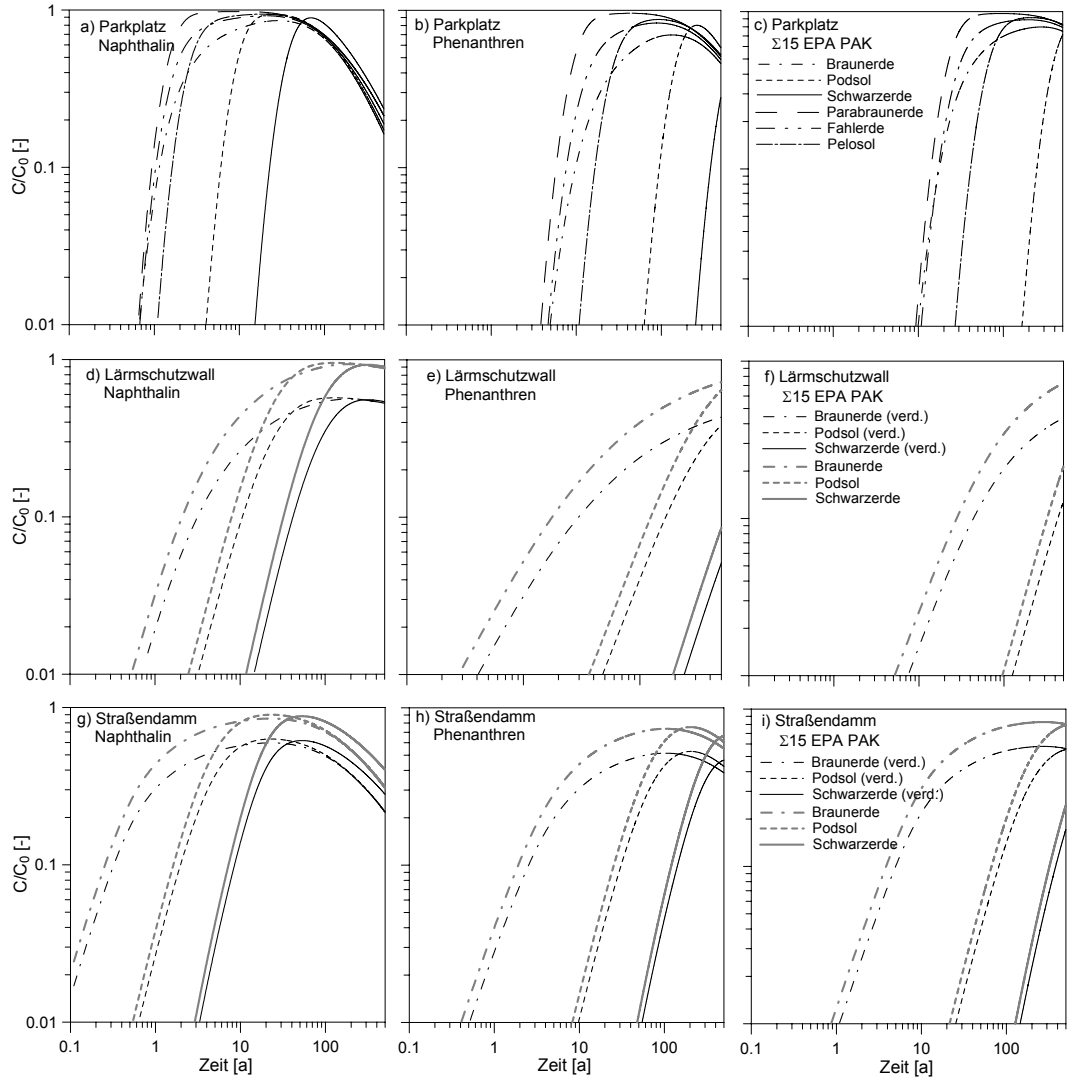

Abb. 8: Durchbruchskurven der sorbierbaren Stoffe Naphthalin (schwach sorptiv, links) und Phenanthren (mäßig gut sorptiv, Mitte) und des Summenparameters Σ15 EPA-PAK *(stark sorptiv, rechts) für die drei Szenarien Parkplatz ((a)-(c)), Lärmschutzwall ((d)-(f)) und Straßendamm ((g)-(i)). Gezeigt werden für Lärmschutzwall und Straßendamm jeweils Durchbruchskurven für den Schadstofftransportpfad (graue dicke Kurven) bzw. auf das Gesamtbauwerk bezogene Durchbruchskurven unter Berücksichtigung der Verdünnung durch nicht belastetes Sickerwasser (schwarze dünne Kurven).*

Abb. 8 (d)-(f) zeigt die NAP-, PHE- und Σ15 EPA-PAK- Durchbruchskurven des LSW-Szenarios. Ein deutlicher Unterschied zum PP ist das längere Anhalten hoher Konzentrationen, welches aus den im Durchschnitt niedrigeren Strömungsgeschwindigkeiten resultiert. Für NAP werden unter Berücksichtigung der Verdünnung durch am RCB vorbeiströmendes Sickerwasser Maximaldurchbrüche von C/C_0 = 0.56 erreicht (Abb. 8 (d)). Für PHE und Σ15 EPA-PAK zeigen sich bei allen betrachteten Böden nach 500 a noch deutlich ansteigende Konzentrationen (Abb. 8 (e) und (f)).

Im Vergleich dazu zeigen sich für das SD-Szenario aufgrund der stark erhöhten Infiltrationsraten steilere Durchbruchskurven und somit ein früheres Erreichen der Konzentrationspeaks (Abb. 8 (g)-(i)). NAP zeigt seine Maximaldurchbrüche bei der Braunerde bereits nach 19 a (C/C_0 = 0.59), bei der Schwarzerde nach 46 a (C/C_0 = 0.60).

Ohne Abbau erfolgt langfristig der Eintrag der gesamten Schadstoffmasse des RCB ins Grundwasser. Wird Abbau bei der Simulation mit berücksichtigt (Abb. 9 (a)– (i)), ist die Massenreduktion bei gegebener Abbauratenkonstante nur von der Verweilzeit der Substanzen im Bodenwasser abhängig. Retardation hat

keinen Einfluss auf die abgebaute Masse, da Mikroorganismen idR. nur zum Abbau in Lösung vorliegender Schadstoffe fähig sind. So zeigen Abb. 9 (a)-(c) für den PP, dass der Abbau bei der Parabraunerde trotz früherer Durchbruchszeiten effektiver ist, als z.B. bei der Braunerde oder dem Podsol. Dies liegt an der geringeren Abstandsgeschwindigkeit $v_a = q / \theta$ (= Transportgeschwindigkeit des Tracers) bzw. dem höheren Wassergehalt der feinkörnigen gegenüber den sandigen Böden bei vorgegebener Infiltrationsrate (= Darcyfluss q), woraus sich eine längere effektive Aufenthaltszeit der Substanzen im Bodenwasser des Profils ergibt. Insgesamt ist bei der angenommenen Halbwertzeit von 70 d eine Reduktion der Durchbruchkonzentrationen für den PP um einen Faktor von bis zu 30 möglich.

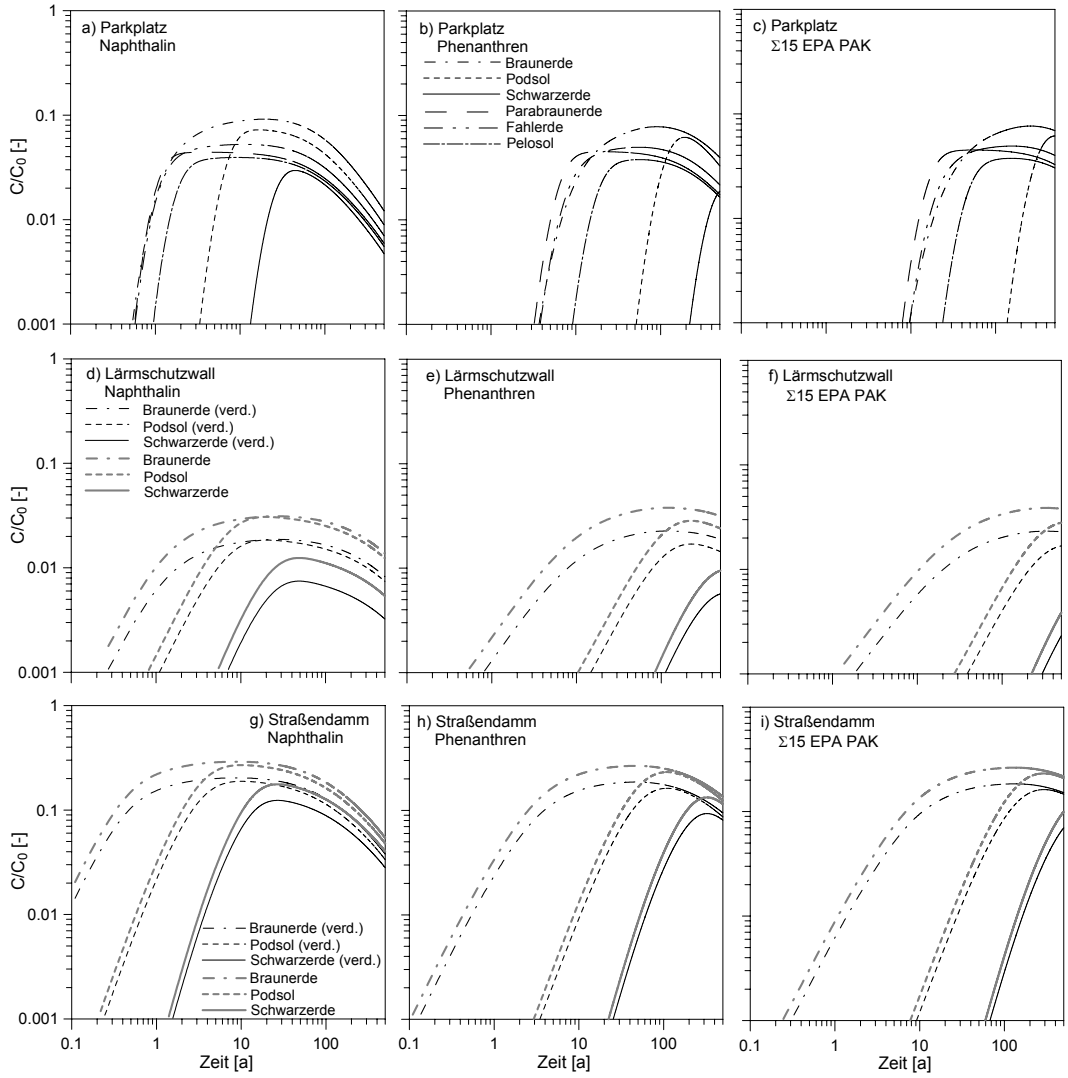

Abb. 9: Durchbruchskurven der sorbierbaren Stoffe Naphthalin (schwach sorptiv, links) und Phenanthren (mäßig gut sorptiv, Mitte) und des Summenparameters Σ15 EPA-PAK *(stark sorptiv, rechts) unter Berücksichtigung des biologischen Abbaus für die drei Szenarien Parkplatz ((a)-(c)), Lärmschutzwall ((d)-(f)) und Straßendamm ((g)-(i)). Gezeigt werden für Lärmschutzwall und Straßendamm jeweils Durchbruchskurven für den Schadstofftransportpfad (graue dicke Kurven) bzw. auf das Gesamtbauwerk bezogene Durchbruchskurven unter Berücksichtigung der Verdünnung durch nicht belastetes Sickerwasser (schwarze dünne Kurven).*

Aufgrund der langsameren Strömungsgeschwindigkeiten ist beim LSW die durchschnittliche Verweilzeit der gelösten Schadstoffe im Boden höher als beim PP. Dies führt zu einer stärkeren Konzentrationsreduktion bei Abbau (Minderungsfaktoren zwischen 25 und 150; Abb. 9 (d)-(f)). Umgekehrt zeigen sich beim SD auf Grund höherer Strömungsgeschwindigkeiten deutlich geringere Aufenthaltszeiten, sodass sich trotz des Abbaus nur geringe Minderungsfaktoren zwischen 2.5 und 5 ergeben (Abb. 9 (g)–(i)).

Schlussfolgerungen

Die in dieser Studie durchgeführten umfangreichen Typ-Szenarien-Simulationen ergänzen die im BMBF-Verbundprojekt „Sickerwasserprognose“ erarbeiteten wissenschaftlichen Grundlagen und methodischen Instrumentarien durch die Anwendung auf praxisrelevante Fallbeispiele. Aus den dabei gewonnenen Ergebnissen lassen sich folgende Schlussfolgerungen ableiten:

- Dispersive Konzentrationsminderung ist nur bedingt wirksam. Eine nennenswerte Abschwächung der Durchbruchskonzentrationen ist nur für Fälle möglich, in denen das Abklingen der Quellkonzentrationen deutlich vor dem Durchbruch des Schadstoffpeaks an der GWO erfolgt. Bei länger anhaltenden Quellstärken (z.B. für Salze wie Sulfat) ist dagegen mit weitgehend unvermindertem Konzentrationsdurchbruch zu rechnen.
- Für stärker sorbierende Schadstoffe (PHE, Σ15 EPA-PAK) zeigt sich schon bei geringem C_{org} der Unterböden eine Retardation der Peak-Durchbruchszeitpunkte um viele Jahrzehnte bis Jahrhunderte. Mit signifikanten Stoffeinträgen (in Abhängigkeit der Quellstärke) ins Grundwasser ist so bei „natürlichen“ Grundwasserneubildungsverhältnissen erst nach sehr langen Zeiträumen zu rechnen.
- Auch bei relativ niedrigen Ratenkonstanten ist eine deutliche Reduktion der Konzentrationen organischer Schadstoffe durch mikrobiellen Abbau möglich. Bezüglich der Effektivität des Abbaus ergeben sich jedoch erhebliche Unterschiede zwischen den drei betrachteten Verwertungsszenarien, die aus den unterschiedlichen Strömungs- bzw. Transportgeschwindigkeiten resultieren.
- Die Stoffverlagerung in den in zwei Raumdimensionen betrachteten Szenarien Lärmschutzwall und Straßendamm zeigt darüber hinaus einen ausgeprägten Einfluss der räumlich variablen Sickerwassermenge. Bereiche hoher Strömungsgeschwindigkeit führen zu früheren Ankunftszeiten der Schadstoffe im Grundwasser. Transportprognosen unter Vernachlässigung dieser Effekte können deshalb zu einer Unterschätzung der Schadstoffverlagerung führen und sind nicht konservativ.
- Die Strömungsbilanzen für Lärmschutzwall und Straßendamm legen nahe, dass mit geeigneten Bauwerksgeometrien und Materialien eine Reduktionen der Infiltration in das Verwertungsmaterial und des Austrags von Schadstoffen ins Grundwasser durch das Ausnutzen von Kapillarsperreneffekten zu erzielen ist. Der hier vorgestellte Modellansatz schafft grundsätzlich die Möglichkeit, das Design von Verwertungsszenarien ohne großen Mehraufwand in der Umsetzung durch numerische Simulationen in Richtung einer möglichst geringen Umweltbelastung bei hoher Verwertungsquote optimieren zu können.

Danksagung: Die Untersuchungen wurden im Rahmen des BMBF-Förderschwerpunkts „Sickerwasserprognose“ (Projektnummer 02WP0517) durchgeführt. Dem BMBF sei für die Förderung gedankt. Des Weiteren danken wir Herrn Dr. Utermann und Herrn Dr. Duijnisveld (BGR, Hannover), Herrn Dr. Susset und Herrn Dr. Leuchs (LANUV, Recklinghausen), Herrn Dr. Henzler (UFZ, Leipzig) und Frau Dr. Kocher (BaST, Bergisch Gladbach) für ausführliche und hilfreiche Diskussionen sowie Frau Dr. Kouznetsova und Herrn Duran für Hilfe bei der Durchführung der Simulationen.

Literaturangaben

Allen-King, R. M. Grathwohl, P., Ball, W. P.: New modelling paradigms for the sorption of hydrophobic organic chemicals to heterogeneous carbonaceous matter in soils, sediments and rocks.- Adv. Wat. Res. **25**, 985-1016 (2002)

Arya, L.M., Paris, J.F.: A physicoempirical model to predict soil moisture characteristics from particle-size distribution and bulk density data. Soil Sci. Soc. Am. J. **45,** 1023-1030 (1981)

BBodSchV: Bundes-Bodenschutz- und Altlastenverordnung vom 16. Juli 1999. Bundesgesetzblatt Jahrgang 1999, Teil I Nr.36, 1554-1682 (1999)

BGR (Bundesanstalt für Geowissenschaften und Rohstoffe): Nutzungsdifferenzierte Bodenübersichtskarte der Bundesrepublik Deutschland 1:1.000.000 (BÜK 1000 N2.3). Auszugskarten Acker, Grünland, Wald; Digit. Archiv FISBo BGR; Hannover und Berlin (2006)

BMU (Bundesministerium für Umwelt, Naturschutz und Reaktorsicherheit): Hydrologischer Atlas von Deutschland, 3. Lieferung 2003; Berlin (2000)

Bold, S.: Processed-based prediction of long-term risk of groundwater pollution by organic non-volatile contaminants. Dissertation, Tübinger Geowissenschaftliche Arbeiten (TGA), C72, 76 S.; Tübingen (2004)

Brakensiek, D.L., Rawls, W.J.: Soil containing rock fragments: Effects on infiltration.- Catena **23** (1-2), 99–110 (1994)

Carsell, R. F., Parish, R. S.: Developing joint probability distributions of soil water retention characteristics. Water Resour. Res. **24** (5), 755-769 (1988)
Du, Y., Wang, W. Kolditz, O.: Richards Flow Modelling. 5. Workshop “Porous Media" Proceedings CD, 2. Ausgabe, Center for Applied Geosciences, University of Tübingen (2005)
FGSV: RAS-Q 96, Richtlinien für die Anlage von Straßen – Teil: Querschnitte. 62 S.; Köln (1996)
FGSV: ZTV E-StB 94, Zusätzliche Technische Vertragsbedingungen und Richtlinien für Erdarbeiten im Straßenbau. 108 S.; Köln (1997)
FGSV: Merkblatt für wasserdurchlässige Befestigung von Verkehrsflächen. 36 S.; Köln (1998)
FGSV: RStO 01, Richtlinien für die Standardisierung des Oberbaues von Verkehrsflächen. 52 S.; Köln (2001)
FGSV: ZTV T-StB 95, Zusätzliche Technische Vertragsbedingungen und Richtlinien für Tragschichten im Straßenbau. Ausgabe 1955 / Fassung 2002. 126 S.; Köln (2002)
FGSV: ZTV SoB-StB 04, Zusätzliche Technische Vertragsbedingungen und Richtlinien für den Bau von Schichten ohne Bindemittel im Straßenbau. 48 S.; Köln (2004)
FGSV: RAS-EW, Richtlinien für die Anlage von Straßen – Teil: Entwässerung. 82 S.; Köln (2005)
Finkel, M.: Quantitative Beschreibung des Transports von polyzyklischen aromatischen Kohlenwasserstoffen (PAK) und Tensiden in porösen Medien. Tübinger Geowissenschaftliche Arbeiten (TGA), C47. 98 S.; Tübingen (1998)
Finkel M., Liedl R., Teutsch G.: Modelling surfactant-enhanced remediation of polycyclic aromatic hydrocarbons. J. Environ. Modelling & Software **14**, 203-211 (1998)
Flöter, O.: Wasserhaushalt gepflasterter Straßen und Gehwege. Lysimeterversuche an drei Aufbauten unter praxisnahen Bedingungen unter Hamburger Klima. Dissertation, Hamburger Bodenkundliche Arbeiten, 58, 329 S.; Hamburg (2006)
Glugla, G., Jankiewicz, P., Rachimow, C., Lojek, K., Richter, K., Fürtig, G., Krahe, P.: Wasserhaushaltsverfahren zur Berechnung vieljähriger Mittelwerte der tatsächlichen Verdunstung und des Gesamtabflusses. BfG-Bericht, Nr. 1342, 106 S.; (2003)
Grathwohl, P.: Diffusion controlled desorption of organic contaminants in various soils and rocks.- In Kharaka, K.Y., Maest, A.S. (Hrsg.): Water rock Interaction - Proceedings of the Utah Conference, 283-286 (1992)
Grathwohl, P.: Diffusion in Natural Porous Media: Contaminant Transport, Sorption/Desorption and Dissolution Kinetics. 224 S.; Kluwer Academic Publishers, Boston (1998)
Grathwohl, P.: Gutachten zur Beschreibung von fachlichen Eckpunkten für die Festlegung von Zuordnungswerten der Einbauklasse 1.1 (Z 1.1) für organische Schadstoffe in mineralischen Abfällen. Umweltbundesamt (Hrsg.) Texte 37/2004. Umweltforschungsplan des Bundesministeriums für Umwelt, Naturschutz und Reaktorsicherheit, Forschungsbericht 36301047, UBA-FB 000721. 71 S.; Berlin (2004)
Grathwohl, P., Susset, B.: Sickerwasserprognose - Grundlagen, Möglichkeiten, Grenzen, Modelle. In "Belastung von Böden und Gewässern" Gemeinschaftstagung ATV-DVWK, 28./29.05.01 Hannover (2001)
Grathwohl, P., Liedl, R., Beyer, C. Konrad, W.: Übertragung der Ergebnisse des BMBF - Förderschwerpunktes „Sickerwasserprognose“ auf repräsentative Fallbeispiele. Abschlussbericht des Teilprojekts 1a des Forschungsvorhabens „Entwicklung und Validierung eines Modells zur Abschätzung der Stoffkonzentration am Beurteilungsort“ im Rahmen des BMBF-Förderschwerpunkts „Sickerwasserprognose“ (Förderkennzeichen 02WP0517) (2006)
Grathwohl, P., Halm, D., Bonilla, A., Broholm, M., Burganos, V., Christophersen, M., Comans, R., Gaganis, P., Gorostiza, I., Höhener, P., Kjeldsen, P. and van der Sloot, H.: Guideline for Groundwater Risk Assessment at Contaminated Sites.- Final Report EU-Project EVK1-CT-1999-00029; (2003)
Hansson, K., Lundin, L.C., Simunek, J.: Modeling water flow patterns in flexible pavements. Transportation Research Record **1936,** 133-141 (2006)
Hayduk, W., Laudie, H.: Prediction of diffusion coefficients for nonelectrolytes in dilute aqueous solutions. AIChE Journal **20** (3), 611-615 (1974)
Hennings, V.: Methodendokumentation Bodenkunde. Auswertungsmethoden zur Beurteilung der Empfindlichkeit und Belastbarkeit von Böden. In: Geologisches Jahrbuch/ Sonderheft Reihe G, Band 1, 2. Auflage, 232 S.; (2000)
Henzler R.: Quantifizierung und Modellierung der PAK-Elution aus verfestigten und unverfestigten Abfallmaterialien. Dissertation, Tübinger Geowissenschaftliche Arbeiten (TGA), C76, 118 S.; Tübingen (2004)
Henzler, R., Rügner, H., Grathwohl, P.: Bewertung der Filter- und Pufferfunktion von Unterböden für organische Schadstoffe. Bodenschutz **1/2006**, 8-14 (2006)
Hjelmar, O., Holm J., Crillesen, K.: Utilisation of MSWI bottom ash as sub-base in road construction: First results from a large-scale test site. J. Hazard. Mater. **139** (3), 471-480 (2007)
Höhener, P, Dakhel, N., Christophersen, M., Broholm, M, Kjeldsen, P.: Biodegradation of hydrocarbons vapors: Comparison of laboratory studies and field investigations in the vadose zone at the emplaced fuel source experiment, Airbase Værløse, Denmark. J. Contam. Hydrol. **88** (3-4), 337-358 (2006)

Jäger, R., Liedl, R.: Prognose der Sorptionskinetik organischer Schadstoffe in heterogenem Aquifermaterial. Grundwasser **2**, 57-66 (2000)
Kellermann, C.: Zur Bewertung des Infiltrationsverhaltens von Tragschichten ohne Bindemittel. Dissertation, Schriftenreihe des Lehrstuhls für Verkehrswegebau der Ruhr-Universität Bochum, Heft 19, 165 S.; Bochum (2003)
Kleineidam, S., Rügner, H., Grathwohl, P.: Impact of grain scale heterogeneity on slow sorption kinetics. Environ. Tox. Chem. **18** (8), 1673–1678 (1999a)
Kleineidam, S., Rügner, H., Ligouis, B., Grathwohl, P.: Organic matter facies and equilibrium sorption of phenanthrene. Environ. Sci. Tech. **33** (10), 1637–1644 (1999b)
Kolditz, O., Bauer, S.: A process-oriented approach to computing multifield problems in porous media. J. Hydroinf. **6** (3), 225-244 (2004)
Kolditz, O., Xie, M., Kalbacher, T., Bauer, S., Wang, W., McDermott, C., Chen, C., Beyer, C., Gronewold, J., Kemmler, D., Legeida, D., Walsh, R., Du, Y., Park, C.H.: GeoSys/Rockflow version 4.3.21 - Theory and users manual, Center for Applied Geoscience, University of Tübingen (2006)
Krass, K., Brüggemann, M., Görener, E.: Anfall, Aufbereitung und Verwertung von Recycling-Baustoffen und industriellen Nebenprodukten im Wirtschaftsjahr 2001 – Teil 1; Recycling-Baustoffe. Straße + Autobahn **4**, 193-202 (2004a)
Krass, K., Brüggemann, M., Görener, E.: Anfall, Aufbereitung und Verwertung von Recycling-Baustoffen und indstriellen Nebenprodukten im Wirtschaftsjahr 2001 – Teil 2; Industrielle Nebenprodukte. Straße + Autobahn **5**, 275-281 (2004b)
KrW/AbfG: Gesetz zur Förderung der Kreislaufwirtschaft und Sicherung der umweltverträglichen Beseitigung von Abfällen (Kreislaufwirtschafts- und Abfallgesetz – KrW/AbfG). BGBl I 1994, 2705 (1994)
Maier, U., Grathwohl, P.: Natural Attenuation in the unsaturated zone and shallow groundwater: coupled modeling of vapor phase diffusion, biogeochemical processes and transport across the capillary fringe. In: Nützmann, G., Viotti, P., Aagard, P.: Reactive transport in soil and groundwater., 141-155; Springer, Berlin (2005)
Mesters, K.: Abschätzung der Mobilisierbarkeit von leichtlöslichen Salzen aus Müllverbrennungsasche am Beispiel eines Lärmschutzwalles.- Dissertation, Schriftenreihe des Lehrstuhls für Verkehrswegebau der Ruhr-Universität Bochum, Heft 5, 170 S.; Bochum (1993)
Mishra, S., Parker, J. C. , Singhal, N.: Estimation of soil hydraulic properties and their uncertainty from particle size distribution data. J. Hydrol. **108**, 1-18 (1989)
Mualem, Y.: A new model for predicting the hydraulic conductivity of unsaturated porous media. Water Resour. Res. **12**, 513–522 (1976)
Richter, T.: Regenwasserversickerung durch Pflasterdecken. Zement-Merkblatt Straßenbau S15 http://www.vdz-online.de/fileadmin/gruppen/vdz/3LiteraturRecherche/Zementmerkblaetter/S15.pdf (2003)
Ross, B.: The diversion capacity of capillary barriers. Water Resour. Res. **26** (10), 2625–2629 (1990)
Rügner, H., Henzler, R., Grathwohl, P.: Beurteilung der Empfindlichkeit der Filter- und Pufferfunktion von Böden (i.B. Unterböden) nach Maßstäben des vorsorgenden Bodenschutzes für organische Schadstoffe - Abschlussbericht. Projekt: „LABO 2003 B 2.03" (Programm: "Wasser und Boden" 2002 der Bund/Länder-Arbeitsgemeinschaft Bodenschutz) (2005)
Rügner, H., Kleineidam, S., Grathwohl, P.: Sorptions- und Transportverhalten organischer Schadstoffe in heterogenen Materialien am Beispiel des Phenanthrens. Grundwasser **3**, 133-138 (1997)
Rügner, H., Kleineidam, S., Grathwohl, P.: Long-term sorption kinetics of phenanthrene in aquifer materials. Environ. Sci. Tech. **33** (10), 1645–1651 (1999)
Seth, R., Mackay, D., Muncke, J.: Estimating of organic carbon partition coefficient and its variability for hydrophobic chemicals. Environ. Sci. Technol. **33** (14), 2390-2394 (1999)
Stieber, M., Kraßnitzer, S., dos Santos Coutinho, C., Tiehm, A.: Untersuchung der Bedeutung des mikrobiellen Abbaus für den Transport persistenter organischer Schadstoffe in der ungesättigten Zone. Abschlussbericht des Teilprojekts 3 des Forschungsvorhabens „Entwicklung und Validierung eines Modells zur Abschätzung der Stoffkonzentration am Beurteilungsort“ im Rahmen des BMBF-Förderschwerpunkts „Sickerwasserprognose“ (Förderkennzeichen 02WP0515) (2006)
Stoppka, B.: Prognose des Salzaustrags aus Straßenbaustoffen in der Sickerzone.- Dissertation, Schriftenreihe des Lehrstuhls für Verkehrswegebau der Ruhr-Universität Bochum, Heft 16, 232 S.; Bochum (2002)
Susset, B.: Materialien zur Sickerwasserprognose.- In: Förstner, U., Grathwohl, P.: Ingenieurgeochemie, Technische Geochemie - Konzepte und Praxis. Textbeitrag und Folien im CD-Anhang der 2. neu bearbeiteten Auflage, 471 S.; Springer, Berlin (2007)
Utermann, J., Kladivko, E.J., Jury, W.A.: Evaluation pesticide migration in tile drained soils with a transfer function model. J. Environ. Quality **19,** 707-714 (1990)
Vanderborght, J., Vereecken, H.: One-Dimensional Modeling of Transport in Soils with Depth-Dependent Dispersion, Sorption and Decay. Vadose Zone J. **6**, 140-148 (2007)

van Genuchten, M.T.: A closed form equation for predicting the hydraulic conductivity of unsaturated soils. Soil Sci. Soc. Am. J. **44**, 892-898 (1980)
Wörner, T., Löcherer, L., Westiner, E.: Untersuchung über das Verhalten von Recycling-Baustoffen in Tragschichten ohne Bindemittel unter längerer Verkehrsbeanspruchung. Beitrag zum Statusseminar Verbundvorhaben "Reststoffverwertung im Straßenbau", TV 4, FKZ 147 10 43 0, Bochum (2001)
Wösten, J. H. M., Lilly, A., Nemes, A., Le Bas, C.: Using existing soil data to derive hydraulic parameters for simulation models and in land use planning. – Final Report on the European Union Funded project. DLO-Staring Centre, Report 156, Wageningen /The Netherlands (1998)